

Synthesis and Biological Activity of Chondroitin Sulfate Biopolymers

Thesis by

Sarah Erin Tully

In Partial Fulfillment of the Requirements

for the Degree of

Doctor of Philosophy



California Institute of Technology

Pasadena, California

2007

(Defended 19 July 2006)

© 2007

Sarah Erin Tully

All Rights Reserved

...for my parents, Wendy and Richard...

Acknowledgments

Without the help and support of many people, the work completed in this thesis would not have been possible. I would like to thank my advisor, Linda Hsieh-Wilson, for her advice and guidance. It was stressful setting up a new lab, but exciting. From raiding the chemistry stockroom to trying to set-up the lyophilizer late in the night, the early times were fun, and it is great to see how the group has progressed. I look forward to seeing the fantastic science that will continue to come from the lab in the future.

I would like to thank the members of my committee, Harry Gray, Peter Dervan and David MacMillan. They have been very supportive and provided excellent scientific insight at my candidacy and proposal exams. Also, even though he is not technically on my committee, I am thankful to Dennis Dougherty for letting our group join his group meetings and for being a second mentor to our lab.

My undergraduate professors deserve special thanks, as well. Dr. Jeanne Poindexter, at Barnard College, inspired me to go into research and was the best mentor a young scientist could have. I learned the basics of organic synthesis from Dr. Christian Rojas, and I know I was able to get started in lab right away when I got here because of him. Dr. Koji Nakanishi and Dr. Yukari Fujimoto taught me how to think about biological problems from a chemical perspective, and are responsible for my original interest in bioorganic chemistry.

The members of the Hsieh-Wilson lab have been wonderful colleagues during my time here. There could not have been a better group of people with whom to start a lab than the original crew: Raymond Doss, Nelly Khidekel, Cristal Gama, Katherine Poulin-Kerstien, Sherry Tsai, Nathan Lamarre-Vincent, and Lori Lee. Working across from Ray

for the first year was an unforgettable experience, and he has made me laugh harder than any person ever has. I forgive him for the Backstreet Boys and N'Sync he subjected me to, and for the all the jokes that he and Uttam made at my expense during that time. His support pulled me through some of the tough times and I value our friendship beyond words. Nelly, Sherry, and Katherine have been great friends in and out of lab. Along with Sarah Miller (now Lamarre-Vincent!), we have had a lot of great talks, dinners, game nights, and parties. Nelly has been a fantastic roommate for the last year and I find it remarkable how well two stressed-out sixth-years can live together. Cristal was a wonderful partner on the chondroitin sulfate project and I am definitely indebted to her for her skills with neurons. Nathan has always been a source of jokes and craziness in the lab and I thank him for his help in organizing parties for major sporting events and for teaching me how to culture cells.

The people who have joined the lab through the years have also been fantastic. Ross Mabon joined the chondroitin sulfate project my second year, and I am not sure if we would have been able to do it without him. His Scottish charm and stories kept the lab interesting. Sabine Arndt was a lovely mentor and friend and showed me that you can do great science and raise a family, too. Heather Murrey was very helpful when I needed to learn how to run gels, and celebrating my 27th birthday with her was definitely memorable. Eric Shipp has been a wonderful bay-mate and microarray partner, and Manish Rawat and Katie Saliba have been great additions on the chondroitin sulfate project. I am indebted to Claude Rogers for finishing up the microarray data for my thesis, making figures for me when I had no idea what I was doing and for being a great friend to me over the last year. Peter Clark has really done some nice modeling work on

the chondroitin sulfate project and provided me with pictures for this thesis. I would also like to thank the other members of the lab: Dr. Marian Bryan, Dr. Helen Cheng, Tammy Campbell, Wendy Mercer, Rob Moncure, Monica Luo, Dr. Stacey Kalovidouris, Bruce Tai, and Dr. Xuewei Liu for their help and support.

The staff at Caltech is fantastic. I need to thank Dr. Scott Ross for all of his efforts in the NMR facility. It would not have been possible to characterize any of the tetrasaccharides without him. Dr. Susan Ou was wonderful to work with on antibody generation, and Dr. Jose Luis Riechmann was helpful in the production of microarrays. I would also like to thank Gary Hathaway and Mona Shahgholi for their hard work on obtaining mass spectral data for my synthetic compounds.

There are many people outside of lab who have supported me and made my time here a bit more enjoyable. Sarah Spessard has been a terrific friend and I miss all of our tennis matches, tennis watching, road-trips, and delicious Thanksgivings and Easters. My friend Danette Martin always seems to call when I need her, and I thank her for worrying about me, making sure I am okay, and for all of her Ohio stories. Joyce Park let me escape to her place in L.A. if things got too crazy and I needed a break, and she showed me all the best places to eat around here. Finally, I need to thank my parents. Without their love and guidance I would have never made it this far, and I thank them from the bottom of my heart.

Abstract

Chondroitin sulfate glycosaminoglycans are ubiquitously expressed linear, sulfated polysaccharides involved in cell growth, neuronal development and spinal cord injury. The different sulfation motifs presented by chondroitin sulfate may regulate its activity, but efforts to understand the precise biological roles of this glycosaminoglycan have been hampered by its complexity and heterogeneity. Here, we report the synthesis of well-defined chondroitin sulfate oligosaccharides through a convergent approach that permits installation of sulfate groups at precise positions along the carbohydrate backbone, biological evaluation of the synthetic molecules, and generation of antibodies that recognize the distinct sulfation motifs.

Using the chondroitin sulfate oligosaccharide library, we demonstrate that specific sulfation patterns act as molecular recognition elements for growth factors, and modulate neuronal growth. We identified a chondroitin sulfate tetrasaccharide, CS-E, which stimulates the growth and differentiation of multiple neuron types. Through use of carbohydrate microarrays, we found that the CS-E tetrasaccharide binds to a variety of proteins involved in promoting neurite outgrowth. A CS-E disaccharide, an unsulfated tetrasaccharide, and three other sulfated tetrasaccharides, CS-A, CS-C, and CS-R, were also investigated, and showed little effect on neurite outgrowth and reduced growth factor binding compared to the CS-E tetrasaccharide. These studies represent the first, direct investigations into the structure-activity relationships of chondroitin sulfate using homogeneous synthetic molecules, define a tetrasaccharide as a minimal motif required for function, and reveal the importance of sulfation in chondroitin sulfate bioactivity.

Table of Contents

Acknowledgments.....		iv
Abstract.....		vii
Table of Contents.....		viii
List of Figures.....		ix
List of Schemes.....		xvii
List of Tables.....		xix
List of Abbreviations.....		xx
Chapter 1	Chondroitin Sulfate Glycosaminoglycans.....	1
Chapter 2	Chemical Synthesis of Chondroitin Sulfate Oligosaccharides.....	28
Chapter 3	Synthesis and Neurobiological Evaluation of Chondroitin Sulfate Oligosaccharides Bearing the CS-E Sulfation Pattern.....	48
Appendix for Chapter 3	Relevant Spectral Data for Compounds of Chapter 3.....	137
Chapter 4	Elucidating the “Sulfation Code” of Chondroitin Sulfate Glycosaminoglycans.....	185
Appendix for Chapter 4	Relevant Spectral Data for Compounds of Chapter 4.....	229
Chapter 5	Development of Chondroitin Sulfate Microarrays.....	243
Appendix for Chapter 5	Keys for the Microarray Grids of Chapter 5 and Binding Curve Data for Midkine and BDNF.....	288
Chapter 6	Generation of Chondroitin Sulfate Antibodies.....	303
Chapter 7	Chondroitin Sulfate as a Modulator of Tumor Necrosis Factor- alpha Activity.....	332

List of Figures

Chapter 1		Page
Figure 1.1	The structures of GAG classes	2
Figure 1.2	GAGs at the cell surface	3
Figure 1.3	NMR structure of a heparin dodecasaccharide	5
Figure 1.4	The biosynthesis of heparin, heparan sulfate and chondroitin sulfate	6
Figure 1.5	Structure of a synthetic HS pentasaccharide with ATIII binding	9
Figure 1.6	Synthetic HS library for FGF-1 binding studies	10
Figure 1.7	X-ray crystal structure of a CS-A hexasaccharide coordinated to sodium ions	12
Figure 1.8	X-ray crystal structure of a CS-A tetrasaccharide coordinated to calcium ions	12
Figure 1.9	The most prevalent chondroitin sulfate sulfation motifs <i>in vivo</i>	13
Chapter 2		
Figure 2.1	Known chondroitin sulfate disaccharides	28
Figure 2.2	Structure of a CS-E tetrasaccharide	31
Figure 2.3	The structures of donors used in CS synthesis	32
Chapter 3		
Figure 3.1	Structures of the initial library of synthetic CS oligosaccharides	50
Figure 3.2	¹ H NMR (300 MHz, D ₂ O) of CS-E disaccharide 73	68
Figure 3.3	¹ H NMR (600 MHz, D ₂ O) of CS-E tetrasaccharide 79	71
Figure 3.4	¹ H NMR (600 MHz, D ₂ O) of compound 81	72

Figure 3.5 CS-E tetrasaccharide **79** stimulates outgrowth of hippocampal neurons 73

**Appendix for
Chapter 3**

Figure A3.1	¹ H NMR (600 MHz, CDCl ₃) of compound 37	138
Figure A3.2	¹ H NMR (300 MHz, CDCl ₃) of compound 38	139
Figure A3.3	¹ H NMR (300 MHz, CDCl ₃) of compound 39	140
Figure A3.4	¹ H NMR (300 MHz, CDCl ₃) of compound 40	141
Figure A3.5	¹ H NMR (300 MHz, CDCl ₃) of compound 42	142
Figure A3.6	¹ H NMR (300 MHz, CDCl ₃) of compound 43	143
Figure A3.7	¹ H NMR (300 MHz, CDCl ₃) of compound 44	144
Figure A3.8	¹ H NMR (300 MHz, CDCl ₃) of compound 45	145
Figure A3.9	¹ H NMR (300 MHz, CD ₃ OD) of compound 46	146
Figure A3.10	¹ H NMR (300 MHz, CDCl ₃) of compound 47	147
Figure A3.11	¹ H NMR (300 MHz, CDCl ₃) of compound 48	148
Figure A3.12	¹ H NMR (300 MHz, CDCl ₃) of compound 48a	149
Figure A3.13	¹ H NMR (300 MHz, CDCl ₃) of compound 49	150
Figure A3.14	¹ H NMR (300 MHz, CDCl ₃) of compound 50	151
Figure A3.15	¹ H NMR (300 MHz, CDCl ₃) of compound 50a	152
Figure A3.16	¹ H NMR (300 MHz, CDCl ₃) of compound 51	153
Figure A3.17	¹ H NMR (300 MHz, CDCl ₃) of compound 52	154
Figure A3.18	¹ H NMR (300 MHz, CDCl ₃) of compound 53	155
Figure A3.19	¹ H NMR (300 MHz, CDCl ₃) of compound 54	156
Figure A3.20	¹ H NMR (300 MHz, CDCl ₃) of compound 55	157

Figure A3.21	^1H NMR (300 MHz, CDCl_3) of compound 56	158
Figure A3.22	^1H NMR (300 MHz, CDCl_3) of compound 57	159
Figure A3.23	^1H NMR (300 MHz, CD_3OD) of compound 58	160
Figure A3.24	^1H NMR (300 MHz, CDCl_3) of compound 59	161
Figure A3.25	^1H NMR (300 MHz, CDCl_3) of compound 60	162
Figure A3.26	^1H NMR (300 MHz, CDCl_3) of compound 61	163
Figure A3.27	^1H NMR (300 MHz, CDCl_3) of compound 62	164
Figure A3.28	^1H NMR (300 MHz, CDCl_3) of compound 64	165
Figure A3.29	^1H NMR (300 MHz, CDCl_3) of compound 64a	166
Figure A3.30	^1H NMR (300 MHz, CDCl_3) of compound 64b	167
Figure A3.31	^1H NMR (300 MHz, CDCl_3) of compound 65	168
Figure A3.32	^1H NMR (600 MHz, CDCl_3) of compound 67	169
Figure A3.33	^1H NMR (600 MHz, CDCl_3) of compound 68	170
Figure A3.34	^1H NMR (300 MHz, CDCl_3) of compound 69	171
Figure A3.35	^1H NMR (300 MHz, CDCl_3) of compound 70	172
Figure A3.36	^1H NMR (300 MHz, CD_3OD) of compound 71	173
Figure A3.37	^1H NMR (300 MHz, CD_3OD) of compound 71a	174
Figure A3.38	^1H NMR (300 MHz, CD_3OD) of compound 72	175
Figure A3.39	^1H NMR (300 MHz, CD_3OD) of compound 72a	176
Figure A3.40	^1H NMR (300 MHz, D_2O) of compound 73	177
Figure A3.41	^1H NMR (300 MHz, CDCl_3) of compound 74	178
Figure A3.42	^1H NMR (300 MHz, CDCl_3) of compound 75	179
Figure A3.43	^1H NMR (300 MHz, CDCl_3) of compound 76	180

Figure A3.44	^1H NMR (600 MHz, CD_3OD) of compound 77	181
Figure A3.45	^1H NMR (600 MHz, CD_3OD) of compound 78	182
Figure A3.46	^1H NMR (600 MHz, D_2O) of compound 79: CS-E	183
Figure A3.47	^1H NMR (600 MHz, D_2O) of compound 81	184

Chapter 4

Figure 4.1	Major chondroitin sulfate disaccharides of the embryonic rat brain	185
Figure 4.2	Structures of the second library of synthetic CS oligosaccharides	188
Figure 4.3	^1H NMR (600 MHz, D_2O) of CS-A tetrasaccharide 85	190
Figure 4.4	^1H NMR (600 MHz, D_2O) of CS-C tetrasaccharide 88	192
Figure 4.5	^1H NMR (600 MHz, D_2O) of CS-R tetrasaccharide 92	194
Figure 4.6	^1H NMR (600 MHz, D_2O) of CS-E dimer 95	196
Figure 4.7	Average structures from molecular dynamics simulations of the CS tetrasaccharides in water	198
Figure 4.8	The sulfation pattern directs the neurotogenic activity of CS	199
Figure 4.9	The CS-E sulfation motif stimulates neuronal growth through activation of midkine-PTP ζ and BDNF-TrkB signaling pathways	202
Figure 4.10	Class-matched IgG control antibodies do not effect neurite outgrowth in the presence or absence of CS-E	202
Figure 4.11	Antibodies against BDNF or midkine, but not control IgG antibodies, block the binding of BDNF or midkine to CS-E on the microarray	203

Appendix for Chapter 4

Figure A4.1	^1H NMR (300 MHz, CDCl_3) of compound 82	230
Figure A4.2	^1H NMR (300 MHz, CD_3OD) of compound 83	231
Figure A4.3	^1H NMR (300 MHz, CD_3OD) of compound 84	232

Figure A4.4	¹ H NMR (600 MHz, D ₂ O) of compound 85: CS-A	233
Figure A4.5	¹ H NMR (600 MHz, CD ₃ OD) of compound 86	234
Figure A4.6	¹ H NMR (600 MHz, CD ₃ OD) of compound 86a	235
Figure A4.7	¹ H NMR (300 MHz, CD ₃ OD) of compound 87	236
Figure A4.8	¹ H NMR (600 MHz, D ₂ O) of compound 88: CS-C	237
Figure A4.9	¹ H NMR (300 MHz, CDCl ₃) of compound 89	238
Figure A4.10	¹ H NMR (600 MHz, CD ₃ OD) of compound 90	239
Figure A4.11	¹ H NMR (600 MHz, D ₂ O) of compound 92: CS-R	240
Figure A4.12	¹ H NMR (600 MHz, D ₂ O) of compound 93	241
Figure A4.13	¹ H NMR (600 MHz, D ₂ O) of compound 95	242

Chapter 5

Figure 5.1	Surface display of oligosaccharides for SPR analysis using the biotin-streptavidin interaction	244
Figure 5.2	Non-covalent display of isolated polysaccharides	245
Figure 5.3	Immobilization of neoglycolipids to nitrocellulose arrays	246
Figure 5.4	Pohl's approach to fluoros-based microarrays	247
Figure 5.5	Wong's generation of lipid-linked oligosaccharide microtiter plates	248
Figure 5.6	Formation of covalently attached carbohydrate microarrays through use of a Diels-Alder reaction	249
Figure 5.7	Shin's approach to covalent attachment of oligosaccharides	250
Figure 5.8	Seeberger's approach to covalent conjugation of oligosaccharides to microarrays	250
Figure 5.9	Covalent attachment of unmodified oligosaccharides to hydrazide- or aminoxy-coated slides	251
Figure 5.10	Wong and Paulson's approach to NHS-activated microarrays	252
Figure 5.11	Synthetic chondroitin sulfate library for microarray analysis	254

Figure 5.12	pH-dependence of aminoxy oligosaccharide conjugation to aldehyde-coated slides	258
Figure 5.13	Binding analysis of the anti-CS-A, anti-CS-C or anti-CS-E antibodies to the microarrays	261
Figure 5.14	Binding analysis of MK, PTN or FGF-16 to the microarrays	264
Figure 5.15	Binding analysis of BDNF, NGF or TrkB to the microarrays	268
Figure 5.16	Binding analysis of GDNF, Nogo-A or Nogo-R to the microarrays	269
 Appendix for Chapter 5		
Figure A5.1	Representative portion of the microarrays illustrating spot morphology and fluorescence intensity after incubation with anti-CS-A antibody 10G9-2B5	289
Figure A5.2	Representative portion of the microarrays illustrating spot morphology and fluorescence intensity after incubation with anti-CS-C antibody 2D5-1D2	290
Figure A5.3	Representative portion of the microarrays illustrating spot morphology and fluorescence intensity after incubation with anti-CS-E antibody 2D11-2A10	291
Figure A5.4	Representative portion of the microarrays illustrating spot morphology and fluorescence intensity after incubation with midkine	292
Figure A5.5	Representative portion of the microarrays illustrating spot morphology and fluorescence intensity after incubation with pleiotrophin	293
Figure A5.6	Representative portion of the microarrays illustrating spot morphology and fluorescence intensity after incubation with FGF-16	294
Figure A5.7	Representative portion of the microarrays illustrating spot morphology and fluorescence intensity after incubation with BDNF	295
Figure A5.8	Representative portion of the microarrays illustrating spot morphology and fluorescence intensity after incubation with NGF	296
Figure A5.9	Representative portion of the microarrays illustrating spot morphology and fluorescence intensity after incubation with TrkB	297
Figure A5.10	Representative portion of the microarrays illustrating spot morphology and fluorescence intensity after incubation with GDNF	298

Figure A5.11	Representative portion of the microarrays illustrating spot morphology and fluorescence intensity after incubation with Nogo-A	299
Figure A5.12	Representative portion of the microarrays illustrating spot morphology and fluorescence intensity after incubation with Nogo-R	300
Figure A5.13	Binding curves obtained from microarray data of the CS tetrasaccharides bound to midkine	301
Figure A5.14	Binding curves obtained from microarray data of the CS tetrasaccharides bound to BDNF	302

Chapter 6

Figure 6.1	Compounds for antibody generation	306
Figure 6.2	Dot blots of antibody pre-bleeds	307
Figure 6.3	Dot blot characterization of anti-CS-A 10G9-2B5 and anti-CS-C 5D2-1D2 monoclonal antibodies	309
Figure 6.4	Dot blot characterization of commercial CS-A and CS-C antibodies	310
Figure 6.5	Dot blot characterization of anti-CS-E monoclonal 2D11-2A10 and commercially available CS-56	311
Figure 6.6	Western blot of adult rat brain lysates probed with anti-CS-A monoclonal antibody 10G9-2B5	312
Figure 6.7	Western blot of adult rat brain lysates probed with anti-CS-C monoclonal antibody 5D2-1D2	313
Figure 6.8	Western blot of adult rat brain lysates probed with anti-CS-E monoclonal antibody 2D11-2A10	314
Figure 6.9	Western blot of embryonic day 20 rat brain lysates probed with anti-CS-E monoclonal antibody 2D11-2A10	315
Figure 6.10	Staining of DRG neurons from embryonic day 20 rat spinal cord cultured for 15 hours in vitro with the anti-CS-E antibody 2D11-2A10	316
Figure 6.11	Coomassie stained 3 – 8% Tris-acetate minigel of the column fractions from the 10G9-2B5 anti-CS-A monoclonal antibody purification	323
Figure 6.12	Coomassie stained 3 – 8% Tris-acetate minigel of the column fractions from the 5D2-1D2 anti-CS-C monoclonal antibody purification	324
Figure 6.13	Coomassie stained 3 – 8% Tris-acetate minigel of the column fractions from the 2D11-2A10 anti-CS-E monoclonal antibody purification	325

Chapter 7

Figure 7.1	TNF- α binding to chondroitin sulfate microarrays	334
Figure 7.2	Computational modeling of the TNF- α /CS-E tetrasaccharide interaction	335
Figure 7.3	ELISA analysis of the TNF- α /TNFR1 binding in the presence of chondroitin sulfate	337
Figure 7.4	ELISA analysis of the TNF- α /TNFR2 binding in the presence of chondroitin sulfate	337
Figure 7.5	CS polysaccharides enriched in the CS-E motif and CS-E tetrasaccharide 79 inhibit TNF- α -induced apoptosis	338
Figure 7.6	CS-E tetrasaccharide 79 inhibits TNF- α -induced apoptosis and a protective effect is observed.	339
Figure 7.7	Representative portion of the microarrays illustrating spot morphology and fluorescence intensity after incubation with TNF- α	343
Figure 7.8	Optimization of the biotinylated TNF- α concentration for TNFR1 and TNFR2 ELISA studies	345
Figure 7.9	Optimization of the caspase assay	346

List of Schemes

Chapter 2		Page
Scheme 2.1	Activation of donors with C-2 participating groups	32
Scheme 2.2	Azidonitration of tri- <i>O</i> -acetylgalactal with cerium ammonium nitrate and sodium azide.	33
Scheme 2.3	The first synthesis of a CS-A disaccharide by Marra and Sinäy	35
Scheme 2.4	Jacquinet's synthesis of CS-A and CS-C disaccharides	36
Scheme 2.5	Synthesis of Tamura and Ogawa's fully protected tetrasaccharide	37
Scheme 2.6	Synthesis of Tamura and Ogawa's CS-A, CS-C, and CS-E tetrasaccharides	39
Scheme 2.7	Synthesis of Karst and Jacquinet's fully protected hexasaccharide	40
Scheme 2.8	Karst and Jacquinet's CS-D hexasaccharide	41
Chapter 3		
Scheme 3.1	Retrosynthetic analysis 1 and retrosynthetic analysis 2 of CS tetrasaccharides	52
Scheme 3.2	Synthesis of glucuronic acid monomer 39	54
Scheme 3.3	Synthesis of the galactosamine monomer 40	55
Scheme 3.4	Formation of disaccharide 38	56
Scheme 3.5	Intermolecular aglycon transfer	57
Scheme 3.6	Synthesis of the galactosamine monomer 60	58
Scheme 3.7	Formation of disaccharide 61	58
Scheme 3.8	Synthesis of the glucuronic acid monomer 44	59
Scheme 3.9	Formation of disaccharide 42	60
Scheme 3.10	Isomerization of the GalNAc anomeric allyl group	61
Scheme 3.11	Generation of the disaccharide donor 64 and acceptor 65	62

Scheme 3.12	Formation of tetrasaccharide 37	63
Scheme 3.13	Rearrangement of the disaccharide donor 64	63
Scheme 3.14	Formation of tetrasaccharide acceptor 67 and hexasaccharide 68	64
Scheme 3.15	Stepwise synthesis of the CS-E disaccharide 73	66
Scheme 3.16	Streamlined synthesis of the CS-E disaccharide 73	67
Scheme 3.17	Generation of key tetrasaccharide tetraol 76	70
Scheme 3.18	Generation of the CS-E tetrasaccharide 79	70
Scheme 3.19	Generation of the unsulfated CS tetrasaccharide 81	70
 Chapter 4		
Scheme 4.1	Synthesis of the CS-A tetrasaccharide 85	189
Scheme 4.2	Synthesis of the CS-C tetrasaccharide 88	191
Scheme 4.3	Synthesis of the CS-R tetrasaccharide 92	193
Scheme 4.4	Synthesis of the CS-E dimer 95	195
 Chapter 5		
Scheme 5.1	Attachment of an aminoxy linker to chondroitin sulfate tetrasaccharides	256

List of Tables

Chapter 3		Page
Table 3.1	Conditions attempted for generation of disaccharide 38	56
Table 3.2	Allyl isomerization conditions	61
Table 3.3	Conditions attempted for the generation of tetrasaccharide 37	63
Chapter 5		
Table 5.1	Conditions tested for the conjugation of aminoxy oligosaccharides to aldehyde-coated slides	257
Table 5.2	Conditions tested for the blocking of aldehyde-coated slides	258
Table 5.3	Conditions tested for protein incubations on aldehyde microarrays	259
Table 5.4	Binding of proteins to heparan sulfate polysaccharides on polylysine microarrays and chondroitin sulfate tetrasaccharides on aldehyde microarrays	262
Chapter 6		
Table 6.1	Commercially available chondroitin sulfate antibodies	305
Table 6.2	List of anti-CS-A, -C, and -E monoclonal antibodies generated from the synthetic chondroitin sulfate oligosaccharides 85: CS-A , 88: CS-C , and 79: CS-E	307

List of Abbreviations

[α] _D	specific rotation at wavelength of sodium D line
A	CS-A tetrasaccharide
Å	angstrom
A ₂₈₀	absorbance at 280 nm
ABTS	2,2'-azino-bis(3-ethylbenzthiazoline-6-sulfonic acid)
Ac	acetyl, acetate
Adam-10	a disintegrin and metalloproteinase
AIBN	2,2'-azobis(2-methylpropionitrile)
All	allyl
aq	aqueous
ATIII	antithrombin III
BDNF	brain-derived neurotrophic factor
Bn	benzyl
BSA	bovine serum albumin
Bu	butyl
Bz	benzoyl
C	CS-C tetrasaccharide
°C	degrees Celsius
calcd	calculated
CAN	cerium ammonium nitrate
Cereb	cerebellum
COD	<i>cis,cis</i> -1,5-cyclooctadiene
CS	chondroitin sulfate
CSA	(±)-DL-camphor-10-sulfonic acid
CXCL-16	CXC-chemokine ligand-16
Cy	cyclohexyl
d	doublet
D	aspartic acid
DABCO	1,4-diazabicyclo[2.2.2]octane
DBU	1,8-diazabicyclo[5.4.0]undec-7-ene
DCC	deleted in colorectal cancer
dd	doubly distilled or doublet of doublets
DDQ	2,3-dichloro-5,6-dicyano- <i>p</i> -benzoquinone
di	disaccharide
DIPEA	<i>N,N</i> -diisopropylethylamine
DLAR	<i>Drosophila</i> LAR receptor
DMA	<i>N,N</i> -dimethylacetamide
DMAP	4-dimethylaminopyridine

DMF	<i>N,N</i> -dimethylformamide
DNA	deoxyribonucleic acid
dppp	1,3-bis(diphenylphosphino)propane
DRG	dorsal root ganglion
DS	dermatan sulfate
E	CS-E tetrasaccharide or glutamic acid
ECD	extracellular domain
EGF	epidermal growth factor
EGFR	epidermal growth factor receptor
ELISA	enzyme-linked immunosorbent assay
equiv	equivalent
ESI	electrospray ionization
Et	ethyl
FAB	fast atom bombardment
FGF	fibroblast growth factor
FGFR	fibroblast growth factor receptor
FU	fluorescence units
g	gram(s)
GAG	glycosaminoglycan
Gal	galactose
GalNAc	<i>N</i> -acetylgalactosamine
GDNF	glial-derived neurotrophic factor
GlcA	glucuronic acid
GlcN	glucosamine
GlcNAc	<i>N</i> -acetylglucosamine
GPI	glycosylphosphatidylinositol
h	hour(s)
HB-EGF	heparin-binding epidermal growth factor
Hh	Hedgehog
Hippo	hippocampus
HPLC	high-performance liquid chromatography
HRMS	high resolution mass spectrometry
HRP	horse radish peroxidase
HS	heparan sulfate
Hz	hertz
IC ₅₀	inhibitory concentration 50%
IdoA	iduronic acid
IgG	immunoglobulin
IP-10	inducible protein-10
IR	infrared spectroscopy

<i>J</i>	coupling constant
KLH	keyhole limpet hemocyanin
λ	wavelength
L	liter
LC	liquid chromatography
Lev	levulinoyl
m	multiplet, milli or messenger
<i>m/z</i>	mass to charge ratio
μ	micro
MAG	myelin-associated glycoprotein
MAPK	mitogen associated protein kinase
MCA	monochloroacetyl
Me	methyl
MHz	megahertz
min	minute(s)
MK	midkine
mol	mole(s)
MS	mass spectrometry
MS	molecular sieves
n	nano
NDST	<i>N</i> -deacetylase/sulfotransferase
NF- κ B	nuclear factor kappa B
NGF	nerve growth factor
NHS	<i>N</i> -hydroxysuccinimide
NIS	<i>N</i> -iodosuccinimide
NMR	nuclear magnetic resonance
Olf	olfactory
<i>p</i>	para
PAPS	3' phosphoadenosine 5' phosphosulfate
PBS	phosphate buffered saline
PDC	pyridinium dichromate
PG	proteoglycan
Ph	phenyl
pH	hydrogen concentration in aqueous solution
PhMe	tolyl
Phth	phthaloyl
PI3-K	phosphatidylinositol-3 kinase
Piv	pivolate
PMB	<i>para</i> -methoxybenzyl
<i>p</i> MP	<i>para</i> -methoxyphenyl
ppm	parts per million
PTN	pleiotrophin

PTP ζ	protein-tyrosine phosphatase zeta
pyr	pyridine
q	quartet
QEq	charge equilibrium
R	CS-R tetrasaccharide
R γ	retention factor
RNA	ribonucleic acid
rt	room temperature
RT-PCR	reverse transcription polymerase chain reaction
s	singlet
SDF-1 β	stromal cell-derived factor-1 β
SDS-PAGE	sodium dodecyl sulfate polyacrylamide gel electrophoresis
sem	standard error of the mean
Ser	serine
SLC	secondary lymphoid-tissue chemokine
SPR	surface plasmon resonance
t	triplet
TBAF	tetrabutylammonium fluoride
TBS	<i>tert</i> -butyldimethylsilyl
TBS	tris buffered saline
TCA	trichloroacetyl
TEA	triethylamine
tetra	tetrasaccharide
Tf	trifluoromethanesulfonate
THF	tetrahydrofuran
TIPS	triisopropylsilyl
TLC	thin-layer chromatography
TMA	trimethylamine
TMS	trimethylsilyl
TNFR1	tumor necrosis factor-alpha receptor 1
TNFR2	tumor necrosis factor-alpha receptor 2
TNF- α	tumor necrosis factor-alpha
TOCSY	total correlated spectroscopy
TrkA	tyrosine kinase A receptor
TrkB	tyrosine kinase B receptor
Troc	trichloroethoxycarbonyl
U	units
UDP	uridine diphosphate
UV	ultraviolet
V	valine
Wg	Wingless
Xyl	xylose

Chapter 1: Chondroitin Sulfate Glycosaminoglycans

The glycosaminoglycan family

Glycosaminoglycans (GAGs) are linear, sulfated oligosaccharides that are involved in numerous biological functions, ranging from tissue structure and cell growth to protein activity regulation. Assembled from repeating disaccharide subunits, GAGs exhibit subtle variations in stereochemistry, length, and patterns of sulfation (Figure 1.1). Depending on the type of amino sugar found in the polymer, GAGs can be classified into two broad categories: the glucosaminoglycans, based on D-glucosamine (hyaluronan, keratan sulfate, heparin, and heparan sulfate), and the galactosaminoglycans, based on D-galactosamine (chondroitin sulfate and dermatan sulfate). Chondroitin sulfate (CS) contains only glucuronic acid moieties, whereas, heparan sulfate (HS), heparin, and dermatan sulfate (DS) contain both iduronic (IdoA) and glucuronic acid (GlcA) units, adding another level of stereochemical complexity. Various sulfation motifs are created through modification of the carbohydrate backbone.^{1,2} For example, heparin and HS can be sulfated at the C-2 hydroxyl of IdoA and the C-3 and C-6 hydroxyls of glucosamine (GlcN). The C-2 amine can be sulfated acetylated or remain unmodified. Due to this complexity, an HS tetrasaccharide can present over 2000 sulfation motifs. CS also is diversely sulfated and can be modified at any of the free hydroxyls. Potentially, a simple CS tetrasaccharide can present 256 sulfation patterns.

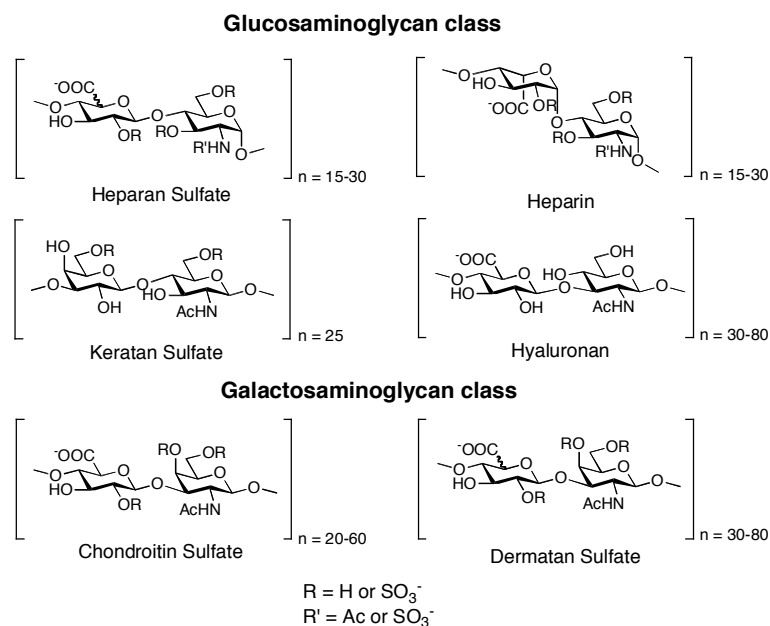


Figure 1.1: The structures of GAG classes.

In animals, GAGs can exist independently or are attached to core proteins, called proteoglycans, via a common GAG-protein linkage region tetrasaccharide on specific serine residues.^{3,4} Proteoglycans are major constituents of the extracellular matrix and cell membranes, and are important in a variety of functions, including cancer metastasis, embryonic development, viral entry and attachment, angiogenesis, and axonal guidance. They modulate cell-cell and cell-matrix interactions, contribute to the maintenance of normal tissue architecture and function, and participate in cell adhesion and growth control.³⁻⁷ Potentially, GAGs and their associated core proteins recruit protein ligands to the cell surface and act as templates to bring ligands and their corresponding receptors into the optimal alignment for productive binding (Figure 1.2).^{8,9} The number of GAGs attached to a proteoglycan can differ, as can the length, sugar composition, and sulfation pattern of the attached GAGs.^{5,6} These aspects are regulated depending on the location of

the proteoglycan, and the developmental and pathological state of the tissues where the proteoglycan exists. The sulfation patterns of GAGs are highly controlled and presumably dictate the ligands a proteoglycan can bind,¹⁰ but the difficulty in isolating GAG chains of defined sulfation sequence for protein-binding analyses has hampered an understanding of the roles of specific sulfation sequences and the reasons exquisite pattern regulation is important.

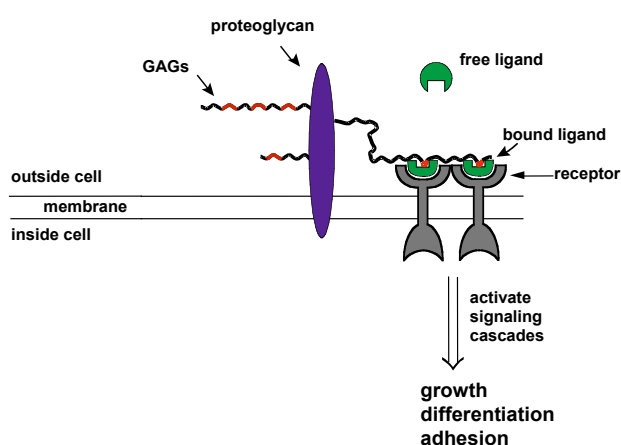


Figure 1.2: GAGs at the cell surface.

In developing nervous tissue, proteoglycans have been implicated in various cellular processes such as cell proliferation, regulation of cell morphology, cell migration, cell differentiation, neurite formation, synapse stabilization and signal transduction. In central nervous tissues, the majority of the proteoglycans carry either CS or HS side chains. Some of them are constituents of the extracellular matrix, others are bound to the cell surface through a glycosylphosphatidylinositol (GPI) anchor and some are transmembrane proteins.^{4,6,8} Proteoglycans in the brain display affinity to a variety of

ligands, including growth factors, cell adhesion molecules, matrix components, enzymes, and enzyme inhibitors. During histogenesis of the central nervous system, proteoglycans and their putative binding partners frequently colocalize, so it is likely that proteoglycans mediate crucial events in brain development.^{3,4,8,9}

Heparan sulfate and heparin glycosaminoglycans

Understanding the importance and function of GAGs *in vivo* has been the focus of numerous investigations, and the majority of these studies concentrated on heparin and HS. Consisting of GlcN and either IdoA or GlcA, heparin and HS are joined by repeating $\alpha(1,4)$ and $\beta(1,4)$ linkages. Heparin is usually localized to specialized granule cells but HS is present on multiple cell types and is more prevalent *in vivo*. HS displays a variety of sulfation patterns and has greater structural diversity than heparin.^{1,11}

Studies using NMR, X-ray crystallography and molecular modeling have shown that HS and heparin are helical molecules but the pitch of the helix can vary upon protein binding or with different counterions (Figure 1.3).^{11,12} The conformational flexibility of the IdoA subunit provides an additional level of 3-dimensional complexity, and is proposed to enhance heparin/HS-protein interactions.^{11,13}

The biosynthesis of heparin and HS begins in the Golgi apparatus, and starts with generation of the tetrasaccharide linkage region, GlcA $\beta(1,3)$ -galactose $\beta(1,3)$ -galactose $\beta(1,4)$ -xylose β -1-*O*-Ser, common to heparan sulfate, heparin and CS GAGs (Figure 1.4). Xylose, from uridine diphosphate-xylose, is linked to select proteoglycan core protein serines followed by the addition of two galactose units and a GlcA moiety through three distinct transferases.^{14,15} This region can be sulfated or phosphorylated.¹⁶ The addition of

N-acetylglucosamine (GlcNAc) to the linker determines the chain will be HS or heparin and is followed by alternating addition of GlcA and GlcNAc by EXT1 and EXT2, the HS and heparin polymerases.¹⁵

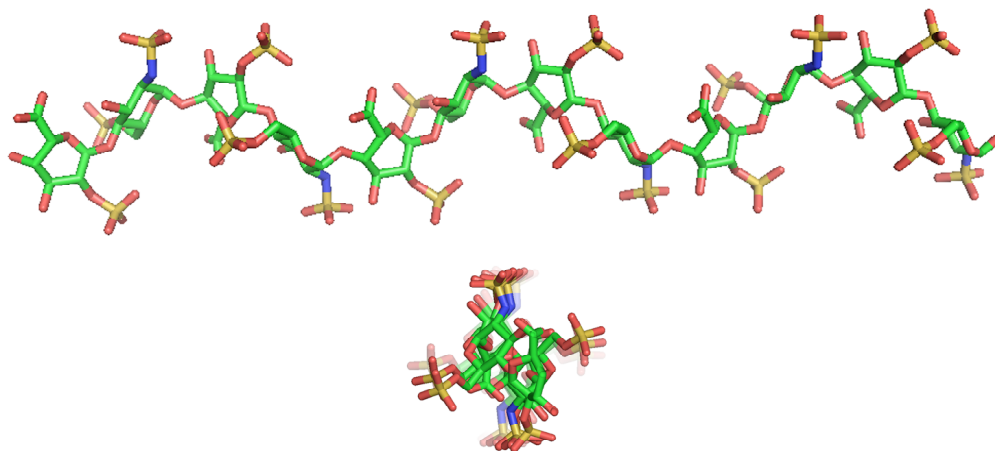


Figure 1.3: NMR structure of a heparin dodecasaccharide. The top structure shows the view parallel to the helical axis and the bottom structure the view perpendicular to the helical axis.¹²

Sulfation of HS or heparin GAGs also takes place in the Golgi apparatus and sulfotransferases add sulfate groups from 3' phosphoadenosine-5' phosphosulfate (PAPS) to the growing oligosaccharides. How the resulting sulfation pattern is determined and the organization of the sulfotransferases in the Golgi apparatus are unknown, but the enzymes are believed to form complexes with other enzymes in the pathway. Fifteen HS/heparin sulfotransferases have been identified in mice and humans. The first sulfotransferase to modify the HS/heparin chain is NDST (*N*-deacetylase/sulfotransferase), a bifunctional enzyme that deacetylates and subsequently sulfates the GlcNAc C-2 amines.^{2,17,18}

After *N*-sulfation, some of the GlcA moieties are converted to IdoA by a C-5 epimerase. This is followed by sulfation of the C-2 positions of IdoA and GlcA,^{19,20} C-6 sulfation of GlcN^{21,22} and C-3 sulfation of GlcN, the rarest form of HS/heparin sulfation.^{23,24,25}

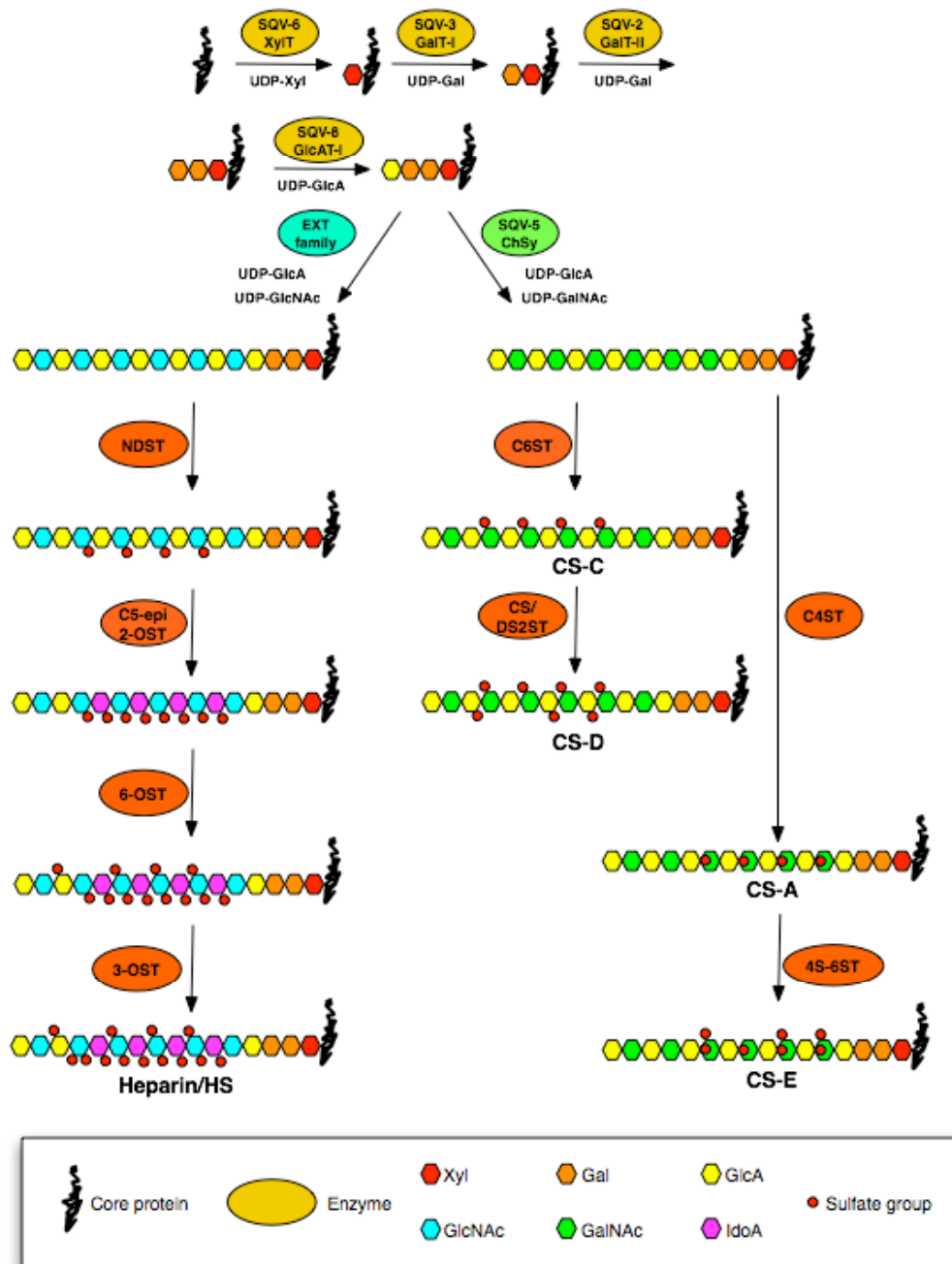


Figure 1.4: The biosynthesis of heparin, heparan sulfate and chondroitin sulfate. SQV enzymes are from *Caenorhabditis elegans*.

HS and heparin have been linked to Alzheimer's disease,²⁶ cancer metastasis,²⁷ entry of herpes simplex virus type I²⁴ and malaria,²⁸ embryonic development,^{29,30} nerve cell communication, and axonal guidance.³⁰⁻³³ Genetic investigations have shown that deletion of the HS and heparin polymerase EXT1 leads to severe defects in mammalian brain morphogenesis, irregular midline axon guidance, and embryonic death in mice, demonstrating the importance of HS and heparin in central nervous system formation.³¹

The fine structures of HS and heparin have been implicated in dictating their protein binding partners and functions *in vivo*.^{11,14} Knockout studies of the HS-modifying enzymes C-5 epimerase, 2-*O*-sulfotransferase and 6-*O*-sulfotransferase in *Caenorhabditis elegans* suggest that some neuron types have a dependence on certain HS motifs and that specific sulfation patterns are necessary for normal growth.³⁴ The chemorepellent protein Slit is involved in axonal guidance, and is dependent on HS to bind to its receptor, Robo, at the tip of axons to repel axonal growth.³³ The specific sulfation sequence needed for the HS to interact with Slit is unknown, but *O*-sulfation is required.³⁵

Two important developmental pathways are regulated by differentially sulfated HS GAGs, Wnt and Hedgehog (Hh) signaling. Disruptions in a *Drosophila* NDST displayed a complete loss of activity in the Wingless (Wg), a Wnt family member, and Hh pathways.³⁶ Mutation of the gene *tout velu*, a gene encoding an HS polymerase, had defective Hh signaling.^{37,38} Recently, an extracellular sulfatase, QSulf1, has been found to remove the 6-*O* sulfates from HS to form a low affinity HS-Wnt complex and promote the interaction of Wnt with its receptor, Frizzled.^{39,40} Interestingly, this suggests that sulfation of HS and heparin is dynamic and remodeling of sulfate groups can occur at the cell surface, not only in the Golgi. The generation of a low affinity HS-Wnt complex

upon sulfate group cleavage and the effects on Wnt signaling in *Drosophila* after the loss of NDST suggest a sulfation pattern dependence for HS-Wnt binding.

The mechanisms through which HS and heparin modulate the events described earlier are not well understood but it has been suggested that HS and heparin form complexes with growth factors and their receptors in a sulfation-dependent manner. The best-studied examples of the importance of sulfation on HS bioactivity and in ligand-receptor complex formation are the fibroblast growth factors (FGFs). The FGFs are a family of proteins involved in morphogenesis, angiogenesis, and development,⁴¹ and crystal structures of HS oligosaccharides with FGF1-FGF receptor 2 (FGFR2)⁴² or FGF2-FGFR1⁴³ demonstrate that HS forms a complex with FGFs and FGFRs to promote signaling. Binding of FGF-1 to its receptor requires both 2-*O*-sulfation and 6-*O*-sulfation, and FGF-2 requires 2-*O*-sulfation but not 6-*O*-sulfation.⁴⁴ As mentioned earlier, isolation of GAGs with defined sulfation is extremely difficult, and the heterogeneous nature of biochemical HS and heparin preparations has hampered attempts to determine the precise sulfation motifs necessary for FGF binding. Without access to defined HS sequences, understanding the roles of sulfation in HS-protein binding is not possible.

Chemical approaches enable synthesis of sulfated oligosaccharides with distinct structures, and thus, systematic investigation of HS-protein binding and bioactivity. The structural requirements for HS recognition of both antithrombin III (ATIII) and FGF-1 have been determined through use of synthetic small molecules. A sulfated HS pentasaccharide synthesized by Choay *et al.* interacted with ATIII to prevent blood coagulation, and led to an understanding of the mechanism of heparin anticoagulant activity (Figure 1.5).⁴⁵

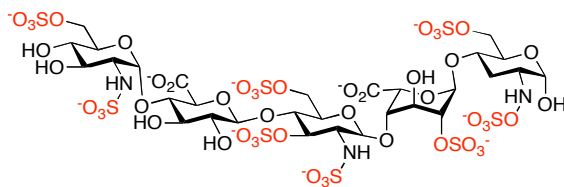


Figure 1.5: Structure of a synthetic HS pentasaccharide with ATIII binding.

Angulo *et al.* performed investigation of FGF-1 binding to HS with a library of synthetic HS hexa- and octasaccharides (Figure 1.6).⁴⁶ Oligosaccharides **1** and **2** display the major sulfation motif found in heparin, and the distribution of the negatively-charged groups is on both sides of the helix adopted by these two molecules. Hexasaccharide **3** has a lower overall charge than **1** or **2** and the sulfate groups are presented on only one face of the helix. The anionic charge of hexasaccharides **4** and **5** is similar to **3**, but the distributions of the sulfate groups are altered. Octasaccharide **2** and hexasaccharide **3** promoted FGF-1-mediated cell proliferation, whereas the other oligosaccharides had poor mitogenic activity. The precise arrangement of sulfate groups appears to be important for the HS-FGF-1 interaction and subtle changes can lead to dramatic effects in the biological properties of HS. These studies with HS small molecules are remarkable as GAG chains are typically hundreds of monosaccharides long, but synthetically accessible pentasaccharide, hexasaccharide, and octasaccharide motifs captured the activities of these long polysaccharides. The ability to understand HS-protein binding and the biological functions of HS with defined, synthetic molecules enables investigation into GAG structure-activity relationships.

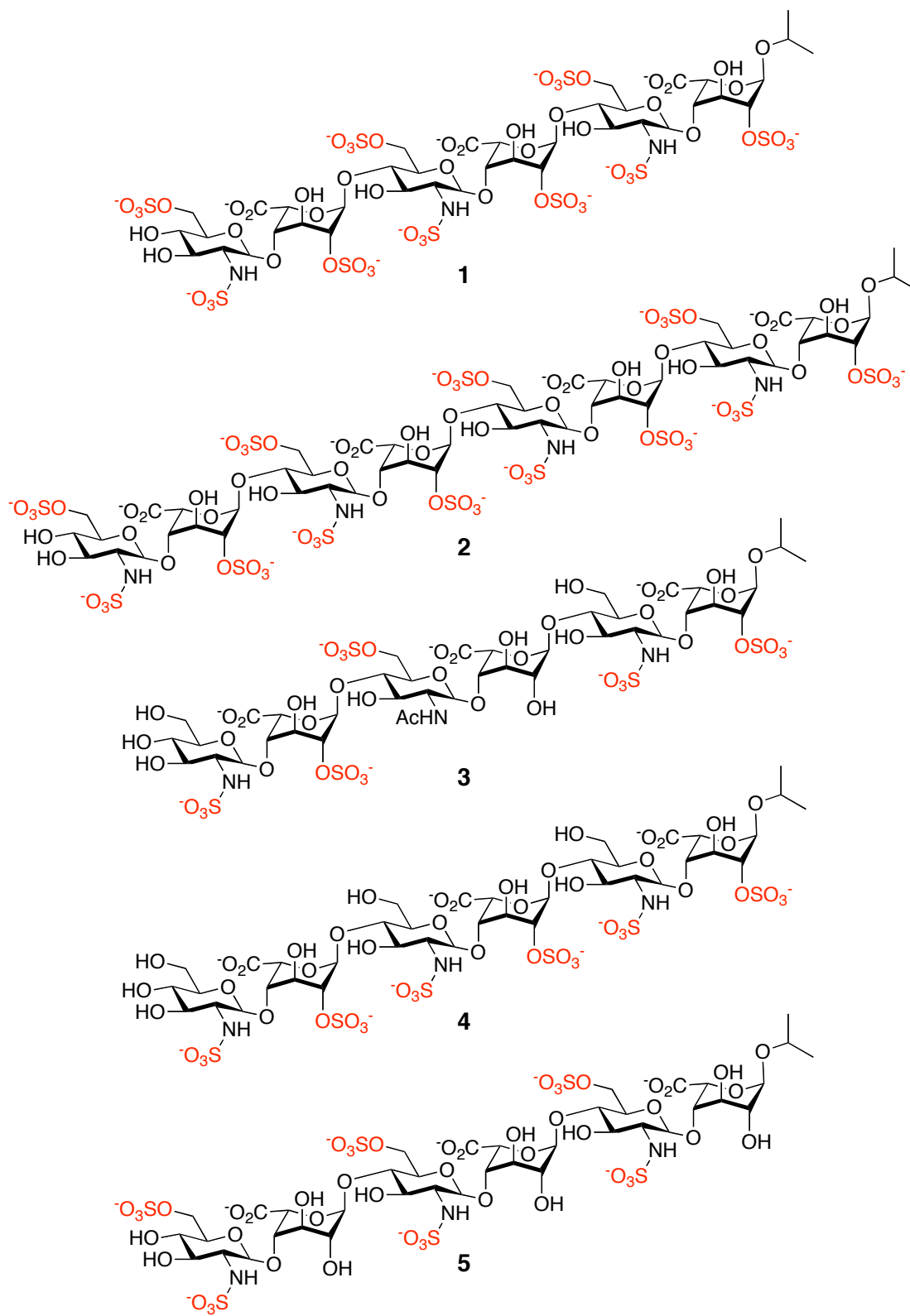


Figure 1.6: Synthetic HS library for FGF-1 binding studies.

Chondroitin sulfate glycosaminoglycans

Historically, research on GAGs has focused on heparin and HS, despite the ubiquitous expression of CS oligosaccharides. CS consists of repeating disaccharide units of GlcA and *N*-acetylgalactosamine (GalNAc) linked through β -(1,3) and (1,4) glycosidic bonds. As described earlier, CS displays a variety of sulfation patterns, and CS polysaccharides can range from 10 to 100 disaccharide units in length.¹

CS GAGs have a non-rigid, helical structure, like HS and heparin, and the presence of different counterions changes the shape of the helix. For example, X-ray crystallographic analysis of a CS-A [GlcA-GalNAc(4-*O*-SO₃⁻)] hexasaccharide in the presence of sodium ions⁴⁷ (Figure 1.7) afforded a tighter helix than a crystal structure of a tetrasaccharide with bulkier calcium ions coordinated (Figure 1.8).⁴⁸ The flexibility of CS allows for multiple protein binding conformations and different sulfate group orientations.

Similar to HS, the biosynthesis of CS begins in the Golgi apparatus and with the placement of the tetrasaccharide linker on specific serine residues (Figure 1.4). GalNAc is the next monomer added and then CS synthases add alternating units of GlcA and GalNAc.^{49,50} Sulfotransferases use PAPS to add sulfate groups to the chains, and there are three major families of CS sulfotransferases: one transfers sulfate groups to the C-4 hydroxyl of GalNAc residues, the second to the C-6 hydroxyls of GalNAc and the last to the C-2 hydroxyls of GlcA units. In total, seven CS sulfotransferases have recently been identified and cloned.² Sulfation of the C-4 GalNAc hydroxyl to afford the pattern called CS-A or the C-6 GalNAc hydroxyl to yield CS-C happens first and these motifs are the most commonly displayed. Additional sulfation of the C-4 sulfated product usually

occurs at the C-6 hydroxyl to generate CS-E, and the C-6 sulfated product is normally modified at the C-2 hydroxyl of GlcA to generate CS-D (Figure 1.9).² The variety of sulfotransferases leads to the generation of multiple sulfation motifs and creates the structural complexity observed in CS GAGs.

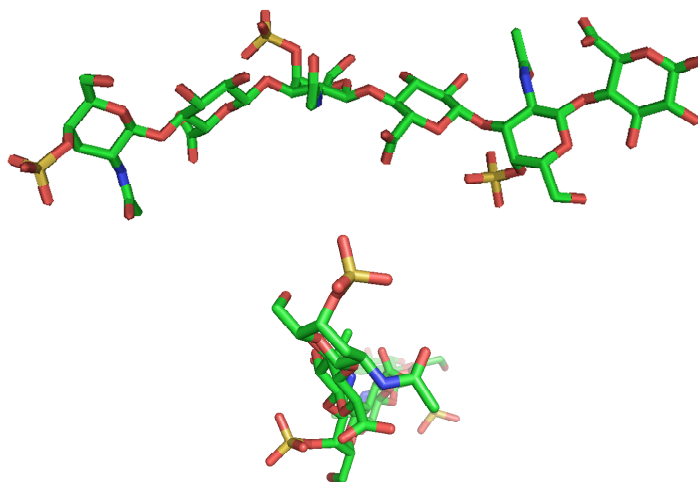


Figure 1.7: X-ray crystal structure of a CS-A hexasaccharide coordinated to sodium ions. The top structure shows the view parallel to the helical axis and the bottom structure the view perpendicular to the helical axis.⁴⁷

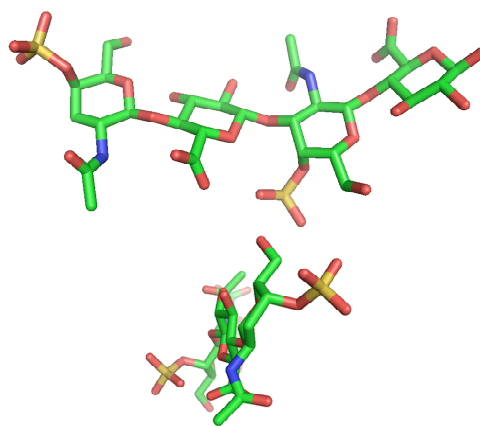


Figure 1.8: X-ray crystal structure of a CS-A tetrasaccharide coordinated to calcium ions. The top structure shows the view parallel to the helical axis and the bottom structure the view perpendicular to the helical axis.⁴⁸

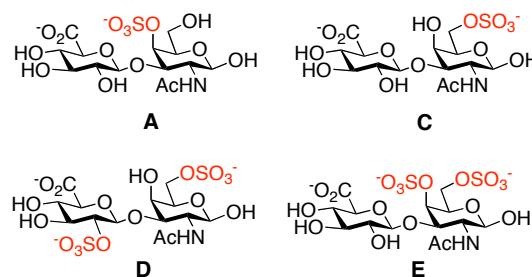


Figure 1.9: The most prevalent chondroitin sulfate sulfation motifs *in vivo*.

CS is important in proper embryonic development and the sulfation motifs presented are carefully regulated during this crucial time. Proper development of the brain is dependent on the regulation of CS chains by chondroitin-4-sulfotransferase and chondroitin-6-sulfotransferase enzymes.¹⁰ RNA-mediated interference of the CS synthase gene of *Caenorhabditis elegans* led to defects in vulval morphogenesis and embryogenesis.⁵¹ Despite the lack of sulfation present on *Caenorhabditis elegans* CS, these studies still show the importance of CS in the embryo. Mice with a mutant form of chondroitin-4-sulfotransferase 1 had severe chondrodysplasia and a disorganized cartilage growth plate resulting in osteoarthritis, demonstrating the necessity of C-4 sulfation and the importance of CS structure in proper cartilage formation.⁵² Knockout mice lacking one of the chondroitin-6-sulfotransferase genes were generated to understand the importance of CS-D sulfation on development but the mice displayed normal growth, yet had decreased numbers of lymphocytes in the spleen.⁵³ Compensation of the loss of the highly sulfated CS-D motif by other highly sulfated motifs (such as CS-E) or by other sulfotransferases may be why a dramatic effect was not observed. In humans, this same deletion led to severe skeletal defects, and the difference between what was detected in mice is unclear.⁵⁴ More knockout models are needed to better

understand the significance of CS and the impact of specific sulfation patterns in the embryo, but these models provide only limited amounts of information. Multiple motifs may be affected by the loss of the sulfotransferase and distinct sulfation types cannot be targeted.

Differentially sulfated CS structures have been implicated in a variety of processes related to disease and injury. For example, *Plasmodium falciparum*, the malarial parasite, has evolved to use CS as a method for cell attachment. Erythrocytes infected by malarial parasites bind to the placenta through a CS-A dodecasaccharide and adversely affect both mother and child. Interestingly, binding is inhibited by the CS-E motif, thus preventing adhesion to the placenta.⁵⁵⁻⁵⁷ In cancer, melanoma chondroitin sulfate proteoglycan is an early cell surface melanoma progression marker that stimulates cancer cell proliferation, migration, and invasion.⁵⁸ The structure of the attached CS chain has not been elucidated but its activity appears to be regulated by sulfation.⁵⁹ CS is the most common component in wound fluid, and binds several factors involved in leukocyte adhesion, including L-selectin, P-selectin, and CD44.^{60,61} The binding appears to be sulfation dependent as L-selectin and P-selectin bind only to motifs enriched in CS-E and CS-B [IdoA-GalNAc(4-*O*-SO₃⁻)], but CD44 is capable of binding all CS sulfation motifs. Versican, a CS proteoglycan (CSPG) containing high amounts of CS-E and CS-B, has been shown to bind to the inflammatory chemokines SLC, IP-10, and SDF-1β.^{61,62}

CS is essential in the development of the central nervous system by regulating axonal growth and pathfinding,^{63,64} and, paradoxically, CS has been described as both growth promoting and inhibitory to neurons. CSPGs can repel migrating neurons or extending axons in brain development or following injury, but tissues that strongly

express CS do not always exclude the entry of axons.^{65,66} During the migration of neural crest cells, the temporal and spatial changes of CSPG expression patterns are inversely correlated with the pathways of the cells, suggesting an inhibitory role.⁶⁷ In contrast, CS has been found in the tracts of developing axons and the CS-E-enriched chains of the proteoglycan phosphacan promote neurite outgrowth of both embryonic rat mesecephalic and hippocampal neurons.^{68,69} A CSPG cannot be simply classified as neurite outgrowth supportive or inhibitory as its spatial and temporal regulation, its interactions with protein ligands, like growth factors, and potentially its sulfation pattern define its properties on neurite outgrowth.

Numerous proteins have been identified as CS binders, and CS fine structure is believed to regulate these recognition events. Through assays with CSPGs and heterogeneous preparations of CS polysaccharides, the neuronal growth factors pleiotrophin, midkine, FGF-2, and FGF-16 were found to interact with CS.⁷⁰⁻⁷² It is unknown if CS molecules form complexes with ligands and their receptors to promote signaling in a manner similar to HS, FGF, and FGFR, and no crystal structures have been reported. Pleiotrophin and midkine are related proteins involved in the promotion of neurite outgrowth, and they both bind to the CS-E-enriched proteoglycan phosphacan and polysaccharides concentrated in CS-E.⁷⁰⁻⁷² Intriguingly, CS-E polysaccharides have been shown to promote the outgrowth of neurons, perhaps through pathways regulated by midkine and pleiotrophin.⁷³ Unfortunately, as with HS and heparin, the heterogeneity of the CS molecules used in the studies described does not allow an understanding of the roles of precise sulfation patterns, making a chemical approach that provides defined

oligosaccharides necessary to determine the biological relevance of different CS sulfation motifs.

Our knowledge of the physiological importance of CS oligosaccharides would be significantly enhanced by an ability to correlate structure with function. As demonstrated with HS, synthetic small molecules can recapitulate the activity of large polysaccharides and bind proteins like ATIII and FGF-1 in a sulfation pattern dependent manner. Synthesis of a library of CS oligosaccharides with differential sulfation would provide access to defined structures not obtainable from natural sources, and allow us to elucidate what impact precise motifs have on ligand binding and the development and function of neurons. It would also enable evaluation of the somewhat contradictory nature of CS GAGs, as they are both neuronal growth inhibitory and stimulatory. Such detailed structure-function analyses have not yet been performed for CS and are needed to fully understand its activities. This thesis describes our approach to a synthetic library of CSs, identification of the biologically relevant motifs, and determination of the roles of specific CS motifs in neuronal development and function.

References

1. Gama, C.I. & Hsieh-Wilson, L.C. (2005). Chemical approaches to deciphering the glycosaminoglycan code. *Curr. Opin. Chem. Biol.* **9**, 609-619.
2. Kursche-Gullberg, M. & Kjellen, L. (2003). Sulfotransferases in glycosaminoglycan biosynthesis. *Curr. Opin. Struct. Biol.* **5**, 605-611.
3. Small, D.H., Mok, S.S., Williamson, T.G. & Nurcombe, V. (1996). Role of proteoglycans in neural development, regeneration, and the aging brain. *J. Neurochem.* **67**, 889-899.
4. Krishna, N.R. & Agrawal, P.K. (2001). Molecular structure of the carbohydrate-protein linkage region fragments from connective-tissue proteoglycans. *Adv. in Carbohydr. Chem. and Biochem.* **56**, 201-234.
5. Bandtlow, C.E. & Zimmerman, D.R. (2000). Proteoglycans in the developing brain: new conceptual insights for old proteins. *Physiological Rev.* **80**, 1267-1290.
6. Matsui, F., Nishizuka, M. & Oohira, A. (1999). Proteoglycans in perineuronal nets. *Acta Histochem. Cytochem.* **32**, 141-147.
7. Snow, D.M. (1994). Neurite outgrowth in response to patterns of chondroitin sulfate proteoglycan: inhibition and adaptation. *Neuroprotocols* **4**, 146-157.
8. Lyon, M. & Gallagher, J.T. (1998). Bio-specific sequences and domains in heparan sulphate and the regulation of cell growth and adhesion. *Matrix Biol.* **17**, 485-493.
9. Carey, D.J. (1997). Syndecans: multifunctional cell-surface co-receptors. *Biochem. J.* **327**, 1-16.

10. Kitagawa, H., Tsutsumi, K., Tone, Y. & Sugahara, K. (1997). Developmental regulation of the sulfation profile of chondroitin sulfate chains in the chicken embryo brain. *J. Biol. Chem.* **272**, 31377-31381.
11. Capila, I. & Linhardt, R.J. (2002). Heparin-protein interactions. *Angew. Chem. Int. Ed. Engl.* **41**, 391-412.
12. Mulloy, B., Forster, M.J., Jones, C. & Davies, D.B. (1993). NMR and molecular-modelling studies of the solution conformation of heparin. *Biochem. J.* **293**, 849-858.
13. Das, S.K., Mallet, J.M., Esnault, J., Driguez, P.A., Duchaussoy, P., Sizun, P., Hérault, J.P., Herbert, J.M., Petitou, M. & Sinay, P. (2001). Synthesis of conformationally locked carbohydrates: a skew-boat conformation of L-iduronic acid governs the antithrombotic activity of heparin. *Angew. Chem. Int. Ed. Engl.* **40**, 1670-1673.
14. Esko, J.D. & Selleck, S.B. (2002). Order out of chaos: assembly of ligand binding sites in heparan sulfate. *Annu. Rev. Biochem.* **71**, 435-471.
15. Sugahara, K. & Kitagawa, H. (2000). Recent advances in the study of the biosynthesis and functions of sulfated glycosaminoglycans. *Curr. Opin. Struct. Biol.* **10**, 518-527.
16. Silbert, J.E. & Sugumaran, G. (2002). Biosynthesis of chondroitin/dermatan sulfate. *IUBMB Life* **54**, 177-186.
17. Grobe, K., Ledin, J., Ringvall, M., Holmborn, K., Forsberg, E., Esko, J.D., & Kjellen, L. (2002). Heparan sulfate and development: differential roles of the *N*-

- acetylglucosamine *N*-deacetylase/*N*-sulfotransferase isozymes. *Biochim. Biophys. Acta.* **1573**, 209-215.
18. Grobe, K. & Esko, J.D. (2002). Regulated translation of heparan sulfate GlcNAc *N*-deacetylase/*N*-sulfotransferase isozymes by structured 5'-untranslated regions and internal ribosome entry sites. *J. Biol. Chem.* **277**, 30699-30706.
19. Rong, J., Habuchi, H., Kimata, K., Lindahl, U. & Kusche-Gullberg, M. (2001). Substrate specificity of the heparan sulfate hexuronic acid 2-*O*-sulfotransferase. *Biochemistry* **40**, 5548-5555.
20. Merry, C.L. & Wilson, V.A. (2002). Role of heparan sulfate-2-*O*-sulfotransferase in the mouse. *Biochim. Biophys. Acta.* **1573**, 319-327.
21. Habuchi, H., Tanaka, M., Habuchi, O., Yoshida, K., Suzuki, H., Ban, K. & Kimata, K. (2000). The occurrence of three isoforms of heparan sulfate 6-*O*-sulfotransferase having different specificities for hexuronic acid adjacent to the targeted *N*-sulfoglucosamine. *J. Biol. Chem.* **275**, 2859-2868.
22. Smeds, E., Habuchi, H., Do, A.T., Hjertson, E., Grundberg, H., Kimata, K., Lindahl, U. & Kusche-Gullberg, M. (2003). Substrate specificities of mouse heparan sulphate glucosaminyl 6-*O*-sulphotransferases. *Biochem. J.* **372**, 371-380.
23. Shworak, N.W., Liu, J., Petros, L.M., Zhang, L., Kobayashi, M., Copeland, N.G., Jenkins, N.A. & Rosenberg, R.D. (1999). Multiple isoforms of heparan sulfate D-glucosaminyl 3-*O*-sulfotransferase. Isolation, characterization, and expression of human cDNAs and identification of distinct genomic loci. *J. Biol. Chem.* **274**, 5170-5184.

24. Xia, G., Chen, J., Tiwari, V., Ju, W., Li, J.P., Malmstrom, A., Shukla, D. & Liu, J. (2002). Heparan sulfate 3-*O*-sulfotransferase isoform 5 generates both an antithrombin-binding site and an entry receptor for herpes simplex virus, type 1. *J. Biol. Chem.* **277**, 37912-37919.
25. Mochizuki, H., Yoshida, K., Gotoh, M., Sugioka, S., Kikuchi, N., Kwon, Y.D., Tawada, A., Maeyama, K., Inaba, N., Hiruma, T., Kimata, K. & Narimatsu, H. (2003). Characterization of a heparan sulfate 3-*O*-sulfotransferase-5, an enzyme synthesizing a tetrasulfated disaccharide. *J. Biol. Chem.* **278**, 26780-26787.
26. van Horsen, J., Wesseling, P., van den Heuvel, L.P., de Waal, R.M. & Verbeek, M.M. (2003). Heparan sulphate proteoglycans in Alzheimer's disease and amyloid-related disorders. *Lancet Neurol.* **2**, 482-492.
27. Sasisekharan, R., Shriver, Z., Venkataraman, G. & Narayanasami, U. (2002). Roles of heparan-sulphate glycosaminoglycans in cancer. *Nat. Rev.* **2**, 521-528.
28. Vogt, A.M., Winter, G., Wahlgren, M. & Spillmann, D. (2004). Heparan sulphate identified on human erythrocytes: a *Plasmodium falciparum* receptor. *Biochem. J.* **381**, 593-597.
29. Perrimon, N. & Bernfield, M. (2000). Specificities of heparan sulphate proteoglycans in developmental processes. *Nature* **404**, 725-728.
30. Bernfield, M., Gotte, M., Park, P.W., Reizes, O., Fitzgerald, M.L., Lincecum, J. & Zako, M. (1999). Functions of cell surface heparan sulfate proteoglycans. *Ann. Rev. Biochem.* **68**, 729-777.

31. Inatani, M., Irie, F., Plump, A.S., Tessier-Lavigne, M. & Yamaguchi, Y. (2003). Mammalian brain morphogenesis and midline axon guidance require heparan sulfate. *Science* **302**, 1044-1046.
32. Yamaguchi, Y. (1998). Heparan sulfate proteoglycans in neural development. *Trends Glycosci. Glycotech.* **10**, 161-173.
33. Hu, H. (2001). Cell-surface heparan sulfate is involved in the repulsive guidance activities of Slit2 protein. *Nat. Neurosci.* **4**, 695-701.
34. Bulow, H.E. & Hobert, O. (2004). Differential sulfations and epimerization define heparan sulfate specificity in nervous system development. *Neuron* **41**, 723-736.
35. Ronca, F., Andersen, J.S., Paech, V. & Margolis, R.U. (2001). Characterization of Slit protein interactions with glypican-1. *J. Biol. Chem.* **276**, 29141-29147.
36. Lin, X. & Perrimon, N. (1999). Dally cooperates with *Drosophila* Frizzled 2 to transduce Wingless signaling. *Nature* **400**, 281-284.
37. Bellaïche, Y., The, I. & Perrimon, N. (1998). Tout-velu is a *Drosophila* homologue of the putative tumour suppressor EXT-1 and is needed for Hh diffusion. *Nature* **394**, 85-88.
38. The, I., Bellaïche, Y. & Perrimon, N. (1999). Evidence that heparan sulfate proteoglycans are involved in the movement of Hedgehog molecules through fields of cells. *Mol. Cell* **4**, 633-639.
39. Dhoot, G.K., Gustafsson, M.K., Ai, X., Sun, W., Standiford, D.M. & Emerson Jr., C.P. (2001). Regulation of Wnt signaling and embryo patterning by an extracellular sulfatase. *Science* **293**, 1663-1666.

40. Ai, X., Do, A.T., Lozynska, O., Kusche-Gullberg, M., Lindahl, U. & Emerson Jr., C.P. (2003). QSulf remodels the 6-O sulfation states of cell surface heparan sulfate proteoglycans to promote Wnt signaling. *J. Cell Biol.* **162**, 341-351.
41. Ornitz, D.M. & Itoh, N. (2001). Fibroblast growth factors. *Genome Biol.* **2**, 1-12.
42. Pellegrini, L., Burke, D.F., von Delft, F., Mulloy, B. & Blundell, T.L. (2000). Crystal structure of fibroblast growth factor receptor ectodomain bound to ligand and heparin. *Nature* **407**, 1029-1034.
43. Schlessinger, J., Plotnikov, A.N., Ibrahimi, O.A., Eliseenkova, A.V., Yeh, B.K., Yayon, A. & Linhardt, R.J. (2000). Crystal structure of a ternary FGF-FGFR-heparin complex reveals a dual role for heparin in FGFR binding and dimerization. *Mol. Cell* **6**, 743-750.
44. Ostrovsky, O., Berman, B., Gallagher, J., Mulloy, B., Fernig, D.G., Delehede, M. & Ron, D. (2002). Differential effects of heparin saccharides on the formation of specific fibroblast growth factor (FGF) and FGF receptor complexes. *J. Biol. Chem.* **277**, 2444-2453.
45. Choay, J., Petitou, M., Lormeau, J.C., Sinay, P., Casu, B. & Gatti, G. (1983). Structure-activity relationship in heparin: a synthetic pentasaccharide with high affinity for anti-thrombin-III and eliciting high anti-factor Xa activity. *Biochem. Biophys. Res.* **116**, 492-499.
46. Angulo, J., Ojeda, R., de Paz, J.L., Lucas, R., Nieto, P.M., Lozano, R.M., Redondo-Horcajo, M., Gimenez-Gallego, G. & Martin-Lomas, M. (2004). The activation of fibroblast growth factors (FGFs) by glycosaminoglycans: influence of the sulfation pattern on the biological activity of FGF-1. **5**, 55-61.

47. Winter, W.T., Arnott, S., Isaac, D.H. & Atkins, E.D.T. (1978). Chondroitin 4-sulfate: the structure of a sulfated glycosaminoglycan. *J. Mol. Biol.* **125**, 1-19.
48. Cael, J.J., Winter, W.T. & Arnott, S. (1978). Calcium chondroitin 4-sulfate: molecular conformation and organization of polysaccharide chains in a proteoglycan. *J. Mol. Biol.* **125**, 21-42.
49. Kitagawa, H., Uyama, T. & Sugahara, K. (2001). Molecular cloning and expression of a human chondroitin synthase. *J. Biol. Chem.* **276**, 38721-38726.
50. Yada, T., Gotoh, M., Sato, T., Shionyu, M., Go, M., Kaseyama, H., Iwasaki, H., Kikuchi, N., Kwon, Y.D., Togayachi, A., Kudo, T., Watanabe, H., Narimatsu, H. & Kimata, K. (2003). Chondroitin sulfate synthase 2: molecular cloning and characterization of a novel human glycosyltransferase homologous to chondroitin sulfate glucuronyltransferase, which has dual enzymatic activities. *J. Biol. Chem.* **278**, 30235-30247.
51. Hwang, H.Y., Olson, S.K., Esko, J.D. & Horvitz, H.R. (2003). *Caenorhabditis elegans* early embryogenesis and vulval morphogenesis require chondroitin biosynthesis. *Nature* **423**, 439-443.
52. Kluppel, M., Wight, T.N., Chan, C., Hinek, A. & Wrana, J.L. (2005). Maintenance of chondroitin sulfation balance by chondroitin-4-sulfotransferase 1 is required for chondrocyte development and growth factor signaling during cartilage morphogenesis. *Development* **132**, 3989-4003.
53. Uchimura, K., Kadomatsu, K., Nishimura, H., Muramatsu, H., Nakamura, E., Kurosawa, N., Habuchi, O., El-Fasakhany, F.M., Yoshikai, Y. & Muramatsu, T. (2002). Functional analysis of the chondroitin 6-sulfotransferase gene in relation

- to lymphocyte subpopulations, brain development, and oversulfated chondroitin sulfates. *J. Biol. Chem.* **277**, 1443-1450.
54. Thiele, H., Sakano, M., Kitagawa, H., Sugahara, K., Rajab, A., Hohne, W., Ritter, H., Leschik, G., Nurnberg, P. & Mundlos, S. (2004). Loss of chondroitin 6-*O*-sulfotransferase-1 function results in severe human chondrodysplasia with progressive spinal involvement. *Proc. Natl. Acad. Sci. USA* **101**, 10155-10160.
55. Gamain, B., Gratepanche, S., Miller, L.H. & Baruch, D.I. (2002). Molecular basis for the dichotomy in *Plasmodium falciparum* adhesion to CD36 and chondroitin sulfate A. *Proc. Natl. Acad. Sci. USA* **99**, 10020-10024.
56. Achur, R.N., Valiyaveetil, M. & Gowda, D.C. (2003). The low sulfated chondroitin sulfate proteoglycans of human placenta have sulfate group-clustered domains that can efficiently bind *Plasmodium falciparum*-infected erythrocytes. *J. Biol. Chem.* **278**, 11705-11713.
57. Chai, W., Beeson, J.G. & Lawson, A.M. (2002). The structural motif in chondroitin sulfate for adhesion of *Plasmodium falciparum*-infected erythrocytes comprises disaccharide units of 4-*O*-sulfated and non-sulfated *N*-acetylgalactosamine linked to glucuronic acid. *J. Biol. Chem.* **277**, 22438-22446.
58. Yang, J., Price, M.A., Neudauer, C.L., Wilson, C., Ferrone, S., Xia, H., Iida, J., Simpson, M.A. & McCarthy, J.B. (2004). Melanoma chondroitin sulfate proteoglycans enhances FAK and ERK activation by distinct mechanisms. *J. Cell Biol.* **165**, 881-891.
59. Heredia, A., Villena, J., Romaris, M., Molist, A. & Bassols, A. (1996). Transforming growth factor beta 1 increases the synthesis and shedding of the

- melanoma-specific proteoglycan in human melanoma cells. *Arch. Biochem. Biophys.* **333**, 198-206.
60. Taylor, K.R & Gallo, R.L (2006). Glycosaminoglycans and their proteoglycans: host-associated molecular patterns for initiation and modulation of inflammation. *FASEB J.* **20**, 9-22.
61. Kawashima, H., Hirose, M., Hirose, J., Nagakubo, D., Plaas, A.H. & Miyasaka, M. (2000). Binding of a large chondroitin sulfate/dermatan sulfate proteoglycan, versican, to L-selectin, P-selectin, and CD44. *J. Biol. Chem.* **275**, 35448-35456.
62. Kawashima, H., Atarashi, K., Hirose, M., Hirose, J., Yamada, S., Sugahara, K. & Miyasaka, M. (2002). Oversulfated chondroitin/dermatan sulfates containing GlcAbeta1/IdoAalpha1-3GalNAc(4,6-O-disulfate) interact with L- and P-selectin and chemokines. *J. Biol. Chem.* **277**, 12921-12930.
63. Morgenstern, D.A., Asher, R.A. & Fawcett, J.W. (2002). Chondroitin sulphate proteoglycans in the CNS injury response. *Prog. Brain Res.* **137**, 313-332.
64. Ichijo, H. (2004). Proteoglycans as cues for axonal guidance in formation of retinotectal or retinocollicular projections. *Mol. Neurobiol.* **30**, 23-33.
65. Bradbury, E.J., Moon, L.D., Popat, R.J., King, V.R., Bennett, G.S., Patel, P.N., Fawcett, J.W. & McMahon, S.B. (2002). Chondroitinase ABC promotes functional recovery after spinal cord injury. *Nature* **416**, 636-640.
66. Emerling, D.E. & Lander, A.D. (1996). Inhibitors and promoters of thalamic neuron adhesion and outgrowth in embryonic neocortex: functional association with chondroitin sulfate. *Neuron* **17**, 1089-1100.

67. Kubota, Y., Morita, T., Kusakabe, M., Sakakura, T. & Ito, K. (1999). Spatial and temporal changes in chondroitin sulfate distribution in the sclerotome play an essential role in the formation of migration patterns of mouse neural crest cells. *Dev. Dyn.* **214**, 55-65.
68. Fernaud-Espinosa, I., Nieto-Sampedro, M. & Bovolenta, P. Developmental distribution of glycosaminoglycans in embryonic rat brain: relationship to axonal tract formation. (1996). *J. Neurobiol.* **30**, 410-424.
69. Clement, A.M., Nadanaka, S., Masayama, K., Mandl, C., Sugahara, K. & Faissner, A. (1998). The DSD-1 carbohydrate epitope depends on sulfation, correlates with chondroitin sulfate D motifs, and is sufficient to promote neurite outgrowth. *J. Biol. Chem.* **273**, 28444-28453.
70. Deepa, S.S., Umehara, Y., Higashiyama, S., Itoh, N. & Sugahara, K. (2002). Specific molecular interactions of oversulfated chondroitin sulfate E with various heparin-binding growth factors. Implications as a physiological binding partner in the brain and other tissues. *J. Biol. Chem.* **277**, 43707-43716.
71. Zou, K., Muramatsu, H., Ikematsu, S., Sakuma, S., Salama, R.H., Shinomura, T., Kimata, K. & Muramatsu, T. (2000). A heparin-binding growth factor, midkine, binds to a chondroitin sulfate proteoglycan, PG-M/versican. *Eur. J. Biochem.* **267**, 4046-4053.
72. Maeda, N., Nishiwaki, T., Shintani, T., Hamanaka, H. & Noda, M. (1996). 6B4 proteoglycan/phosphacan, an extracellular variant of receptor-like protein-tyrosine phosphatase zeta/RPTPbeta, binds pleiotrophin/heparin-binding growth-associated molecule (HB-GAM). *J. Biol. Chem.* **271**, 21446-21452.

73. Clement, A.M., Sugahara, K. & Faissner, A. (1999). Chondroitin sulfate E promotes neurite outgrowth of rat embryonic day 18 hippocampal neurons. *Neurosci. Lett.* **269**, 125-128.

Chapter 2: Chemical Synthesis of Chondroitin Sulfate Oligosaccharides

Chondroitin sulfate glycosaminoglycans

Chondroitin sulfate (CS) glycosaminoglycans (GAGs) are highly sulfated sugars composed of the repeating β -linked disaccharide unit *N*-acetylgalactosamine (GalNAc) and glucuronic acid (GlcA, Figure 2.1). On the cell surface and in the extracellular matrix, CS chains can be hundreds of monosaccharide units long, display multiple sulfation patterns, and are attached to proteoglycan core proteins via serine residues. Together, CS chains and their associated core proteins have been proposed to recruit protein ligands, such as growth factors and cytokines, to the cell surface and may act as templates to bring ligands and their corresponding receptors into the optimal alignment for productive binding.^{1,2,3} CS proteoglycans (CSPGs) modulate cell-cell and cell-matrix interactions, contribute to the maintenance of normal tissue architecture and function, and

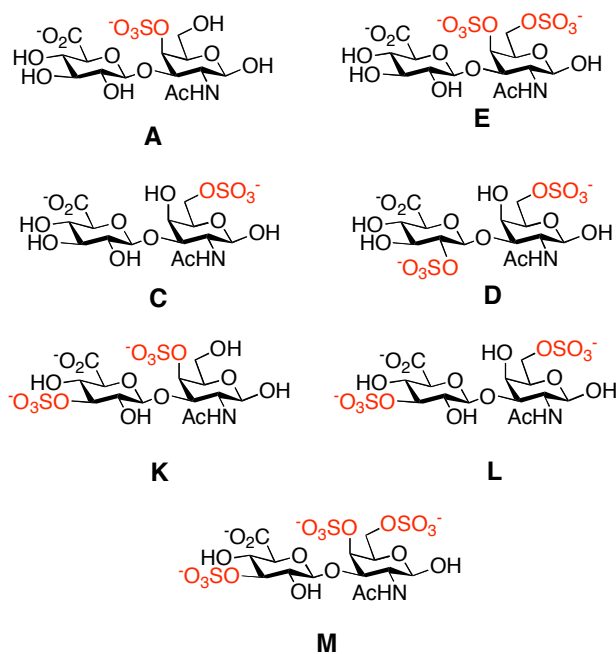


Figure 2.1: Known chondroitin sulfate disaccharides. Ac = acetyl.

participate in cell adhesion and growth control.⁴⁻⁸ The sulfation patterns of CSPGs are highly regulated, differentially expressed in distinct tissues⁹ and they potentially dictate the proteins a proteoglycan can bind.

While CS binds growth factors and potentially regulates cell surface interactions,¹⁰ the importance of specific sulfation motifs in modulating binding and the impact of distinct patterns on chondroitin sulfate bioactivity are unclear. Interest has grown in elucidating how sulfation directs recognition events and affects the functions of CS *in vivo*. An understanding of the physiological role of chondroitin sulfate (CS) oligosaccharides would be significantly enhanced by an ability to correlate structure with function. Although several strategies have been developed, there are currently no methods to systematically explore the role of specific sulfation sequences. For instance, genetic approaches that target a sulfotransferase gene perturb multiple sulfation patterns throughout the polysaccharide chain and cannot be used to study the impact of a single structural motif.^{11,12} Biochemical methods afford a mixture of heterogeneously sulfated compounds of poorly defined linear sequence,¹³ thereby complicating efforts to relate a biological function to a specific sulfation sequence.

Chemical synthesis and chemoenzymatic synthesis of GAGs provide access to well-defined structures for biological evaluation. While investigations into the chemoenzymatic synthesis of CS have not been pursued until recently as not all of the enzymes involved are fully characterized,¹⁴ carbohydrate chemists have used chemical synthesis to generate CS disaccharides,¹⁵⁻²⁰ trisaccharides,^{20,21} tetrasaccharides,^{20,22,23} pentasaccharides,²⁴ and hexasaccharides,^{22,25} but the bioactivities of these molecules have not yet been described.

We reasoned that the combination of chemical synthesis and systematic biological studies would advance an understanding of the physiological roles of CS. As shown with synthetic heparan sulfate small molecules (see Chapter 1), slight changes in sulfation can have dramatic effects on protein interactions and the cellular response to HS.^{26,27} A library of synthetic CS oligosaccharides with precise sulfation motifs should provide crucial information regarding the possible existence of a “sulfation code” for CS, where distinct sulfation sequences have specific protein-binding and neurobiological properties. Our studies would be the first reported to use defined CS small molecules for biological evaluation.

Chemical synthesis of chondroitin sulfate oligosaccharides

Unlike for DNA and peptides, no general synthetic method exists for the synthesis of carbohydrates. Selective protection and deprotection of hydroxyl protecting groups and generation of glycosidic linkages at different positions along the carbohydrate ring makes development of a general method for carbohydrate synthesis difficult.²⁸ Due to their high degree of functionality, the synthesis of CS glycosaminoglycans is challenging and lengthy, with more than 40 chemical steps required for a single oligosaccharide.²⁹ To be practical for biological studies, a modular, efficient approach must be designed to minimize the number of steps and afford sufficient quantities of oligosaccharides for analysis. Construction of CS necessitates stereospecific formation of β -glycosidic linkages, the use of uronic acid donors or acceptors of low reactivity, and regiospecific functionalization of hydroxyl groups of comparable reactivity to install distinct sulfation sequences. Protecting group strategies must be carefully selected as they determine not

only the pattern of sulfation, but also the reactivities of the glycosyl donor and acceptor. Slight changes in protecting groups have been reported to lead to dramatic changes in the stereochemistry and yield of the glycosidic bond formed.³⁰

CS is composed of two types of glycosidic linkages, the $\beta(1,4)$ -linkage between the C-4 hydroxyl of GlcA and GalNAc, and the $\beta(1,3)$ -linkage between the C-3 hydroxyl of GalNAc and GlcA (Figure 2.2). As the $\beta(1,4)$ -linkage is the more hindered and difficult to form a glycosidic bond, it is usually generated at the disaccharide formation stage of the synthesis and then the $\beta(1,3)$ -linkage is formed to make larger oligosaccharides. The C-4 hydroxyl also can have reduced nucleophilicity during coupling due to the electron-withdrawing nature of the C-5 ester present on the GlcA monomer. As a result, oxidation of the C-6 hydroxyl group is often performed after the coupling reaction, though oxidation can be difficult on larger substrates. For the synthesis of CS oligosaccharides, Koenigs-Knorr glycosylation using glycosyl bromides¹⁵ and Schmidt's trichloroacetimidate method^{26,27} (Figure 2.3) have been the conventional methods for generating glycosidic linkages. Trichloroacetamides are very active and these donors compensate for the less reactive oxidized GlcA monomer.

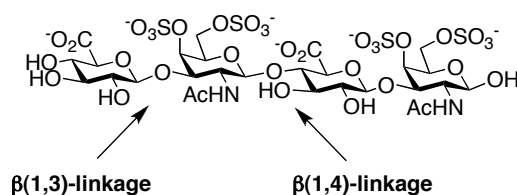


Figure 2.2: Structure of a CS-E tetrasaccharide.

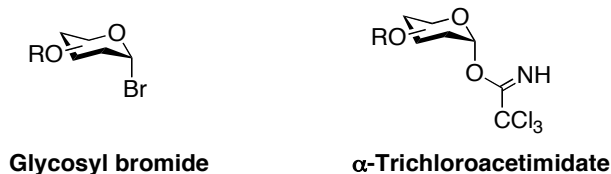
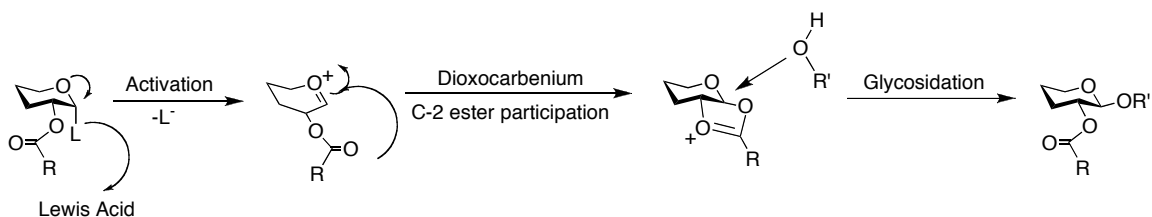
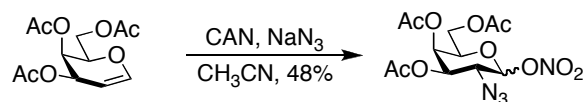


Figure 2.3: The structures of donors used in CS synthesis.

All of the linkages in CS are β -glycosidic linkages, so a neighboring participating group at the C-2 position is commonly used to direct the stereochemistry during the coupling reaction (Scheme 2.1).²² The C-2 position of the GlcA monomer is usually protected with an ester protecting group, such as a benzoyl or an acetyl. Unfortunately, the *N*-acetyl group present on the C-2 position of the GalNAc residues in the final molecules is a poor participating group during coupling reactions, so the amine of the GalNAc donor is typically masked as an azide or with a protecting group like trichloroacetyl. While azides are not participating groups, β -linkages have been successfully generated using α -trichloroacetimidate donors containing C-2 azides.²⁰ C-2 azides are quite common at some stage of most CS syntheses and they are readily accessed through an azidonitration reaction of tri-*O*-acetylgalactal (Scheme 2.2).^{15,19,20,31} The expense of galactosamine inhibits its ability to be an accessible starting material for the synthesis of CS.



Scheme 2.1: Activation of donors with C-2 participating groups.



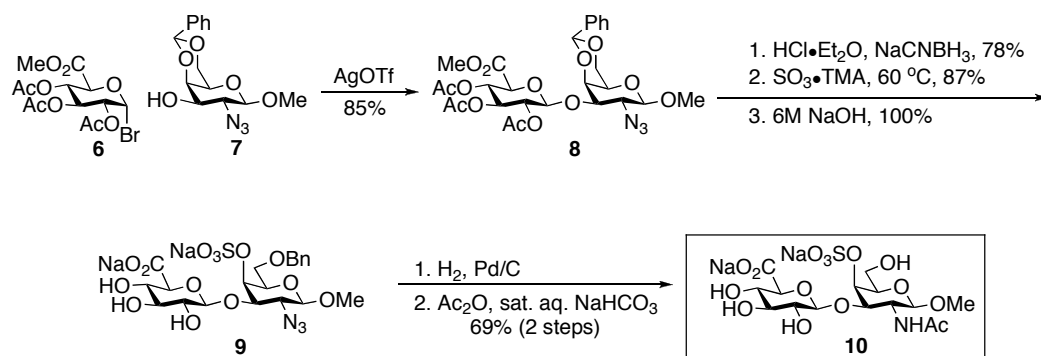
Scheme 2.2: Azidonitration of tri-*O*-acetylgalactal with cerium ammonium nitrate and sodium azide.

One of the most challenging tasks in the synthesis of CS glycosaminoglycans is the development of an orthogonal protecting group strategy. Protecting groups chosen for the synthesis must withstand acidic coupling conditions and harsh, sometimes acidic sulfation reactions. Early CS syntheses utilized benzyl and acetate protecting groups,¹⁵ because these groups do not tend to negatively affect the reactivities of the donor and acceptor. Ester protecting groups larger than acetates, such as benzoyl, are electron withdrawing and can decrease coupling reaction yields when present on either the donor or acceptor. One problem with acetyl groups is that they can readily migrate around the carbohydrate ring under basic conditions.³⁰ For this reason, the repertory of protecting groups for CS synthesis has been expanded. Benzylidene rings, benzoyl esters, *p*-methoxybenzyl groups, silyl ethers, pivalate esters, and levulinoyl esters are some of the protecting groups successfully used in CS syntheses.¹⁶⁻²⁵ The deactivating nature of the larger ester groups is compensated by their stability. The protecting group present at the reducing end sugar must also be carefully chosen, as this group has to mimic the native carbohydrate. CS oligosaccharides lacking a protecting group at this position are difficult to characterize because anomerization complicates NMR analysis. The methyl group is a commonly used group at the reducing end due to its small size, but it can only be cleaved with acid hydrolysis, and therefore cannot be readily removed from the oligosaccharide.^{15,16}

The presence of sulfate esters on the final CS product adds complexity to the synthesis since sulfate groups are both acid and base sensitive, and decrease the solubility of the CS oligosaccharide in organic solvents. For these reasons, sulfation generally occurs at the end of the synthesis.

Sinäy's approach to a CS-A disaccharide

The first synthesis of a CS disaccharide was reported in 1989 by Marra *et al.*¹⁵ (Scheme 2.3). Glycosyl bromide **6**, synthesized in 3 steps from D-glucurono-6,3-lactone, was coupled to glycosyl acceptor **7**, synthesized in 3 steps from tri-*O*-acetylgalactal, in the presence of silver triflate to provide the desired β -disaccharide in 85% yield. The disaccharide was further elaborated by a regioselective benzylidene ring opening to provide the free C-4 hydroxyl group in 78% yield, which was then sulfonated with sulfur trioxide-trimethylamine. Deprotection of the benzyl ethers and reduction of the azide to the amine was performed using H₂ and palladium on carbon. The resulting amine was acetylated to yield the final CS-A disaccharide **10**. While this route could provide access to other CS sulfation patterns such as CS-E and potentially CS-C, the presence of a methyl group at the reducing end prevents further elongation of the oligosaccharide because acid cleavage of this group would also lead to removal of the benzylidene ring.

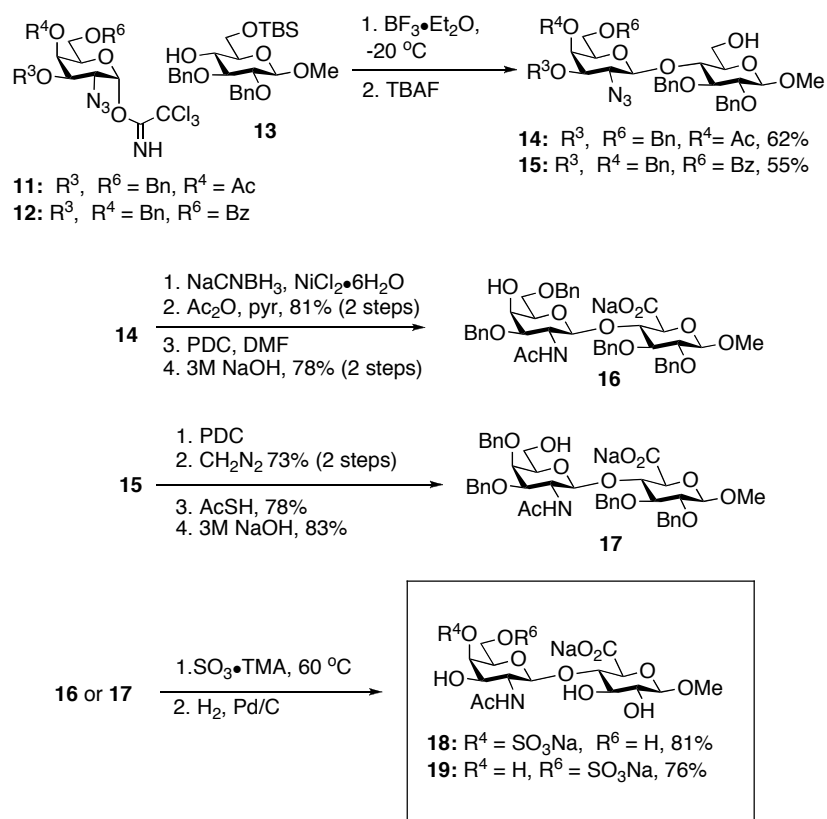


Scheme 2.3: The first synthesis of a CS-A disaccharide by Marra and Sinäy. Ph = phenyl, Ac = acetyl, Me = methyl, TMA = trimethylamine, Tf = trifluoromethanesulfonate, Bn = benzyl.

Jacquet's approach to CS-A and CS-C disaccharides

In 1990, the Jacquet group developed syntheses of $\beta(1,4)$ -linked CS disaccharides (Scheme 2.4).¹⁹ This more sterically hindered linkage can be difficult to generate and the reactive α -glycosyl trichloroacetimidate group was exploited to construct it. With non-participating groups at C-2 and treatment with $\text{BF}_3 \cdot \text{OEt}_2$ at low temperature, α -glycosyl trichloroacetimidates undergo inversion at the anomeric center to give β -linked products.³² Glycosyl imidates **11** and **12** were synthesized from galactal (6 steps for **11** and 5 steps for **12**) and reacted with **13** in the presence of $\text{BF}_3 \cdot \text{OEt}_2$ followed by tetrabutylammonium fluoride (TBAF) cleavage of the 6-*O*-silyl ether to afford **14** and **15** in 62% and 55% yields, respectively. The modest yields demonstrate the challenge associated with formation of the $\beta(1,4)$ -linkage and generation of the α -disaccharide when using a non-participating group at the C-2 position. Elaboration of **14** and **15** led to formation of CS-A disaccharide **18** and CS-C disaccharide **19**. As with the previous synthesis, production of longer oligosaccharides would be difficult due to the methyl protecting group at the reducing end position. In addition, multiple sulfation patterns cannot be generated from one disaccharide. Two disaccharides must be synthesized and

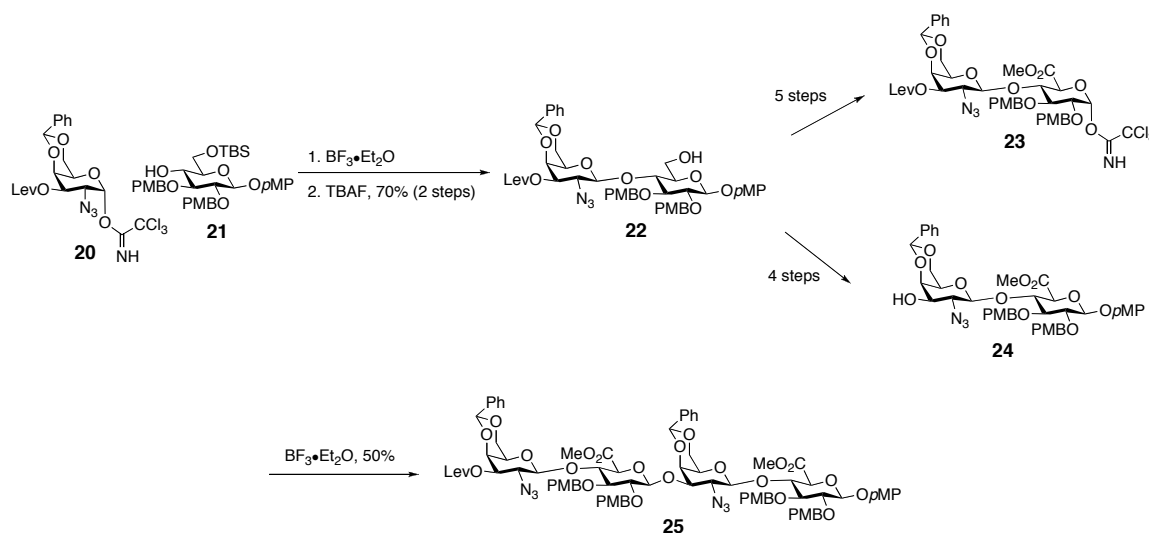
two GalNAc monomers, making synthesis of large amounts of the CS oligosaccharides tedious and more challenging.



Scheme 2.4: Jacquinet's synthesis of CS-A and CS-C disaccharides. Bn = benzyl, Bz = benzoyl, Ac = acetyl, TBS = *t*-butyldimethylsilyl, TBAF = tetrabutylammonium fluoride, PDC = pyridinium dichromate, TMA = trimethylamine, Me = methyl.

Ogawa's synthesis of CS-A, CS-C, and CS-E tetrasaccharides

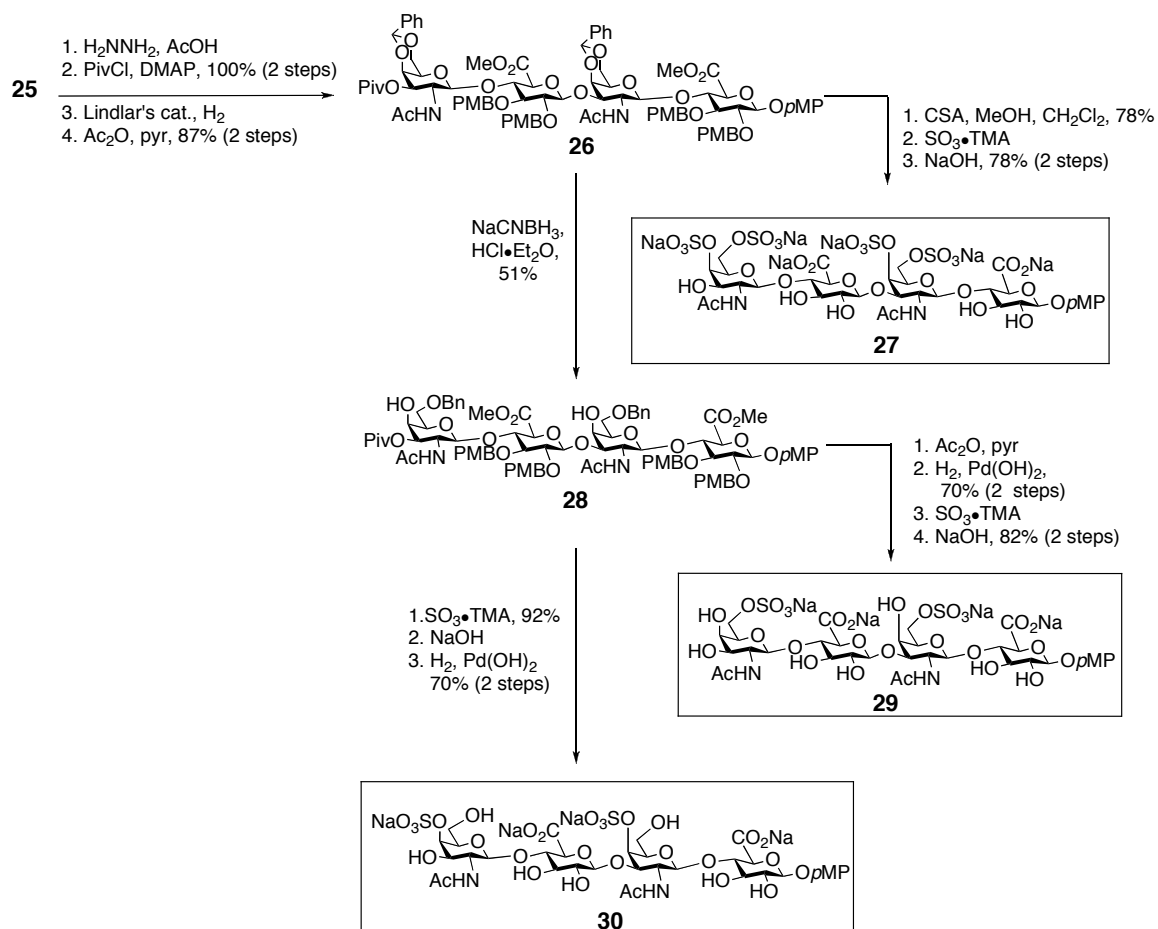
In 1995, Tamura *et al.*²³ reported the synthesis of the first CS-A tetrasaccharide and in 1997, the syntheses of CS-C and CS-E tetrasaccharides (Schemes 2.5 and 2.6).²⁰ As in the previous example, glycosyl imidates were used to generate the $\beta(1,3)$ - and $\beta(1,4)$ -glycosidic linkages. Glycosyl imidate **20** was synthesized from galactose in 11 steps and acceptor **21** from known compound *p*-methoxyphenyl β -D-glucopyranoside in 4 steps.³³ Coupling of these two compounds with subsequent 6-*O*-silyl ether deprotection gave the key disaccharide **22** in 70% yield. Opting to form the less hindered 1,3-linkage during tetrasaccharide construction, disaccharide **22** was converted into donor **23** or acceptor **24**. Reaction of these molecules with $\text{BF}_3 \cdot \text{OEt}_2$ afforded tetrasaccharide **25** in 50% yield.



Scheme 2.5: Synthesis of Tamura and Ogawa's fully protected tetrasaccharide. Ph = phenyl, TBS = *t*-butyldimethylsilyl, TBAF = tetrabutylammonium fluoride, PMB = *p*-methoxybenzyl, *p*MP = *p*-methoxyphenyl, Lev = levulinoyl, Me = methyl.

Tetrasaccharide **25** was converted to **26** in 4 steps. Since the levulinoyl group can be cleaved during benzylidene acetal removal, it was replaced with the more stable and less migratable pivolate group. The azides were reduced to amines and acetylated. **26** was subsequently reacted in two ways. First, it was converted to CS-E tetrasaccharide **27** by cleavage of the benzylidene acetal, followed by sulfonation with sulfur trioxide-trimethylamine and saponification of the esters. The authors had planned to use this approach to synthesize **29**, but selective C-6 sulfonation was not observed. Others have reported difficulty with this type of simultaneous sulfation of the C-4 and C-6 hydroxyls.³⁴ To access **29**, a more stepwise approach was required. **26** was converted to **23** by regioselective ring opening of the benzylidene ring using sodium cyanoborohydride and HCl-ether. Protection of the C-4 hydroxyl group as an acetate, benzyl deprotection, sulfonation, and ester cleavage gave CS-C tetrasaccharide **29** in good yield. CS-A tetrasaccharide **30** was synthesized in a similar manner by sulfonation, debenzylation, and ester hydrolysis. All three CS molecules were made from key disaccharide **22**, making this an efficient synthesis of CS. The relatively low-yielding regioselective ring-opening is one disadvantage of this method, and the multiple products of this reaction are difficult to separate. Methods to selectively sulfate or benzoilate the C-6 positions would provide access to all of the sulfation patterns from the tetraol generated through removal of the benzylidene rings of **26**. Another weakness of this method is the protection of the anomeric positions of the reducing end sugars with *p*-methoxyphenyl groups. This group does provide a UV active moiety to simplify purification of the oligosaccharides, but it is bulky and does not mimic the native oligosaccharide structure. Biological evaluation of these oligosaccharides would most

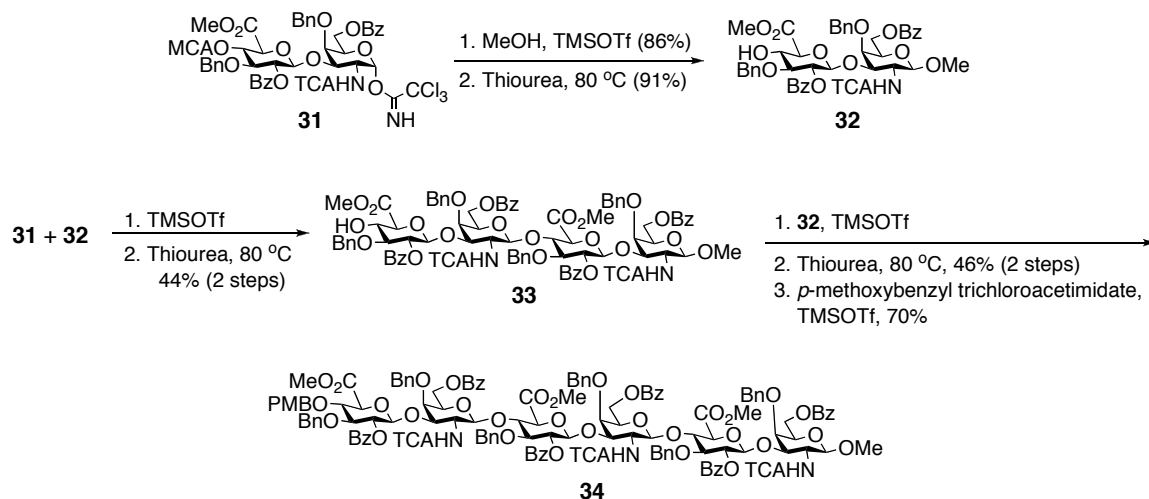
likely require replacement of the anomeric *p*-methoxyphenyl with a smaller, less intrusive protecting group.



Scheme 2.6: Synthesis of Tamura and Ogawa's CS-A, CS-C, and CS-E tetrasaccharides. Ph = phenyl, Piv = pivalate, Ac = acetate, PMB = *p*-methoxybenzyl, *p*MMP = *p*-methoxyphenyl, TMA = trimethylamine, Me = methyl, CSA = (±)-DL-camphor-10-sulfonic acid, DMAP = 4-dimethylaminopyridine.

Karst and Jacquinet's synthesis of a CS-D hexasaccharide

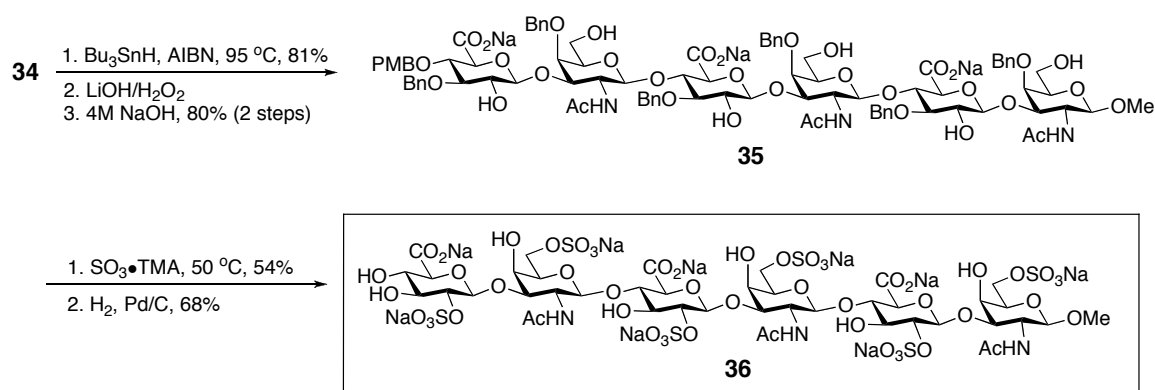
In 2002, Karst *et al.* reported the first synthesis of a CS hexasaccharide, CS-D (Schemes 2.7 and 2.8).²² Disaccharide imidate **31** was synthesized in 14 steps from known starting materials.^{26,34} **31** was converted to acceptor **32** by treatment with methanol and TMSOTf followed by reaction with thiourea to remove the C-4 chloroacetate group. Glycosyl imidate **31** and acceptor **32** were coupled in the presence of TMSOTf, and the product was immediately reacted with thiourea to afford tetrasaccharide **33** in 44% yield. Even though the more hindered 1,4-linkage was formed, the yield was similar to that of Ogawa *et al.*^{20,23} This demonstrates the influence of protecting groups in activating or deactivating the glycosidic bond forming reaction, and the presence of a C-2 trichloroacetamide on the donor promotes formation of the β -glycosidic linkage. Acceptor **33** was treated with TMSOTf and **32** to afford the hexasaccharide in good yield. The chloroacetate group was removed with thiourea and exchanged for a *p*-methoxybenzyl group to afford **34**. Exchange was necessary because



Scheme 2.7: Synthesis of Karst and Jacquinet's fully protected hexasaccharide. Me = methyl, MCA = monochloroacetyl, Bn = benzyl, Bz = benzoyl, TCA = trichloroacetyl, TMSOTf = trimethylsilyl trifluoromethane sulfonate, PMB = *p*-methoxybenzyl.

the chloroacetate group would be cleaved under the basic conditions needed to remove the benzoyl groups at sites of sulfation.

Hexasaccharide **34** was transformed to **35** by conversion of the *N*-trichloroacetyl groups to *N*-acetyl groups using tributyltin hydride and AIBN,³⁵ followed by treatment of this product with base to cleave the esters.³⁶ Sulfonation with sulfur trioxide-trimethylamine proceeded rapidly at the C-6 position, but sluggishly at C-2. A large excess of reagent was required to drive the reaction to completion. The final CS-D hexasaccharide **36** was obtained by hydrogenolysis of the benzyl ethers using H₂ and palladium on carbon.



Scheme 2.8: Karst and Jacquinet's CS-D hexasaccharide. Me = methyl, Bn = benzyl, Bz = benzoyl, PMB = *p*-methoxybenzyl, Ac = acetyl, AIBN = 2,2'-azobis(2-methylpropionitrile), TMA = trimethylamine, Bu = butyl.

Conclusion

The chemical synthesis of CS GAGs is a formidable challenge. In the past two decades, much progress has been made to generate oligosaccharides of different lengths and sulfation patterns. New, modular syntheses are needed for rapid formation of focused libraries of sulfated CS compounds, and defined saccharides should provide a means to dissect systematically the structure-function relationships of CS GAGs. Notably, the biological activities of the oligosaccharides constructed in the previous studies described in this chapter have not been reported in the literature. Access to these sugars should enable an understanding of their roles in a biological context, and we began our studies with this goal in mind.

References

1. Lyon, M. & Gallagher, J.T. (1998). Bio-specific sequences and domains in heparan sulphate and the regulation of cell growth and adhesion. *Matrix Biol.* **17**, 486-493.
2. Carey, D.J. (1997). Syndecans: multifunctional cell-surface co-receptors. *Biochem. J.* **327**, 1-16.
3. Gama, C.I. & Hsieh-Wilson, L.C. (2005). Chemical approaches to deciphering the glycosaminoglycan code. *Curr. Opin. Chem. Biol.* **9**, 609-619.
4. Small, D.H., Mok, S.S., Williamson, T.G. & Nurcombe, V. (1996). Role of proteoglycans in neural development, regeneration, and the aging brain. *J. Neurochem.* **67**, 889-899.
5. Krishna, N.R. & Agrawal, P.K. (2001). Molecular structure of the carbohydrate-protein linkage region fragments from connective-tissue proteoglycans. *Adv. in Carbohydr. Chem. and Biochem.* **56**, 201-234.
6. Bandtlow, C.E. & Zimmerman, D.R. (2000). Proteoglycans in the developing brain: new conceptual insights for old proteins. *Physiological Rev.* **80**, 1267-1290.
7. Matsui, F., Nishizuka, M. & Oohira, A. (1999). Proteoglycans in perineuronal nets. *Acta Histochem. Cytochem.* **32**, 141-147.
8. Snow, D.M. (1994). Neurite outgrowth in response to patterns of chondroitin sulfate proteoglycan: inhibition and adaptation. *Neuroprotocols* **4**, 146-157.
9. Kitagawa, H., Tsutsumi, K., Tone, Y. & Sugahara, K. (1997). Developmental regulation of the sulfation profile of chondroitin sulfate chains in the chicken embryo brain. *J. Biol. Chem.* **272**, 31377-31381.

10. Sugahara, K., Mikami, T., Uyama, T., Mizuguchi, S., Nomura, K. & Kitagawa, H. (2003). Recent advances in the structural biology of chondroitin sulfate and dermatan sulfate. *Curr. Opin. Struct. Biol.* **13**, 612-620.
11. Bradbury, E.J., Moon, L.D., Popat, R.J., King, V.R., Bennett, G.S., Patel, P.N., Fawcett, J.W. & McMahon, S.B. (2002). Chondroitinase ABC promotes functional recovery after spinal cord injury. *Nature* **416**, 636-640.
12. Holt, C.E. & Dickson, B.J. (2005). Sugar codes for axons? *Neuron* **46**, 169-172.
13. Nandini, C.D., Mikami, T., Ohta, M., Itoh, N., Akiyama-Nambu, F. & Sugahara, K. (2004). Structural and functional characterization of oversulfated chondroitin sulfate/dermatan sulfate hybrid chains from the notochord of hagfish. Neuritogenic and binding activities for growth factors and neurotrophic factors. *J. Biol. Chem.* **279**, 50799-50809.
14. Fujikawa, S., Ohmae, M. & Kobayashi, S. (2005). Enzymatic synthesis of chondroitin 4-sulfate with well-defined structure. *Biomacromolecules* **6**, 2935-2942.
15. Marra, A., Dong, X., Petitou, M. & Sinay, P. (1989). Synthesis of disaccharide fragments of dermatan sulfate. *Carbohydr. Res.* **195**, 39-50.
16. Karst, N. & Jacquinet, J.C. (2000). Chemical synthesis of β -D-GlcpA(2SO₄)-(1→3)-D-GalpNAc(6SO₄), the disaccharide repeating unit of shark cartilage chondroitin sulfate D, and of its methyl β -D-glycoside derivative. *J. Chem. Soc., Perkin Trans. 1*, 2709-2717.

17. Jaquinet, J.C., Rochepeau-Jobron, L. & Combal, J.P. (1998). Multigram syntheses of the disaccharide repeating units of chondroitin 4- and 6-sulfates. *Carbohydr. Res.* **314**, 283-288.
18. Lubineau, A. & Bonnaffe, D. (1999). Access to molecular diversity in glycosaminoglycans: combinatorial synthesis of eight chondroitin sulfate disaccharides. *Eur. J. Org. Chem.* 2523-2532.
19. Jaquinet, J.C. (1990). Syntheses of the methyl glycosides of the repeating units of chondroitin 4- and 6-sulfate. *Carbohydr. Res.* **199**, 153-181.
20. Tamura, J., Neumann, K.W., Kurono, S. & Ogawa, T. (1997). Synthetic approach towards sulfated chondroitin di-, tri-, and tetrasaccharides corresponding to the repeating unit. *Carbohydr. Res.* **305**, 43-63.
21. Coutant, C. & Jaquinet, J.C. (1995). 2-Deoxy-2-trichloroacetamido-D-glucopyranose derivatives in oligosaccharide synthesis: from hylauronic acid to chondroitin 4-sulfate trisaccharides. *J. Chem. Soc., Perkin Trans. 1*, 1573-1581.
22. Karst, N. & Jaquinet, J.C. (2002). Stereocontrolled total syntheses of shark cartilage chondroitin sulfate D-related tetra- and hexasaccharide methyl glycosides. *Eur. J. Org. Chem.* 815-825.
23. Tamura, J., Neumann, K.W. & Ogawa, T. (1995). A regio- and stereoselective synthesis of a 4-O-sulfated chondroitin di- and tetrasaccharide based on the strategy designed for the elongation of the repeating unit. *Bioorg. Med. Chem. Lett.* **5**, 1351-1354.

24. Belot, F. & Jacquinet, J.C. (2000). Syntheses of chondroitin 4- and 6-sulfate pentasaccharide derivatives having a methyl β -D-glucopyranosiduronic acid at the reducing end. *Carbohydr. Res.* **326**, 88-97.
25. Tamura, J. & Tokuyoshi, M. (2004). Synthesis of chondroitin sulfate E hexasaccharide in the repeating region by an effective elongation strategy toward longer chondroitin oligosaccharides. *Biosci. Biotechnol. Biochem.* **68**, 2436-2443.
26. Choay, J., Petitou, M., Lormeau, J.C., Sinay, P., Casu, B. & Gatti, G. (1983). Structure-activity relationship in heparin: a synthetic pentasaccharide with high affinity for anti-thrombin-III and eliciting high anti-factor Xa activity. *Biochem. Biophys. Res. Commun.* **116**, 492-499.
27. Angulo, J., Ojeda, R., de Paz, J.L., Lucas, R., Nieto, P.M., Lozano, R.M., Redondo-Horcado, M., Gimenez-Gallego, G. & Martin-Lomas, M. (2004). The activation of fibroblast growth factors (FGFs) by glycosaminoglycans: influence of the sulfation pattern on the biological activity of FGF-1. *ChemBiochem.* **5**, 55-61.
28. Sears, P. & Wong, C.H. (2001). Toward automated synthesis of oligosaccharides and glycoproteins. *Science* **291**, 2344-2350.
29. Karst, N.A. & Linhardt, R.J. (2003). Recent chemical and enzymatic approaches to the synthesis of glycosaminoglycan oligosaccharides. *Curr. Med. Chem.* **10**, 1993-2031.
30. *Carbohydrates in Chemistry and Biology*, 1st ed.; Ernst, B.; Hart, G.W.; Sinay, P., Eds.; Wiley-VCH: New York, NY 2000; Vol. 1.

31. Lemieux, R.U. & Ratcliffe, R.M. (1979). The azidonitration of tri-*O*-acetyl-D-glucal. *Can. J. Chem.* **57**, 1244-1251.
32. Schmidt, R.R. (1986). New methods for the synthesis of glycosides and oligosaccharides - are there alternatives to the Koenigs-Knorr method? *Angew. Chem. Int. Ed.* **25**, 212-235.
33. Yamaguchi, M., Horiguchi, A., Fukuda, A. & Minami, T. (1990). Novel synthesis of aryl 2,3,4,6-tetra-*O*-acetyl-D-glucopyranosides. *J. Chem. Soc., Perkin Trans. 1*, 1079-1082.
34. Belot, F. & Jacquinet, J.C. (2000). Unexpected stereochemical outcome of activated 4,6-*O*-benzylidene derivatives of the 2-deoxy-2-trichloroacetamido-D-galacto series in glycosylation reactions during the synthesis of a chondroitin 6-sulfate trisaccharide methyl glycoside. *Carbohydr. Res.* **325**, 93-106.
35. Blatter, G., Beau, J.M. & Jacquinet, J.C. (1994). The use of 2-deoxy-2-trichloroacetamido-D-glucopyranose derivatives in syntheses of oligosaccharides. *Carbohydr. Res.* **260**, 189-202.
36. Lucas, H., Basten, J.E.M., van Dinther, T.G., Meuleman, J.G., van Aelst, S.F. & van Boeckel, C.A.A. (1990). Syntheses of heparin-like pentamers containing opened uronic-acid moieties. *Tetrahedron* **46**, 8207-8228.

Chapter 3: Synthesis and Neurobiological Evaluation of Chondroitin Sulfate Oligosaccharides Bearing the CS-E Sulfation Pattern*†

Background

Glycosaminoglycans (GAGs) have an inherent capacity to encode functional information that rivals DNA, RNA and proteins. On the cell surface and in the extracellular matrix, chondroitin sulfate (CS) GAGs are hundreds of monosaccharide units in length, and they display a variety of sulfation patterns that are tightly regulated *in vivo* (see Figure 2.1 of Chapter 2).^{1,2} Over the past several decades, genetic and biochemical studies have established the importance of GAGs in regulating many physiological processes, including morphogenesis and development, viral invasion, cancer metastasis and spinal cord injury.³⁻⁶ However, a key unresolved question is whether and how glycosaminoglycans utilize specific sulfation sequences to modulate biological processes.

In the central nervous system, CS and their associated proteoglycans have been shown to prevent axonal growth and inhibit neural regeneration in areas of injury, but tissues that strongly express CS do not always exclude the entry of axons.^{6,7} Several methods have been employed to understand this paradox, but none of these strategies can determine the importance of specific sulfation sequences. For example, mutations of sulfotransferase genes disrupt multiple sulfation patterns on the GAG chain and cannot be

* Syntheses of chondroitin sulfate oligosaccharides were done in collaboration with Ross Mabon, a former postdoctoral scholar in the Hsieh-Wilson laboratory, Sherry M. Tsai, a former graduate student in the Hsieh-Wilson laboratory, and Manish Rawat, a postdoctoral scholar in the Hsieh-Wilson laboratory. Neurobiological studies were done in collaboration with Cristal I. Gama, a graduate student in the Hsieh-Wilson laboratory.

† Portions of this chapter were taken from S.E. Tully *et al.* (2004) *J. Am. Chem. Soc.* **126**, 7736-7737 and C.I. Gama *et al.* (2006) *Nat. Chem. Biol.* accepted.

used to elucidate the impact of a single motif.^{3,8} Biochemical preparations of CS polysaccharides have been shown both to stimulate and attenuate the growth of cultured neurons,⁹⁻¹¹ and the contradictory observations may be due to the difficulty in isolating defined CS molecules from natural sources such as shark cartilage. The heterogeneity of CS polysaccharides obtained through such methods has hampered efforts to relate precise CS structure with function.¹²

Among the sulfation patterns implicated in the modulation of cell growth is the disulfated CS-E motif, a sulfation pattern enriched in the developing central nervous system (Figure 3.1).^{13,14} Heterogeneous polysaccharides enriched in CS-E have been shown to promote neurite outgrowth in hippocampal neurons,¹⁵ and they bind numerous growth factors active in the brain such as midkine, pleiotrophin, and fibroblast growth factor-2 (FGF-2).¹⁶ CS-E represented only 65% of the overall sulfation pattern of the molecules used in these studies, raising some doubt as to whether other motifs might be contributing to the observed effects.

To investigate the biological properties of CS-E and establish the minimal structural determinants for activity, we sought to develop a modular and efficient synthesis of di- and tetrasaccharides bearing this sulfation pattern. Many heparan sulfate glycoaminoglycan binding proteins recognize tetra- or pentasaccharide motifs,^{17,18} but literature reports of CS proteoglycan-protein interactions suggest CS motifs of octasaccharides or larger are necessary for recognition.¹⁹ We wanted to determine if synthetic CS-E di- or tetrasaccharides could recapitulate the activities of the CS-E enriched polysaccharides. We also decided to generate a tetrasaccharide lacking sulfation

for comparison in our studies in order to understand the importance of sulfation in CS activity (Figure 3.1).

To evaluate the biological activities of the synthetic molecules, we planned to analyze their abilities to promote neurite outgrowth of hippocampal neurons. The hippocampus is a region of the brain important in learning and memory²⁰ and it is also one of the first regions affected during Alzheimer's disease.²¹ Synthetic, neurite outgrowth promoting CS small molecules could prove to be quite powerful in curing the dementia caused by Alzheimer's and in understanding the importance of CS GAGs in learning and memory.

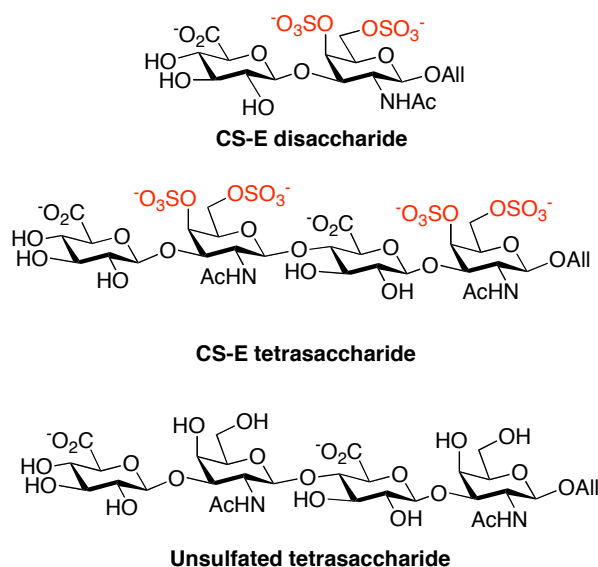


Figure 3.1: Structures of the initial library of synthetic CS oligosaccharides. All = allyl, Ac = acetyl.

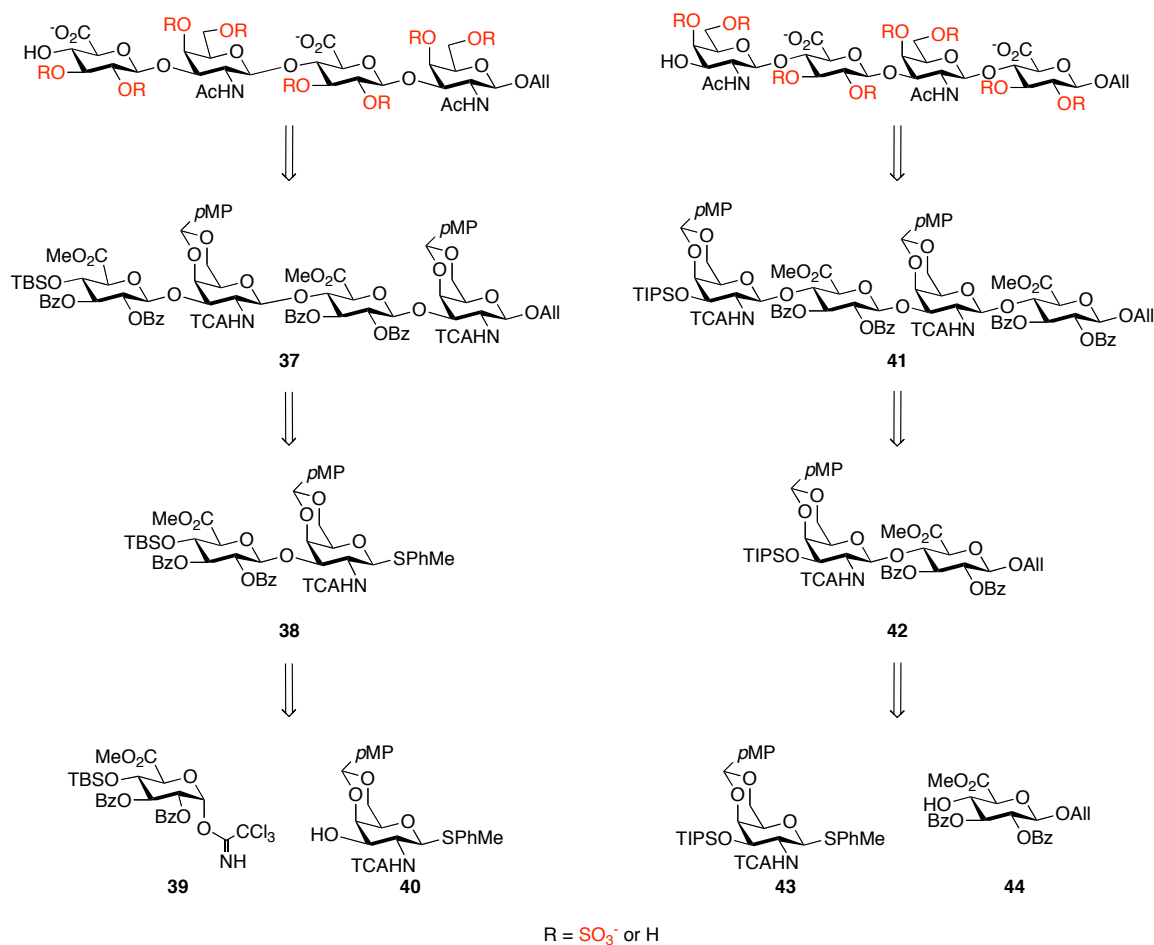
Development of a synthetic route to chondroitin sulfate oligosaccharides

As described in Chapter 2, the synthesis of CS oligosaccharides is challenging and requires stereospecific formation of glycosidic linkages and regiospecific

functionalization of hydroxyl groups of comparable reactivity to install distinct sulfation sequences. While we first wanted to create di- and tetrasaccharides bearing the CS-E sulfation motif, we sought to design a modular synthetic approach that would allow us to rapidly generate multiple sulfation patterns from a single disaccharide intermediate. Retrosynthetic analysis of CS di- and tetrasaccharides afforded two possible routes and led to glucuronic acid (GlcA) monomers **39** and **44** and *N*-acetylgalactosamine (GalNAc) monomers **40** and **43** (Scheme 3.1). Coupling **39** and **40** places the GalNAc subunit at the reducing end, whereas, coupling of **43** to **44** places the GlcA moiety at the reducing end. In retrosynthesis 1, the hindered $\beta(1,4)$ -glycosidic linkage is constructed when coupling disaccharides, but for retrosynthesis 2, this linkage is generated during monomer coupling. We pursued the two syntheses in parallel to determine the highest yielding method. This is possible as both the GlcA monomers can be generated through one synthetic pathway and both the GalNAc monomers through another pathway.

We decided to oxidize the C-6 position of the glucuronic acid monomer at the monomer stage as oxidation is easier to perform on monosaccharides than on oligosaccharides. The methyl ester is deactivating, but there is precedent for high yielding and stereoselective coupling reactions with glucuronic methyl ester monomers.^{22,23}

To direct the β -stereochemistry of the glycosidic bond forming reaction, we planned to exploit C-2 *N*-trichloroacetyl (TCA) or *O*-benzoyl (Bz) participating groups in a manner comparable to previous syntheses (see Chapter 2).²⁴ α -Trichloroacetimidates and thioglycosides are more activated leaving groups than glycosyl bromides and thus were chosen as donors. The versatility of thioglycosides enables conversion to the more activated α -trichloroacetimidate, if necessary. Additionally, for retrosynthesis 1, an α -



Scheme 3.1: Retrosynthetic analysis 1 (left) and retrosynthetic analysis 2 (right) of CS tetrasaccharides. Me = methyl, All = allyl, Ac = acetyl, *p*MP = *p*-methoxyphenyl, TBS = *t*-butyldimethylsilyl, Bz = benzoyl, TCA = trichloroacetyl, PhMe = tolyl, TIPS = triisopropylsilyl.

trichloroacetimidate was chosen as the donor in the formation of the disaccharide because it should be selectively activated in the presence of a thioglycoside, allowing for orthogonal coupling reactions.²⁵ The thioglycoside present at the reducing end allows for extension to tetrasaccharides and longer oligosaccharides.

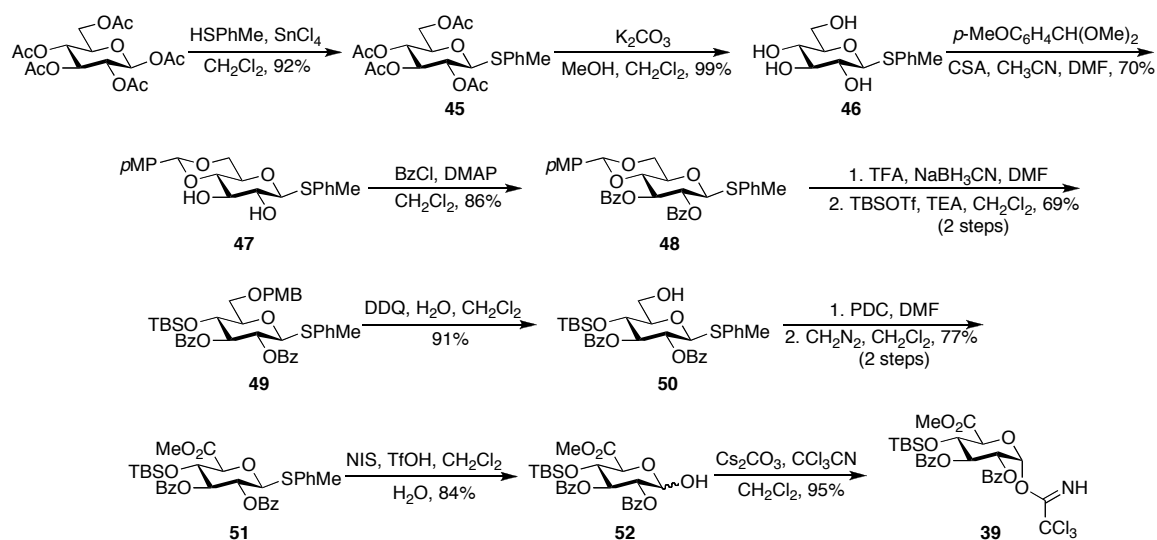
An orthogonal protecting group strategy was designed to install specific sulfation sequences. We chose the *p*-methoxybenzylidene group to mask positions that are exposed at late stages of the synthesis for sulfation. Unlike a benzylidene ring, this group is readily cleaved through oxidative cleavage with DDQ, eliminating the need to perform an

acidic cleavage and minimizing side reactions such as loss of other protecting groups and destruction of glycosidic linkages. In addition, it is more amenable to cleavage on solid support, which would be valuable for future extension of the synthesis to solid-phase. To elongate the carbohydrate chain, a silyl ether (TIPS or TBS) is used to protect the C-4 position of GlcA or C-3 position of GalNAc and liberate a hydroxyl group nucleophile for reaction with a glycosylating agent. In addition to their abilities as participating groups, the *N*-TCA group is also readily converted to the acetamide during late stages of the synthesis and the Bz groups are easily cleaved. Finally and unique to our synthesis, we utilize the allyl moiety at the reducing end of the oligosaccharides as a convenient chemical handle for conjugation to proteins, small molecules and surfaces.

Monomer synthesis for retrosynthesis 1

Glucuronic acid monomer **39** was synthesized in 11 steps and 21% overall yield from β -D-glucose pentaacetate, and importantly, this synthesis was readily performed on a multigram scale to obtain pure monomer (Scheme 3.2). β -D-Glucose pentaacetate was converted to thioglycoside **45** in 92% yield using tin (IV) tetrachloride and *p*-toluenethiol, and the thioglycoside was then transformed to **46** through a methanolysis reaction in 99% yield. Tetraol **46** generated *p*-methoxybenzylidene **47** in 70% yield using *p*-methoxybenzylidene dimethyl acetal and a catalytic amount of DL-camphor-10-sulfonic acid. A small amount of DMF was added to the reaction to enhance the solubility of **46**, but running the reaction in DMF instead of acetonitrile led to prolonged reaction times. Dibenzoylation of the diol using benzoyl chloride and DMAP afforded **48**, and regioselective ring opening of the acetal using TFA and NaBH_3CN ²⁶ followed by silyl protection of the C-4 hydroxyl yielded **49** in 69% yield. Next, the PMB group was

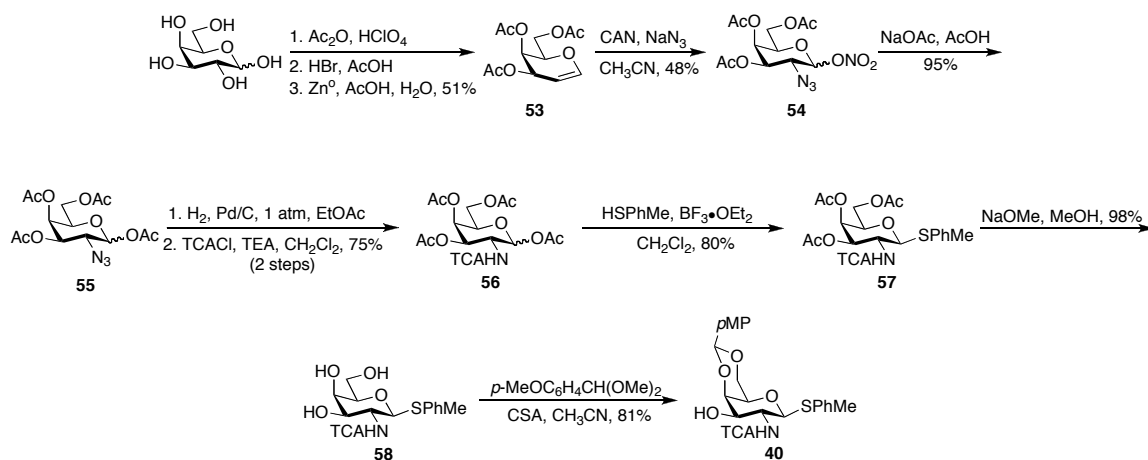
removed by oxidative cleavage with DDQ and the resulting primary alcohol **50** was oxidized with pyridinium dichromate in DMF to afford the acid over the aldehyde and leave the thiol unoxidized.^{27,28} The acid was then esterified under standard conditions using diazomethane, and conversion of thioglycoside **51** to the corresponding imidate furnished the monomer **39** in 80% yield over the two steps. The imidate was chosen over the thioglycoside for the final monomer as it should be more reactive in the coupling reaction to the GalNAc monomer.²⁹



Scheme 3.2: Synthesis of the glucuronic acid monomer **39**. Ac = acetyl, Me = methyl, All = allyl, *p*MP = *p*-methoxyphenyl, TBS = *t*-butyldimethylsilyl, Bz = benzoyl, PhMe = tolyl, *p*-MeOC₆H₄CH(OMe)₂ = *p*-methoxybenzaldehyde dimethyl acetal, CSA = (±)-DL-camphor-10-sulfonic acid, TFA = trifluoroacetic acid, TBSOTf = *t*-butyldimethylsilyl trifluoromethane sulfonate, TEA = triethylamine, PMB = *p*-methoxybenzyl, DDQ = 2,3-dichloro-5,6-dicyano-*p*-benzoquinone, PDC = pyridinium dichromate, NIS = *N*-iodosuccinimide.

Synthesis of the galactosamine monomer **40** was accomplished on a multigram scale in eleven steps from D-galactose and an 11% overall yield (Scheme 3.3). D-Galactose was converted to tri-*O*-acetylgalactal **53** in a three-step reaction sequence for a yield of 51%.³⁰ D-Galactose was first acetylated using acetic anhydride and catalytic perchloric acid. The peracetylated galactose was converted to the glycosyl bromide using

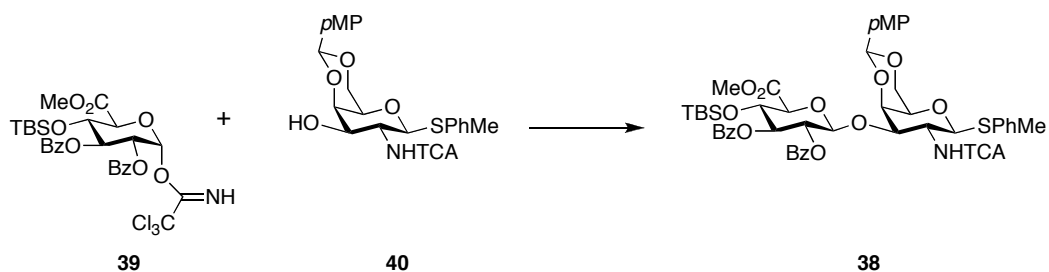
hydrogen bromide in acetic acid, and the bromide was reduced to tri-*O*-acetylgalactal **53** using elemental zinc and aqueous acetic acid. Azidonitration using cerium ammonium nitrate and sodium azide afforded nitrate **54** as a mixture of α - and β -anomers in 48% yield.³¹ Acetate **55** was prepared from **54** in 95% yield utilizing sodium acetate and acetic acid, and subsequently, the azide was reduced and converted to the trichloroacetamide **56**. Formation of thioglycoside **57** using boron trifluoride diethyl etherate and *p*-toluenethiol followed by deacetylation under Zemplén conditions afforded **58** in 78% yield from **56**. Monomer **40** was completed through installation of a *p*-methoxybenzylidene ring on the C-4 and C-6 hydroxyls utilizing *p*-methoxybenzylidene dimethyl acetal and a catalytic amount of DL-camphor-10-sulfonic acid.



Scheme 3.3: Synthesis of the galactosamine monomer **40**. Ac = acetyl, CAN = cerium ammonium nitrate, TCACl = trichloroacetyl chloride, TEA = triethylamine, PhMe = tolyl, *p*MP = *p*-methoxyphenyl, *p*-MeOC₆H₄CH(OMe)₂ = *p*-methoxybenzaldehyde dimethyl acetal, CSA = (\pm)-DL-camphor-10-sulfonic acid

Generation of the disaccharide for retrosynthesis 1

With the protected donor and acceptors in hand, Ross Mabon and I undertook construction of disaccharide building block **38** (Scheme 3.4 and Table 3.1). Unexpectedly, the yields for this coupling were quite low even though it generates the less hindered $\beta(1,3)$ -linkage. While some of the $\alpha(1,3)$ -linked disaccharide was observed, the major by-product was monosaccharide **51** (Scheme 3.2) in yields ranging from 20% – 60%. This product was presumably formed through an intermolecular aglycon transfer reaction (Scheme 3.5) and demonstrates one of the difficulties in coupling to thioglycoside acceptors.³²

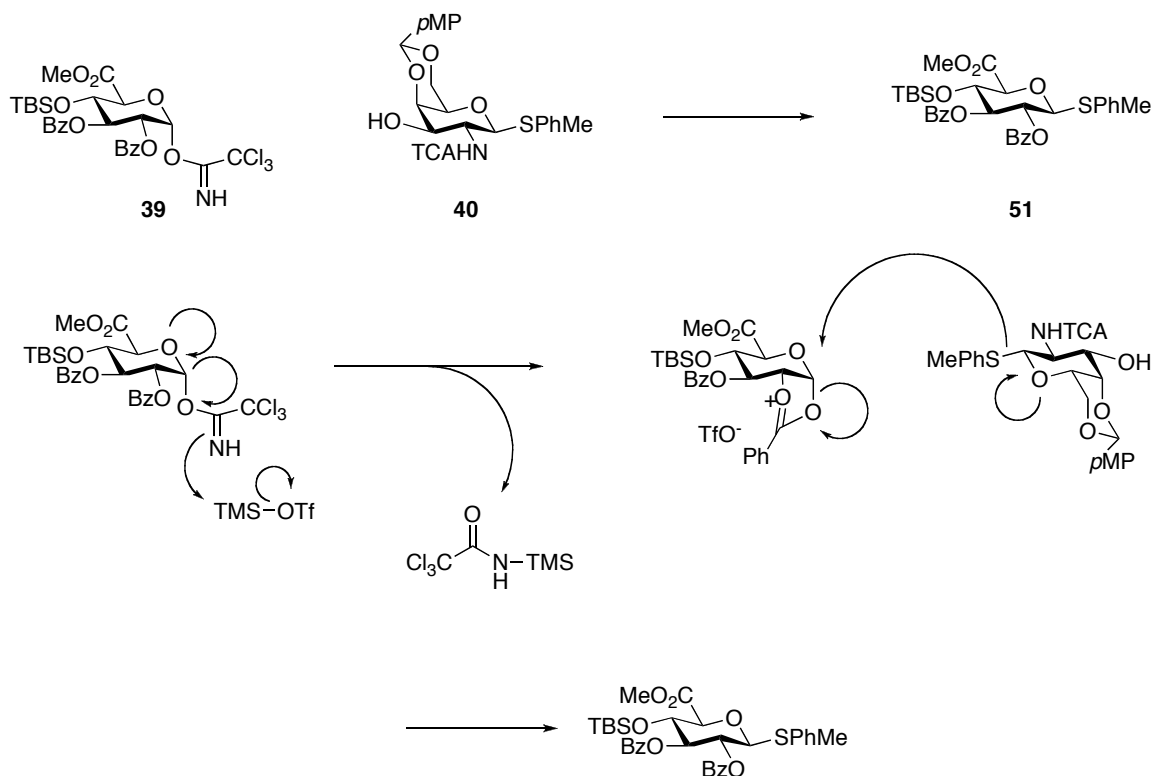


Scheme 3.4: Formation of disaccharide **38**. Me = methyl, TBS = *t*-butyldimethylsilyl, Bz = benzoyl, PhMe = tolyl, *p*MP = *p*-methoxyphenyl, TCA = trichloroacetyl.

Donor (eq)	Acceptor (eq)	Activator (eq)*	Solvent	Temp (°C)	Time (h)	β -di
1.2	1.0	BF ₃ ·OEt ₂ (0.1)	Toluene/CH ₂ Cl ₂	0	1	21%
1.8	1.0	BF ₃ ·OEt ₂ (0.3)	CH ₂ Cl ₂	-15	2	18%
1.2	1.0	BF ₃ ·OEt ₂ (0.3)	CH ₂ Cl ₂	-45	2	32%
1.0	1.7	BF ₃ ·OEt ₂ (0.3)	CH ₂ Cl ₂	-45 to rt	3	46%
1.1	1.0	TMSOTf (0.2)	Toluene/CH ₂ Cl ₂	rt	1	16%
1.8	1.0	TMSOTf (0.4)	Toluene/CH ₂ Cl ₂	-15	3	17%
1.2	1.0	TMSOTf (0.2)	CH ₂ Cl ₂	-15	1	21%
1.2	1.0	TMSOTf (0.2)	CH ₂ Cl ₂	-78 to rt	3	28%
1.2	1.0	TMSOTf (1.1)	CH ₂ Cl ₂	-78 to rt	18	32%

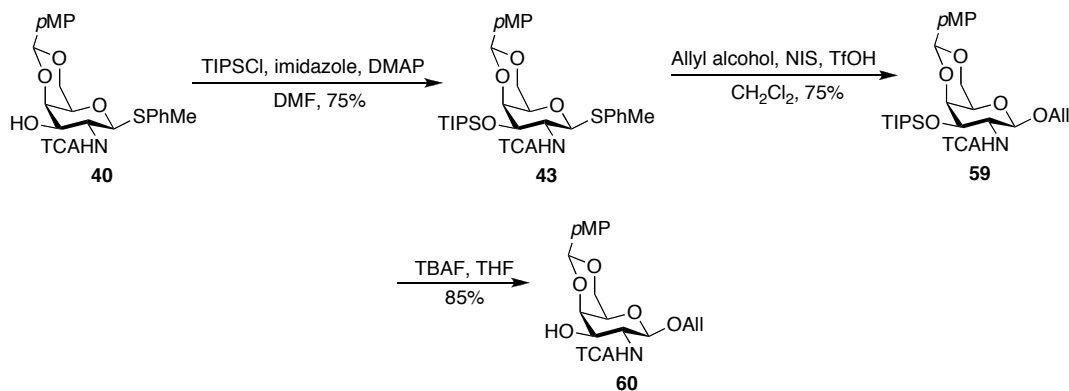
*NIS also used in each condition (1.4 eq)

Table 3.1: Conditions attempted for generation of disaccharide **38**. NIS = *N*-iodosuccinimide, TMSOTf = trimethylsilyl trifluoromethanesulfonate, Et = ethyl.



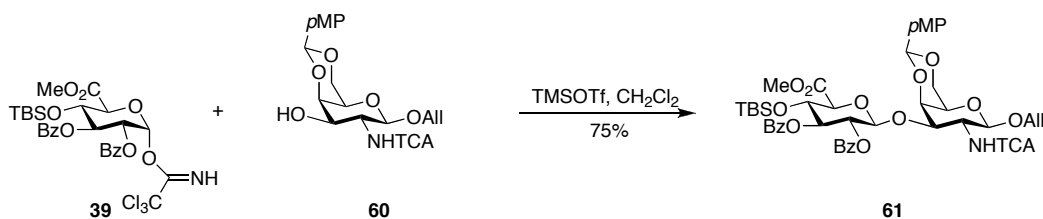
Scheme 3.5: Intermolecular aglycon transfer. Me = methyl, TBS = *t*-butyldimethylsilyl, Bz = benzoyl, PhMe = tolyl, *p*MP = *p*-methoxyphenyl, TCA = trichloroacetyl, TMS = trimethylsilyl.

To avoid this transfer, we placed the allyl group on the reducing end of GalNAc at an earlier stage in the synthesis. The allyl group should be stable to all coupling conditions and not sensitive to aglycon transfer. We envisioned that for generation of larger oligosaccharides, the allyl group could be cleaved to afford an anomeric mixture of alcohols and the imidate generated for coupling reactions.³³ The new GalNAc monomer **60** was made in three steps from **40** (Scheme 3.6). First, a TIPS group was added to the C-3 hydroxyl using triisopropylsilyl chloride and imidazole. This was followed by allylation through activation of the thioglycoside with triflic acid and *N*-iodosuccinimide and coupling to allyl alcohol to afford **59** in 75% yield. The silyl group was then cleaved to afford GalNAc acceptor **60**.



Scheme 3.6: Synthesis of the galactosamine monomer **60**. All = allyl, *p*MP = *p*-methoxyphenyl, PhMe = tolyl, NIS = *N*-iodosuccinimide, TIPSCl = triisopropylsilyl chloride, TfOH = triflic acid, TCA = trichloroacetyl, TBAF = tetrabutylammonium fluoride, DMAP = 4-dimethylaminopyridine.

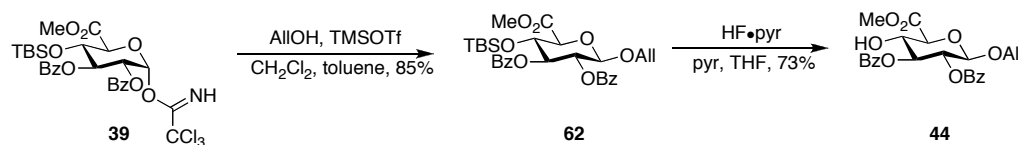
Imidate **39** was coupled to allyl glycoside acceptor **60** using TMSOTf in CH_2Cl_2 at $-40\text{ }^\circ\text{C}$ to afford disaccharide **61** in 75% yield (Scheme 3.7). As anticipated, formation of the $\beta(1,3)$ -glycosidic linkage was exclusively observed at low temperature due to the presence of a C-2 participating group and an α -trichloroacetimidate in the glycosyl donor. Upon generating the key disaccharide for retrosynthesis 1, we were then able to explore generation of larger oligosaccharides and the remaining sulfation and deprotection steps for the synthesis of the CS-E disaccharide.



Scheme 3.7: Formation of disaccharide **61**. Me = methyl, All = allyl, *p*MP = *p*-methoxyphenyl, TBS = *t*-butyldimethylsilyl, Bz = benzoyl, TCA = trichloroacetyl, PhMe = tolyl, TMSOTf = trimethylsilyl trifluoromethane sulfonate.

Monomer synthesis for retrosynthesis 2

In parallel to retrosynthesis 1, we investigated the generation of CS oligosaccharides through retrosynthesis 2. The GlcA monomer for retrosynthesis 2 was readily generated using monomer **39** from retrosynthesis 1 (Scheme 3.8). Coupling imidate **39** to allyl alcohol through activation with TMSOTf proceeded in 85% yield to afford **62**. GlcA acceptor **44** was then formed by HF•pyridine cleavage of the TBS group. HF•pyridine was chosen over TBAF as β -elimination of the C-4 hydroxyl was observed when TBAF was employed.



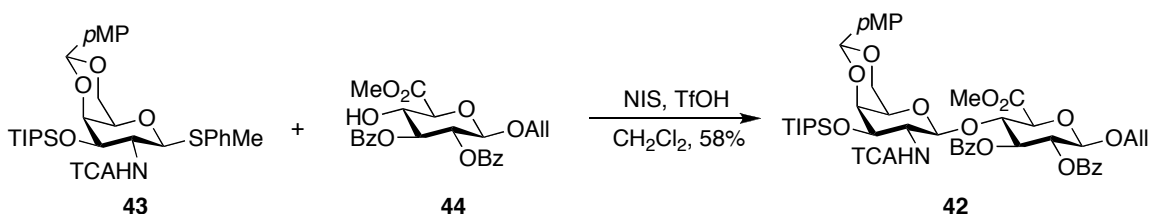
Scheme 3.8: Synthesis of the glucuronic acid monomer **44**. Me = methyl, All = allyl, TBS = *t*-butyldimethylsilyl, Bz = benzoyl, TMSOTf = trimethylsilyl trifluoromethane sulfonate, pyr = pyridine.

The GalNAc monomer for retrosynthesis 2 is intermediate **43** from Scheme 3.6 for the monomers of revised retrosynthesis 1.

Generation of the disaccharide for retrosynthesis 2

Sherry M. Tsai investigated coupling of donor **43** to acceptor **44** to form the key disaccharide in retrosynthesis 2. In the presence of *N*-iodosuccinimide and triflic acid, the coupling afforded the β -disaccharide **42** in 58% yield and the corresponding α -disaccharide in 32% yield (Scheme 3.9). Separation of the anomeric mixture was tedious and only possible by preparative thin layer chromatography, making generation of multiple grams of this disaccharide difficult. In contrast, key disaccharide **61** of

retrosynthesis 1 is easily purified through standard large-scale silica gel chromatographic methods and can be readily synthesized on a multigram scale necessary to complete the synthesis of CS oligosaccharides. For this reason, and the reduced yield compared to the previous coupling, we decided to continue the remaining synthesis utilizing retrosynthesis 1 in order to obtain multigram amounts of the disaccharide building block.

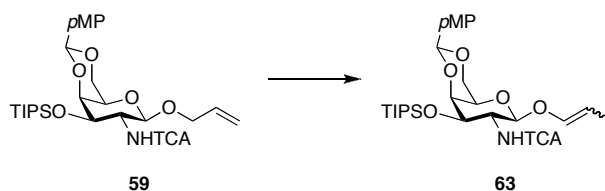


Scheme 3.9: Formation of disaccharide **42**. Me = methyl, All = allyl, *p*MP = *p*-methoxyphenyl, Bz = benzoyl, TCA = trichloroacetyl, PhMe = tolyl, TMSOTf = trimethylsilyl trifluoromethane sulfonate, NIS = *N*-iodosuccinimide, TfOH = triflic acid, TIPS = triisopropylsilyl.

Tetrasaccharide **37** and Hexasaccharide **68** Formation

To synthesize the fully-protected tetrasaccharide, both a disaccharide acceptor and donor were generated from **61**. Activation of the disaccharide was envisioned to proceed through conversion of the C-1 allyl group to the lactol followed by formation of the trichloroacetimidate. Ross Mabon used GalNAc monomer **59** as a model system to test the isomerization of the olefin (Scheme 3.10). As summarized in Table 3.2, conventional methods such as Pd(PPh₃)₄,³⁴ PdCl₂,³⁵ Wilkinson's catalyst,³⁶⁻³⁸ NiCl₂(dppp)₂ in the presence of Et₃Al,³⁹ palladium on carbon,⁴⁰ sodium borohydride in the presence of iodine,⁴¹ and [Ir(COD)(PMePh₂)₂]₂PF₆,⁴² did not yield the desired isomerization. This is presumably due to interference by the C-2 trichloroacetamide, as the 2-acetamido derivative readily isomerized upon treatment with [Ir(COD)(PMePh₂)₂]₂PF₆. Fortunately, treatment with Grubbs' second-generation catalyst⁴³ led to the desired product likely

through either hydride addition-elimination or π -allyl metal coordination and a 1,3-hydride shift.⁴⁴ Running the reaction in H₂ accelerated the reaction time, but the reaction proceeded smoothly in the presence or absence of H₂.



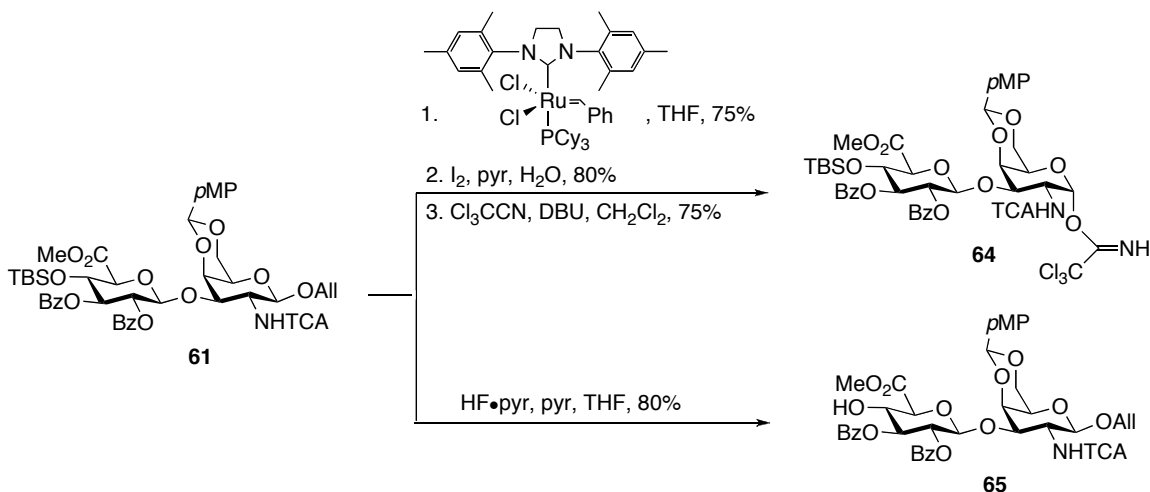
Scheme 3.10: Isomerization of the GalNAc anomeric allyl group. *p*MP = *p*-methoxyphenyl, TCA = trichloroacetyl, TIPS = triisopropylsilyl.

Catalyst	Additives	Solvent	Yield
Pd(PPh ₃) ₄	AcOH	MeOH	no reaction
PdCl ₂	none	MeOH	no reaction
(Ph ₃ P) ₃ RhCl	DBU	EtOH/toluene/H ₂ O	no reaction
(Ph ₃ P) ₃ RhCl	DABCO	EtOH/benzene/H ₂ O	no reaction
(Ph ₃ P) ₃ RhCl	DIPEA	toluene	no reaction
NiCl ₂ (dppp) ₂	Et ₃ Al, then H ₂ O	MeOH	no reaction
10% Pd/C	none	MeOH	no reaction
NaBH ₄	I ₂	MeOH	no reaction
[Ir(COD)(PMePh ₂) ₂] ₂ PF ₆	H ₂	THF	no reaction
Grubbs' second-generation catalyst	with or without H ₂	THF	70%

Table 3.2: Allyl isomerization conditions. dppp = 1,3-bis(diphenylphosphino)propane, COD = *cis,cis*-1,5-cyclooctadiene, Ph = phenyl, AcOH = acetic acid, Et = ethyl, DBU = 1,8-diazabicyclo[5.4.0]undec-7-ene, DABCO = 1,4-diazabicyclo[2.2.2]octane, DIPEA = *N,N*-diisopropylethylamine.

Reaction of disaccharide **61** with Grubbs' second-generation catalyst was followed by hydrolysis of the enol ether and conversion to the imidate under standard conditions to afford donor **64** (Scheme 3.11). Disaccharide **61** also provided access to glycosyl acceptor **65** via desilylation with HF•pyridine. Sherry M. Tsai attempted a similar olefin isomerization strategy with disaccharide **42** in order to advance the

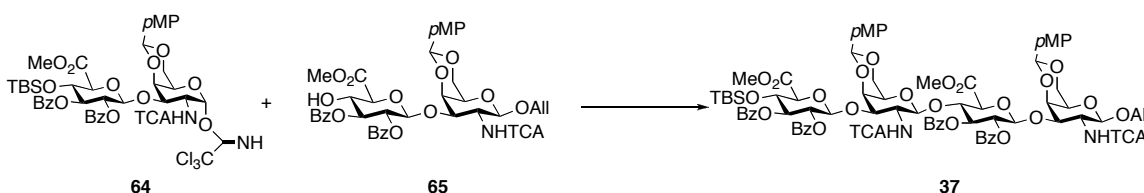
synthetic route of retrosynthesis 2, but the reaction was low-yielding, and further confirmed our decision to proceed forward with retrosynthesis 1.



Scheme 3.11: Generation of the disaccharide donor **64** and acceptor **65**. Me = methyl, All = allyl, *p*MP = *p*-methoxyphenyl, TBS = *t*-butyldimethylsilyl, Bz = benzoyl, TCA = trichloroacetyl, pyr = pyridine, DBU = 1,8-diazabicyclo[5.4.0]undec-7-ene, Ph = phenyl, Cy = cyclohexyl.

Ross Mabon and Manish Rawat screened numerous conditions for the coupling of **64** and **65** (Scheme 3.12 and Table 3.3) and ultimately, activation of the imidate with TMSOTf at low temperature provided the highest yield and excellent β -stereoselectivity. The lower yields for the glycosylation reaction compared to those observed for disaccharide generation were due to the ability of the imidate donor to readily hydrolyze (10 – 20%) and also to rearrange and generate an unreactive amide by-product **66** (20 – 30%) (Scheme 3.13). Katie Saliba and Manish Rawat are currently investigating alternative coupling reactions. By increasing the bulk of the C-2 amine-protecting group, it should be possible to eliminate rearrangement of the imidate donor to an amide such as **66**. Replacement of the TCA group with phthaloyl (Phth) or a trichloroethoxycarbonyl (Troc) should increase yields and prevent formation of the unreactive amide species. Also, donors containing 4,6-benzylidene rings can have unexpected stereochemical

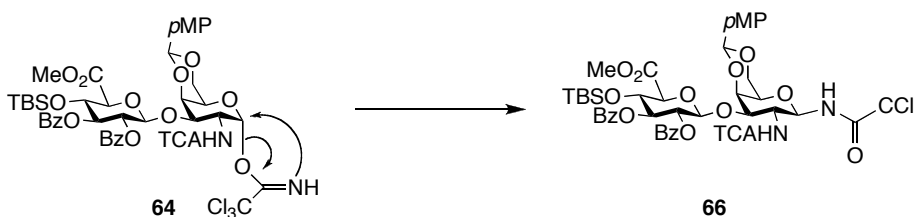
results during coupling reactions.⁴⁵ While formation of the α -linked product was not a problem in our case, replacement of the *p*-methoxybenzylidene ring with two protecting groups might increase the reaction yield in future syntheses. With the current method, we were able to generate gram quantities of the key tetrasaccharide intermediate and proceed with the synthesis of CS tetrasaccharides.



Scheme 3.12: Formation of tetrasaccharide **37**. Me = methyl, All = allyl, *p*MP = *p*-methoxyphenyl, TBS = *t*-butyldimethylsilyl, Bz = benzoyl, TCA = trichloroacetyl.

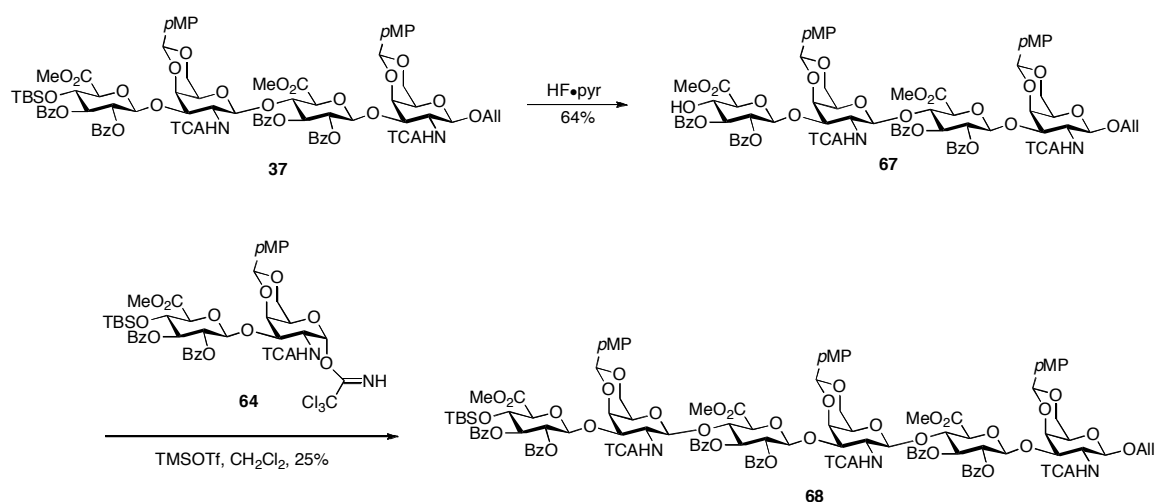
Activator (eq)	Solvent	Temp (°C)	β -tetra
TMSOTf (0.2)	CH ₂ Cl ₂	-15	35%
TMSOTf (0.4)	CH ₂ Cl ₂	-15	22%
BF ₃ •Et ₂ O (0.2)	CH ₂ Cl ₂	-15	18%
ZnCl ₂ •Et ₂ O (0.6)	CH ₂ Cl ₂	-15	trace
TBSOTf (0.2)	CH ₂ Cl ₂	-15	40%
MeOTf (0.6)	CH ₂ Cl ₂	-15	trace
BF ₃ •Et ₂ O (0.4)	CH ₂ Cl ₂ /toluene (1:1)	-10	25%
TMSOTf (0.2)	CH ₂ Cl ₂ /toluene (1:1)	-10	28%
TMSOTf (0.2)	THF	-15	trace
TMSOTf (0.2)	MeCN	-15	trace
TBSOTf (0.3)	CH ₂ Cl ₂	0	34%
TMSOTf (0.2)	CH₂Cl₂	-78 to -20	44%

Table 3.3: Conditions attempted for generation of tetrasaccharide **37**. TBSOTf = *t*-butyldimethylsilyl trifluoromethane sulfonate, TMSOTf = trimethylsilyl trifluoromethane sulfonate, Et = ethyl, Me = methyl.



Scheme 3.13: Rearrangement of disaccharide donor **64**. Me = methyl, *p*MP = *p*-methoxyphenyl, TBS = *t*-butyldimethylsilyl, Bz = benzoyl, TCA = trichloroacetyl.

Hexasaccharide **68** was made in a manner similar to tetrasaccharide **37**. First, acceptor **67** was formed through silyl deprotection of the TBS group of tetrasaccharide **37** (Scheme 3.14), followed by coupling to donor **64** in an unoptimized yield of 25%. While we could generate fully-protected hexasaccharides, we decided to focus the synthesis on CS-E di- and tetrasaccharides first elucidate their neurobiological activities. In addition, we thought optimization of the final deprotection and sulfation steps and the purification of these highly-charged molecules would be more straightforward on the smaller carbohydrates.

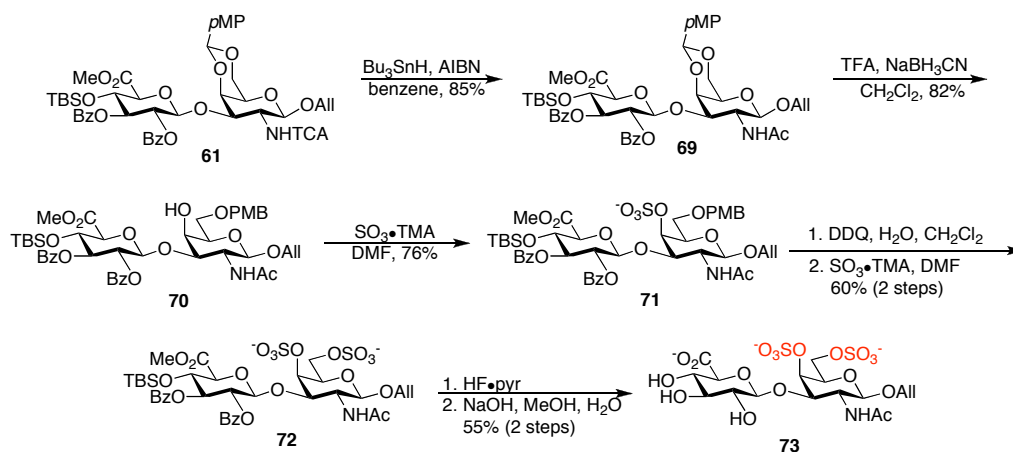


Scheme 3.14: Formation of tetrasaccharide acceptor **67** and hexasaccharide **68**. Me = methyl, All = allyl, *p*MP = *p*-methoxyphenyl, TBS = *t*-butyldimethylsilyl, Bz = benzoyl, TCA = trichloroacetyl, pyr = pyridine, TMSOTf = trimethylsilyl trifluoromethane sulfonate.

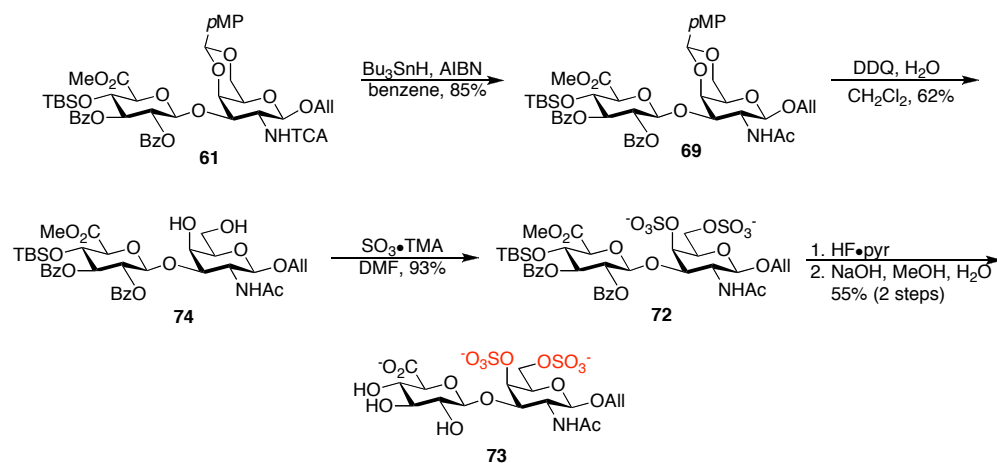
Elaboration of protected di- and tetrasaccharides to form CS-E oligosaccharides

With fully-protected di- and tetrasaccharides, we embarked on the final deprotection and sulfation steps necessary to create CS-E oligosaccharides. Due to the relative ease of obtaining large amounts of disaccharide versus tetrasaccharide, we decided to optimize the end game on disaccharide **61**. Two routes were designed due to an earlier report suggesting that simultaneous sulfation of the C-4 and C-6 hydroxyls might be challenging.⁹ One method involved regioselective ring-opening of the *p*-methoxybenzylidene ring and sequential sulfation of the two hydroxyl groups (Scheme 3.15), and the other concurrent sulfation of the C-4 and C-6 hydroxyls (Scheme 3.16). Both methods began with radical-mediated conversion of the *N*-trichloroacetyl group to *N*-acetyl with tributyltin hydride and AIBN provided disaccharide **69** in 85% yield.⁴⁶ For the more stepwise approach, several conditions were attempted for the regioselective ring opening of **69**, such as, TFA and sodium cyanoborohydride in DMF,²⁶ HCl in ether and sodium cyanoborohydride in THF,⁴⁷ and triethylsilane and triflic acid in CH₂Cl₂,⁴⁸ and these conditions mostly led to hydrolysis of the *p*-methoxybenzylidene ring and only a small amount of the desired product. Ultimately, treatment with TFA and sodium cyanoborohydride in CH₂Cl₂ afforded the product in 82% yield. Sulfation of the C-4 hydroxyl proceeded rapidly, and was followed by cleavage of the PMB group and C-6 sulfation to afford the disulfated product **72**. The target CS-E disaccharide **73** was obtained after silyl deprotection, saponification, and gel filtration chromatography using Sephadex G-10 resin and sodium ion-exchange chromatography with Sephadex C-25. In addition to generating the CS-E motif, this approach can also produce the CS-A disaccharide, a motif with only C-4 sulfation, if the second sulfation is not performed.

The shorter, less stepwise approach also readily yielded the CS-E tetrasaccharide. Oxidative cleavage of the *p*-methoxybenzylidene ring of **69** was performed with DDQ,⁴⁹ as the anomeric allyl group, unlike primary allyl protecting groups, is not sensitive to DDQ cleavage.⁵⁰ A small amount of TBS group loss was observed, most likely due to the acidity of the reaction. This was followed by sulfation of the resulting diol **74** with a large excess of sulfur trioxide-trimethylamine and cleavage of the silyl group and esters to afford 45 milligrams of **73**. Biological studies require nanogram to microgram amounts of material to perform, so the route afforded more than enough material to study the activity of the carbohydrate. Since this method is shorter, we decided to proceed with it for the synthesis of the CS-E tetrasaccharide.



Scheme 3.15: Stepwise synthesis of the CS-E disaccharide **73**. Me = methyl, All = allyl, *p*MP = *p*-methoxyphenyl, TBS = *t*-butyldimethylsilyl, Bz = benzoyl, TCA = trichloroacetyl, pyr = pyridine, TFA = trifluoroacetic acid, TMA = trimethylamine, Bu = butyl, PMB = *p*-methoxybenzyl, DDQ = 2,3-dichloro-5,6-dicyano-*p*-benzoquinone, AIBN = 2,2'-azobis(2-methylpropanitrile).



Scheme 3.16: Streamlined synthesis of the CS-E disaccharide **73**. Me = methyl, All = allyl, *p*MP = *p*-methoxyphenyl, TBS = *t*-butyldimethylsilyl, Bz = benzoyl, TCA = trichloroacetyl, pyr = pyridine, TMA = trimethylamine, Bu = butyl, DDQ = 2,3-dichloro-5,6-dicyano-*p*-benzoquinone, AIBN = 2,2'-azobis(2-methylpropionitrile).

The ^1H NMR spectrum of the pure CS-E disaccharide is shown in Figure 3.2. The doublet for the anomeric GlcA proton is located at 4.46 ppm and has a J value of 7.8 Hz. The anomeric GalNAc proton is at 4.54 ppm and, due to a long-range splitting with an allyl group proton, it is not the expected doublet, but a multiplet. The C-4 and C-6 protons of the GalNAc moiety are at 4.80 ppm and 4.05 – 4.02 ppm, respectively. The C-4 proton can appear as a singlet or have an extremely small splitting value.

STANDARD 1H OBSERVE

```

exp1 std1h
SAMPLE
date Dec 10 2002 dfrq DEC. & VT
solvent D2O dn 299.868 H1
file exp 36 H1
ACQUISITION exp 0
strq 299.868 dm nnn
tn 1.81 dnm 7900 C
rt 16384 dnr
sv 4500.5 wtf file
fb 2600 proc ft
bs 4 fn not used
tpwr 56 react
pw 14.0 werr
d1 1.000 wexp
tof 0 wbs
nt 256 wnt
ct 22
alock n
gain not used
flags
il n
in n
dp y
SP DISPLAY
wp -300.3
vs 3148.3
sc 151
wc 0
h2mm 250
is 12.59
rfl 500.00
rfp 754.6
th 0
ins 2
nm cdc ph 2.000
  
```

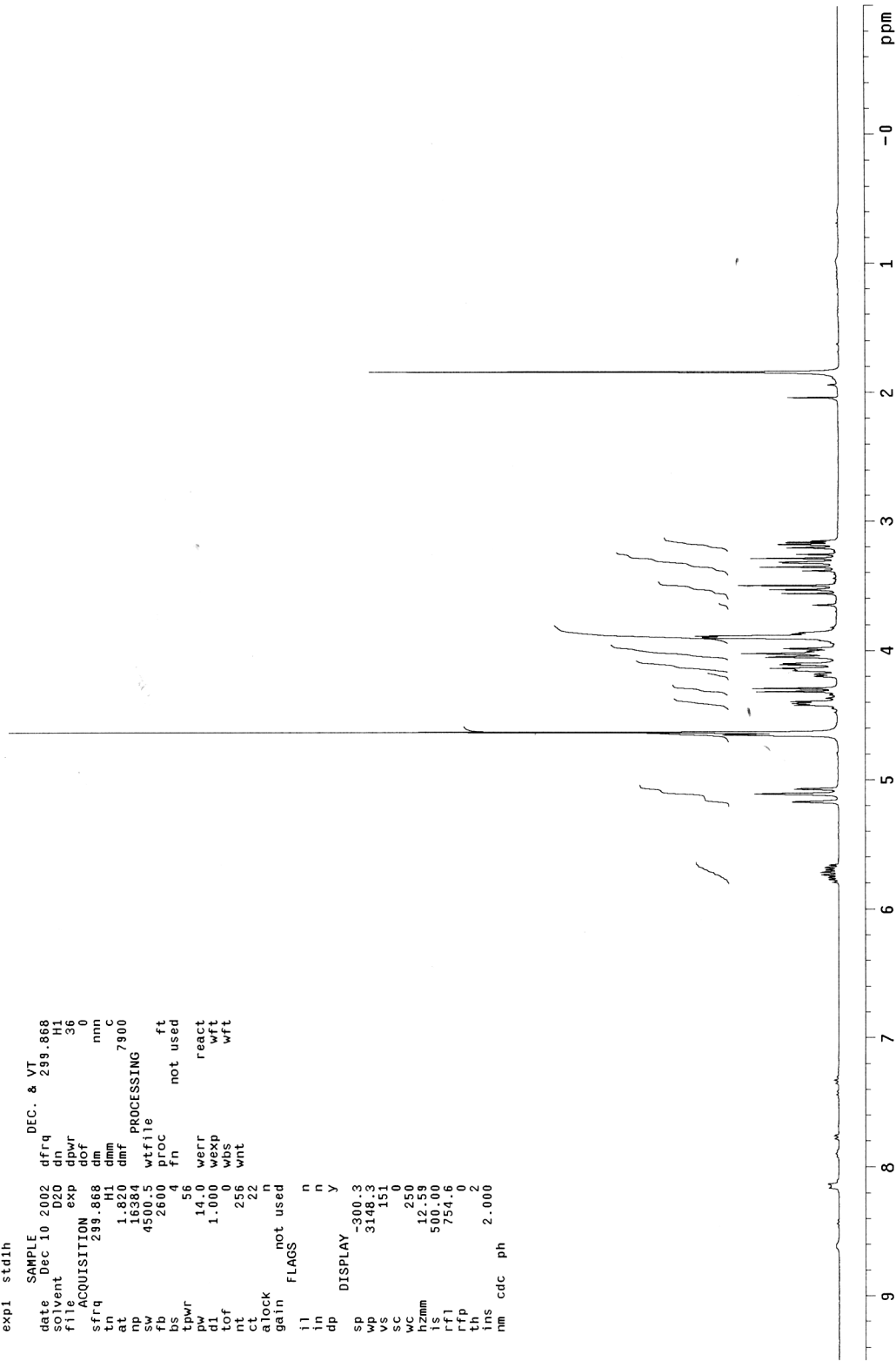
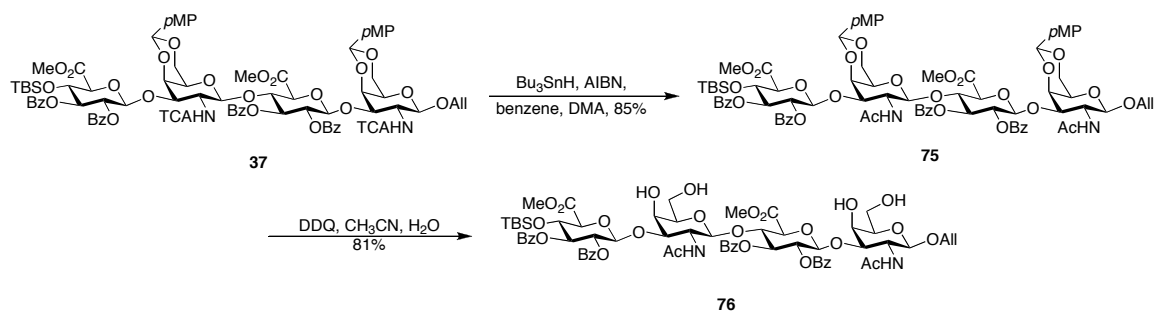
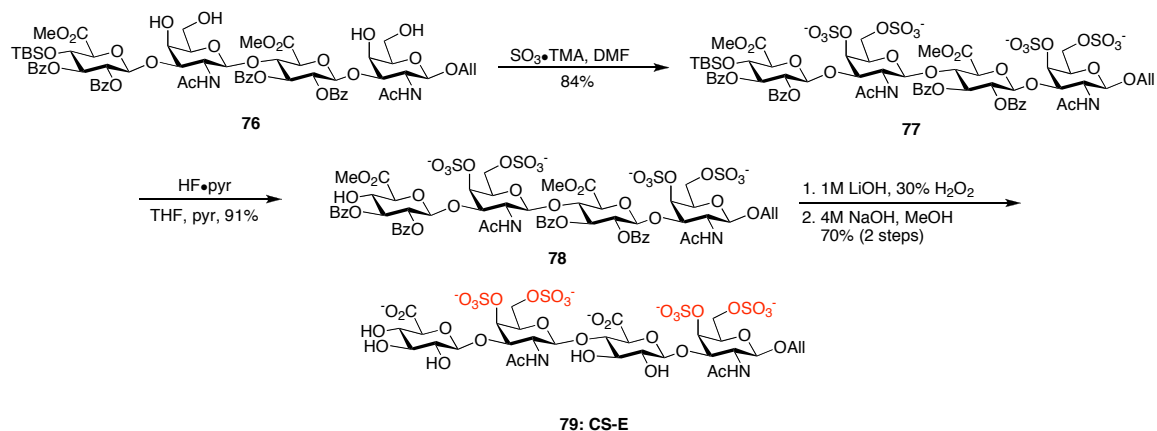


Figure 3.2: ¹H NMR (300 MHz, D₂O) of CS-E disaccharide 73.

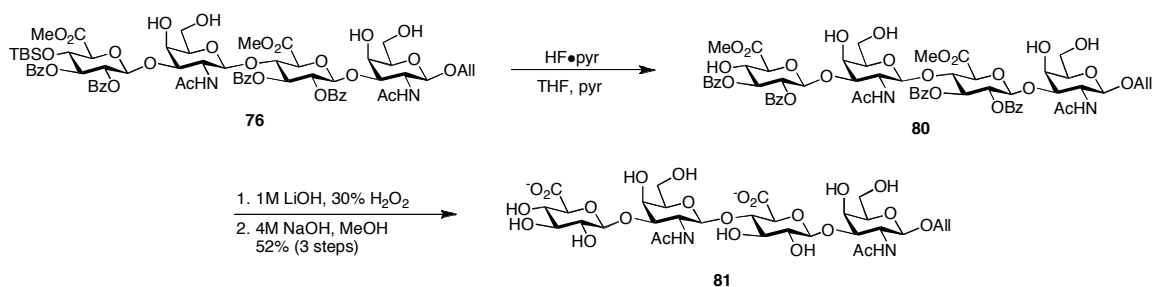
The synthesis of CS-E tetrasaccharide **79** began with generation of tetraol **76** through radical mediated formation of the acetamide followed by DDQ cleavage of the *p*-methoxybenzylidene acetal (Scheme 3.17). Unlike the reaction sequence for the formation of the CS-E disaccharide, the DDQ cleavage was performed in acetonitrile instead of methylene chloride. The change of solvents resulted in a shorter reaction time and eliminated loss of the TBS group. This tetraol is a key intermediate in the synthesis, as it can be used to generate several CS sulfation patterns (see Chapter 4). Elaboration of tetraol **76** through sulfation with sulfur trioxide-trimethylamine followed by deprotection of the silyl group and ester hydrolysis provided the desired CS-E tetrasaccharide **79** in 54% yield over three steps (Scheme 3.18). Sequential LiOOH-NaOH treatment was used during the saponification reaction to minimize β -elimination at the GlcA C-4 position,⁵¹ and the sulfation reaction was carefully monitored to ensure that the pH did not drop below pH 5.0. The unsulfated tetrasaccharide **81** was generated from tetraol **76** through cleavage of the TBS group and the ester protecting groups in a three-step reaction series to yield the final product (Scheme 3.19). Both products were purified by Sephadex G-25 gel filtration chromatography and the ¹H NMR spectra of the pure products are shown in Figures 3.3 and 3.4. Complete assignments were done with proton decoupling experiments, and the C-4 GalNAc protons of **79** were located at 4.85 and 4.79 ppm, indicating the presence of C-4 sulfation. The doublets of doublets ranging from 3.77 – 3.34 Hz are characteristic for the C-2, C-3 and C-4 protons of the GlcA monomers. With the three desired CS oligosaccharides synthesized, we began to investigate the biological activities of these molecules.



Scheme 3.17: Generation of key tetrasaccharide tetraol **76**. Me = methyl, All = allyl, *p*MP = *p*-methoxyphenyl, TBS = *t*-butyldimethylsilyl, Bz = benzoyl, TCA = trichloroacetyl, Bu = butyl, DDQ = 2,3-dichloro-5,6-dicyano-*p*-benzoquinone, AIBN = 2,2'-azobis(2-methylpropionitrile), DMA = *N,N*-dimethylacetamide.



Scheme 3.18: Generation of the CS-E tetrasaccharide **79**. Me = methyl, All = allyl, TBS = *t*-butyldimethylsilyl, Bz = benzoyl, pyr = pyridine, TMA = trimethylamine.



Scheme 3.19: Generation of the unsulfated CS tetrasaccharide **81**. Me = methyl, All = allyl, TBS = *t*-butyldimethylsilyl, Bz = benzoyl, pyr = pyridine, TMA = trimethylamine.

```

STANDARD PROTON PARAMETERS
exp1  s2pu1
date  SAMPLE      DEC. & VT
solvent Jun 16 2005  dfrq 599.655
file  D2O          dn   H1
      exp         dpwr 30
      dof         dof  0
ACQUISITION
sfrq  599.655    dm   nnn
tn    0.800      dmm  200
np    16000     dmf   1.0
sw    10000.0   dres  n
bs    not used  homo  n
ss    4         dfrq2 0
tpwr  55       dn2   0
pw    5.5      dpwr2 1
d1    1.000    dof2  0
tof   0        dm2   n
nt    1e+09    dmm2  c
ct    80       dmf2  200
alock gain      n     dseq2 1.0
      gain      n     dres2  n
      gain      n     homo2  n
il    n        dfrq3  0
in    n        dn3   0
dp    y        dpwr3  1
hs    nn       dof3  0
sp    -299.9   dm3   n
wp    4796.8  dmm3  c
vs    945     dmf3  200
sc    35      dseq3  1.0
wc    215     dres3  n
hzmm  22.28   homo3  n
ls1   431.73  gfs   0.550
ls2   2001.0  wfile not used
rfp   7       proc  ft
ins   cdc    ph    1.000
nm    32768  fn    32768
      math   f
      werr
      wexp
      wbs
      wnt
      wft

```

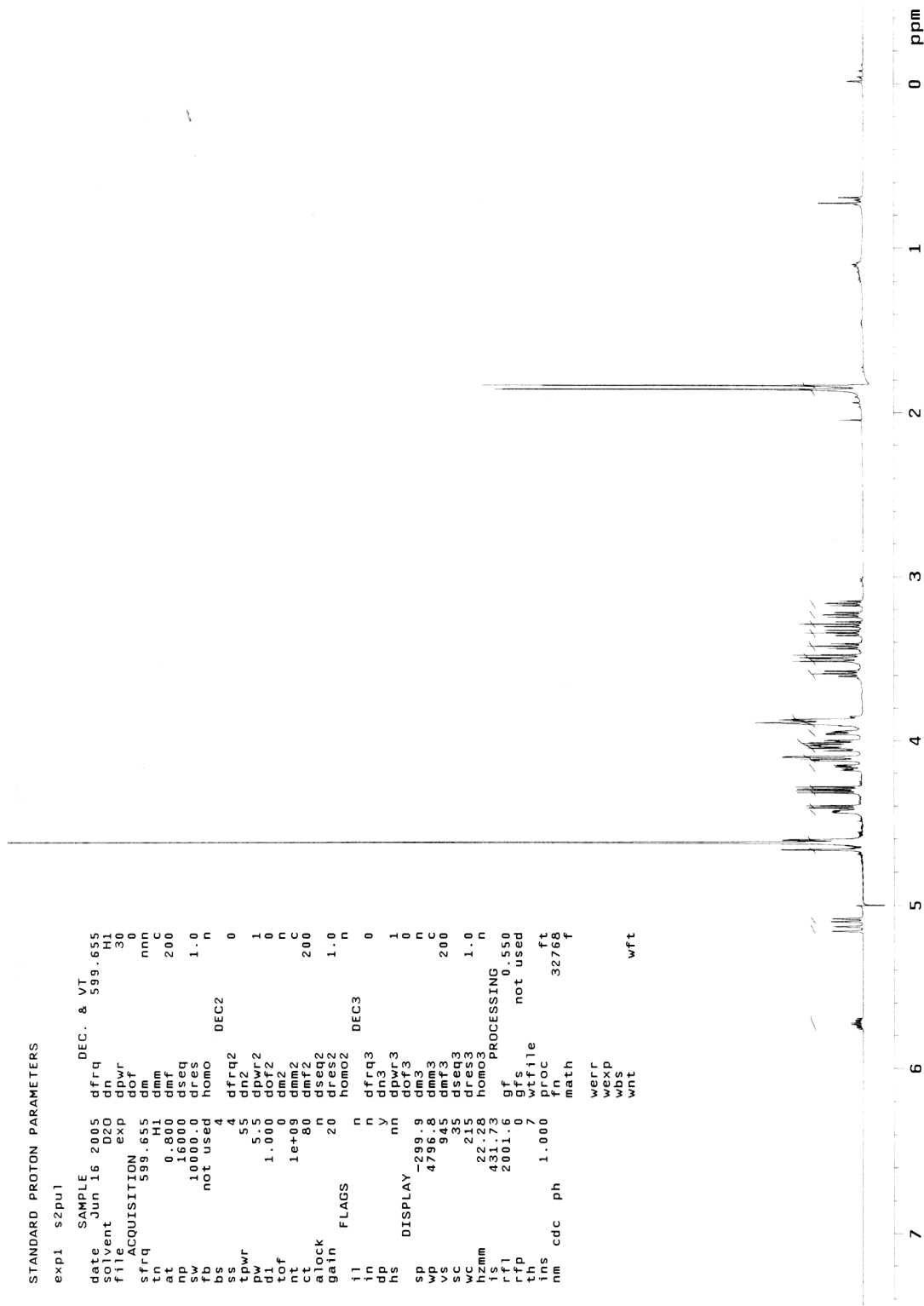
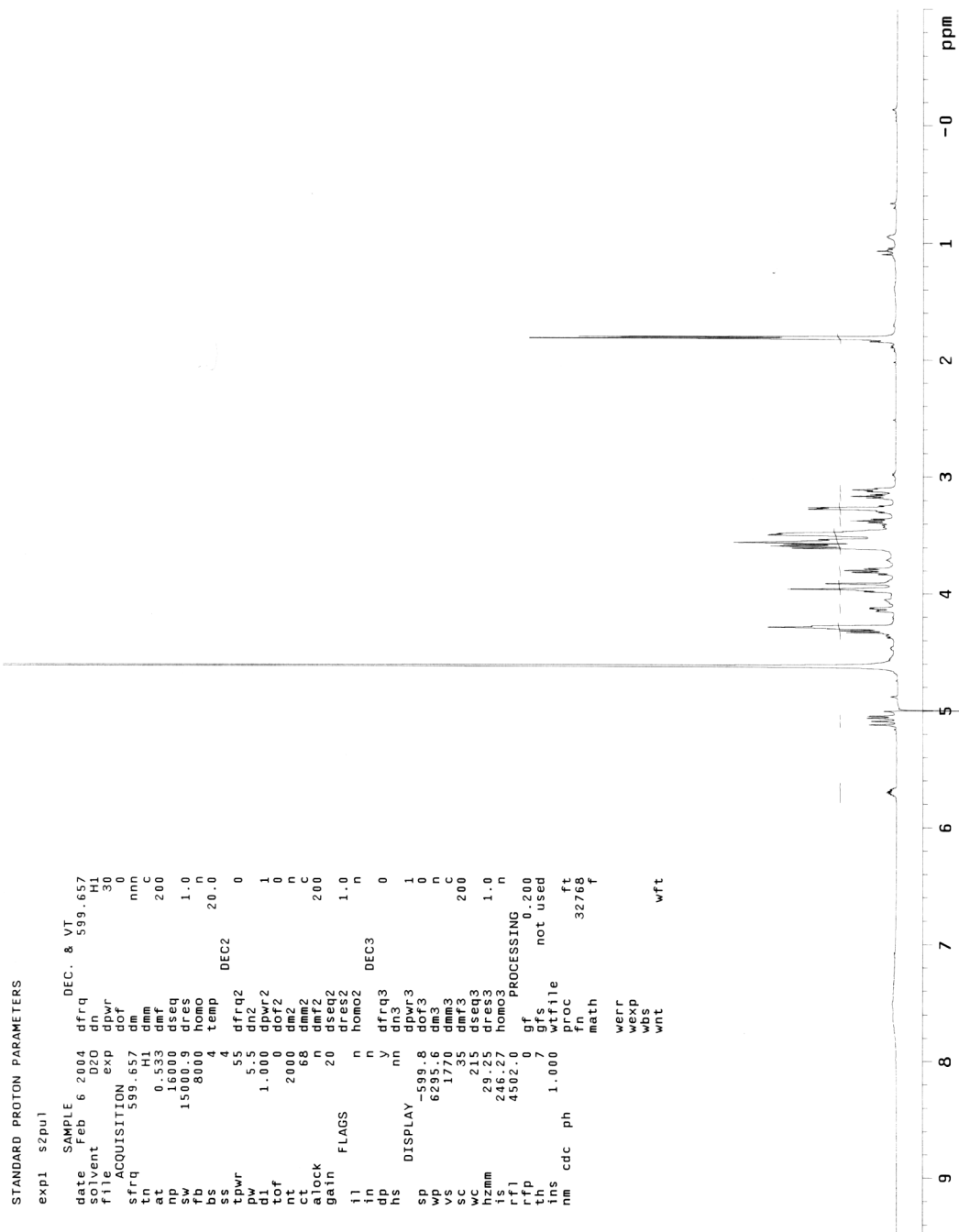


Figure 3.3: ¹H NMR (600 MHz, D₂O) of CS-E tetrasaccharide 79.



Neurobiological evaluation of synthetic CS oligosaccharides

To explore the abilities of **73**, **79**, and **81** to modulate neuronal growth, Cristal Gama cultured primary hippocampal neurons on poly-DL-ornithine-coated coverslips with or without each compound. After 48 h, the neurons were fixed, immunostained with anti-tau antibodies, and examined by confocal microscopy.⁵² Sulfated tetrasaccharide **79** exhibited striking effects on neuronal morphology and growth (Figure 3.5). The number of neurites emanating from the cell body was enhanced, and the growth of the major extension was dramatically stimulated by $39.3 \pm 3.6\%$ relative to the poly-DL-ornithine control. In contrast, sulfated disaccharide **73** and unsulfated tetrasaccharide **81** had no significant effects on neuronal outgrowth. Notably, these studies are the first biological

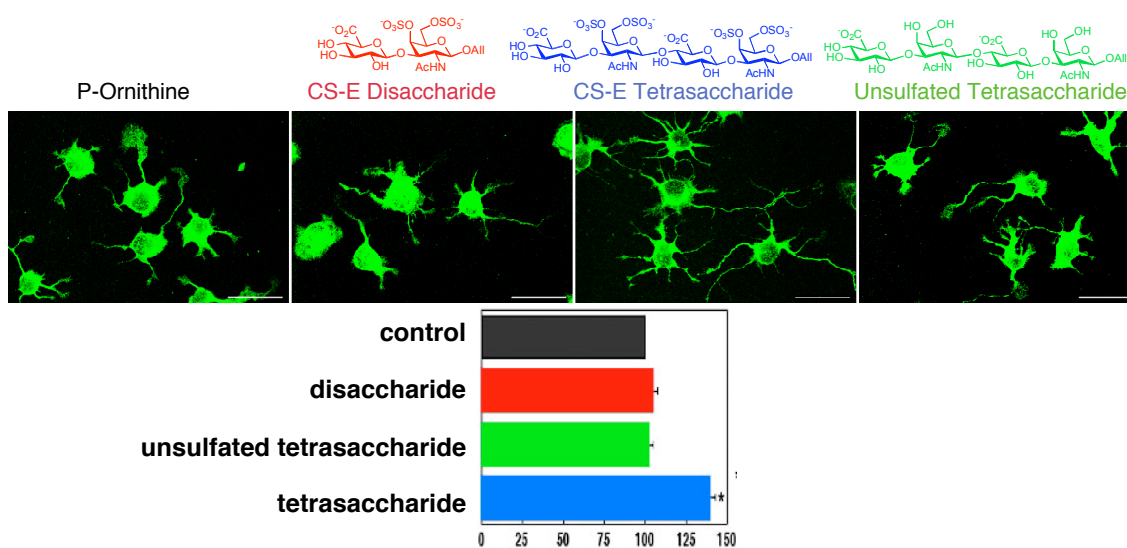


Figure 3.5: CS-E tetrasaccharide **79** stimulates the outgrowth of hippocampal neurons. Top: Immunofluorescence images of neurons 48 h after treatment with the indicated compound. Bottom: Statistical analysis of neurite length. * $p < 0.0001$.

investigation using well-defined CS structures. We find that a specific sulfation motif, CS-E, promotes the outgrowth of neurons, and a tetrasaccharide was identified as a minimum structural motif with biological activity. Sulfation was a prerequisite for function, as the unsulfated tetrasaccharide failed to promote neurite outgrowth.

Discussion

One of the primary goals of this work was to develop an efficient, modular synthesis of CS oligosaccharides. Starting from β -D-glucose pentaacetate and D-galactose, we generated gram quantities of key disaccharide intermediate **61** and key tetrasaccharide intermediate **37**. From these compounds, we were able to synthesize CS-E di- and tetrasaccharides and an unsulfated tetrasaccharide in milligram amounts, more than enough needed for biological studies that usually require nanogram to microgram amounts of material. The synthesis is versatile enough to create a library of CS oligosaccharides with differing sulfation patterns, as will be demonstrated in Chapter 4.

The ability of the CS-E tetrasaccharide to stimulate the outgrowth of hippocampal neurons suggests that CS GAGs may be important in directing neuronal growth during the formation of the central nervous system. The observed effects of CS-E tetrasaccharide **79** support previous studies implicating the CS-E motif in the growth and development of neurons. For example, CS-E is found on the protein appican, an isoform of the amyloid precursor protein that exhibits neurotrophic activity.⁵³ CS-E is also associated with the proteoglycans syndecan-1 and -4, neuroglycan C and phosphacan.^{13,54} It is a motif enriched in the developing brain^{13,14} and may line axonal growth tracts to guide neurons

to their proper targets. Moreover, polysaccharides enriched in the CS-E motif have been shown to promote the outgrowth of neurons.¹⁰

The discovery that CS small molecules can recapitulate the activities of larger polysaccharides was significant. As mentioned earlier, heparan sulfate glycosaminoglycan protein-binding motifs are generally tetra- and pentasaccharides,^{17,18} but previous studies with CS-protein interactions have suggested binding motifs of octasaccharides or larger.¹⁹ The ability of the CS-E tetrasaccharide to stimulate growth indicates that CS binding proteins can recognize this small, synthetically accessible unit. It also validates our approach to use CS small molecules to understand the structural determinants and mechanisms of CS activity.

Since the unsulfated CS tetrasaccharide had no activity with hippocampal neurons, sulfation must be crucial for the growth-promoting effects observed. It is unknown whether a specific orientation of the sulfate groups is necessary for activity, perhaps by engaging growth factors or other proteins. Through synthesis of a variety of sulfation patterns (see Chapter 4) and discovery of new CS protein binding partners with biochemical assays (see Chapter 4) and microarrays (see Chapter 5), we plan to elucidate the molecular determinants necessary for CS activity and establish whether CS acts through a “sulfation code” where proteins recognize distinct sulfation sequences.

Conclusion

In summary, we have developed a modular synthesis of CS oligosaccharides with defined sulfation patterns, synthesized di- and tetrasaccharides bearing the CS-E motif, and discovered that the CS-E tetrasaccharide stimulates the growth and differentiation of neurons. Our studies provide the first, direct investigations into the structure-activity relationships of CS using homogeneous, synthetic molecules.⁵² The findings indicate that the CS-E sulfation motif is likely an important structural determinant for CS activity *in vivo*, endowing CS polysaccharides with the ability to induce neuronal growth. CS small molecules should provide new chemical approaches to understand and manipulate neuronal growth and regeneration.

Experimental Procedures for Chapter 3

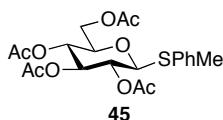
General methods

Unless stated otherwise, reactions were performed in flame-dried glassware under a nitrogen or an argon environment, using freshly-distilled solvents. Acetonitrile used for LC/MS was HPLC grade, and all aqueous solutions were made from nanopure water. All other commercially obtained reagents were used as received. Thin-layer chromatography (TLC) was performed using E. Merck silica gel 60 F254 precoated plates (0.25 mm). Visualization of the developed chromatogram was performed by fluorescence quenching, cerium ammonium molybdate stain, or ninhydrin stain, as necessary. ICN silica gel (particle size 0.032 - 0.063 mm) was used for flash chromatography. Gel filtration chromatography (Sephadex® LH-20, G-10 and G-25 ultrafine) and ion exchange chromatography [Sephadex® C-25 (Na⁺)] were used in order to achieve purification of the final products.

¹H NMR and proton decoupling spectra were recorded on Varian Mercury 300 (300 MHz) and Varian Mercury 600 (600 MHz) spectrometers and the ¹H NMR spectra are reported in parts per million (δ) relative to the residual solvent peak. Data for ¹H are reported as follows: chemical shift (δ ppm), multiplicity (s = singlet, d = doublet, t = triplet, q = quartet, m = multiplet), coupling constant in Hz, and integration. ¹³C NMR spectra were obtained on a Varian Mercury 300 (75 MHz) spectrometer and are reported in parts per million (δ) relative to the residual solvent peak. IR spectra were recorded on a Perkin Elmer Paragon 1000 spectrometer and are reported in terms of frequency of absorption (cm⁻¹). A JASCO P-1010 was used to measure optical rotation. Mass spectra

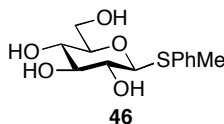
were obtained from the Protein/Peptide MicroAnalytical Laboratory on a Perkin Elmer/Sciex API 365 triple quadrupole/electrospray tandem mass spectrometer and the Mass Spectrometry Facility at the California Institute of Technology on a JEOL JMS-600H High Resolution Mass Spectrometer.

Synthetic methods

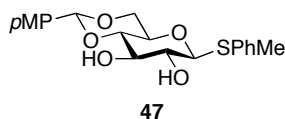


***p*-Methylphenyl 2,3,4,6-Tetra-*O*-acetyl-1-thio- β -D-glucopyranoside (45).**⁵⁵ β -D-Glucose pentaacetate (2.0 g, 5.1 mmol) was dissolved in CH₂Cl₂ (20 mL). *p*-Toluenethiol (0.7 g, 5.6 mmol) was added and the solution was cooled to -20 °C. SnCl₄ in CH₂Cl₂ (1 M in CH₂Cl₂, 3.6 mL, 3.6 mmol) was added dropwise over a period of 5 min, and the reaction was stirred at -20 °C for 3 h. The reaction was quenched with saturated aqueous NaHCO₃ (10 mL) and warmed to rt. The organic layer was extracted, dried (MgSO₄), filtered, and concentrated to afford a yellow-white solid. Purification by flash chromatography (25% → 30% EtOAc:hexanes) yielded **45** (2.14 g, 92%) as a white solid. The spectral data agreed with published data. R_f 0.57 (50% EtOAc:hexanes). ¹H NMR (300 MHz, CDCl₃): δ = 7.41 (d, *J* = 8.4 Hz, 2H, SC₆H₄Me), 7.12 (d, *J* = 8.1 Hz, 2H, SC₆H₄Me), 5.20 (t, *J* = 9.45 Hz, 1H), 5.01 (t, *J* = 9.8 Hz, 1H), 4.92 (t, *J* = 9.6 Hz, 1H), 4.63 (d, *J* = 10.2 Hz, 1H), 4.20 – 4.15 (m, 2H), 3.69 (dq, *J* = 3.0, 2.1 Hz, 1H), 2.34 (s, 3H, SPhCH₃), 2.08 (s, 3H, OC(O)CH₃), 2.08 (s, 3H, OC(O)CH₃), 2.01 (s, 3H,

OC(O)CH₃), 1.98 (s, 3H, OC(O)CH₃). ESI MS: *m/z*: calcd for C₂₁H₂₆NaO₉S: 477.12; found: 477.0 [*M* + Na]⁺.

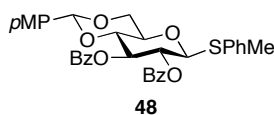


***p*-Methylphenyl-1-thio- β -D-glucopyranoside (46).**⁵⁵ **45** (9.1 g, 20 mmol) was dissolved in MeOH (80 mL) and CH₂Cl₂ (40 mL). To this solution was added K₂CO₃ (2.8 g, 20 mmol), and the reaction was stirred at rt until all of the starting material had been converted to the lowest R_f product. The reaction was acidified to pH 6 with Dowex 50X8-200, filtered, and concentrated to afford **46** (5.6 g, 99%) as a white solid. The spectral data agreed with published data. R_f 0.11 (75% EtOAc:hexanes). ¹H NMR (300 MHz, CD₃OD): δ = 7.26 (d, *J* = 8.4 Hz, 2H, SC₆H₄Me), 7.12 (d, *J* = 8.4 Hz, 2H, SC₆H₄Me), 4.57 (d, *J* = 9.6 Hz, 1H), 3.73 (dd, *J* = 11.9, 1.5 Hz, 1H), 3.58 (dd, *J* = 12.0, 4.8 Hz, 1H), 3.34 – 3.21 (m, 3H), 3.11 (t, *J* = 9.5 Hz, 1H), 2.28 (s, 3H, SPhCH₃). ESI MS: *m/z*: calcd for C₁₃H₁₈NaO₅S: 309.08; found: 309.0 [*M* + Na]⁺.



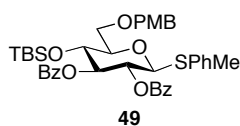
***p*-Methylphenyl 4,6-*O*-*p*-methoxybenzylidene-1-thio- β -D-glucopyranoside (47).** The procedure for the preparation of **47** was adapted from Ye *et. al.*⁵⁶ *p*-Methylphenyl-1-thio- β -D-glucopyranoside **46** (36.7 g, 128 mmol) was dissolved in DMF (30.0 mL) and CH₃CN (300 mL). *p*-Anisaldehyde dimethyl acetal (44.0 mL, 256 mmol) and DL-10-

camphorsulfonic acid (6.00 g, 25.6 mmol) were added. The reaction was stirred at rt for 12 h. The reaction was quenched with TEA and concentrated to afford an orange syrup. The product was purified by flash chromatography (50% → 70% EtOAc:hexanes) to afford **47** (36 g, 70%) as a white crystalline solid. R_f 0.26 (50% EtOAc:hexanes). $[\alpha]_D^{21} = -38$ ($c = 1.0$, CH_2Cl_2); IR (thin film on NaCl): $\nu = 3447, 2869, 1614, 1518, 1250, 1104, 1084, 1033 \text{ cm}^{-1}$; ^1H NMR (300 MHz, CDCl_3): $\delta = 7.43$ (d, $J = 8.1$ Hz, 2H, $\text{SC}_6\text{H}_4\text{Me}$), 7.39 (d, $J = 9.0$ Hz, 2H, $\text{C}_6\text{H}_4\text{OMe}$), 7.15 (d, $J = 7.5$ Hz, 2H, $\text{SC}_6\text{H}_4\text{Me}$), 6.88 (d, $J = 9.0$ Hz, 2H, $\text{C}_6\text{H}_4\text{OMe}$), 5.48 (s, 1H, MeOPhCH), 4.56 (d, $J = 9.9$ Hz, 1H, H-1), 4.35 (dd, $J = 3.9, 10.5$ Hz, 1H), 3.85 – 3.72 (m, 5H), 3.50 – 3.39 (m, 3H), 2.80 (br s, 1H, OH), 2.67 (br s, 1H, OH), 2.36 (s, 3H, SPhCH_3); ^{13}C NMR (75 MHz, CDCl_3): $\delta = 138.8, 138.2, 133.6, 132.1, 129.9, 129.4, 127.7, 113.7, 101.8, 88.7, 80.2, 74.5, 72.5, 70.5, 68.6, 55.3, 21.2$; HR-FAB MS: m/z : calcd for $\text{C}_{21}\text{H}_{25}\text{O}_6\text{S}$: 405.1372; found: 405.1359 [$M + \text{H}$] $^+$.



***p*-Methylphenyl 2,3-di-*O*-benzoyl-4,6-*O*-*p*-methoxybenzylidene-1-thio- β -D-glucopyranoside (48).** **47** (23.7 g, 58.6 mmol) was dissolved in CH_2Cl_2 (670 mL). In a separate flask, benzoyl chloride (17.0 mL, 146 mmol) was added dropwise to a solution of 4-(dimethylamino)pyridine (25.1 g, 205 mmol) in CH_2Cl_2 (225 mL). The benzoyl chloride/4-(dimethylamino)pyridine solution was then slowly added to the solution of **47**. An additional volume of CH_2Cl_2 (19.0 mL) was used to complete the transfer of solution. The reaction was allowed to stir at rt for 25 min and then quenched with saturated

aqueous NaHCO₃. The aqueous layer was extracted with CH₂Cl₂ (2x). The combined organic layers were washed with brine, dried over Na₂SO₄, filtered, and concentrated to yield a pale yellow solid. This crude material was washed with MeOH and crystallization from EtOAc afforded **48** as a white solid (31 g, 86%). R_f 0.43 (30% EtOAc:hexanes). [α]_D²² = +25 (c = 0.42, CH₂Cl₂); IR (thin film on NaCl): ν = 2934, 1740, 1735, 1730, 1715, 1700, 1617, 1614, 1517, 1272, 1251, 1095 cm⁻¹; ¹H NMR (300 MHz, CDCl₃): δ = 7.98 – 7.90 (m, 4H, ArH), 7.56 – 7.30 (m, 10H, ArH), 7.12 (d, J = 8.1 Hz, 2H, SC₆H₄Me), 6.82 (d, J = 8.7 Hz, 2H, C₆H₄OMe), 5.76 (dd, J = 9.3, 9.3 Hz, 1H, H-3), 5.49 (s, 1H, MeOPhCH), 5.43 (dd, J = 9.3, 9.3 Hz, 1H, H-2), 4.95 (d, J = 10.5 Hz, 1H, H-1), 4.43 (dd, J = 4.5, 10.8 Hz, 1H), 3.90 – 3.82 (m, 2H), 3.76 – 3.67 (m, 4H), 2.35 (s, 3H, SPhCH₃); ¹³C NMR (75 MHz, CDCl₃): δ = 165.6, 165.2, 160.1, 138.8, 133.8, 133.3, 133.1, 129.9, 129.8, 129.8, 129.4, 129.3, 129.2, 128.4, 128.3, 127.9, 127.5, 113.6, 101.5, 87.3, 78.5, 73.4, 71.1, 71.0, 68.5, 55.3, 21.3; HR-FAB MS: m/z: calcd for C₃₅H₃₃O₈S: 613.1896; found: 613.1879 [M + H]⁺.

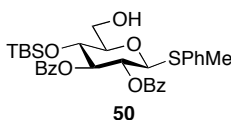


***p*-Methylphenyl 2,3-di-*O*-benzoyl-4-*O*-*tert*-butyldimethylsilyl-6-*O*-*p*-methoxybenzyl-1-thio-β-D-glucopyranoside (49).** The procedure for the regioselective ring opening of **48** was adapted from Johansson *et al.*²⁶ Typically, **48** (12.0 g, 19.6 mmol) was dissolved in DMF (261 mL) and sodium cyanoborohydride (6.15 g, 97.9 mmol), and activated 3Å powdered molecular sieves (12.0 g) were added to the solution. The reaction was cooled to 0 °C, and trifluoroacetic acid (15.3 mL, 196 mmol) was added dropwise to the

reaction. The reaction was stirred at 0 °C for 1 h, and then allowed to warm to rt. After stirring at rt for 1 d, the reaction was filtered, diluted with CH₂Cl₂, and quenched with cold saturated aqueous NaHCO₃. The aqueous layer was separated and extracted with CH₂Cl₂ (2x). The combined organic layers were washed with saturated aqueous NaHCO₃ (1x) and brine (1x), dried over Na₂SO₄, filtered, and concentrated. To remove the remaining sodium cyanoborohydride, the crude material was re-dissolved in CH₂Cl₂ (250 mL) and washed with brine (3x). The organic layer was dried over Na₂SO₄, filtered, and concentrated to afford a white solid containing the desired alcohol. R_f 0.23 (30% EtOAc:hexanes).

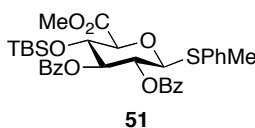
The crude alcohol was dissolved in CH₂Cl₂ (476 mL), TEA (8.20 mL, 58.6 mmol) was added, and the reaction cooled to 0 °C. *tert*-Butyldimethylsilyl trifluoromethanesulfonate (11.2 mL, 48.8 mmol) was added dropwise to the reaction. The reaction was allowed to warm to rt and stirred for 3 h. It was then quenched with saturated aqueous NaHCO₃ and diluted with CH₂Cl₂. The aqueous layer was separated and extracted with CH₂Cl₂ (3x). The combined organic layers were washed with brine, dried over Na₂SO₄, filtered, and concentrated to afford an orange syrup. The product was purified by flash chromatography (10% → 12% EtOAc:hexanes) to afford **49** (13 g, 94%) as a white foam. R_f 0.64 (30% EtOAc:hexanes). $[\alpha]_D^{22} = +36$ ($c = 1.0$, CH₂Cl₂); IR (thin film on NaCl): $\nu = 2953, 2928, 2856, 1734, 1612, 1602, 1513, 1451, 1272, 1251, 1106, 1089, 1069$ cm⁻¹; ¹H NMR (300 MHz, CDCl₃): $\delta = 7.92 - 7.87$ (m, 4H, ArH), $7.51 - 7.27$ (m, 10H, ArH), 7.03 (d, $J = 7.8$ Hz, 2H, SC₆H₄Me), $6.94 - 6.91$ (m, 2H, ArH), 5.59 (dd, $J = 9.2, 9.2$ Hz, 1H, H-3), 5.30 (dd, $J = 9.6, 9.6$ Hz, 1H, H-2), 4.88 (d, $J = 9.6$ Hz, 1H, H-1), 4.60 (d, $J =$

11.4 Hz, 1H, CH_2PhOMe), 4.51 (d, $J = 11.7$ Hz, 1H, CH_2PhOMe), 4.01 (dd, $J = 9.0, 9.0$ Hz, 1H, H-4), 3.84 – 3.64 (m, 6H, H-5, H-6, H-6, PhOCH_3), 2.32 (s, 3H, SPhCH_3), 0.74 (s, 9H, $(\text{CH}_3)_3\text{CSi}$), 0.02 (s, 3H, CH_3Si), -0.22 (s, 3H, CH_3Si); ^{13}C NMR (75 MHz, CDCl_3): $\delta = 165.9, 165.3, 159.2, 138.2, 133.4, 133.1, 133.0, 130.5, 129.9, 129.9, 129.8, 129.7, 129.5, 129.3, 128.6, 128.4, 128.3, 113.9, 86.1, 81.0, 77.5, 73.3, 71.3, 69.4, 68.7, 55.5, 25.9, 21.5, 18.1, -3.9, -4.4$; HR-FAB MS: m/z : calcd for $\text{C}_{41}\text{H}_{47}\text{O}_8\text{SSi}$: 727.2785; found: 727.2761 $[M]^+$.



***p*-Methylphenyl 2,3-di-*O*-benzoyl-4-*O*-*tert*-butyldimethylsilyl-1-thio- β -D-glucopyranoside (50).** The preparation of **50** was performed by using a modified procedure from Zhang *et al.*⁴⁹ In a flask covered with aluminum foil, **49** (13.2 g, 18.1 mmol) was dissolved in CH_2Cl_2 (440 mL). Water (23.0 mL) and 2,3-dichloro-5,6-dicyano-1,4-benzoquinone (4.93 g, 21.7 mmol) were added. The reaction was stirred at rt for 13 h. The reaction was then quenched with aqueous NaHCO_3 , and water was added to dissolve all solids. The aqueous layer was separated and extracted with CH_2Cl_2 (3x). The combined organic layers were washed with brine, dried over Na_2SO_4 , filtered, and concentrated to yield a peach solid. The product was purified by flash chromatography (40% CH_2Cl_2 :hexanes \rightarrow 100% CH_2Cl_2 \rightarrow 10% EtOAc: CH_2Cl_2) to afford **50** (9.4 g, 86%) as a white foam. R_f 0.41 (20% EtOAc:hexanes). $[\alpha]_D^{22} = +62$ ($c = 1.0, \text{CH}_2\text{Cl}_2$); IR (thin film on NaCl): $\nu = 3442, 2951, 2928, 2856, 1733, 1602, 1493, 1451, 1273, 1088, 1070, 1027 \text{ cm}^{-1}$; ^1H NMR (300 MHz, CDCl_3): $\delta = 7.92 - 7.88$ (m, 4H, ArH), 7.52

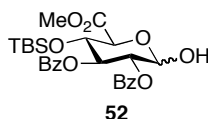
– 7.45 (m, 2H, ArH), 7.38 – 7.32 (m, 6H, ArH), 7.12 (d, $J = 8.1$ Hz, 2H, SC₆H₄Me), 5.62 (dd, $J = 9.3, 9.3$ Hz, 1H, H-3), 5.29 (dd, $J = 9.6, 9.6$ Hz, 1H, H-2), 4.93 (d, $J = 9.9$ Hz, 1H, H-1), 4.02 – 3.92 (m, 2H), 3.81 – 3.73 (m, 1H), 3.60 – 3.55 (d, $J = 11.4$ Hz, 1H), 2.35 (s, 3H, SPhCH₃), 1.95 (br s, 1H, OH), 0.76 (s, 9H, (CH₃)₃CSi), 0.07 (s, 3H, CH₃Si), -0.20 (s, 3H, CH₃Si); ¹³C NMR (75 MHz, CDCl₃): $\delta = 165.9, 165.4, 138.7, 133.5, 133.3, 133.2, 130.0, 130.0, 129.9, 129.8, 129.4, 128.5, 128.5, 128.4, 86.4, 81.1, 77.2, 71.3, 69.0, 62.0, 25.9, 21.6, 18.2, -3.9, -4.3$; HR-FAB MS: m/z : calcd for C₃₃H₄₁O₇SSi: 609.2342; found: 609.2321 [$M + H$]⁺.



***p*-Methylphenyl (methyl 2,3-di-*O*-benzoyl-4-*O*-*tert*-butyldimethylsilyl-1-thio- β -D-glucopyranosyluronate (51).** **50** (9.42 g, 15.5 mmol) was dissolved in DMF (115 mL). Pyridinium dichromate (34.9 g, 92.8 mmol) was added, and the reaction was stirred at rt for 3 d. To precipitate and remove the chromium salts, EtOAc was added, and the reaction was filtered and concentrated (3x). The remaining salts were removed by flash chromatography (100% EtOAc) to yield a white foam containing the desired carboxylic acid. R_f 0.17 (30% EtOAc:hexanes).

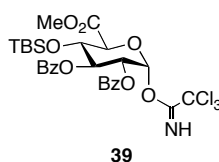
The crude acid was placed in a round bottom flask that had no scratches, dissolved in CH₂Cl₂ (187 mL), put behind a blast shield, and cooled to 0 °C. Using a glass pipet with a rounded tip, diazomethane⁵⁷ (93.0 mL, 0.2 M in diethyl ether, 18.6 mmol) was slowly added. After stirring at 0 °C for 1 h, a few drops of glacial acetic acid were added until

the reaction turned colorless. The reaction mixture was then concentrated and purified by flash chromatography (10% → 15% EtOAc:hexanes) to yield **51** (6.0 g, 61%) as a white solid. R_f 0.67 (30% EtOAc:hexanes). $[\alpha]_D^{22} = +54$ ($c = 1.0$, CH_2Cl_2); IR (thin film on NaCl): $\nu = 3443, 2953, 2928, 2857, 1732, 1601, 1493, 1451, 1437, 1269, 1085, 1069$ cm^{-1} ; ^1H NMR (300 MHz, CDCl_3): $\delta = 7.90 - 7.86$ (m, 4H, ArH), 7.52 – 7.46 (m, 2H, ArH), 7.38 – 7.31 (m, 6H, ArH), 7.10 (d, $J = 8.1$ Hz, 2H, $\text{SC}_6\text{H}_4\text{Me}$), 5.59 (dd, $J = 9.3, 9.3$ Hz, 1H, H-3), 5.30 (dd, $J = 9.6, 9.6$ Hz, 1H, H-2), 4.90 (d, $J = 9.9$ Hz, 1H, H-1), 4.26 (dd, $J = 9.2, 9.2$ Hz, 1H, H-4), 4.08 (d, $J = 8.7$ Hz, 1H, H-5), 3.82 (s, 3H, CO_2CH_3), 2.33 (s, 3H, SPhCH_3), 0.71 (s, 9H, $(\text{CH}_3)_3\text{CSi}$), -0.05 (s, 3H, CH_3Si), -0.22 (s, 3H, CH_3Si); ^{13}C NMR (75 MHz, CDCl_3): $\delta = 168.3, 168.3, 165.9, 165.3, 138.8, 133.7, 133.4, 133.4, 130.0, 130.0, 130.0, 129.7, 129.5, 128.5, 128.2, 87.2, 80.4, 76.6, 70.9, 70.7, 52.8, 25.6, 21.4, 18.0, -4.2, -4.9$; HR-FAB MS: m/z : calcd for $\text{C}_{34}\text{H}_{41}\text{O}_8\text{SSi}$: 637.2291; found: 637.2284 $[M + \text{H}]^+$.



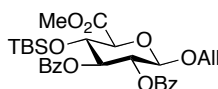
Methyl 2,3-di-O-benzoyl-4-O-tert-butyltrimethylsilyl- α/β -D-glucopyranosyluronate (52). **51** (6.09 g, 9.56 mmol) was dissolved in CH_2Cl_2 (67.0 mL) and water (0.70 mL) was added. A solution was prepared containing 2.93 g *N*-iodosuccinimide, 127 mL CH_2Cl_2 , 3.10 mL THF, and 78.0 μL triflic acid. 130 mL of this solution was slowly added to the reaction mixture via an additional funnel. The reaction stirred at rt for 5.5 h. It was then quenched with 1 M $\text{Na}_2\text{S}_2\text{O}_3$ and diluted with CH_2Cl_2 . The aqueous layer was separated and extracted with CH_2Cl_2 (3x). The combined organic layers were washed

with brine, dried over Na₂SO₄, filtered, and concentrated. The product was purified by flash chromatography (15% → 30% EtOAc:hexanes) to afford **52** (4.3 g, 84%, 6.2β:1α) as a white foam. R_f 0.30, 0.36 (30% EtOAc:hexanes). [α]_D²² = +99 (c = 1.0, CH₂Cl₂); IR (thin film on NaCl): ν = 3455, 2954, 2930, 2857, 1732, 1602, 1451, 1275, 1110, 1070 cm⁻¹; ¹H NMR (300 MHz, CDCl₃): δ = 8.18 – 8.07 (m, 4H, ArH), 7.99 – 7.90 (m, 4H, ArH), 7.69 – 7.31 (m, 12H, ArH), 6.55 (d, J = 3.3 Hz, 1H, H-1, α), 5.94 (dd, J = 9.0, 9.9 Hz, 1H), 5.72 – 5.58 (m, 3H), 5.22 – 5.14 (m, 2H), 4.62 (d, J = 9.3 Hz, 1H, H-1, β), 4.40 – 4.27 (m, 2H), 4.13 (d, J = 9.3 Hz, 1H), 3.81 (s, 3H, CO₂CH₃), 3.80 (s, 3H, CO₂CH₃), 3.46 (d, J = 3.6 Hz, 1H), 0.76 (s, 9H, (CH₃)₃CSi), 0.75 (s, 9H, (CH₃)₃CSi), -0.01 (s, 6H, CH₃Si), -0.15 (s, 6H, CH₃Si); ¹³C NMR (75 MHz, CDCl₃): δ = 169.8, 169.0, 168.7, 167.4, 167.3, 166.1, 165.9, 165.0, 134.2, 133.9, 133.8, 133.6, 133.4, 130.3, 130.2, 130.1, 129.9, 129.1, 129.0, 128.8, 128.6, 128.6, 92.2, 90.9, 75.8, 74.8, 74.6, 74.6, 72.5, 72.4, 72.3, 71.1, 70.5, 70.2, 52.9, 25.7, 25.6, 18.0, -4.2, -4.9; HR-FAB MS: m/z: calcd for C₂₇H₃₅O₉Si: 531.2050; found: 531.2041 [M + H]⁺.



Methyl 2,3-di-O-benzoyl-4-O-tert-butyldimethylsilyl-α-D-glucopyranosyluronate trichloroacetimidate (39). The preparation of **39** was performed by using a procedure modified from Driguez *et al.*⁵⁸ **52** (3.32 g, 6.26 mmol) was azeotroped by co-evaporated with toluene (2 x 20 mL) and dried under vacuum overnight. It was then dissolved in CH₂Cl₂ (49.0 mL). Trichloroacetonitrile (3.80 mL, 37.5 mmol) and Cs₂CO₃ (0.820 g,

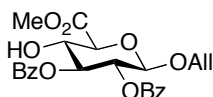
2.50 mmol) were added. After stirring at rt for 4 h, additional trichloroacetonitrile (0.950 mL, 9.50 mmol) and Cs₂CO₃ (0.200 g, 0.600 mmol) were added. The reaction was allowed to stir an additional 4 h and then concentrated. The product was purified by flash chromatography (10% EtOAc:hexanes + 0.1% TEA) to afford **39** (3.8 g, 89%), with a trace amount of the β anomer, as a white foam. The compound was stored at -20 °C and under Ar to prevent hydrolysis and rearrangement of the imidate to an amide by-product, and was stable under these conditions. R_f 0.57 (30% EtOAc:hexanes). [α]_D²² = +99 (*c* = 1.0, CH₂Cl₂); IR (thin film on NaCl): ν = 3343, 2954, 2930, 2858, 1757, 1735, 1676, 1602, 1451, 1315, 1267, 1111, 1095 cm⁻¹; ¹H NMR (300 MHz, CDCl₃): δ = 8.60 (s, 1H, C=NH), 7.96 – 7.87 (m, 4H, ArH), 7.53 – 7.29 (m, 6H, ArH), 6.74 (d, *J* = 3.9 Hz, 1H, H-1), 5.99 (dd, *J* = 9.0, 10.2 Hz, 1H, H-3), 5.43 (dd, *J* = 3.9, 10.5 Hz, 1H, H-2), 4.51 (d, *J* = 9.3 Hz, 1H, H-5), 4.38 (dd, *J* = 9.3, 9.3 Hz, 1H, H-4), 3.81 (s, 3H, CO₂CH₃), 0.74 (s, 9H, (CH₃)₃CSi), -0.01 (s, 3H, CH₃Si), -0.15 (s, 3H, CH₃Si); ¹³C NMR (75 MHz, CDCl₃): δ = 168.7, 165.7, 165.7, 160.8, 133.7, 133.5, 130.1, 129.9, 129.7, 128.7, 128.6, 128.6, 93.4, 74.6, 72.5, 70.9, 70.8, 53.0, 53.0, 25.7, 18.0, -4.1, -4.9; ESI MS: *m/z*: calcd for C₂₉H₃₄Cl₃NNaO₉Si: 696.1; found: 696.2 [*M* + Na]⁺.



62

Allyl methyl 2,3-di-O-benzoyl-4-O-tert-butyl dimethylsilyl-β-D-glucopyranosyluronate (62). **39** (100 mg, 0.15 mmol) was azeotroped by co-evaporation with toluene (3x) and placed under high vacuum to dry for 3 h. CH₂Cl₂ (1.2 mL) and 4Å powdered molecular sieves were then added and stirred. To this solution were added allyl

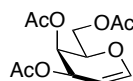
alcohol (100 μ L, 1.48 mmol) and trimethylsilyl trifluoromethanesulfonate (1 *N* in toluene, 30 μ L, 0.03 mmol). After stirring at rt for 12 h, the reaction was quenched with TEA, filtered through Celite, and concentrated to afford a yellow syrup. Purification of this oil by flash chromatography (30% EtOAc:hexanes) afforded **62** (72 mg, 85%) as a white solid. R_f 0.78 (4.5:4.5:1 CH_2Cl_2 :hexanes:EtOAc). ^1H NMR (300 MHz, CDCl_3): δ = 7.92 – 7.87 (m, 4H, ArH), 7.51 – 7.45 (m, 2H, ArH), 7.37 – 7.31 (m, 4H, ArH), 5.81 – 5.68 (m, 1H, $\text{OCH}_2\text{CH}=\text{CH}_2$), 5.59 (dd, J = 9.3, 9.3 Hz, 1H, H-2), 5.38 (dd, J = 8.6, 8.6 Hz, 1H, H-3), 5.21 (dd, J = 1.5, 17.4 Hz, 1H, $\text{OCH}_2\text{CH}=\text{CH}_2$), 5.11 (dd, J = 1.6, 10.4 Hz, 1H, $\text{OCH}_2\text{CH}=\text{CH}_2$), 4.80 (d, J = 7.8 Hz, 1H, H-1), 4.38 – 4.29 (m, 2H, H-4, $\text{OCH}_2\text{CH}=\text{CH}_2$), 4.13 – 4.06 (m, 2H, H-5, $\text{OCH}_2\text{CH}=\text{CH}_2$), 3.81 (s, 3H, CO_2CH_3), 0.73 (s, 9H, $(\text{CH}_3)_3\text{CSi}$), -0.03 (s, 3H, CH_3Si), -0.20 (s, 3H, CH_3Si). ESI MS: m/z : calcd for $\text{C}_{30}\text{H}_{39}\text{O}_9\text{Si}$: 571.7; found 571.7 [$M + \text{H}$] $^+$.



44

Allyl methyl 2,3-di-O-benzoyl- β -D-glucopyranosyluronate (44). To a solution of **62** (72 mg, 0.13 mmol) in dry THF (01.8 mL) and pyridine (1.8 mL) cooled to 0 $^\circ\text{C}$ was added HF•pyridine (0.64 mL). The reaction mixture was warmed to rt and stirred for 12 h. The mixture was then diluted with EtOAc and washed with 10% aqueous CuSO_4 . The aqueous phase was extracted with EtOAc (3x) and the combined organics washed with saturated aqueous NaHCO_3 and dried over MgSO_4 . The solvent was removed *in vacuo* to afford a white solid. Purification of this solid by flash chromatography (40 EtOAc:hexanes) afforded **44** (42 mg, 73%) as a white solid. R_f 0.25 (30%

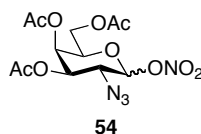
EtOAc:hexanes). $^1\text{H NMR}$ (300 MHz, CDCl_3): $\delta = 7.98 - 7.94$ (m, 4H, ArH), 7.53 – 7.48 (m, 2H, ArH), 7.40 – 7.34 (m, 4H, ArH), 5.84 – 5.71 (m, 1H, $\text{OCH}_2\text{CH}=\text{CH}_2$), 5.54 (dd, $J = 8.7, 9.9$ Hz, 1H, H-2), 5.47 (dd, $J = 7.8, 9.3$ Hz, 1H, H-3), 5.24 (dd, $J = 1.6, 17.6$ Hz, 1H, $\text{OCH}_2\text{CH}=\text{CH}_2$), 5.14 (dd, $J = 0.9, 10.5$ Hz, 1H, $\text{OCH}_2\text{CH}=\text{CH}_2$), 4.81 (d, $J = 7.2$ Hz, 1H, H-1), 4.38 (dd, $J = 4.5, 13.2$ Hz, 1H, $\text{OCH}_2\text{CH}=\text{CH}_2$), 4.25 – 4.07 (m, 3H, H-4, H-5, $\text{OCH}_2\text{CH}=\text{CH}_2$), 3.86 (s, 3H, CO_2CH_3), 3.38 (d, $J = 3.6$ Hz, 1H, OH). ESI MS: m/z : calcd for $\text{C}_{30}\text{H}_{39}\text{O}_9\text{Si}$: 457.4; found 457.5 $[M + \text{H}]^+$.



53

Tri-*O*-acetylgalactal (53).³⁰ Tri-*O*-acetylgalactal was prepared in the manner of Kozikowski *et al.*³⁰ A stirred suspension of D-galactose (0.071 g, 0.39 mmol) in acetic anhydride (40 mL) was treated dropwise with 70% perchloric acid (0.250 mL). Additional D-galactose (9.97 g, 55.3 mmol) was added in small portions over a period of 45 min. The reaction mixture was maintained at 40 °C during the addition by periodic cooling in an ice bath. When the addition of D-galactose was complete, the solution was cooled to 23 °C and 30% HBr in acetic acid (44 mL) was added. The reaction was stirred for 1.5 h. The reaction mixture was then diluted with CH_2Cl_2 (93 mL), washed with cold water (2 x 30 mL), and washed with cold 5% aqueous NaHCO_3 (2 x 30 mL). The organic layer was dried (Na_2SO_4), filtered, and concentrated to afford a yellow syrup that was immediately used in the next step. The syrup was added over a period of 1 h to Zn^0 (25.2 g, 386 mmol) in 50 % aqueous acetic acid (160 mL) with mechanical stirring while keeping the temperature at -15 °C to -20 °C. After the addition, the reaction was stirred

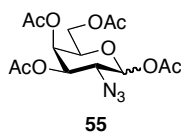
at 0 °C for 1 h. The reaction mixture was then filtered through celite and diluted with CH₂Cl₂ (100 mL). It was extracted with ice water (3 x 35 mL), and the organic extract was washed with cold saturated aqueous NaHCO₃ (2 x 30 mL) and with brine (30 mL). The solution was dried (Na₂SO₄), filtered, and concentrated to afford a white syrup. This was purified by flash chromatography (30% EtOAc:hexanes) to afford tri-*O*-acetylgalactal **53** (7.6 g, 51%) as a white syrup. The work-up procedures for this reaction series must be carefully followed and the ratios of organic layer to water layer exactly measured. The spectral data agreed with published data. R_f 0.59 (50% EtOAc:hexanes). ¹HNMR (300 MHz, CDCl₃): δ = 6.45 (dd, *J* = 6.3, 1.8 Hz, 1H), 5.55 – 5.54 (m, 1H), 5.43 – 5.41 (m, 1H), 4.72 (dq, *J* = 2.1, 1.5 Hz, 1H), 4.29 – 4.21 (m, 3H), 2.12 (s, 3H, OC(O)CH₃), 2.08 (s, 3H, OC(O)CH₃), 2.02 (s, 3H, OC(O)CH₃). ESI MS: *m/z*: calcd for C₁₂H₁₆NaO₇: 295.08; found: 295.2 [*M* + Na]⁺.



Nitro 2-deoxy-2-azido-3,4,6-tri-*O*-acetyl- α,β -D-galactopyranoside (54).³¹

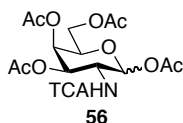
Azidonitration was performed in the manner of Lemieux *et al.*³¹ Tri-*O*-acetylgalactal **53** (1.5 g, 5.5 mmol) was dissolved in CH₃CN (20 mL) and this was added to a dry mix of NaN₃ (0.54 g, 8.27 mmol) and cerium ammonium nitrate (9.1 g, 16.5 mmol) under N₂ at –15 °C (dry ice/ethylene glycol). The reaction was stirred at –15 °C for 20 h. After that, cold diethyl ether (25 mL) and water (25 mL) were added. The organic layer was separated and washed with ice-cold water (3 x 25 mL), dried (Na₂SO₄), filtered, and concentrated to afford a white-yellow syrup. The product was purified by flash

chromatography (40% EtOAc:hexanes) to afford nitrate **54** (1.0 g, 48%, 1:1 α/β) as a white syrup. The work-up procedures for this reaction series must be carefully followed and the ratios of organic layer to water layer exactly measured. The spectral data agreed with published data. R_f 0.80 (50% EtOAc:hexanes). IR (thin film on NaCl) ν_{\max} : 2124 (N_3), 1753 (OAc), 1668 (ONO_2) cm^{-1} ; 1H NMR (300 MHz, $CDCl_3$): δ = 6.34 (d, J = 3.9 Hz, 1H, α -isomer), 5.57 (d, J = 9.0 Hz, 1H, β -isomer), 5.50 (dd, J = 3.3, 1.5 Hz, 1H, α -isomer), 5.39 (dd, J = 3.3, 0.9 Hz, 1H, β -isomer), 5.25 (dd, J = 11.3, 3.3 Hz, 1H, α -isomer), 4.95 (dd, J = 10.2, 3.3 Hz, 1H, β -isomer), 4.15 – 4.04 (m, 4H, α -isomer), 4.15 – 4.04 (m, 3H, β -isomer), 3.82 (q, J = 9.6, 8.7 Hz, 1H, β -isomer), 2.17 (s, 3H, $OC(O)CH_3$, α -isomer), 2.17 (s, 3H, $OC(O)CH_3$, β -isomer), 2.08 (s, 3H, $OC(O)CH_3$, β -isomer), 2.07 (s, 3H, $OC(O)CH_3$, α -isomer), 2.04 (s, 3H, $OC(O)CH_3$, β -isomer), 2.03 (s, 3H, $OC(O)CH_3$, α -isomer). ESI MS: m/z : calcd for $C_{12}H_{16}N_4NaO_{10}$: 399.08; found: 399.0 [$M + Na$] $^+$.



Acetyl 2-Deoxy-2-azido-3,4,6-tri-O-acetyl- α,β -D-galactopyranoside (55).³¹ Nitrate **54** (1.5 g, 4 mmol) was dissolved in acetic acid (9.4 mL) and to this mixture was added anhydrous sodium acetate (0.65 g). The reaction was heated to 100 °C for 1.5 h. It was then cooled to rt and diluted with CH_2Cl_2 (50 mL). The organic layer was treated with ice water (40 mL), saturated aqueous $NaHCO_3$ (2 x 20 mL), and water (25 mL). The organic layer was dried (Na_2SO_4), filtered, and concentrated to afford a yellow syrup that later

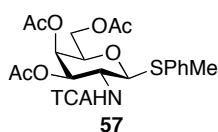
crystallized to afford white, crystalline acetate **55** (1.41 g, 95%, 1:1 α/β). The spectral data agreed with published data. R_f 0.70 (50% EtOAc:hexanes). ^1H NMR (300 MHz, CDCl_3): δ = 6.32 (d, J = 3.9 Hz, 1H, α -isomer), 5.54 (d, J = 8.7 Hz, 1H, β -isomer), 5.47 (dd, J = 3.0, 1.2 Hz, 1H, α -isomer), 5.40 (dd, J = 3.45, 1.2 Hz, 1H, β -isomer), 5.31 (dd, J = 10.8, 3.3 Hz, 1H, α -isomer), 4.89 (dd, J = 10.8, 3.3 Hz, 1H, β -isomer), 4.15 – 4.04 (m, 3H, α -isomer), 4.15 – 4.04 (m, 3H, β -isomer), 3.93 (q, J = 11.1, 3.6 Hz, 1H, α -isomer), 3.84 (q, J = 9.8, 8.7 Hz, 1H, β -isomer), 2.20 (s, 3H, OC(O)CH_3 , α -isomer), 2.17 (s, 3H, OC(O)CH_3 , β -isomer), 2.16 (s, 3H, OC(O)CH_3 , β -isomer), 2.09 (s, 3H, OC(O)CH_3 , α -isomer), 2.07 (s, 3H, OC(O)CH_3 , β -isomer), 2.06 (s, 3H, OC(O)CH_3 , α -isomer), 2.04 (s, 3H, OC(O)CH_3 , α -isomer), 2.03 (s, 3H, OC(O)CH_3 , β -isomer). ESI MS: m/z : calcd for $\text{C}_{14}\text{H}_{19}\text{N}_3\text{O}_9$: 396.10; found: 396.0 [$M + \text{Na}$] $^+$.



1,3,4,6-tetra-*O*-acetyl-2-deoxy-2-trichloroacetamido- α/β -D-galactopyranoside (56).

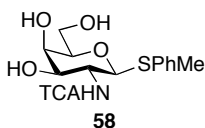
To 1,3,4,6-tetra-*O*-acetyl-2-azido-2-deoxy-D-galactopyranoside **55** (0.100 g, 0.268 mmol) in THF (5.00 mL) was added *p*-tosic acid monohydrate (0.051 g, 0.27 mmol) followed by Pd/C (0.017 g, 6 mol%). The reaction was placed under an atmosphere of H_2 and stirred at rt for 18 h. The Pd/C was removed by filtration through Celite and the solvent concentrated to afford an anomeric mixture of crude amines as a pale yellow foam. The crude mixture was used for the next step without purification.

To a solution of crude amines in THF (5 mL) cooled to 0 °C, was added trichloroacetylchloride (0.22 g, 0.13 mL, 1.2 mmol) followed by TEA (0.25 mL, 1.8 mmol). After stirring at 0 °C for 15 min, the reaction mixture was quenched with saturated aqueous NaHCO₃. The water layer was separated and extracted with CH₂Cl₂ (2x), the combined organics dried over Na₂SO₄, and the solvent removed *in vacuo* to afford a yellow oil. Purification of this oil by flash chromatography (30% → 40% EtOAc:hexanes) afforded **56** (0.099 g, 75%, 3.1β:1α) as a white solid R_f 0.61 and 0.53 (60% EtOAc:hexanes). ¹H NMR (300 MHz, CDCl₃): δ = 6.73 (d, *J* = 9.0 Hz, 2H, NHTCA), 6.30 (d, *J* = 3.9 Hz, 1H, H-1, α), 5.45 (d, *J* = 3.3 Hz, 3H), 5.32 (dd, *J* = 3.5 Hz and 11.3 Hz, 2H), 4.58 (m, 2H), 4.26 (dd, *J* = 6.6 Hz, 6.6 Hz, 2H), 4.20 – 4.03 (m, 4H), 2.17 (s, 6H, OC(O)CH₃), 2.15 (s, 6H, OC(O)CH₃), 2.02 (s, 6H, OC(O)CH₃), 2.00 (s, 6H, OC(O)CH₃); ¹³C NMR (75 MHz, CDCl₃): δ = 171.2, 170.5, 170.2, 168.7, 162.2, 90.5, 69.0, 67.8, 66.8, 61.5, 49.6, 21.2, 21.0; HR-FAB MS: *m/z*: calcd for C₁₆H₁₉C₁₃NO₁₀: 490.0075; found: 490.0073 [*M* - H].



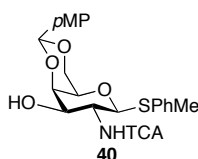
***p*-Methylphenyl 2-deoxy-2-trichloroacetamido-3,4,6-tri-*O*-acetyl-1-thio-β-D-galactopyranoside (57).** To a solution of **56** (0.050 g, 0.10 mmol) in dry CH₂Cl₂ (0.35 mL) was added *p*-toluenethiol (0.042 g, 0.34 mmol) followed by BF₃•OEt₂ (0.043 g, 38 μL, 0.30 mmol) and the reaction mixture stirred at rt. After 2 h, a further addition of *p*-toluenethiol (0.012 g, 0.10 mmol) and BF₃•OEt₂ (0.014 g, 13 μL, 0.10 mmol) was made,

followed by stirring at rt for 1 h. The reaction mixture was quenched with saturated aqueous NaHCO₃ and the organic phase washed twice with saturated aqueous NaHCO₃ and water. The aqueous layers were back-extracted with CH₂Cl₂ (3x), and the combined organics washed with brine and dried over Na₂SO₄ to afford an amber oil. Purification of this oil by flash chromatography (20% → 25% EtOAc:hexanes) afforded **57** (0.044 g, 80%) as a white solid. R_f 0.51 (50% EtOAc:hexanes). [α]_D²³ = -2.4 (*c* = 0.5, CH₂Cl₂); IR (thin film on NaCl): ν = 3450, 1752, 1655, 1529, 1493, 1370, 1230, 1082, 1045 cm⁻¹; ¹H NMR (300 MHz, CDCl₃): δ = 7.42 (d, *J* = 8.3 Hz, 2H, SC₆H₄Me), 7.12 (d, *J* = 8.3 Hz, 2H, SC₆H₄Me), 6.77 (d, *J* = 8.7 Hz, 1H, NHTCA), 5.39 (d, *J* = 3.3 Hz, 1H, H-4), 5.29 (dd, *J* = 3.3, 11.1 Hz, 1H, H-3), 4.89 (d, *J* = 10.5 Hz, 1H, H-1), 4.22 – 4.09 (m, 3H, H-2, H-6), 3.94 (dd, *J* = 6.6, 6.6 Hz, 1H, H-5), 2.34 (s, 3H, SPhCH₃), 2.13 (s, 3H, OC(O)CH₃), 2.04 (s, 3H, OC(O)CH₃), 1.97 (s, 3H, OC(O)CH₃); ¹³C NMR (75 MHz, CDCl₃): δ = 170.6, 170.5, 170.2, 161.9, 138.8, 133.5, 129.9, 128.5, 92.5, 87.2, 74.9, 70.9, 67.1, 62.0, 51.7, 21.6, 21.1, 21.0, 20.9; HR-FAB MS: *m/z*: calcd for C₂₁H₂₅Cl₃NO₈S: 556.0367; found: 556.0369 [*M* + H]⁺.



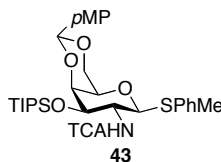
***p*-Methylphenyl 2-deoxy-2-trichloroacetamido-3-*O*-triisopropylsilyl-4,6-*O*-*p*-methoxybenzylidene-1-thio-β-D-galactopyranoside (**58**).** A solution of **57** (17.9 g, 0.0320 mol) in dry CH₂Cl₂ (85 mL) and MeOH (435 mL) was stirred at rt for 30 min and NaOMe (25 wt% solution in MeOH, 0.52 g, 2.1 mL, 9.6 mmol) was then added. After stirring for 2 h, Dowex 50X8-200 was added and stirring continued for an additional 30

min. The Dowex beads were removed by filtration and the solvent removed *in vacuo* to afford **58** (13.5 g, 98%) as a yellow solid. This compound was suitable for the next step without purification. R_f 0.11 (75% EtOAc:hexanes). $^1\text{H NMR}$ (300 MHz, CD_3OD): δ = 7.42 (d, J = 8.3 Hz, 2H, $\text{SC}_6\text{H}_4\text{Me}$), 7.09 (d, J = 8.3 Hz, 2H, $\text{SC}_6\text{H}_4\text{Me}$), 4.91 (d, J = 10.5 Hz, 1H, H-1), 4.05 (dd, J = 8.7, 9.1 Hz, 1H, H-2), 3.87 (d, J = 1.8 Hz, 1H, H-6), 3.81 – 3.68 (m, 3H, H-3, H-4, H-6), 3.55 (dd, J = 6.6, 6.6 Hz, 1H, H-5), 2.34 (s, 3H, SPhCH_3).



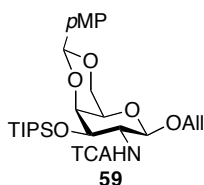
***p*-Methylphenyl 2-deoxy-2-trichloroacetamido-4,6-*O*-*p*-methoxybenzylidene-1-thio- β -D-galactopyranoside (**40**).** To a solution of **58** (13.5 g, 0.0310 mol) in acetonitrile (800 mL, minimum amount) was added *p*-anisaldehyde dimethyl acetal (11 g, 12 mL, 0.063 mol) and DL-10-camphorsulfonic acid (10 mol%) and the mixture stirred at rt for 12 h. The reaction mixture was quenched with TEA and the solvent concentrated to afford a yellow solid. Purification of this solid by flash chromatography (40% \rightarrow 80% EtOAc:hexanes) afforded **40** (13 g, 76%) as a white solid. R_f 0.25 (50% EtOAc:hexanes). $[\alpha]_D^{24} = -14.6$ ($c = 0.5$, CH_2Cl_2); IR (thin film on NaCl): $\nu = 3333, 1687, 1615, 1519, 1492, 1403, 1364, 1301, 1248, 1167, 1095, 1055 \text{ cm}^{-1}$; $^1\text{H NMR}$ (300 MHz, CDCl_3): δ = 7.55 (d, J = 8.4 Hz, 2H, $\text{SC}_6\text{H}_4\text{Me}$), 7.34 (d, J = 8.7 Hz, 2H, $\text{C}_6\text{H}_4\text{OMe}$), 7.12 (d, J = 8.4 Hz, 2H, $\text{SC}_6\text{H}_4\text{Me}$), 6.88 (d, J = 8.7 Hz, 2H, $\text{C}_6\text{H}_4\text{OMe}$), 6.81 (d, J = 7.5 Hz, 1H, NHTCA), 5.48 (s, 1H, MeOPhCH), 5.03 (d, J = 9.9 Hz, 1H, H-1), 4.37 (dd, J = 1.5, 12.6 Hz, 1H, H-6), 4.20 – 4.10 (m, 2H, H-3, H-4), 4.01 (dd, J = 1.5, 12.6 Hz, 1H, H-6), 3.83

(s, 3H, PhOCH₃), 3.69 (m, 1H, H-2), 3.57 (s, 1H, H-5), 2.58 (d, *J* = 10.5 Hz, 1H, OH), 2.37 (s, 3H, SPhCH₃); ¹³C NMR, (75 MHz, CDCl₃): δ = 162.1, 160.5, 139.0, 134.7, 130.2, 130.0, 128.1, 126.9, 113.8, 101.4, 84.0, 75.2, 70.7, 70.3, 69.5, 55.7, 54.4, 21.7; HR-FAB MS: *m/z*: calcd for C₂₃H₂₅Cl₃NO₆S: 548.0469; found: 548.0448 [*M* + H]⁺.



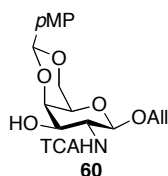
***p*-Methylphenyl 2-deoxy-2-trichloroacetamido-3-*O*-triisopropylsilyl-4,6-*O*-*p*-methoxybenzylidene-β-D-galactopyranoside (43).** To a solution of **40** (5.6 g, 0.010 mol) in dry DMF (50 mL) at rt was added triisopropylsilyl chloride (6.3 g, 0.033 mol, 7.0 mL), imidazole (2.7 g, 0.040 mol) and 4-(dimethylamino)pyridine (0.49 g, 40 mol%). The reaction mixture was stirred for 4 h, whereupon further addition of triisopropylsilyl chloride (3.2 g, 3.5 mL, 0.016 mol), imidazole (1.4 g, 0.020 mol) and 4-(dimethylamino)pyridine (0.25 g, 20 mol%) were added. The reaction mixture was stirred for 12 h and quenched with saturated aqueous NaHCO₃. The aqueous layer was extracted with EtOAc (3x) and the combined organics washed with brine and dried over MgSO₄ to afford a pale yellow oil. Purification of this oil by flash chromatography (10% → 15% EtOAc:hexanes) afforded **43** (5.3 g, 75%) as a white solid. *R*_f 0.57 (30% EtOAc:hexanes). [α]_D²³ = +5.9 (*c* = 0.5, CH₂Cl₂); IR (thin film on NaCl): ν = 2943, 2866, 1705, 1616, 1519, 1493, 1464, 1365, 1249, 1170, 1139, 1083, 1051 cm⁻¹; ¹H NMR (300 MHz, CDCl₃): δ = 7.57 (d, *J* = 8.1 Hz, 2H, SC₆H₄Me), 7.38 (d, *J* = 8.7 Hz, 2H, C₆H₄OMe), 7.07 (d, *J* = 8.1 Hz, 2H, SC₆H₄Me), 6.87 (d, *J* = 8.7 Hz, 2H, C₆H₄OMe),

6.85 (m, 1H, NHTCA), 5.45 (s, 1H, MeOPhCH), 5.39 (d, $J = 9.9$ Hz, 1H, H-1), 4.62 (dd, $J = 3.2, 10.2$ Hz, 1H, H-3), 4.37 (dd, $J = 1.7, 12.5$ Hz, 1H, H-6), 4.13 (d, $J = 3.2$ Hz, 1H, H-4), 4.01 (dd, $J = 1.7, 12.5$ Hz, 1H, H-6), 3.83 (s, 3H, PhOCH₃), 3.71 (m, 1H, H-2), 3.55 (s, 1H, H-5), 2.34 (s, 3H, SPhCH₃), 1.01 (s, 21H, [(CH₃)₂CH]₃), ¹³C NMR (75 MHz, CDCl₃): $\delta = 161.3, 160.1, 138.5, 134.1, 130.7, 130.0, 128.0, 127.9, 113.5, 101.1, 83.4, 76.7, 71.0, 70.3, 69.7, 55.6, 54.8, 21.7, 18.5, 18.4, 13.1$; HR-FAB MS: m/z : calcd for C₃₂H₄₅Cl₃NO₆SSi: 704.1621; found: 704.1623 [$M + H$]⁺.



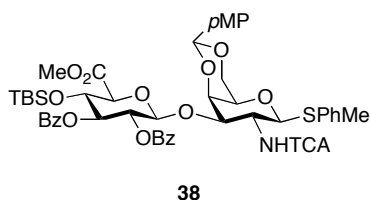
Allyl 2-deoxy-2-trichloroacetamido-3-*O*-triisopropylsilyl-4,6-*O*-*p*-methoxybenzylidene- β -D-galactopyranoside (59**).** To a solution of **43** (11 g, 0.016 mol) in dry CH₂Cl₂ (675 mL) were added 4Å powdered molecular sieves. After stirring for 1 h at rt, allyl alcohol (9.3 g, 11 mL, 0.16 mol) and *N*-iodosuccinimide (5.3 g, 0.023 mol) were added, and the mixture was cooled to 0 °C. Triflic acid (0.5 *N* solution in CH₂Cl₂, 1.44 g, 9.60 mmol, 19.2 mL) was added and the reaction stirred at 0 °C for 10 min. The mixture was quenched with TEA, washed with brine, and dried over MgSO₄. The solvent was removed *in vacuo* to afford a yellow oil. Purification of this oil by flash chromatography (5% → 15% EtOAc:hexanes) afforded **59** (8.1 g, 79%) as a white solid. R_f 0.41 (30% EtOAc:hexanes). $[\alpha]_D^{24} = +38.1$ ($c = 0.5, \text{CH}_2\text{Cl}_2$); IR (thin film on NaCl): $\nu = 3445, 1644, 1520, 1463, 1368, 1249, 1171, 1123, 1060 \text{ cm}^{-1}$; ¹H NMR (300 MHz, CDCl₃): $\delta = 7.45$ (d, $J = 8.9$ Hz, 2H, C₆H₄OMe), 6.97 (d, $J = 7.2$ Hz, 1H, NHTCA), 6.87

(d, $J = 8.9$ Hz, 2H, C_6H_4OMe), 5.96 – 5.83 (m, 1H, $OCH_2CH=CH_2$), 5.49 (s, 1H, $MeOPhCH$), 5.26 (dd, $J = 1.4, 17.3$ Hz, 1H, $OCH_2CH=CH_2$), 5.17 (dd, $J = 1.4, 10.5$ Hz, 1H, $OCH_2CH=CH_2$), 5.16 (d, $J = 8.1$ Hz, 1H, H-1), 4.65 (dd, $J = 3.3, 10.5$ Hz, 1H, H-3), 4.37 (m, 2H, $OCH_2CH=CH_2$, H-6), 4.13 – 4.05 (m, 3H, $OCH_2CH=CH_2$, H-4, H-6), 3.81 (s, 3H, $PhOCH_3$), 3.75 (m, 1H, H-2), 3.48 (s, 1H, H-5), 1.05 (s, 21H, $[(CH_3)_2CH]_3$); ^{13}C NMR (75 MHz, $CDCl_3$): $\delta = 161.7, 160.1, 134.0, 130.5, 127.8, 118.2, 113.6, 101.2, 97.8, 76.6, 70.6, 69.9, 69.5, 66.7, 64.2, 57.6, 55.6, 18.5, 18.4, 13.1$; HR-FAB MS: m/z : calcd for $C_{25}H_{37}Cl_3NO_6Si$: 580.1456; found: 580.1474 [$M^+ - OAlI$].



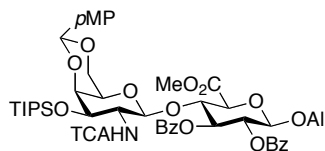
Allyl 2-deoxy-2-trichloroacetamido-4,6-*O*-*p*-methoxybenzylidene- β -D-galactopyranoside (60). To a solution of **59** (8.00 g, 12.5 mmol) in THF (290 mL) was added tetrabutylammonium fluoride (1 *N* solution in THF, 4.91 g, 18.8 mL, 18.8 mmol) and the mixture stirred at rt for 8 h. At this time, a second addition of tetrabutylammonium fluoride (2.5 g, 9.4 mmol, 9.4 mL) was made and the reaction stirred for an additional 12 h. The solvent was removed *in vacuo* to afford a yellow oil. Purification of this oil by flash chromatography (40% \rightarrow 80% EtOAc:hexanes) yielded **60** (5.14 g, 85%) as a white solid. R_f 0.17 (50% EtOAc:hexanes). $[\alpha]_D^{24} = +0.62$ ($c = 0.5$, CH_2Cl_2); IR (thin film on NaCl): $\nu = 3423, 1686, 1616, 1531, 1402, 1366, 1303, 1249, 1170, 1097, 1060$ cm^{-1} ; 1H NMR (300 MHz, $CDCl_3$): $\delta = 7.43$ (d, $J = 8.7$ Hz, 2H, C_6H_4OMe), 6.89 (d, $J = 8.7$ Hz, 2H, C_6H_4OMe), 6.87 (m, 1H, *NHTCA*), 5.95 – 5.82 (m,

1H, OCH₂CH=CH₂), 5.54 (s, 1H, MeOPhCH), 5.29 (dd, *J* = 1.4, 17.7 Hz, 1H, OCH₂CH=CH₂), 5.19 (dd, *J* = 1.4, 10.5 Hz, 1H, OCH₂CH=CH₂), 4.84 (d, *J* = 8.4 Hz, 1H, H-1), 4.44 – 4.32 (m, 2H, H-3, H-6), 4.26 – 4.07 (m, 4H, OCH₂CH=CH₂, H-4, H-6), 3.81 (m, 1H, H-2), 3.81 (s, 3H, PhOCH₃), 3.53 (s, 1H, H-5), 2.71 (d, *J* = 9.9 Hz, 1H, OH); ¹³C NMR (75 MHz, CDCl₃): δ = 162.5, 160.4, 153.6, 133.7, 130.0, 127.9, 118.3, 113.8, 101.6, 98.7, 75.2, 70.4, 69.4, 69.3, 67.0, 57.2, 55.7; HR-FAB MS: *m/z*: calcd for C₁₉H₂₃Cl₃NO₇: 482.0540; found: 482.0531 [*M* + H]⁺.



Methyl 2,3-di-*O*-benzoyl-4-*O*-*tert*-butyldimethylsilyl-β-D-glucopyranosyluronate)-(1 → 3)-4,6-*O*-*p*-methoxybenzylidene-2-deoxy-2-trichloroacetamido-1-thio-β-D-galactopyranoside (38). **39** (20 mg, 0.030 mmol) and **40** (17 mg, 0.026 mmol) were combined, azeotroped by co-evaporation with toluene (3x), and placed under high vacuum overnight to dry. The mixture was dissolved in CH₂Cl₂ (0.6 mL) and 4Å powdered molecular sieves added. The mixture was stirred for 1 h at rt, cooled to –78 °C, and *N*-iodosuccinimide (9.7 mg, 0.042 mmol) was added. Trimethylsilyl trifluoromethanesulfonate (0.1 *N* solution in CH₂Cl₂, 62 μL, 0.005 mmol) was cooled to –78 °C and added dropwise to the reaction mixture. After 45 min, the reaction mixture was warmed to rt, stirred for 30 min and then quenched with TEA. The mixture was filtered and concentrated to afford a yellow oil. Purification of this oil by preparative thin layer chromatography (30% EtOAc:hexanes) afforded **38** (7.5 mg, 28%) as a white solid. *R*_f

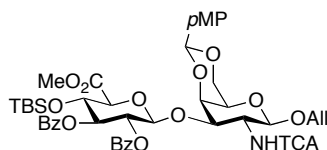
0.53 (40% EtOAc:hexanes). ^1H NMR (300 MHz, CDCl_3): δ = 7.83 – 7.77 (m, 4H, ArH), 7.50 – 7.43 (m, 4H, ArH), 7.33 – 7.27 (m, 6H, ArH), 6.99 (d, J = 8.4 Hz, 2H, $\text{C}_6\text{H}_4\text{OMe}$), 6.86 (d, J = 8.7 Hz, 1H, $\text{SC}_6\text{H}_4\text{Me}$), 6.75 (d, J = 6.6 Hz, 1H, NHTCA), 5.46 – 5.29 (m, 4H, H-1 GalNAc, H-2 GlcA, H-3 GlcA, MeOPhCH), 5.02 (d, J = 7.2 Hz, 1H, H-1 GlcA), 4.69 (dd, J = 3.3, 10.5 Hz, 1H, H-3 GalNAc), 4.39 – 4.27 (m, 3H, H-4 GalNAc, H-4 GlcA, H-6 GalNAc), 4.05 (d, J = 9.3 Hz, 1H, H-5 GlcA), 4.00 (dd, J = 0.9, 10.8 Hz, 1H, H-6 GalNAc), 3.83 (s, 3H, CO_2CH_3), 3.80 (s, 3H, PhOCH_3), 3.69 – 3.60 (m, 1H, H-2 GalNAc), 3.57 (s, 1H, H-5 GalNAc), 0.71 (s, 9H, $(\text{CH}_3)_3\text{CSi}$), -0.09 (s, 3H, CH_3Si), -0.25 (s, 3H, CH_3Si). ESI MS: m/z : calcd for $\text{C}_{50}\text{H}_{57}\text{Cl}_3\text{NO}_{14}\text{SSi}$: 1062.5; found: 1062.5 [$M + \text{H}$] $^+$.



42

Allyl (4,6-*O*-*p*-methoxybenzylidene-3-*O*-triisopropylsilyl-2-deoxy-2-trichloroacetamido- β -D-galactopyranosyl)-(1 \rightarrow 4)-methyl 2,3-di-*O*-benzoyl- β -D-glucopyranosyluronate (**42**). **43** (0.044 g, 0.063 mmol) and **44** (0.016 g, 0.035 mmol) were combined, azeotroped by co-evaporated with toluene (3x), and put under high vacuum overnight to dry. The mixture was dissolved in CH_2Cl_2 (0.5 mL) and 4Å powdered molecular sieves added. The mixture was stirred for 1 h at rt and then cooled to -15 °C. *N*-iodosuccinimide (16 mg, 0.07 mmol) and triflic acid (0.25 *N* solution in CH_2Cl_2 , 15 μL , 0.004 mmol) were added, and the reaction was stirred at -15 °C for 30 min and quenched with TEA. The mixture was filtered and the solvent removed *in vacuo*

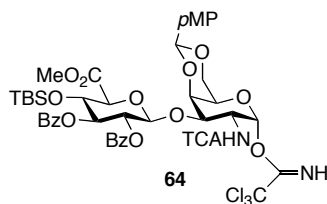
to afford a yellow oil. Purification of this oil by preparative thin layer chromatography (25% EtOAc:hexanes) afforded **42** (21 mg, 58%) as a white solid. The α -linked product was observed in 32% yield. R_f 0.50 (30% EtOAc:hexanes). $^1\text{H NMR}$ (300 MHz, CDCl_3): $\delta = 7.97 - 7.93$ (m, 4H, ArH), 7.53 – 7.48 (m, 1H, ArH), 7.39 – 7.31 (m, 3H, ArH), 7.23 – 7.18 (m, 2H, ArH), 7.07 (d, $J = 9.0$ Hz, 2H, $\text{C}_6\text{H}_4\text{OMe}$), 6.82 (d, $J = 7.8$ Hz, 1H, NHTCA), 6.74 (d, $J = 8.1$ Hz, 2H, $\text{C}_6\text{H}_4\text{OMe}$), 5.84 – 5.71 (m, 1H, $\text{OCH}_2\text{CH}=\text{CH}_2$), 5.71 (dd, $J = 8.7, 9.0$ Hz, 1H, H-2 GlcA), 5.38 (dd, $J = 8.7, 9.3$ Hz, 1H, H-3 GlcA), 5.28 – 5.20 (m, 3H, H-1 GalNAc, MeOPhCH, $\text{OCH}_2\text{CH}=\text{CH}_2$), 5.14 (dd, $J = 1.5, 11.2$ Hz, 1H, $\text{OCH}_2\text{CH}=\text{CH}_2$), 4.83 (d, $J = 7.2$ Hz, 1H, H-1 GlcA), 4.60 (dd, $J = 8.7, 8.7$ Hz, 1H, H-4 GlcA), 4.38 – 4.32 (m, 2H, H-3 GalNAc, $\text{OCH}_2\text{CH}=\text{CH}_2$), 4.18 – 4.09 (m, 2H, H-5 GlcA, $\text{OCH}_2\text{CH}=\text{CH}_2$), 3.96 – 3.67 (m, 4H, H-6 GalNAc, H-6 GalNAc, H-2 GalNAc, H-4 GalNAc) 3.86 (s, 3H, CO_2CH_3), 3.80 (s, 3H, PhOCH_3), 3.31 (s, 1H, H-5 GalNAc), 0.99 (s, 21H, $[(\text{CH}_3)_2\text{CH}]_3$); ESI MS: m/z : calcd for $\text{C}_{49}\text{H}_{61}\text{Cl}_3\text{NO}_{15}\text{Si}$: 1038.4; found 1038.5 $[M + \text{H}]^+$.



61

Allyl (methyl 2,3-di-O-benzoyl-4-O-tert-butyldimethylsilyl- β -D-glucopyranosyluronate)-(1 \rightarrow 3)-4,6-O-p-methoxybenzylidene-2-deoxy-2-trichloroacetamido- β -D-galactopyranoside (61). A mixture of donor **39** (0.50 g, 0.74 mmol) and acceptor **60** (0.30 g, 0.62 mmol) was azeotroped by co-evaporated with toluene (3 x 3 mL) and dried under vacuum overnight. The mixture was dissolved in

CH₂Cl₂ (16 mL), and activated 4Å powdered molecular sieves were added. The reaction was stirred at rt for 1.5 h. The reaction was then cooled to -40 °C and stirred for an additional 30 min. Trimethylsilyl trifluoromethanesulfonate (1 N in CH₂Cl₂, 125 μL, 0.123 mmol) at -40 °C was added to the reaction dropwise. The reaction was allowed to stir an additional 30 min. A carefully controlled temperature gradient was essential to avoid formation of the inseparable ortho ester. It was then warmed to -10 °C over a period of 30 min, quenched with TEA, and allowed to warm to rt. The reaction was filtered and concentrated to afford a yellow syrup. The product was purified by flash chromatography (30% EtOAc:hexanes) to afford **61** (0.46 g, 74%) as a white solid. R_f 0.12 (30% EtOAc:hexanes). ¹H NMR (300 MHz, CDCl₃): δ = 7.87 – 7.82 (m, 4H, ArH), 7.48 – 7.39 (m, 4H, ArH), 7.35 – 7.26 (m, 4H, ArH), 6.86 (d, *J* = 8.7 Hz, 2H, C₆H₄OMe), 6.82 (d, *J* = 7.2 Hz, 1H, NHTCA), 5.89 – 5.76 (m, 1H, OCH₂CH=CH₂), 5.45 (s, 1H, MeOPhCH), 5.52 – 5.39 (m, 2H, H-2 GlcA, H-3 GlcA), 5.22 (dd, *J* = 1.6, 17.6 Hz, 1H, OCH₂CH=CH₂), 5.13 (dd, *J* = 1.0, 10.4 Hz, 1H, OCH₂CH=CH₂), 5.08 (d, *J* = 7.5 Hz, 1H, H-1 GlcA), 5.05 (d, *J* = 8.1 Hz, 1H, H-1 GalNAc), 4.67 (dd, *J* = 3.3, 10.8 Hz, 1H, H-3 GalNAc), 4.36 – 4.27 (m, 4H, OCH₂CH=CH₂, H-4 GalNAc, H-4 GlcA, H-6 GalNAc), 4.10 (d, *J* = 9.3 Hz, 1H, H-5 GlcA), 4.07 – 4.01 (m, 2H, OCH₂CH=CH₂, H-6 GalNAc), 3.79 (s, 6H, CO₂CH₃, PhOCH₃), 3.77 – 3.68 (m, 1H, H-2 GalNAc), 3.48 (s, 1H, H-5 GalNAc), 0.72 (s, 9H, (CH₃)₃CSi), -0.08 (s, 3H, CH₃Si), -0.23 (s, 3H, CH₃Si); ¹³C NMR (75 MHz, CDCl₃): δ = 168.7, 165.7, 165.2, 162.3, 160.0, 133.8, 133.4, 133.4, 130.5, 130.0, 129.9, 129.5, 129.2, 128.5, 127.7, 118.2, 113.6, 100.7, 100.6, 97.8, 92.3, 76.4, 75.8, 75.6, 73.6, 72.0, 70.9, 70.6, 69.2, 66.8, 55.6, 55.4, 52.9, 25.7, 18.1, -4.0, -4.7; HR-FAB MS: *m/z*: calcd for C₄₆H₅₃Cl₃NO₁₅Si: 992.2250; found: 992.2255 [*M*]⁺.



Methyl (2,3-di-*O*-benzoyl-4-*O*-*tert*-butyldimethylsilyl- β -D-glucopyranosyluronate)-(1

→ 3)-4,6-*O*-*p*-methoxybenzylidene-2-deoxy-2-trichloroacetamido- α -D-

galactopyranoside trichloroacetimidate (64). To a solution of **61** (2.5 g, 2.5 mmol) in

dry CH₂Cl₂ (40 mL) was added Grubbs' second-generation catalyst (0.43 g, 20 mol%)

and the mixture stirred at rt for 2 h. The solvent was removed *in vacuo* to afford a brown

oil. Purification of this oil by flash chromatography (15% → 20% EtOAc:hexanes)

afforded *E/Z*-prop-2-enyl (methyl 2,3-di-*O*-benzoyl-4-*O*-*tert*-butyldimethylsilyl- β -D-

glucopyranosyluronate)-(1 → 3)-4,6-*O*-*p*-methoxybenzylidene-2-deoxy-2-

trichloroacetamido- β -D-galactopyranoside (1.92 g, 77%) as a white solid. R_f (E and Z)

0.68 (60% EtOAc:hexanes). [α]_D²⁵ = +29.1 (*c* = 1.0, CH₂Cl₂); IR (thin film on NaCl): ν

= 3308, 2954, 2858, 1755, 1734, 1717, 1694, 1617, 1602, 1540, 1520, 1452, 1371, 1268,

1221, 1176, 1147, 1089, 1069, 1040, 1026, 1001 cm⁻¹; ¹H NMR (300 MHz, CDCl₃): δ =

7.85 (m, 3H, ArH), 7.48 – 7.28 (m, 10H, ArH, OCH=CHCH₃), 6.87 (d, *J* = 8.7 Hz, 2H,

C₆H₄OMe), 6.82 (d, *J* = 6.6 Hz, 1H, NHTCA), 6.17 (m, 1H, CH=CHCH₃), 5.52 – 5.40

(m, 3H, MeOPhCH, H-2 GlcA, H-3 GlcA), 5.19 (d, *J* = 8.1 Hz, 1H, H-1 GalNAc), 5.08

(d, *J* = 7.2 Hz, 1H, H-1 GlcA), 4.68 (dd, *J* = 3.8, 11.0 Hz, 1H, H-3 GalNAc), 4.39 – 4.28

(m, 3H, H-4 GalNAc, H-4 GlcA, H-6 GalNAc), 4.16 – 4.02 (m, 2H, H-5 GlcA, H-6

GalNAc), 3.87 (m, 1H, H-2 GalNAc), 3.81 (s, 3H, PhOCH₃), 3.80 (s, 3H, CO₂CH₃), 3.54

(s, 1H, H-5), 1.51 (m, 3H, OCH=CHCH₃), 0.72 (s, 9H, (CH₃)₃CSi), -0.07 (s, 3H, CH₃Si),

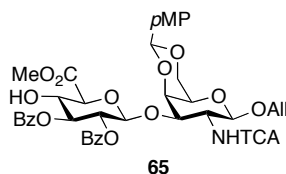
-0.22 (s, 3H, CH₃Si); ¹³C NMR (75 MHz, CDCl₃): δ = 168.7, 165.7, 165.3, 162.4, 162.3, 160.0, 143.5, 142.1, 133.5, 133.4, 130.4, 130.1, 129.9, 129.5, 129.1, 128.5, 127.7, 113.6, 105.7, 104.8, 100.8, 100.6, 100.5, 98.4, 98.0, 76.5, 75.6, 75.5, 73.5, 73.4, 72.0, 70.9, 69.0, 67.2, 67.1, 55.6, 55.1, 55.0, 52.9, 25.7, 18.1, 12.6, 9.7, -4.0, -4.7.

To a solution of *E/Z*-prop-2-enyl (methyl 2,3-di-*O*-benzoyl-4-*O*-*tert*-butyldimethylsilyl-β-D-glucopyranosyluronate)-(1 → 3)-4,6-*O*-*p*-methoxybenzylidene-2-deoxy-2-trichloroacetamido-β-D-galactopyranoside (6.2 g, 6.3 mmol) in dry THF (118 mL), water (24 mL) and pyridine (1.9 mL), was added iodine (3.1 g) and the mixture stirred at ambient temperature for 30 min. The solvent was removed *in vacuo* to afford a yellow oil. The oil was taken up in EtOAc and washed with 5% aqueous Na₂SO₃, saturated aqueous NaHCO₃, brine and dried over MgSO₄. The solvent was removed *in vacuo* to afford a pale yellow oil. Purification of this oil by flash chromatography (40% → 60% EtOAc:hexanes) afforded an anomeric mixture of methyl (2,3-di-*O*-benzoyl-4-*O*-*tert*-butyldimethylsilyl-β-D-glucopyranosyluronate)-(1 → 3)-4,6-*O*-*p*-methoxybenzylidene-2-deoxy-2-trichloroacetamido-α/β-D-galactopyranoside (4.8 g, 81%) as a pale yellow solid. R_f 0.28 and 0.18 (50% EtOAc:hexanes). [α]_D²⁵ = +79.0 (*c* = 1.0, CH₂Cl₂); IR (thin film on NaCl): ν = 3521, 2930, 1738, 1682, 1615, 1519, 1452, 1394, 1251, 1172, 1093, 1069, 1031 cm⁻¹; ¹H NMR (300 MHz, CDCl₃): δ = 7.92 – 7.85 (m, 3H, ArH), 7.54 – 7.45 (m, 3H, ArH), 7.40 – 7.27 (m, 4H, ArH), 7.12 (d, *J* = 9.0 Hz, 2H, C₆H₄OMe), 6.96 (d, *J* = 6.3 Hz, 1H, NHTCA), 6.72 (d, *J* = 9.0 Hz, 2H, C₆H₄OMe), 5.60 (m, 1H, H-1 GalNAc), 5.50 (dd, *J* = 8.2, 8.2 Hz, 1H, H-3 GlcA), 5.42 (dd, *J* = 8.2, 8.2 Hz, 1H, H-2 GlcA), 5.24 (s, 1H, MeOPhCH), 5.21 (d, *J* = 7.5 Hz, 1H, H-1 GlcA), 4.39 – 4.35 (m, 4H, H-3

GalNAc, H-4 GalNAc, H-4 GlcA), 4.23 – 4.02 (m, 3H, H-2 GalNAc, H-5 GlcA, H-6 GalNAc), 3.96 (s, 1H, H-5 GalNAc), 3.79 (s, 3H, PhOCH₃), 3.75 (s, 3H, CO₂CH₃), 3.03 (d, *J* = 3.3 Hz, 1H, OH), 0.73 (s, 9H, (CH₃)₃CSi), -0.08 (s, 3H, CH₃Si), -0.22 (s, 3H, CH₃Si); ESI MS: *m/z*: calcd for C₄₃H₅₀Cl₃NO₁₅Si: 954.2914; found: 954.2910 [M - H].

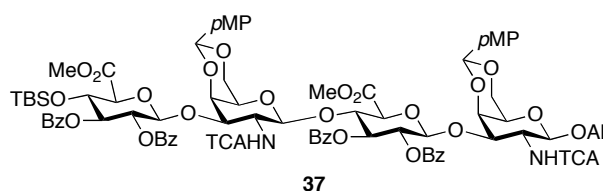
To a solution of methyl (2,3-di-*O*-benzoyl-4-*O*-*tert*-butyldimethylsilyl- β -D-glucopyranosyluronate)-(1 → 3)-4,6-*O*-*p*-methoxybenzylidene-2-deoxy-2-trichloroacetamido- α/β -D-galactopyranoside (4.6 g, 4.8 mmol) in dry CH₂Cl₂ (190 mL) cooled to 0 °C, was added 1,8-diazabicyclo[5.4.0]undec-7-ene (0.29 g, 0.29 mL, 1.9 mmol) and trichloroacetonitrile (10 g, 7.2 mL, 71 mmol). After stirring for 15 min, the mixture was quenched with TEA and concentrated *in vacuo* to afford a yellow oil. Purification of this oil by flash chromatography (35% EtOAc:hexanes, + 2% TEA) afforded **64** (4.7 g, 90%) as a pale yellow foam. The material was stored at -20 °C and under Ar, as it readily hydrolyzes to give an anomeric mixture of alcohols. R_f 0.74, (50% EtOAc:hexanes). $[\alpha]_D^{24} = +12.0$ (*c* = 0.5, CH₂Cl₂); IR (thin film on NaCl): $\nu = 3422, 2956, 2991, 2361, 1731, 1676, 1616, 1519, 1452, 1373, 1271, 1177, 1147, 1094, 1070, 1028$ cm⁻¹; ¹H NMR (300 MHz, CDCl₃): $\delta = 8.69$ (s, 1H, C=NH), 7.90 (m, 4H, ArH), 7.51 (m, 2H, ArH), 7.42 – 7.26 (m, 4H, ArH), 7.00 (d, *J* = 8.9 Hz, 2H, C₆H₄OMe), 6.93 (d, *J* = 5.4 Hz, 1H, NHTCA), 6.77 (d, *J* = 2.1 Hz, 1H, H-1 GalNAc), 6.68 (d, *J* = 8.9 Hz, 2H, C₆H₄OMe), 5.52 (dd, *J* = 8.7, 8.7 Hz, 1H, H-3 GlcA), 5.45 (dd, *J* = 8.7, 8.7 Hz, 1H, H-2 GlcA), 5.27 (d, *J* = 7.8 Hz, 1H, H-1 GalNAc), 5.17 (s, 1H, MeOPhCH), 4.62 (m, 2H, H-4 GalNAc, H-4 GlcA), 4.49 (m, 1H, H-3 GalNAc), 4.31 (m, 2H, H-2 GalNAc, H-6 GalNAc), 4.18 (d, *J* = 9.0 Hz, 1H, H-5 GlcA), 4.00 (d, *J* = 12.6 Hz, 1H, H-6 GalNAc),

3.94 (s, 1H, H-5 GalNAc), 3.75 (s, 3H, PhOCH₃), 3.74 (s, 3H, CO₂CH₃), 0.73 (s, 9H, (CH₃)₃CSi), -0.06 (s, 3H, CH₃Si), -0.19 (s, 3H, CH₃Si); ¹³C NMR (75 MHz, CDCl₃): δ = 168.1, 165.9, 165.6, 162.0, 160.4, 133.9, 133.6, 130.1, 129.9, 129.4, 128.7, 128.6, 127.6, 113.6, 101.1, 98.4, 95.3, 77.2, 75.5, 74.4, 71.2, 70.9, 69.2, 69.0, 65.5, 55.6, 53.0, 50.5, 46.5, 25.7, -4.0, -4.8. The material hydrolyzed too readily to obtain a mass spectrum.



Allyl (methyl 2,3-di-O-benzoyl-β-D-glucopyranosyluronate)-(1 → 3)-4,6-O-p-methoxybenzylidene-2-deoxy-2-trichloroacetamido-β-D-galactopyranoside (65). To a solution of **61** (2.5 g, 2.5 mmol) in dry THF (40 mL) and pyridine (40 mL) cooled to 0 °C, was added HF•pyridine (13 mL, 715 mmol). The reaction mixture was warmed to rt and stirred for 18 h. The mixture was then diluted with EtOAc and washed with 10% aqueous CuSO₄. The aqueous phase was extracted with EtOAc (3x) and the combined organics washed with saturated aqueous NaHCO₃ and dried over MgSO₄. The solvent was removed *in vacuo* to afford a yellow oil. Purification of this oil by flash chromatography (30 → 60% EtOAc:hexanes) afforded **65** (1.9 g, 85%) as a white solid. R_f 0.35 (60% EtOAc:hexanes). [α]_D²⁵ = +32.8 (c = 1.0, CH₂Cl₂); IR (thin film on NaCl): ν = 3422, 1731, 1616, 1519, 1452, 1369, 1251, 1173, 1093, 1069 cm⁻¹; ¹H NMR (300 MHz, CDCl₃): δ = 7.93 – 7.87 (m, 4H, ArH), 7.50 – 7.42 (m, 4H, ArH, C₆H₄OMe), 7.36 – 7.26 (m, 4H, ArH), 7.01 (d, J = 6.6 Hz, 1H, NHTCA), 6.89 (d, J = 8.7 Hz, 2H, C₆H₄OMe), 5.89 – 5.77 (m, 1H, OCH₂CH=CH₂), 5.47 (m, 3H, MeOPhCH, H-2 GlcA, H-

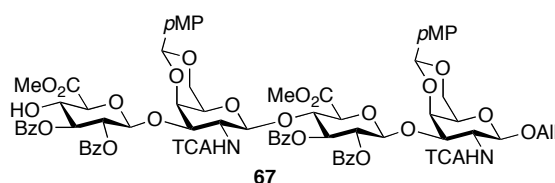
3 GlcA), 5.26 – 5.12 (m, 4H, OCH₂CH=CH₂, H-1 GalNAc, H-1 GlcA), 4.73 (dd, *J* = 3.6, 11.4 Hz, 1H, H-3 GalNAc), 4.41 – 4.28 (m, 3H, OCH₂CH=CH₂, H-4 GalNAc, H-6 GalNAc), 4.19 (m, 1H, H-4 GlcA), 4.12 – 4.02 (m, 3H, OCH₂CH=CH₂, H-5 GlcA, H-6 GalNAc), 3.83 (s, 3H, PhOCH₃), 3.81 (s, 3H, CO₂CH₃), 3.72 (m, 1H, H-2 GalNAc), 3.48 (s, 1H, H-5 GalNAc), 3.45 (d, *J* = 3.3 Hz, 1H, OH); ¹³C NMR (75 MHz, CDCl₃): δ = 169.3, 166.6, 165.2, 162.3, 160.1, 133.8, 133.6, 133.5, 130.4, 130.1, 130.0, 129.2, 129.1, 128.7, 128.6, 127.5, 118.2, 113.7, 100.8, 100.7, 97.7, 76.1, 75.4, 74.3, 74.1, 71.4, 70.7, 69.3, 66.8, 55.7, 53.4; ESI MS: *m/z*: calcd for C₄₀H₃₉Cl₃NO₁₅; 880.1; found: 880.2 [*M* – H][–].



Allyl (methyl 2,3-di-*O*-benzoyl-4-*O*-*tert*-butyldimethylsilyl-β-D-glucopyranosyluronate)-(1 → 3)-(4,6-*O*-*p*-methoxybenzylidene-2-deoxy-2-trichloroacetamido-β-D-galactopyranosyl)-(1 → 4)-(methyl 2,3-di-*O*-benzoyl-β-D-glucopyranosyluronate)-(1 → 3)-4,6-*O*-*p*-methoxybenzylidene-2-deoxy-2-trichloroacetamido-β-D-galactopyranoside (37). **64** (0.10 g, 0.088 mmol) and **65** (0.065 g, 0.074 mmol) were combined and azeotroped by co-evaporation with toluene (3x) and placed under high vacuum overnight to dry. The mixture was dissolved in CH₂Cl₂ (3.0 mL), 4Å powdered molecular sieves added. The mixture was stirred for 1 h at rt and then cooled to –78 °C. Trimethylsilyl trifluoromethanesulfonate (0.5 *N* solution in CH₂Cl₂, 0.0033 g, 30 μL, 0.015 mmol) was cooled to –78 °C and added dropwise to the reaction mixture. After 10 min, the reaction mixture was warmed to –20 °C, stirred

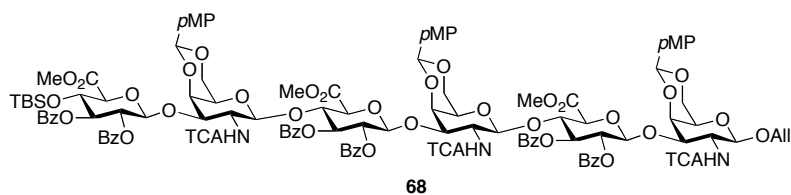
for 30 min and then quenched with TEA. The mixture was filtered and concentrated to afford a yellow oil. Purification of this oil by flash chromatography (30 → 40% EtOAc:hexanes containing 0.1% TEA) followed by preparative thin layer chromatography (10% EtOAc:CH₂Cl₂) afforded **37** (59 mg, 44%) as a white solid. For complete assignment of the ¹H NMR spectra of this compound, ¹H decoupling and TOCSY experiments were performed. R_f 0.43 (60% EtOAc:hexanes). [α]_D²⁵ = +13.4 (*c* = 0.5, CH₂Cl₂); IR (thin film on NaCl): ν = 3424, 2956, 2361, 1732, 1638, 1519, 1452, 1368, 1251, 1173, 1093, 1173, 1093, 1070, 1028; ¹H NMR (600 MHz, CDCl₃): δ = 7.88 – 7.80 (m, 8H, ArH), 7.49 – 7.45 (m, 4H, ArH), 7.38 – 7.28 (m, 8H, ArH), 7.22 – 7.20 (m, 2H, ArH), 7.06 (d, *J* = 8.4 Hz, 2H, C₆H₄OMe), 6.93 (d, *J* = 8.4 Hz, 2H, C₆H₄OMe), 6.85 (d, *J* = 6.6 Hz, 1H, NHTCA), 6.74 (d, *J* = 8.4 Hz, 2H, C₆H₄OMe), 6.66 (d, *J* = 7.2 Hz, 1H, NHTCA), 5.87 – 5.81 (m, 1H, OCH₂CH=CH₂), 5.58 (dd, *J* = 7.8, 7.8 Hz, 1H, H-3 GlcA), 5.49 (s, 1H, MeOPhCH), 5.44 (dd, *J* = 8.7, 8.7 Hz, 1H, H-3 GlcA), 5.35 (m, 2H, H-2 GlcA, H-2 GlcA), 5.23 (d, *J* = 18.0 Hz, 1H, OCH₂CH=CH₂), 5.20 (s, 1H, MeOPhCH), 5.15 – 5.12 (m, 2H, OCH₂CH=CH₂, H-1 GlcA), 5.11 (d, *J* = 7.8 Hz, 1H, H-1 GalNAc), 5.03 (d, *J* = 7.2 Hz, 1H, H-1 GlcA), 5.00 (d, *J* = 8.4 Hz, 1H, H-1 GalNAc), 4.68 (dd, *J* = 3.6, 10.8 Hz, 1H, H-3 GalNAc), 4.58 (dd, *J* = 9.0, 9.0 Hz, 1H, H-4 GlcA), 4.39 – 4.30 (m, 5H, OCH₂CH=CH₂, H-3 GalNAc, H-4 GalNAc, H-4 GlcA, H-6 GalNAc), 4.14 (m, 2H, H-4 GalNAc, H-5 GlcA), 4.06 – 3.91 (m, 3H, OCH₂CH=CH₂, H-5 GlcA, H-6 GalNAc), 3.83 (s, 3H, PhOCH₃), 3.81 – 3.68 (m, 4H, H-2 GalNAc, H-2 GalNAc, H-6 GalNAc, H-6 GalNAc), 3.80 (s, 3H, PhOCH₃), 3.80 (s, 3H, CO₂CH₃), 3.79 (s, 3H, CO₂CH₃), 3.48 (s, 1H, H-5 GalNAc), 3.10 (s, 1H, H-5 GalNAc), 0.72 (s, 9H, (CH₃)₃CSi), -0.09 (s, 3H, CH₃Si), -0.24 (s, 3H, CH₃Si); ¹³C NMR (75 MHz, CDCl₃): δ =

168.8, 168.4, 165.7, 165.4, 165.2, 165.1, 162.2, 161.9, 160.0, 159.8, 133.8, 133.4, 133.3, 133.1, 130.5, 130.4, 130.2, 130.1, 130.0, 129.9, 129.6, 129.5, 129.2, 129.1, 128.6, 128.5, 128.4, 127.9, 127.8, 118.2, 113.7, 113.4, 100.8, 100.5, 100.4, 100.2, 98.6, 97.7, 77.4, 76.4, 75.9, 75.8, 75.3, 75.0, 74.2, 74.1, 73.5, 73.4, 72.1, 71.9, 70.8, 70.6, 69.3, 68.4, 66.9, 55.7, 55.6, 54.8, 53.5, 52.8, 25.7, 18.1, -4.1, -4.8. ESI MS: m/z : calcd for $C_{83}H_{89}Cl_6N_2O_{29}Si$: 1819.4; found 1819.5 $[M + H]^+$.



Allyl (methyl 2,3-di-*O*-benzoyl- β -D-glucopyranosyluronate)-(1 \rightarrow 3)-(4,6-*O*-*p*-methoxybenzylidene-2-deoxy-2-trichloroacetamido- β -D-galactopyranosyl)-(1 \rightarrow 4)-(methyl 2,3-di-*O*-benzoyl- β -D-glucopyranosyluronate)-(1 \rightarrow 3)-4,6-*O*-*p*-methoxybenzylidene-2-deoxy-2-trichloroacetamido- β -D-galactopyranoside (67). To a solution of **37** (0.10 g, 0.055 mmol) in dry THF (0.84 mL) and pyridine (0.84 mL) cooled to 0 °C, was added HF • pyridine (0.28 mL, 15 mmol). The reaction mixture was warmed to rt and stirred for 12 h. The mixture was then diluted with EtOAc and washed with 10% aqueous $CuSO_4$. The aqueous phase was extracted with EtOAc (3x) and the combined organics washed with saturated aqueous $NaHCO_3$ and dried over $MgSO_4$. The solvent was removed *in vacuo* to afford a yellow oil. Purification of this oil by flash chromatography (40 \rightarrow 60% EtOAc:hexanes) afforded **67** (60 mg, 64%) as a white solid. R_f 0.24 (60% EtOAc:hexanes). $[\alpha]_D^{25} = +13.8$ ($c = 0.5$, CH_2Cl_2); IR (thin film on NaCl): $\nu = 3528, 2361, 1731, 1616, 1519, 1452, 1368, 1251, 1173, 1094, 1070, 1028$; 1H NMR

(600 MHz, CDCl₃): δ = 7.92 (d, J = 7.8 Hz, 2H, ArH), 7.89 – 7.86 (m, 6H, ArH), 7.51 – 7.47 (m, 5H, ArH), 7.39 – 7.32 (m, 7H, ArH), 7.22 – 7.19 (m, 2H, ArH), 7.11 (d, J = 8.4 Hz, 2H, C₆H₄OMe), 6.91 (d, J = 8.4 Hz, 2H, C₆H₄OMe), 6.87 (d, J = 6.6 Hz, 1H, NHTCA), 6.87 (d, J = 7.2 Hz, 1H, NHTCA), 6.75 (d, J = 8.4 Hz, 2H, C₆H₄OMe), 5.87 – 5.81 (m, 1H, OCH₂CH=CH₂), 5.60 (dd, J = 8.4, 7.8 Hz, 1H, H-3 GlcA), 5.49 (s, 1H, MeOPhCH), 5.42 – 5.34 (m, 3H, H-3 GlcA, H-2 GlcA, H-2 GlcA), 5.25 (s, 1H, MeOPhCH), 5.23 (d, J = 18.0 Hz, 1H, OCH₂CH=CH₂), 5.17 – 5.11 (m, 5H, OCH₂CH=CH₂, H-1 GlcA, H-1 GalNAc, H-1 GlcA, H-1 GalNAc), 4.70 (dd, J = 3.3, 11.1 Hz, 1H, H-3 GalNAc), 4.61 (dd, J = 9.0, 8.4 Hz, 1H, H-4 GlcA), 4.44 (dd, J = 3.0, 11.4 Hz, 1H, H-3 GalNAc), 4.37 – 4.30 (m, 4H, OCH₂CH=CH₂, H-4 GalNAc, H-4 GlcA, H-6 GalNAc), 4.25 (d, J = 3.0 Hz, 1H, H-4 GalNAc), 4.20 (m, 1H, H-2 GalNAc), 4.17 (d, J = 9.0 Hz, 1H, H-5 GlcA), 4.08 – 4.03 (m, 3H, OCH₂CH=CH₂, H-5 GlcA, H-6 GalNAc), 3.86 (s, 3H, PhOCH₃), 3.80 (s, 3H, PhOCH₃), 3.80 (s, 3H, CO₂CH₃), 3.79 (s, 3H, CO₂CH₃), 3.74 – 3.65 (m, 3H, H-2 GalNAc, H-6 GalNAc, H-6 GalNAc), 3.48 (s, 1H, H-5 GalNAc), 3.38 (d, J = 2.4 Hz, 1H, OH), 3.13 (s, 1H, H-5 GalNAc); ¹³C NMR (75 MHz, CDCl₃) δ = 169.4, 168.4, 166.7, 165.5, 165.2, 162.3, 162.0, 160.0, 159.9, 133.7, 133.6, 133.5, 133.1, 129.9, 128.6, 128.4, 127.7, 127.6, 118.2, 113.7, 113.4, 100.8, 100.5, 100.2, 98.2, 97.7, 75.7, 75.6, 75.5, 74.8, 74.2, 74.1, 73.9, 73.4, 69.3, 68.6, 67.9, 66.8, 55.7, 55.6, 55.1, 53.5, 53.3. ESI MS: m/z : calcd for C₈₃H₈₉Cl₆N₂O₂₉Si: 1705.1; found 1705.2 [$M + H$]⁺.

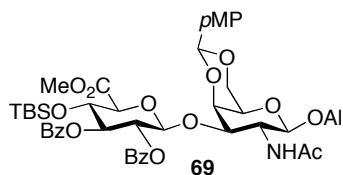


Allyl (methyl 2,3-di-*O*-benzoyl-4-*O*-*tert*-butyldimethylsilyl- β -D-glucopyranosyluronate)-(1 \rightarrow 3)-(4,6-*O*-*p*-methoxybenzylidene-2-deoxy-2-trichloroacetamido- β -D-galactopyranosyl)-(1 \rightarrow 4)-methyl 2,3-di-*O*-benzoyl-4-*O*-*tert*-butyldimethylsilyl- β -D-glucopyranosyluronate)-(1 \rightarrow 3)-(4,6-*O*-*p*-methoxybenzylidene-2-deoxy-2-trichloroacetamido- β -D-galactopyranosyl)-(1 \rightarrow 4)-methyl 2,3-di-*O*-benzoyl- β -D-glucopyranosyluronate)-(1 \rightarrow 3)-4,6-*O*-*p*-methoxybenzylidene-2-deoxy-2-trichloroacetamido- β -D-galactopyranoside (**68**). **64**

(0.073 g, 0.066 mmol) and **67** (0.094 g, 0.055 mmol) were combined, azeotroped by co-evaporation with toluene (3x), and placed under high vacuum overnight to dry. The mixture was dissolved in CH₂Cl₂ (1.2 mL) and 4Å powdered molecular sieves added. After stirring for 1 h at rt, the reaction mixture was cooled to -15 °C. Trimethylsilyl trifluoromethanesulfonate (0.25 *N* in CH₂Cl₂, 60 μ L, 0.011 mmol) was added, and the reaction was stirred at -15 °C for 30 min and quenched with TEA. The mixture was filtered and the solvent removed *in vacuo* to afford a yellow oil. Purification of this oil by flash chromatography (35 \rightarrow 50% EtOAc:hexanes) afforded **68** (32 mg, 25%) as a white solid. *R*_f 0.56 (60% EtOAc:hexanes). For complete assignment of the ¹H NMR spectra of this compound, ¹H decoupling and TOCSY experiments were performed. [α]_D²⁵ = +5.7 (*c* = 1.0, CH₂Cl₂); IR (thin film on NaCl): ν = 3424, 2928, 2360, 1732, 1617, 1519, 1452, 1368, 1251, 1173, 1093, 1070; ¹H NMR (600 MHz, CDCl₃): δ = 7.89 – 7.84 (m, 8H,

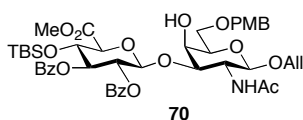
ArH), 7.81 (d, $J = 7.2$ Hz, 2H, ArH), 7.48 – 7.26 (m, 18H, ArH), 7.22 – 7.17 (m, 6H, ArH), 7.05 (d, $J = 8.4$ Hz, 2H, C₆H₄OMe), 6.90 (d, $J = 9.0$ Hz, 2H, C₆H₄OMe), 6.86 (d, $J = 7.2$ Hz, 1H, NHTCA), 6.81 (d, $J = 8.4$ Hz, 2H, C₆H₄OMe), 6.72 (d, $J = 8.4$ Hz, 2H, C₆H₄OMe), 6.63 (d, $J = 7.2$ Hz, 1H, NHTCA), 6.60 (d, $J = 7.2$ Hz, 1H, NHTCA), 5.84 (m, 1H, OCH₂CH=CH₂), 5.59 (dd, $J = 8.1, 8.1$ Hz, 1H H-3 GlcA), 5.52 (dd, $J = 7.5, 7.5$ Hz, 1H, H-3 GlcA), 5.49 (s, 1H, MeOPhCH), 5.44 (dd, $J = 8.4, 8.4$ Hz, 1H H-3 GlcA), 5.36 (m, 2H, H-2 GlcA, H-2 Glc-A), 5.27 (dd, $J = 6.9, 6.9$ Hz, 1H, H-2 GlcA), 5.24 (s, 1H, MeOPhCH), 5.22 (s, 1H, OCH₂CH=CH₂), 5.15 (m, 3H, OCH₂CH=CH₂, H-1 GlcA, MeOPhCH), 5.11 (d, $J = 7.8$ Hz, 1H, H-1 GalNAc), 5.05 (m, 2H, H-1 GalNAc, H-1 GlcA), 5.02 (d, $J = 7.2$ Hz, 1H, H-1 GlcA), 4.86 (d, $J = 7.8$ Hz, 1H, H-1 GalNAc), 4.69 (dd, $J = 3.3, 11.1$ Hz, 1H, H-1 GlcA), 4.59 (dd, $J = 9.0, 9.0$ Hz, 1H, H-4 GlcA), 4.54 (dd, $J = 9.0, 9.0$ Hz, 1H, H-4 GlcA), 4.37 – 4.30 (m, 6H, H-4 GlcA, H-5 GalNAc, H-3 GalNAc, OCH₂CH=CH₂, H-6 GalNAc, H-4 GalNAc), 4.16 – 4.03 (m, 7H, OCH₂CH=CH₂, H-6 GalNAc, H-5 GlcA, H-5 GlcA, H-4 GalNAc, H-5 GlcA, H-4 GalNAc), 3.81 – 3.76 (m, 2H, H-6 GalNAc, H-6 GalNAc), 3.80 – 3.77 (6s, 18H, CO₂CH₃, PhOCH₃), 3.73 – 3.61 (m, 5H, H-6 GalNAc, H-6 GalNAc, H-2 GalNAc, H-2 GalNAc, H-2 GalNAc), 3.48 (s, 1H, H-5 GalNAc), 3.08 (s, 1H, H-5 GalNAc), 3.00 (s, 1H, H-5 GalNAc), 0.72 (s, 9H, (CH₃)₃CSi), -0.10 (s, 3H, CH₃Si), -0.25 (s, 3H, CH₃Si); ¹³C NMR (75 MHz, CDCl₃): $\delta = 168.8, 168.5, 168.4, 165.7, 165.5, 165.4, 165.3, 165.1, 165.0, 162.3, 161.9, 161.8, 160.0, 159.9, 159.8, 133.7, 133.4, 133.3, 133.1, 130.7, 130.5, 130.4, 130.2, 130.1, 130.0, 129.9, 129.5, 129.4, 129.2, 129.1, 128.6, 128.5, 128.4, 128.0, 127.8, 127.7, 118.2, 113.7, 113.4, 113.3, 102.9, 100.7, 100.6, 100.5, 100.1, 98.8, 98.4, 97.7, 97.6, 92.5, 92.4, 92.3, 77.5, 76.4, 75.8, 75.7, 75.3, 75.2, 75.0, 74.3, 74.2, 74.1, 73.8,$

73.6, 73.5, 73.4, 72.1, 71.9, 70.8, 70.6, 69.3, 68.6, 66.8, 55.6, 55.5, 54.9, 54.7, 53.5, 53.4, 52.8, 30.1, 25.7, 18.1, -4.1, -4.8. ESI MS: m/z : calcd for $C_{120}H_{123}Cl_9N_3O_{43}Si$: 2637.4; found 2637.5 $[M + H]^+$.



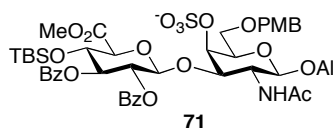
Allyl (methyl 2,3-di-*O*-benzoyl-4-*O*-*tert*-butyldimethylsilyl- β -D-glucopyranosyluronate)-(1 \rightarrow 3)-4,6-*O*-*p*-methoxybenzylidene-2-deoxy-2-acetamido- β -D-galactopyranoside (69). **69** was prepared using a procedure modified from Coutant *et al.*⁴⁶ To a solution of **61** (250 mg, 0.251 mmol) in benzene (7.80 mL). were added tributylstannane (305 μ L, 1.51 mmol) and 2,2'-azobisisobutyronitrile (80.0 mg). The reaction was stirred at rt for 45 min. It was then heated to 80 $^{\circ}$ C and stirred an additional 1.5 h. The reaction was cooled to rt and concentrated to afford a white solid. The product was purified by flash chromatography (50% EtOAc:hexanes) to afford **69** (190 mg, 85%) as a white solid. R_f 0.19 (50% EtOAc:hexanes). 1H NMR (300 MHz, $CDCl_3$): δ = 7.89 – 7.86 (m, 4H, ArH), 7.51 – 7.42 (m, 4H, ArH), 7.37 – 7.31 (m, 4H, ArH), 6.88 (d, J = 8.7 Hz, 2H, C_6H_4OMe), 5.91 – 5.75 (m, 1H, $OCH_2CH=CH_2$), 5.55 (dd, J = 8.9, 8.9 Hz, 1H, H-3'), 5.46 (s, 1H, MeOPhCH), 5.40 – 5.35 (m, 2H, NHAc, H-2 GlcA), 5.20 (dd, J = 1.4, 17.3 Hz, 1H, $OCH_2CH=CH_2$), 5.14 – 5.11 (m, 2H, $OCH_2CH=CH_2$, H-1 GalNAc), 4.97 (d, J = 7.5 Hz, 1H, H-1 GlcA), 4.77 (dd, J = 3.9, 11.1 Hz, 1H, H-3 GalNAc), 4.37 – 4.25 (m, 4H, $OCH_2CH=CH_2$, H-4 GalNAc, H-4 GlcA, H-6 GalNAc), 4.10 (d, J = 9.6 Hz, 1H, H-5 GlcA), 4.10 – 3.98 (m, 2H, $OCH_2CH=CH_2$, H-6 GalNAc), 3.81 (s, 3H, CO_2CH_3), 3.78 (s, 3H, $PhOCH_3$), 3.47 (s, 1H, H-5 GalNAc), 3.34 – 3.26 (m,

¹H, H-2 GalNAc), 1.53 (s, 3H, HNC(O)CH₃), 0.72 (s, 9H, (CH₃)₃CSi), -0.07 (s, 3H, CH₃Si), -0.23 (s, 3H, CH₃Si); ¹³C NMR (75 MHz, CDCl₃): δ = 171.4, 168.7, 165.8, 165.0, 160.0, 134.1, 133.5, 133.4, 130.7, 129.9, 129.8, 129.6, 129.5, 128.6, 128.5, 127.8, 118.0, 113.6, 101.6, 100.8, 98.0, 76.3, 76.1, 75.6, 72.4, 70.9, 70.4, 69.4, 66.7, 55.6, 55.1, 52.9, 25.8, 23.6, 18.1, -4.0, -4.7; ESI MS: *m/z*: calcd for C₄₆H₅₇NNaO₁₅Si: 914.3, found 914.4 [*M* + Na]⁺.



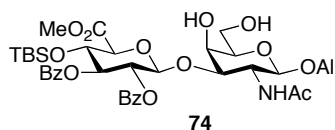
Allyl (methyl 2,3-di-*O*-benzoyl-4-*O*-*tert*-butyldimethylsilyl-β-D-glucopyranosyluronate)-(1 → 3)-6-*O*-*p*-methoxybenzyl-2-deoxy-2-acetamido-β-D-galactopyranoside (70). To **69** (144 mg, 0.162 mmol) dissolved in CH₂Cl₂ (2.8 mL) was added sodium cyanoborohydride (102 mg, 1.62 mmol) in THF (1.8 mL) and 4 Å powdered molecular sieves, and the reaction stirred at rt for 1 h. Trifluoroacetic acid (250 μL, 3.23 mmol) was then added dropwise, and the reaction was stirred overnight. It was then filtered through Celite, diluted with CH₂Cl₂, and washed with saturated aqueous NaHCO₃. The aqueous layer was extracted with CH₂Cl₂ (3x). The combined organic layers was washed with brine, dried over MgSO₄, filtered, and concentrated to afford a colorless syrup. The product was purified by flash chromatography (60% EtOAc:hexanes) to yield **70** (118 mg, 82%) as a white solid. R_f 0.17 (60% EtOAc:hexanes). ¹H NMR (300 MHz, CDCl₃): δ = 7.88 (d, *J* = 7.5 Hz, 4H, ArH), 7.50 – 7.44 (m, 2H, ArH), 7.57 – 7.30 (m, 4H, ArH), 7.24 (d, *J* = 8.7 Hz, 2H, C₆H₄OMe), 6.86 (d, *J* = 8.7 Hz, 2H, C₆H₄OMe), 5.85 – 5.72 (m, 1H, OCH₂CH=CH₂), 5.58 (dd, *J* = 9.2,

9.2 Hz, 1H, H-3 GlcA), 5.47 (d, $J = 6.6$ Hz, 1H, *NHAc*), 5.38 (dd, $J = 7.8, 8.4$ Hz, 1H, H-2 GlcA), 5.17 (dd, $J = 1.4, 17.3$ Hz, 1H, $\text{OCH}_2\text{CH}=\text{CH}_2$), 5.09 (d, $J = 10.5$ Hz, 1H, $\text{OCH}_2\text{CH}=\text{CH}_2$), 4.99 (d, $J = 9.0$ Hz, 1H, H-1 GalNAc), 4.89 (d, $J = 7.5$ Hz, 1H, H-1 GlcA), 4.63 (dd, $J = 3.0, 10.5$ Hz, 1H, H-3 GalNAc), 4.51 (d, $J = 11.7$ Hz, 1H, *MeOPhCH*), 4.46 (d, $J = 11.4$ Hz, 1H, *MeOPhCH*), 4.33 – 4.22 (m, 2H, H-4 GlcA, $\text{OCH}_2\text{CH}=\text{CH}_2$), 4.11 – 4.05 (m, 2H, H-5 GlcA, $\text{OCH}_2\text{CH}=\text{CH}_2$), 3.99 (dd, $J = 6.3, 12.9$ Hz, 1H, H-5 GalNAc), 3.78 – 3.64 (m, 4H, H-2 GalNAc, H-4 GalNAc, H-6 GalNAc, H-6 GalNAc), 3.78 (s, 3H, CO_2CH_3), 3.74 (s, 3H, PhOCH_3), 2.67 (s, 1H, *OH*), 1.30 (s, 3H, $\text{HNC}(\text{O})\text{CH}_3$), 0.72 (s, 9H, $(\text{CH}_3)_3\text{CSi}$), -0.05 (s, 3H, CH_3Si), -0.20 (s, 3H, CH_3Si); ^{13}C NMR (75 MHz, CDCl_3): $\delta = 171.2, 168.4, 165.7, 165.1, 159.3, 134.1, 133.6, 133.4, 130.4, 129.9, 129.9, 129.5, 129.5, 129.2, 128.7, 128.6, 117.8, 114.0, 102.1, 98.1, 78.7, 76.5, 75.1, 73.4, 73.2, 72.2, 70.9, 70.2, 69.2, 68.5, 55.6, 55.1, 53.0, 25.8, 23.3, 18.1, -4.0, -4.7$; HR-FAB MS: m/z : calcd for $\text{C}_{46}\text{H}_{60}\text{NO}_{15}\text{Si}$: 894.3732; found: 894.3696 [$M + \text{H}$] $^+$.



Allyl (methyl 2,3-di-*O*-benzoyl-4-*O*-*tert*-butyldimethylsilyl- β -D-glucopyranosyluronate)-(1 \rightarrow 3)-6-*O*-*p*-methoxybenzyl-4-*O*-sodium sulfonato-2-deoxy-2-acetamido- β -D-galactopyranoside (71). **70** (0.40 g, 0.45 mmol) was dissolved in DMF (13.5 mL), $\text{SO}_3 \cdot \text{TMA}$ (1.9 g, 13.4 mmol) was added, and the reaction was stirred at 50 °C overnight. The reaction was then quenched with MeOH, cooled to rt, and concentrated to afford a white solid. The residue was purified on Sephadex LH-20 (50% CH_2Cl_2 :MeOH, 30 mL resin, 1 cm x 30 cm column), followed by flash chromatography

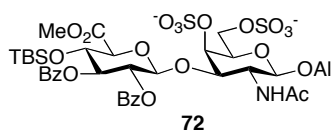
(100% EtOAc) and Sephadex SP C25 (Na⁺) (10% H₂O:MeOH, 50 mL resin, 1 cm x 40 cm column) to afford **71** (0.34 g, 76%) as a white solid. *R*_f 0.11 (60% EtOAc:hexanes). ¹H NMR (300 MHz, CD₃OD): δ = 7.89 – 7.85 (m, 4H, *ArH*), 7.53 – 7.48 (m, 2H, *ArH*), 7.38 – 7.27 (m, 6H, *ArH*), 6.87 (d, *J* = 8.7 Hz, 2H, *ArH*), 5.85 – 5.72 (m, 1H, OCH₂CH=CH₂), 5.64 (dd, *J* = 9.3, 9.3 Hz, 1H, H-3 GlcA), 5.46 (dd, *J* = 8.9, 8.9 Hz, 1H, H-2 GlcA), 5.17 (dd, *J* = 1.2, 17.4 Hz, 1H, OCH₂CH=CH₂), 5.09 – 5.04 (m, 2H, *NHAc*, H-2 GlcA), 4.91 – 4.87 (m, 2H, H-1 GalNAc, OCH₂CH=CH₂), 4.53 – 4.39 (m, 2H, H-3 GalNAc, H-4 GalNAc), 4.20 (d, *J* = 9.3 Hz, 2H, MeOPhCH₂), 4.03 – 3.97 (m, 2H, H-4 GlcA, OCH₂CH=CH₂), 3.92 – 3.76 (m, 6H, H-5 GlcA, H-2 GalNAc, H-5 GalNAc, H-6 GalNAc, H-6 GalNAc, OCH₂CH=CH₂), 3.77 (s, 3H, CO₂CH₃), 3.76 (s, 3H, PhOCH₃), 1.39 (s, 3H, HNC(O)CH₃), 0.73 (s, 9H, (CH₃)₃CSi), -0.01 (s, 3H, CH₃Si), -0.17 (s, 3H, CH₃Si); ¹³C NMR (75 MHz, CD₃OD): δ = 172.2, 169.0, 165.9, 165.8, 159.5, 134.3, 133.4, 130.5, 129.9, 129.6, 129.5, 129.3, 128.3, 128.2, 115.9, 113.5, 102.2, 100.7, 78.7, 76.2, 75.6, 73.7, 72.9, 72.7, 70.8, 70.0, 69.6, 54.6, 52.2, 44.8, 25.0, 21.6, 17.7, -5.0, -5.6; ESI MS: *m/z*: calcd for C₄₆H₅₈NNa₂O₁₈SSi: 1018.4; found: 1019.1 [*M* + Na]⁺.



Allyl (methyl 2,3-di-*O*-benzoyl-4-*O*-*tert*-butyldimethylsilyl-β-D-glucopyranosyluronate)-(1 → 3)-2-deoxy-2-acetamido-β-D-galactopyranoside (74).

To a solution of **69** (190 mg, 0.213 mmol) in CH₂Cl₂ (2.40 mL) and H₂O (0.560 mL) was added 2,3-dichloro-5,6-dicyano-1,4-benzoquinone (73.0 mg, 0.320 mmol). The reaction was stirred at rt for 3 h, quenched with MeOH, and concentrated to yield a red solid. The

product was purified on Sephadex LH-20 (50% CH₂Cl₂:MeOH, 30 mL resin, 1 cm x 30 cm column), followed by flash chromatography (100% EtOAc) to afford an orange solid containing the desired diol **74** (102 mg, 62%). R_f 0.23 (100% EtOAc). ¹H NMR (300 MHz, CD₃OD): δ = 7.90 – 7.86 (m, 4H, ArH), 7.49 – 7.44 (m, 2H, ArH), 7.37 – 7.29 (m, 4H, ArH), 5.83 – 5.74 (m, 1H, OCH₂CH=CH₂), 5.61 (dd, *J* = 9.0, 8.7 Hz, 1H, H-3 GlcA), 5.35 (dd, *J* = 8.1, 9.0 Hz, 1H, H-2 GlcA), 5.18 (dd, *J* = 1.7, 17.6 Hz, 1H, OCH₂CH=CH₂), 5.10 (d, *J* = 9.9 Hz, 1H, OCH₂CH=CH₂), 4.97 (d, *J* = 7.5 Hz, 1H, H-1 GlcA), 4.90 (d, *J* = 7.5 Hz, 1H, H-1 GalNAc), 4.552 (m, 1H, NHAc), 4.29 – 4.17 (m, 3H, H-1 GalNAc, H-4 GalNAc, H-6 GalNAc), 4.03 – 3.93 (m, 4H, OCH₂CH=CH₂, H-3 GalNAc, H-4 GlcA, H-6 GalNAc), 3.89 – 3.86 (m, 2H, OCH₂CH=CH₂, H-5 GalNAc, H-5 GlcA), 3.65 (m, 1H, H-2 GalNAc), 3.78 (s, 3H, CO₂CH₃), 1.26 (s, 3H, HNC(O)CH₃), 0.73 (s, 9H, (CH₃)₃CSi), -0.07 (s, 3H, CH₃Si), -0.20 (s, 3H, CH₃Si); ESI MS: *m/z*: calcd for C₃₈H₅₂NO₁₄Si 774.9; found 774.2 [*M* + H]⁺.



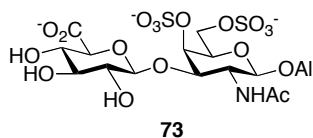
Allyl (methyl 2,3-di-*O*-benzoyl-4-*O*-*tert*-butyldimethylsilyl-β-D-glucopyranosyluronate)-(1 → 3)-4,6-*O*-disodium sulfonato-2-deoxy-2-acetamido-β-D-galactopyranoside (72). To **71** (300 mg, 0.301 mmol) dissolved in CH₂Cl₂ (3.4 mL) and H₂O (0.80 mL) was added 2,3-dichloro-5,6-dicyano-1,4-benzoquinone (103 mg, 0.452 mmol). The reaction was stirred at rt for 4 h at rt, quenched with MeOH, and concentrated to yield a red solid. The product was purified on Sephadex LH-20 (50% CH₂Cl₂:MeOH, 30 mL resin, 1 cm x 30 cm column), followed by flash chromatography

(90% CH₂Cl₂:MeOH), and Sephadex SP C25 (Na⁺) (1:8 H₂O:MeOH, 50 mL resin, 1 cm x 40 cm column) to afford an orange solid containing the desired alcohol. R_f 0.77 (EtOAc:pyr:H₂O:AcOH, 8:5:2:1).

The impure alcohol (303 mg) was dissolved in DMF (9 mL), and SO₃•TMA (1.25 g, 9.04 mmol) was added. The reaction was stirred at 50 °C overnight and then cooled to rt, quenched with MeOH, and concentrated to afford a yellow solid. This was purified on Sephadex LH-20 (50% CH₂Cl₂:MeOH, 30 mL resin, 1 cm x 30 cm column), followed by flash chromatography (100% EtOAc → 8:3:1:0.5 EtOAc:pyr:H₂O:AcOH), and Sephadex SP C25 (Na⁺) (H₂O:MeOH, 1:1, 50 mL, resin 1 cm x 40 cm column). The product was lyophilized to afford **72** (177 mg, 60% from **71**) as a white solid. R_f 0.49 (EtOAc:pyr:H₂O:AcOH, 8:5:3:1).

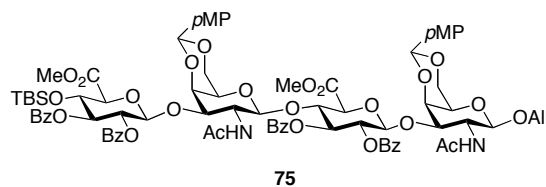
72 was prepared by an alternative method. The sulfation of **74** was performed using a procedure modified from Tamura *et al.*²² The crude diol **74** (102 mg, 0.132 mmol) was dissolved in DMF (5 mL), and SO₃•TMA (0.550 g, 3.96 mmol) was then added. The reaction was stirred at 50 °C overnight. It was cooled to rt, quenched with MeOH, and concentrated to afford a yellow solid. The product was purified on Sephadex LH-20 (50% CH₂Cl₂:MeOH, 30 mL resin, 1 cm x 30 cm column), followed by flash chromatography (10% → 20% MeOH:CH₂Cl₂), to afford **72** (115 mg, 93%) as a white solid. R_f 0.125 (15% MeOH:CH₂Cl₂). ¹H NMR (300 MHz, CD₃OD): δ = 7.88 – 7.85 (m, 4H, ArH), 7.54 – 7.47 (m, 2H, ArH), 7.38 – 7.32 (m, 4H, ArH), 5.86 – 5.73 (m, 1H, OCH₂CH=CH₂), 5.67 (dd, *J* = 9.3, 9.3 Hz, 1H, H-3 GlcA), 5.48 (dd, *J* = 8.1, 9.2 Hz, 1H,

H-2 GlcA), 5.18 (dd, $J = 1.7, 17.6$ Hz, 1H, $\text{OCH}_2\text{CH}=\text{CH}_2$), 5.11 (d, $J = 7.5$ Hz, 1H, H-1 GlcA), 5.05 (dd, $J = 1.8, 10.5$ Hz, 1H, $\text{OCH}_2\text{CH}=\text{CH}_2$), 4.96 (s, 1H, H-4 GalNAc), 4.44 – 4.35 (m, 3H, H-1 GalNAc, H-3 GalNAc, H-4 GlcA), 4.30 – 4.22 (m, 3H, $\text{OCH}_2\text{CH}=\text{CH}_2$, H-5 GlcA, H-6 GalNAc), 4.09 – 3.98 (m, 2H, $\text{OCH}_2\text{CH}=\text{CH}_2$, H-6 GalNAc), 3.95 – 3.91 (m, 2H, H-2 GalNAc, H-5 GalNAc), 3.86 (s, 3H, CO_2CH_3), 1.30 (s, 3H, $\text{HNC}(\text{O})\text{CH}_3$), 0.74 (s, 9H, $(\text{CH}_3)_3\text{CSi}$), -0.02 (s, 3H, CH_3Si), -0.18 (s, 3H, CH_3Si); ^{13}C NMR (75 MHz, CD_3OD): $\delta = 172.3, 170.0, 166.2, 165.8, 134.1, 133.5, 133.4, 130.0, 129.5, 129.4, 129.0, 128.3, 128.2, 115.9, 102.5, 100.8, 79.2, 76.3, 75.9, 75.4, 72.8, 72.6, 70.9, 69.7, 67.6, 54.2, 52.6, 25.0, 21.4, 17.6, -4.9, -5.6$; HR-FAB MS: m/z : calcd for $\text{C}_{38}\text{H}_{49}\text{NNa}_3\text{O}_{20}\text{S}_2\text{Si}$: 1000.175; found: 1000.175 $[M + \text{Na}]^+$.



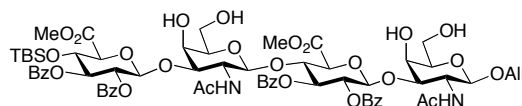
Allyl (sodium β -D-glucopyranosyluronate)-(1 \rightarrow 3)-4,6-di-O-sodium sulfonato-2-deoxy-2-acetamido- β -D-galactopyranoside (73). **72** (115 mg, 0.123 mmol) was dissolved in pyridine (1.7 mL) and THF (1.7 mL). The reaction was cooled to 0 °C, HF•pyridine (0.60 mL, 33 mmol) was added, and it slowly warmed to rt overnight. After 12 h, the mixture was flowed through a Sephadex LH-20 column (50% CH_2Cl_2 :MeOH, 30 mL resin, 1 cm x 30 cm column) and the concentrated residue was purified by flash chromatography (10% \rightarrow 20% MeOH: CH_2Cl_2) to afford a white solid (90.0 mg). R_f 0.50 (EtOAc:pyr:H₂O:AcOH, 8:5:3:1).

The crude alcohol (90 mg, 0.11 mmol) was dissolved in THF (1.8 mL) and H₂O (1.8 mL) and to this was added 2 M NaOH (0.72 mL, 1.4 mmol). After 12 h at rt, the reaction was neutralized with Amberlyst IR-120 resin, filtered, and lyophilized to afford an orange solid. The product was purified by gel filtration chromatography using Sephadex G-10 UF, a resin for compounds with a molecular weight of 700 or less, (100% H₂O, 25 mL resin, 1 cm x 20 cm) and Sephadex SP C25 (Na⁺) (100% H₂O, 25 mL resin, 1 cm x 20 cm), to sharpen the peaks in the ¹H NMR spectrum. The fractions were lyophilized to afford **73** (45 mg, 55%, 2 steps) as a white solid. R_f 0.12 (EtOAc:pyr:H₂O:AcOH, 8:5:3:1). ¹H NMR (300 MHz, D₂O): δ = 5.95 – 5.81 (m, 1H, OCH₂CH=CH₂), 5.32 – 5.22 (m, 2H, OCH₂CH=CH₂), 4.80 (s, 1H, H-4 GalNAc), 4.57 – 4.54 (m, 1H, H-1 GalNAc), 4.46 (d, *J* = 7.8 Hz, 1H, H-1 GlcA), 4.31 – 4.25 (m, 2H, OCH₂CH=CH₂, H-3 GalNAc), 4.20 – 4.13 (m, 2H, OCH₂CH=CH₂, H-2 GalNAc), 4.05 – 4.02 (m, 3H, H-6 GalNAc, H-6 GalNAc, H-5 GalNAc), 3.68 (d, *J* = 9.3, 1H, H-5 GlcA), 3.51 – 3.44 (m, 2H, H-3 GlcA, H-4 GlcA), 3.33 (dd, *J* = 8.1, 8.1 Hz, 1H, H-2 GlcA), 1.99 (s, 3H, HNC(O)CH₃); ¹³C NMR (75 MHz, D₂O): δ = 118.7, 103.4, 100.0, 175.6, 174.8, 133.2, 76.4, 75.2, 75.1, 72.6, 72.4, 71.9, 70.8, 68.0, 51.8, 22.5; HR-FAB MS: *m/z*: calcd for C₁₇H₂₄NNa₂O₁₈S₂: 640.0230; found: 640.0202 [*M* - Na]⁻.



Allyl (methyl 2,3-di-*O*-benzoyl-4-*O*-*tert*-butyldimethylsilyl- β -D-glucopyranosyluronate)-(1 \rightarrow 3)-(4,6-*O*-*p*-methoxybenzylidene-2-deoxy-2-acetamido- β -D-galactopyranosyl)-(1 \rightarrow 4)-(methyl 2,3-di-*O*-benzoyl- β -D-glucopyranosyluronate)-(1 \rightarrow 3)-4,6-*O*-*p*-methoxybenzylidene-2-deoxy-2-acetamido- β -D-galactopyranoside (75). 75 was prepared using a procedure modified from Karst *et al.*²⁴ To a solution of **37** (98 mg, 0.054 mmol) in benzene (1.7 mL) and *N,N*-dimethylacetamide (0.43 mL) were added tributylstannane (0.20 mL, 0.97 mmol) and 2,2'-azobisisobutyronitrile (5.2 mg). The reaction was stirred at rt for 30 min and then was heated at 80 °C for 5 h. It was cooled to rt, concentrated to afford a yellow-white solid, and purified by flash chromatography (80% \rightarrow 100% EtOAc:hexanes) to yield the product as a white solid (80 mg, 92%). R_f 0.69 (100% EtOAc). $^1\text{H NMR}$ (300 MHz, CDCl_3): δ = 7.95 – 7.84 (m, 8H, ArH), 7.52 – 7.43 (m, 6H, ArH), 7.38 – 7.27 (m, 8H, ArH), 7.21 (d, J = 9.0 Hz, 2H, $\text{C}_6\text{H}_4\text{OMe}$), 6.86 (d, J = 8.7 Hz, 2H, $\text{C}_6\text{H}_4\text{OMe}$), 6.80 (d, J = 9.0 Hz, 2H, Ph $\text{C}_6\text{H}_4\text{OMe}$), 5.89 – 5.76 (m, 1H, $\text{OCH}_2\text{CH}=\text{CH}_2$), 5.61 (dd, J = 7.2, 8.1 Hz, 1H, H-3 GlcA), 5.51 (s, 1H, MeOPhCH), 5.44 (dd, J = 8.7, 9.0 Hz, 1H, H-3 GlcA), 5.42 (d, J = 6.6 Hz, 1H, NHAc), 5.31 (dd, J = 6.6, 7.2 Hz, 1H, H-2 GlcA), 5.28 (dd, J = 7.2, 8.7 Hz, 1H, H-2 GlcA), 5.20 (dd, J = 0.9, 17.3 Hz, 1H, $\text{OCH}_2\text{CH}=\text{CH}_2$), 5.18 (s, 1H, MeOPhCH), 5.13 (d, J = 11.4 Hz, 1H, $\text{OCH}_2\text{CH}=\text{CH}_2$), 5.11 (d, J = 8.1 Hz, 1H, H-1 GlcA), 5.05 (d, J = 7.2 Hz, 1H, H-1 GalNAc), 4.98 (d, J = 6.6 Hz, 1H, NHAc), 4.89 (d, J = 7.5 Hz, 1H, H-1 GalNAc), 4.86 (d, J = 9.0 Hz, 1H, H-1GlcA), 4.75 (dd, J = 3.3, 10.8

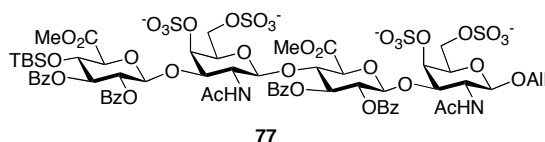
Hz, 1H, H-3 GalNAc), 4.51 (dd, $J = 8.1, 9.3$ Hz, 1H, H-4 GlcA), 4.37 – 4.25 (m, 5H, $\text{OCH}_2\text{CH}=\text{CH}_2$, H-3 GalNAc, H-4 GalNAc, H-4 GlcA, H-6 GalNAc), 4.16 (d, $J = 9.3$ Hz, 1H, H-5 GlcA), 4.06 – 3.98 (m, 4H, $\text{OCH}_2\text{CH}=\text{CH}_2$, H-4 GalNAc, H-5 GlcA, H-6 GalNAc), 3.77 – 3.73 (m, 1H, H-6 GalNAc), 3.80 (s, 3H, PhOCH_3), 3.79 (s, 3H, PhOCH_3), 3.73 (s, 3H, CO_2CH_3), 3.70 (s, 3H, CO_2CH_3), 3.56 – 3.52 (m, 1H, H-6 GalNAc), 3.46 (s, 1H, H-5 GalNAc), 3.35 – 3.26 (m, 2H, H-2 GalNAc, H-2 GalNAc), 2.84 (s, 1H, H-5 GalNAc), 1.54 (s, 3H, $\text{HNC}(\text{O})\text{CH}_3$), 1.50 (s, 3H, $\text{HNC}(\text{O})\text{CH}_3$), 0.70 (s, 9H, $(\text{CH}_3)_3\text{CSi}$), -0.10 (s, 3H, CH_3Si), -0.25 (s, 3H, CH_3Si). ESI MS: m/z : calcd for $\text{C}_{83}\text{H}_{94}\text{N}_2\text{O}_{29}\text{Si}$: 1645.5; found 1645.4 [$M + \text{Cl}$] $^-$.



76

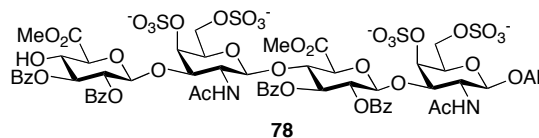
Allyl (methyl 2,3-di-*O*-benzoyl-4-*O*-*tert*-butyldimethylsilyl- β -D-glucopyranosyluronate)-(1 \rightarrow 3)-(2-deoxy-2-acetamido- β -D-galactopyranosyl)-(1 \rightarrow 4)-(methyl 2,3-di-*O*-benzoyl- β -D-glucopyranosyluronate)-(1 \rightarrow 3)-2-deoxy-2-acetamido- β -D-galactopyranoside (76). **75** (42 mg, 0.026 mmol) was dissolved in CH_3CN (840 μL) and H_2O (90 μL) and the reaction was covered with aluminum foil and stirred in the dark. 2,3-Dichloro-5,6-dicyano-1,4-benzoquinone (24 mg, 0.10 mmol) was added and the reaction stirred for 2 h at rt. The reaction mixture was subjected to Sephadex LH-20 (50% CH_2Cl_2 :MeOH, 30 mL resin, 1 cm x 30 cm column) to afford **76** as a pale pink solid (34 mg, 93%). R_f 0.2 (100% EtOAc). ^1H NMR (300 MHz, CD_3OD): $\delta = 7.85 - 7.76$ (m, 8H, ArH), 7.47 – 7.42 (m, 4H, ArH), 7.36 – 7.27 (m, 8H, ArH), 5.79

– 5.66 (m, 1H, OCH₂CH=CH₂), 5.52 (dd, *J* = 8.4, 8.4 Hz, 1H, H-3 GlcA), 5.51 (dd, *J* = 8.4, 9.9 Hz, 1H, H-3 GlcA), 5.27 – 5.19 (m, 3H), 5.12 (dd, *J* = 1.6 Hz, 17.3 Hz, 1H, OCH₂CH=CH₂), 5.00 – 4.96 (m, 4H), 4.43 – 4.42 (m, 1H), 4.32 – 4.26 (m, 2H), 4.20 – 4.10 (m, 5H), 4.00 (d, *J* = 2.4 Hz, 1H), 3.96 – 3.88 (m, 3H), 3.70 (s, 3H, CO₂CH₃), 3.69 (s, 3H, CO₂CH₃), 3.41 – 3.35 (m, 2H), 3.17 – 3.10 (m, 3H), 3.04 – 3.00 (m, 1H), 1.20 (s, 3H, HNC(O)CH₃), 1.18 (s, 3H, HNC(O)CH₃), 0.66 (s, 9H, (CH₃)₃CSi), -0.10 (s, 3H, CH₃Si), -0.26 (s, 3H, CH₃Si). ESI MS: *m/z*: calcd for C₆₇H₈₂N₂NaO₂₇Si: 1397.5; found 1397.6 [*M* + Na]⁺.



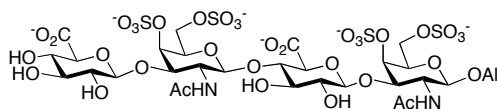
Allyl (methyl 2,3-di-*O*-benzoyl-4-*O*-*tert*-butyldimethylsilyl- β -D-glucopyranosyluronate)-(1 \rightarrow 3)-(4,6-di-*O*-sodium sulfonato-2-deoxy-2-acetamido- β -D-galactopyranosyl)-(1 \rightarrow 4)-(methyl 2,3-di-*O*-benzoyl- β -D-glucopyranosyluronate)-(1 \rightarrow 3)-4,6-di-*O*-sodium sulfonato-2-deoxy-2-acetamido- β -D-galactopyranoside (77). To a solution of **76** (23 mg, 0.017 mmol) in DMF (600 μ L) was added SO₃ • TMA (90 mg, 0.64 mmol). The reaction was stirred at 50 °C for 2 d, at which time additional SO₃ • TMA (50 mg, 0.36 mmol) was added, and the reaction continued at 50 °C for 1 d. The reaction pH was carefully monitored to ensure it did not drop below pH 5.0. It was quenched with MeOH, concentrated to afford a yellow solid, and purified on Sephadex LH-20 (50% CH₂Cl₂:MeOH, 30 mL resin, 1 cm x 30 cm column). The resulting crude product was purified by flash chromatography (6:2:1

EtOAc:MeOH:H₂O) to afford **77** as a white solid (24 mg, 84%). *R_f* 0.51 (6:2:1 EtOAc:MeOH:H₂O). ¹H NMR (300 MHz, CD₃OD): δ = 7.92 – 7.81 (m, 8H, ArH), 7.55 – 7.45 (m, 4H, ArH), 7.43 – 7.33 (m, 8H, ArH), 5.87 – 5.73 (m, 1H, OCH₂CH=CH₂), 5.67 (dd, *J* = 9.0, 9.0 Hz, 1H, H-3 GlcA), 5.61 (dd, *J* = 9.3, 9.3 Hz, 1H, H-3 GlcA), 5.42 – 5.32 (m, 3H), 5.19 (dd, *J* = 1.6, 17.3 Hz, 1H, OCH₂CH=CH₂), 4.93 – 4.79 (m, 4H, H-4 GalNAc, H-4 GalNAc), 4.54 – 4.52 (m, 1H), 4.49 (dd, *J* = 9.0, 9.6 Hz, 1H, H-4 GlcA), 4.40 – 4.33 (m, 5H), 4.28 – 4.22 (m, 3H), 4.18 (d, *J* = 9.3 Hz, 1H, H-5 GlcA), 4.08 – 3.98 (m, 4H), 3.90 – 3.89 (m, 1H), 3.87 (s, 3H, CO₂CH₃), 3.86 – 3.85 (m, 2H), 3.83 (s, 3H, CO₂CH₃), 1.20 (s, 3H, HNC(O)CH₃), 1.18 (s, 3H, HNC(O)CH₃), 0.73 (s, 9H, (CH₃)₃CSi), -0.03 (s, 3H, CH₃Si), -0.19 (s, 3H, CH₃Si). ESI MS: *m/z*: calcd for C₆₇H₇₈N₂Na₃O₃₉S₄Si: 1759.3; found 1759.8 [*M* - Na]⁻.



Allyl (methyl 2,3-di-O-benzoyl-β-D-glucopyranosyluronate)-(1 → 3)-(4,6-di-O-sodium sulfonato-2-deoxy-2-acetamido-β-D-galactopyranosyl)-(1 → 4)-(methyl 2,3-di-O-benzoyl-β-D-glucopyranosyluronate)-(1 → 3)-4,6-di-O-sodium sulfonato-2-deoxy-2-acetamido-β-D-galactopyranoside (78). **77** (32 mg, 0.019 mmol) in a plastic centrifuge tube was dissolved in pyridine (585 μL) and THF (585 μL). The reaction was cooled to 0 °C and to this was added HF • pyridine (94 μL, 5.2 mmol). After stirring at 0 °C for 1 h and at rt overnight, the reaction mixture was loaded onto a Sephadex LH-20 column (50% CH₂Cl₂:MeOH, 30 mL resin, 1 cm x 30 cm column). The product was

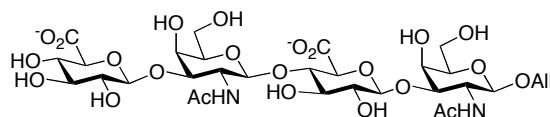
concentrated, taken up in H₂O, and lyophilized to afford a white solid (45 mg, 91%) that was immediately used in the next reaction. R_f 0.36 (6:2:1 EtOAc:MeOH:H₂O). ESI MS: *m/z*: calcd for C₆₁H₆₇N₂O₃₉S₄: 1579.2; found 1579.4 [*M* - H]⁻.



79: CS-E

Allyl (sodium β -D-glucopyranosyluronate)-(1 \rightarrow 3)-(4,6-di-*O*-sodium sulfonato-2-deoxy-2-acetamido- β -D-galactopyranosyl)-(1 \rightarrow 4)-(sodium β -D-glucopyranosyluronate)-(1 \rightarrow 3)-4,6-di-*O*-sodium sulfonato-2-deoxy-2-acetamido- β -D-galactopyranoside (79: CS-E). **78** was deprotected in a manner similar to a procedure from Lucas and coworkers.⁵¹ **78** (45 mg, 0.028 mmol) was dissolved in THF (2.3 mL) and H₂O (1.7 mL) and cooled to 0 °C. To this were added 1 M aq. LiOH (330 μ L, 0.33 mmol) and 30% H₂O₂ (170 μ L, 0.0015 mmol). The reaction was stirred at 0 °C for 1 h and at rt for 12 h. At this time, 4 M NaOH (230 μ L, 0.46 mmol) and MeOH (1.7 mL) were added and the reaction stirred for another 12 h. It was then neutralized with Amberlyst IR-120 resin, filtered, and lyophilized to afford an orange solid. The product was purified by Sephadex G-25 UF, a resin for compounds with a molecular weight of 700 or more, (0.9 % NaCl in H₂O, 30 mL resin, 1 cm x 20 cm column) and desalted with Sephadex G-25 UF (100% H₂O, 30 mL resin, 1 cm x 20 cm column) to afford **79: CS-E** as a white solid upon lyophilization (23 mg, 70%). For complete assignment of the ¹H NMR spectra of this compound, ¹H decoupling experiments were performed. ¹H NMR (600 MHz, D₂O): δ = 5.94 – 5.88 (m, 1H, OCH₂CH=CH₂), 5.33 (dd, *J* = 1.5, 17.1 Hz,

1H, OCH₂CH=CH₂), 5.27 (d, *J* = 10.2 Hz, 1H, OCH₂CH=CH₂), 4.85 (s, 1H, H-4 GalNAc), 4.79 (d, *J* = 1.2 Hz, 1H, H-4 GalNAc), 4.61 (dd, *J* = 3.9, 7.8 Hz, 1H, H-1 GalNAc), 4.59 (d, *J* = 7.8 Hz, 1H, H-1 GalNAc), 4.49 (d, *J* = 7.8 Hz, 1H, H-1 GlcA), 4.47 (d, *J* = 7.8 Hz, 1H, H-1 GlcA), 4.35 (dd, *J* = 5.4, 13.2 Hz, 1H, OCH₂CH=CH₂), 4.29 (dd, *J* = 3.0, 11.4 Hz, 2H, H-6 GalNAc), 4.24 – 4.18 (m, 4H, OCH₂CH=CH₂, H-2 GalNAc, H-5 GalNAc), 4.13 (dd, *J* = 2.7, 8.7 Hz, 1H, H-3 GalNAc), 4.09 – 4.05 (m, 4H, H-6 GalNAc, H-2 GalNAc, H-3 GalNAc), 3.77 (dd, *J* = 9.6, 9.6 Hz, 1H, H-4 GlcA), 3.69 (d, *J* = 9.6 Hz, 1H, H-5 GlcA), 3.67 (d, *J* = 9.6 Hz, 1H, H-5 GlcA), 3.61 (dd, *J* = 9.0, 9.6 Hz, 1H, H-3 GlcA), 3.52 (dd, *J* = 9.0, 9.0 Hz, 1H, H-4 GlcA), 3.47 (dd, *J* = 9.0, 9.6 Hz, 1H, H-3 GlcA), 3.41 (dd, *J* = 8.4, 9.0 Hz, 1H, H-2 GlcA), 3.34 (dd, *J* = 7.8, 9.0 Hz, 1H, H-2 GlcA), 2.04 (s, 3H, HNC(O)CH₃), 2.01 (s, 3H, HNC(O)CH₃). ESI MS: *m/z*: calcd for C₃₁H₄₂N₂Na₅O₃₅S₄: 1245.0; found 1245.0 [*M* - Na]⁻.



81

Allyl (sodium β -D-glucopyranosyluronate)-(1 \rightarrow 3)-(2-deoxy-2-acetamido- β -D-galactopyranosyl)-(1 \rightarrow 4)-(sodium β -D-glucopyranosyluronate)-(1 \rightarrow 3)-2-deoxy-2-acetamido- β -D-galactopyranoside (81). **76** (8.5 mg, 0.0062 mmol) was dissolved in pyridine (110 μ L) and THF (110 μ L). The reaction was cooled to 0 $^{\circ}$ C and to this was added HF \cdot pyridine (30 μ L, 1.7 mmol). After stirring at 0 $^{\circ}$ C for 1 h and at rt overnight, the mixture was loaded onto a Sephadex LH-20 column (50% CH₂Cl₂:MeOH, 30 mL

resin, 1 cm x 30 cm column), and the product was a yellow solid (5.3 mg) that was immediately used in the next reaction. R_f 0.75 (6:2:1 EtOAc:MeOH:H₂O).

The alcohol **80** (5.3 mg, 0.0042 mmol) was dissolved in THF (120 μ L) and H₂O (60 μ L) and cooled to 0 °C. To this were added 1 M aq. LiOH (47 μ L, 0.047 mmol) and 30% H₂O₂ (23 μ L, 0.20 mmol). The reaction was stirred at 0 °C for 1 h and at rt for 12 h. At this time, 4 M NaOH (35 μ L, 0.070 mmol) and MeOH (173 μ L) were added and the reaction stirred for another 12 h. It was neutralized with Amberlyst IR-120 resin, filtered, and lyophilized to afford an orange solid. The product was purified by Sephadex G-25 UF (100% H₂O, 30 mL resin, 1 cm x 20 cm column) and lyophilized to afford **81** as a white solid (2.6 mg, 52% from **76**). For complete assignment of the ¹H NMR spectra of this compound, ¹H decoupling experiments were performed. ¹H NMR (600 MHz, D₂O): δ = 5.91 – 5.84 (m, 1H, OCH₂CH=CH₂), 5.28 (d, J = 17.4 Hz, 1H, OCH₂CH=CH₂), 5.23 (d, J = 10.2 Hz, 1H, OCH₂CH=CH₂), 4.51 – 4.45 (m, 4H), 4.31 (dd, J = 4.8, 12.9 Hz, 1H, OCH₂CH=CH₂), 4.16 – 4.09 (m, 3H), 4.01 – 3.96 (m, 2H), 3.78 – 3.71 (m, 5H), 3.67 – 3.64 (m, 5H), 3.55 (dd, J = 9.0, 9.0 Hz, 1H, H-3 GlcA), 3.48 – 3.42 (m, 3H), 3.34 (dd, J = 8.4, 9.0 Hz, 1H, H-2 GlcA), 3.29 (dd, J = 7.2, 8.4 Hz, 1H, H-2 GlcA), 1.99 (s, 3H, HNC(O)CH₃), 1.98 (s, 3H, HNC(O)CH₃). ESI MS: m/z : calcd for C₃₁H₄₇N₂O₂₃: 815.7; found 815.4 [$M - H$].

References

1. Kitagawa, H., Tsutsumi, K., Tone, Y. & Sugahara, K. (1997). Developmental regulation of the sulfation profile of chondroitin sulfate chains in the chicken embryo brain. *J. Biol. Chem.* **272**, 31377-31381.
2. Plaas, A.H.K., West, L.A., Wong-Palms, S. & Nelson, F.R.T. (1998). Glycosaminoglycan sulfation in human osteoarthritis. Disease-related alterations at the non-reducing termini of chondroitin and dermatan sulfate. *J. Biol. Chem.* **273**, 12642-12649.
3. Hacker, U., Nybakken, K. & Perrimon, N. (2005). Heparan sulphate proteoglycans: the sweet side of development. *Nat. Rev. Mol. Cell Biol.* **6**, 530-541.
4. Capila, I. & Linhardt, R.J. (2002). Heparin-protein interactions. *Angew. Chem. Int. Ed.* **41**, 391-412.
5. Sasisekharan, R., Shriver, Z., Venkataraman, G. & Narayanasami, U. (2002). Roles of heparan-sulphate glycosaminoglycans in cancer. *Nat. Rev. Cancer* **2**, 521-528.
6. Bradbury, E.J., Moon, L.D., Popat, R.J., King, V.R., Bennett, G.S., Patel, P.N., Fawcett, J.W. & McMahon, S.B. (2002). Chondroitinase ABC promotes functional recovery after spinal cord injury. *Nature* **416**, 636-640.
7. Emerling, D.E. & Lander, A.D. (1996). Inhibitors and promoters of thalamic neuron adhesion and outgrowth in embryonic neocortex: functional association with chondroitin sulfate. *Neuron* **17**, 1089-1100.
8. Holt, C.E. & Dickson, B.J. (2005). Sugar codes for axons? *Neuron* **46**, 169-172.

9. Brittis, P.A, Canning, D.R. & Silver, J. (1992). Chondroitin sulfate as a regulator of neuronal patterning in the retina. *Science* **255**, 733-736.
10. Dou, C.L. & Levine, J.M. (1995). Differential effects of glycosaminoglycans on neurite growth on laminin and L1 substrates. *J. Neurosci.* **15**, 8053-8066.
11. Nadanaka, S., Clement, A., Masayama, K., Faissner, A. & Sugahara, K. (1998). Characteristic hexasaccharide sequences in octasaccharides derived from shark cartilage chondroitin sulfate D with a neurite outgrowth promoting activity. *J. Biol. Chem.* **273**, 3296-3307.
12. Nandini, C.D., Mikami, T., Ohta, M., Itoh, N., Akiyama-Nambu, F. & Sugahara, K. (2004). Structural and functional characterization of oversulfated chondroitin sulfate/dermatan sulfate hybrid chains from the notochord of hagfish. Neuritogenic and binding activities for growth factors and neurotrophic factors. *J. Biol. Chem.* **279**, 50799-50809.
13. Shuo, T., Aono, S., Matsui, F., Tokita, Y., Maeda, H., Shimada, K. & Oohira, A. (2004). Neuroglycan C, a brain-specific part-time proteoglycan, with a particular multidomain structure. *Glycoconj. J.* **20**, 267-278.
14. Ueoka, C., Kaneda, N., Okazaki, I., Nadanaka, S., Muramatsu, T. & Sugahara, K. (2000). Neuronal cell adhesion, mediated by the heparin-binding neuroregulatory factor midkine, is specifically inhibited by chondroitin sulfate E. Structural and functional implications of the over-sulfated chondroitin sulfate. *J. Biol. Chem.* **275**, 37407-37413.

15. Clement, A.M., Sugahara, K. & Faissner, A. (1999). Chondroitin sulfate E promotes neurite outgrowth of rat embryonic day 18 hippocampal neurons. *Neurosci. Lett.* **269**, 125-128.
16. Deepa, S.S., Umehara, Y., Higashiyama, S., Itoh, N. & Sugahara, K. (2002). Specific molecular interactions of oversulfated chondroitin sulfate E with various heparin-binding growth factors. Implications as a physiological binding partner in the brain and other tissues. *J. Biol. Chem.* **277**, 43707-43716.
17. Maccarana, M., Casu, B. & Lindahl, U. (1993). Minimal sequence in heparin/heparan sulfate required for binding of basic fibroblast growth factor. *J. Biol. Chem.* **268**, 23898-23905.
18. Guerrini, M., Agulles, T., Bisio, A., Hricovini, M., Lay, L., Naggi, A., Poletti, L., Sturiale, L., Torri, G. & Casu, B. (2002). Minimal heparin/heparan sulfate sequences for binding to fibroblast growth factor-1. *Biochem. Biophys. Res. Comm.* **292**, 222-230.
19. Bao, X., Muramatsu, T. & Sugahara, K. (2005). Demonstration of the pleiotrophin-binding oligosaccharide sequences isolated from chondroitin sulfate/dermatan sulfate hybrid chains of embryonic pig brains. *J. Biol. Chem.* **280**, 35318-35328.
20. Tyler, W.J., Alonso, M., Bramham, C.R. & Pozzo-Miller, L.D. (2002). From acquisition to consolidation: on the role of brain-derived neurotrophic factor signaling in hippocampal-dependent learning. *Learn. Mem.* **9**, 224-237.

21. Morrison, J.H. & Hof, P.R. (2002). Selective vulnerability of corticocortical and hippocampal circuits in aging and Alzheimer's disease. *Prog. Brain Res.* **136**, 467-486.
22. Tamura, J., Neumann, K.W., Kurono, S. & Ogawa, T. (1997). Synthetic approach towards sulfated chondroitin di-, tri-, and tetrasaccharides corresponding to the repeating unit. *Carbohydr. Res.* **305**, 43-63.
23. Jacquinet, J.C., Rochepeau-Jobron, L. & Combal, J.P. (1998). Multigram syntheses of the disaccharide repeating units of chondroitin 4- and 6-sulfates. *Carbohydr. Res.* **314**, 283-288.
24. Karst, N. & Jacquinet, J.C. (2002). Stereocontrolled total syntheses of shark cartilage chondroitin sulfate D-related tetra- and hexasaccharide methyl glycosides. *Eur. J. Org. Chem.* 815-825.
25. Manabe, S., Ito, Y. & Ogawa, T. (1998). Multi-component carbohydrate coupling using solution and polymer support technology. *Molecules Online* **2**, 40-45.
26. Johansson, R. & Samuelsson, B. (1984). Regioselective reductive ring-opening of 4-methoxybenzylidene acetals of hexopyranosides – access to a novel protecting-group strategy. *J. Chem. Soc., Chem. Commun.* 201-202.
27. Nilsson, M., Svahn, C.M. & Westman, J. (1993). Synthesis of the methyl glycosides of a tri- and a tetra-saccharide related to heparin and heparan sulphate. *Carbohydr. Res.* **246**, 161-172.
28. Allanson, N.M., Liu, D., Chi, F., Jain, R.K., Chen, A., Ghosh, M., Hong, L. & Sofia, M.J. (1998). Synthesis of phenyl 1-thioglycopyranosiduronic acids using a sonicated Jones oxidation. *Tet. Lett.* **39**, 1889-1892.

29. *Carbohydrates in Chemistry and Biology*, 1st ed.; Ernst, B.; Hart, G.W.; Sinay, P., Eds.; Wiley-VCH: New York, NY 2000; Vol. 1.
30. Kozikowski, A.P. & Lee, J. (1990). A synthetic approach to the *cis*-fused marine pyranopyrans, (3E)- and (3Z)-dactomelyne. X-ray structure of a rare organomercurial. *J. Org. Chem.* **55**, 863-870.
31. Lemieux, R.U. & Ratcliffe, R.M. (1979). The azidonitration of tri-*O*-acetyl-D-galactal. *Can. J. Chem.* **57**, 1244-1251.
32. Belot, F. & Jacquinet, J.C. (1996). Intermolecular aglycon transfer of a phenyl 1-thiogalactosaminide derivative under trichloroacetimidate glycosylation conditions. *Carbohydr. Res.* **290**, 79-86.
33. Lassaletta, J.M., Carlsson, K., Garegg, P.J. & Schmidt, R.R. (1996). Total synthesis of sialylgalactosylgloboside: stage-specific embryonic antigen 4. *J. Org. Chem.* **61**, 6873-6880.
34. Nakayama, K., Uoto, K., Higashi, K., Soga, T. & Kusama, T. (1992). A useful method for deprotection of the protective allyl group at the anomeric oxygen of carbohydrate moieties using tetrakis(triphenylphosphine)palladium. *Chem. Pharm. Bull.* **40**, 1718-1720.
35. Hanashima, S., Mizushina, Y., Yamazaki, T., Ohta, K., Takahashi, S., Koshino, H., Sahara, H., Sakaguchi, K. & Sugawara, F. (2000). Structural determination of sulfoquinovosyldiacylglycerol by chiral syntheses. *Tet. Lett.* **41**, 4403-4407.
36. Defaye, J. & Guillot, J. M. (1994). A convenient synthesis for anomeric 2-thioglucobioses, 2-thiokojibiose and 2-thiosphorose. *Carbohydr. Res.* **253**, 185-194.

37. Nakahara, Y. & Ogawa, T. (1989). Synthetic studies on plant cell wall glycans. Part 5. A highly stereocontrolled synthesis of the propyl glycoside of a decagalacturonic acid, a model compound for the endogenous phytoalexin elicitor-active oligogalacturonic acids. *Carbohydr. Res.* **194**, 95-114.
38. Lehmann, J. & Moritz, A. (1993). *p*-Benzoquinone as precursor for the synthesis of modified D- and L-hexoses: preparation of 2-acetamido-2,4-dideoxy-D- and L-xylo-hexopyranose. *Carbohydr. Res.* **239**, 317-323.
39. Taniguchi, T. & Ogasawara, K. (1998). Extremely facile and selective nickel-catalyzed allyl ether cleavage. *Angew. Chem. Int. Ed.* **37**, 1136-1137.
40. Smith III, A.B., Rivero, R.A., Hale, K.J. & Vaccaro, H.A. (1991). Phyllanthoside-phyllanthostatin synthetic studies. 8. Total synthesis of (+)-phyllanthoside. Development of the Mitsunobu glycosyl ester protocol. *J. Am. Chem. Soc.* **113**, 2092-2112.
41. Thomas, R.M., Mohan, G.H. & Iyengar, D.S. (1997). A novel, mild and facile reductive cleavage of allyl ethers by the NaBH₄/I₂ system. *Tet. Lett.* **38**, 4721-4724.
42. Lamberth, C. & Bednarski, M.D. (1991). An efficient method for the deprotection of allyl glycosides with adjacent azides: the circumvention of unwanted dipolar cycloaddition products. *Tet. Lett.* **32**, 7369-7372.
43. Scholl, M., Ding, S., Lee, C.W. & Grubbs, R.H. (1999). Synthesis and activity of a new generation of ruthenium-based olefin metathesis catalysts coordinated with 1,3-dimesityl-4,5-dihydroimidazol-2-ylidene ligands. *Org. Lett.* **1**, 953-956.

44. McGrath, D.V. & Grubbs, R.H. (1994). The mechanism of aqueous ruthenium(II)-catalyzed olefin isomerization. *Organometallics* **13**, 224-235.
45. Belot, F. & Jacquinet, J.C. (2000). Unexpected stereochemical outcome of activated 4,6-O-benzylidene derivatives of the 2-deoxy-2-trichloroacetamido-D-galacto series in glycosylation reactions during the synthesis of a chondroitin 6-sulfate trisaccharide methyl glycoside. *Carbohydr. Res.* **325**, 93-106.
46. Coutant, C. & Jacquinet, J.C. (1995). 2-Deoxy-2-trichloroacetamido-D-glucopyranose derivatives in oligosaccharide synthesis: from hyaluronic acid to chondroitin 4-sulfate trisaccharides. *J. Chem. Soc., Perkin Trans. 1*, 1573-1581.
47. Garegg, P.J. & Hultberg, H. (1981). A novel, reductive ring-opening of carbohydrate benzylidene acetals, with unusual regioselectivity. *Carbohydr. Res.* **93**, C10-C11.
48. Sakagami, M. & Hamana, H. (2000). A selective ring opening reaction of 4,6-O-benzylidene acetals in carbohydrates using trialkylsilane derivatives. *Tet. Lett.* **41**, 5547-5551.
49. Zhang, Z. & Magnusson, G. (1996). Conversion of *p*-methoxyphenyl glycosides into the corresponding glycosyl chlorides and bromides, and into thiophenyl glycosides. *J. Org. Chem.* **61**, 2394-2400.
50. Yadav, J.S., Chandrasekhar, G., Sumithra, G. & Kache, R. (1996). Selective and unprecedented oxidative deprotection of allyl ethers with DDQ. *Tet. Lett.* **37**, 6603-6605.

51. Lucas, H., Basten, J.E.M., van Dinther, T.G., Meuleman, J.G., van Aelst, S.F. & van Boeckel, C.A.A. (1990). Syntheses of heparin-like pentamers containing opened uronic-acid moieties. *Tetrahedron* **46**, 8207-8228.
52. Tully, S.E., Mabon, R., Gama, C.I., Tsai, S.M., Liu, X. & Hsieh-Wilson, L.C. (2004). A chondroitin sulfate small molecule that stimulates neuronal growth. *J. Am. Chem. Soc.* **126**, 7736-7737.
53. Tsuchida, K., Shioi, J., Yamada, S., Boghosian, G., Wu, A., Cai, H., Sugahara, K. & Robakis, N.K. (2001). Appican, the proteoglycan form of the amyloid precursor protein, contains chondroitin sulfate E in the repeating disaccharide region and 4-*O*-sulfated galactose in the linkage region. *J. Biol. Chem.* **276**, 37155-37160.
54. Deepa, S.S., Yamada, S., Zako, M., Goldberger, O. & Sugahara, K. (2000). Chondroitin sulfate chains on syndecan-1 and syndecan-4 from normal murine mammary gland epithelial cells are structurally and functionally distinct and cooperate with heparan sulfate chains to bind growth factors. A novel function to control binding of midkine, pleiotrophin, and basic fibroblast growth factor. *J. Biol. Chem.* **279**, 37368-37376.
55. Clingman, A.L. & Richtmyer, N.K. (1964). Aryl thioglycopyranosides, aryl glycopyranosyl sulfones, and the novel oxidation-acetylation of aryl 1-thio- β -D-glucopyranosides to 6-*O*-acetyl- β -D-glucopyranosyl aryl sulfones. *J. Org. Chem.* **29**, 1782-1787.

56. Ye, X.S. & Wong, C.H. (2000). Anomeric reactivity-based one-pot oligosaccharide synthesis: a rapid route to oligosaccharide libraries. *J. Org. Chem.* **65**, 2410-2431.
57. Black, T.H. (1983). The preparation and reactions of diazomethane. *Aldrichimica Acta* **16**, 3-10.
58. Driguez, P.A., Lederman, I., Strassel, J.M., Herbert, J.M. & Petitou, M. (1999). Synthetic carbohydrate derivatives as low sulfated heparin mimetics. *J. Org. Chem.* **64**, 9512-9520.

**Appendix for Chapter 3: Relevant Spectral Data for
Compounds of Chapter 3**

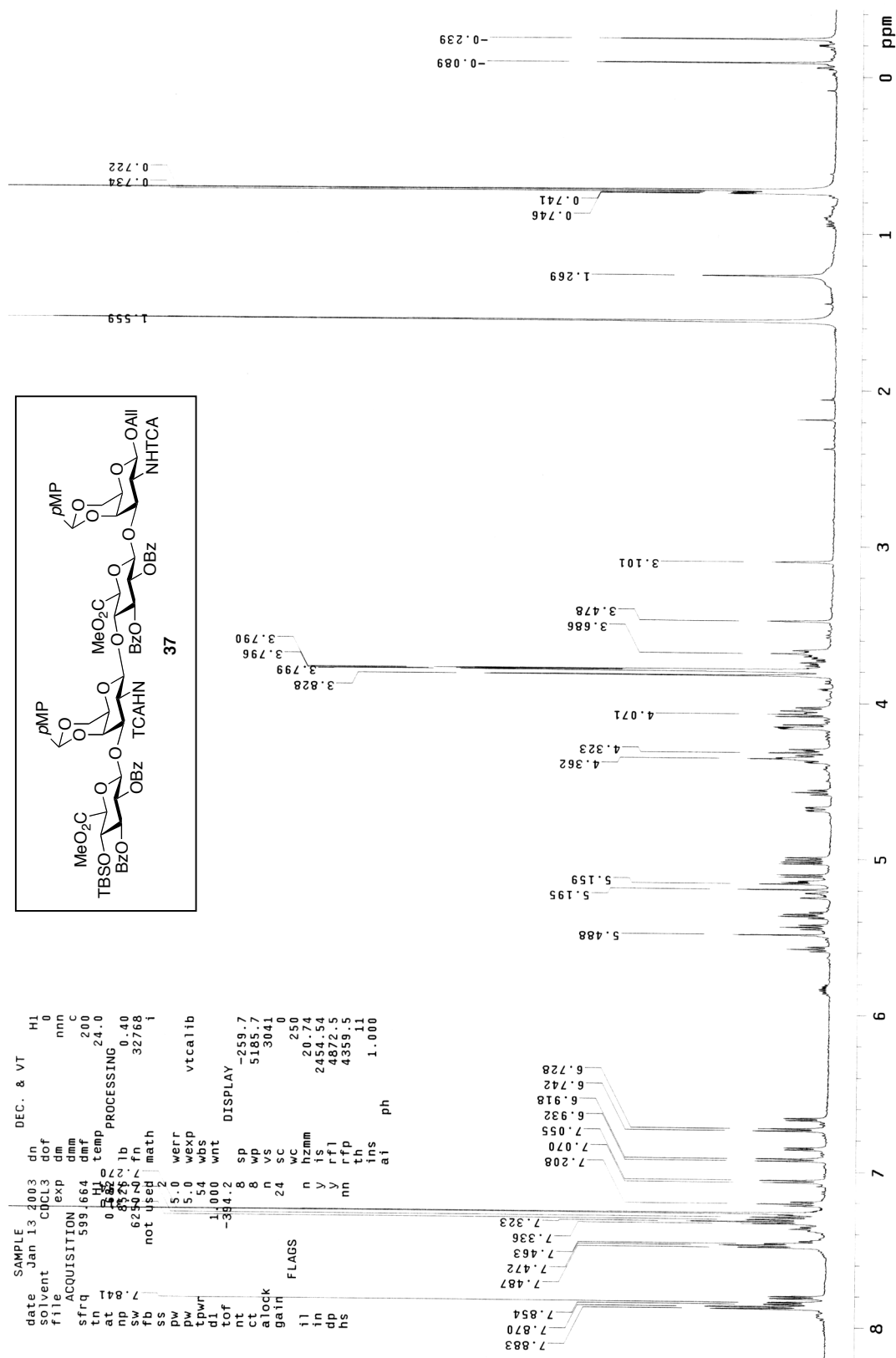


Figure A3.1: ^1H NMR (600 MHz, CDCl_3) of compound **37**.

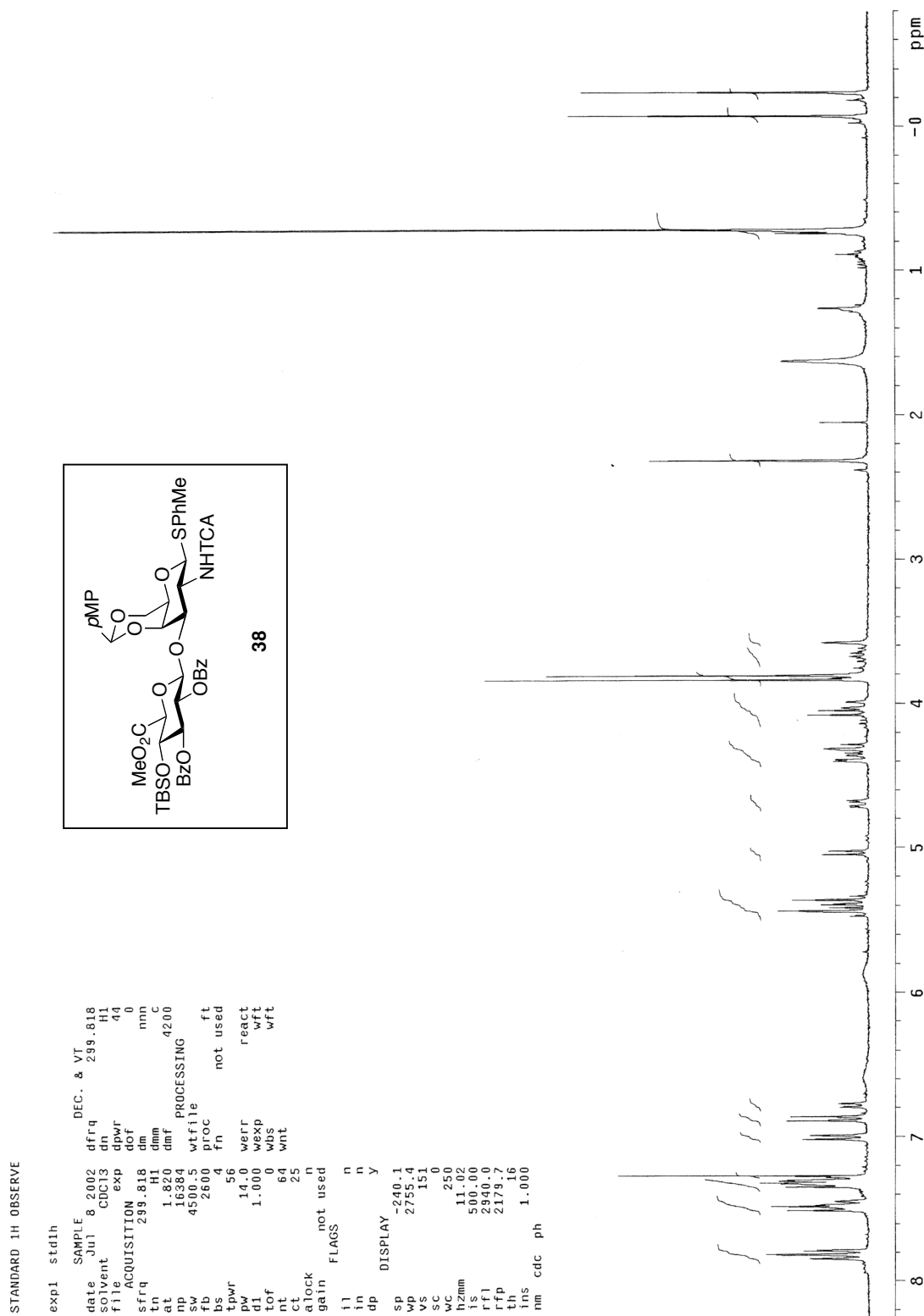


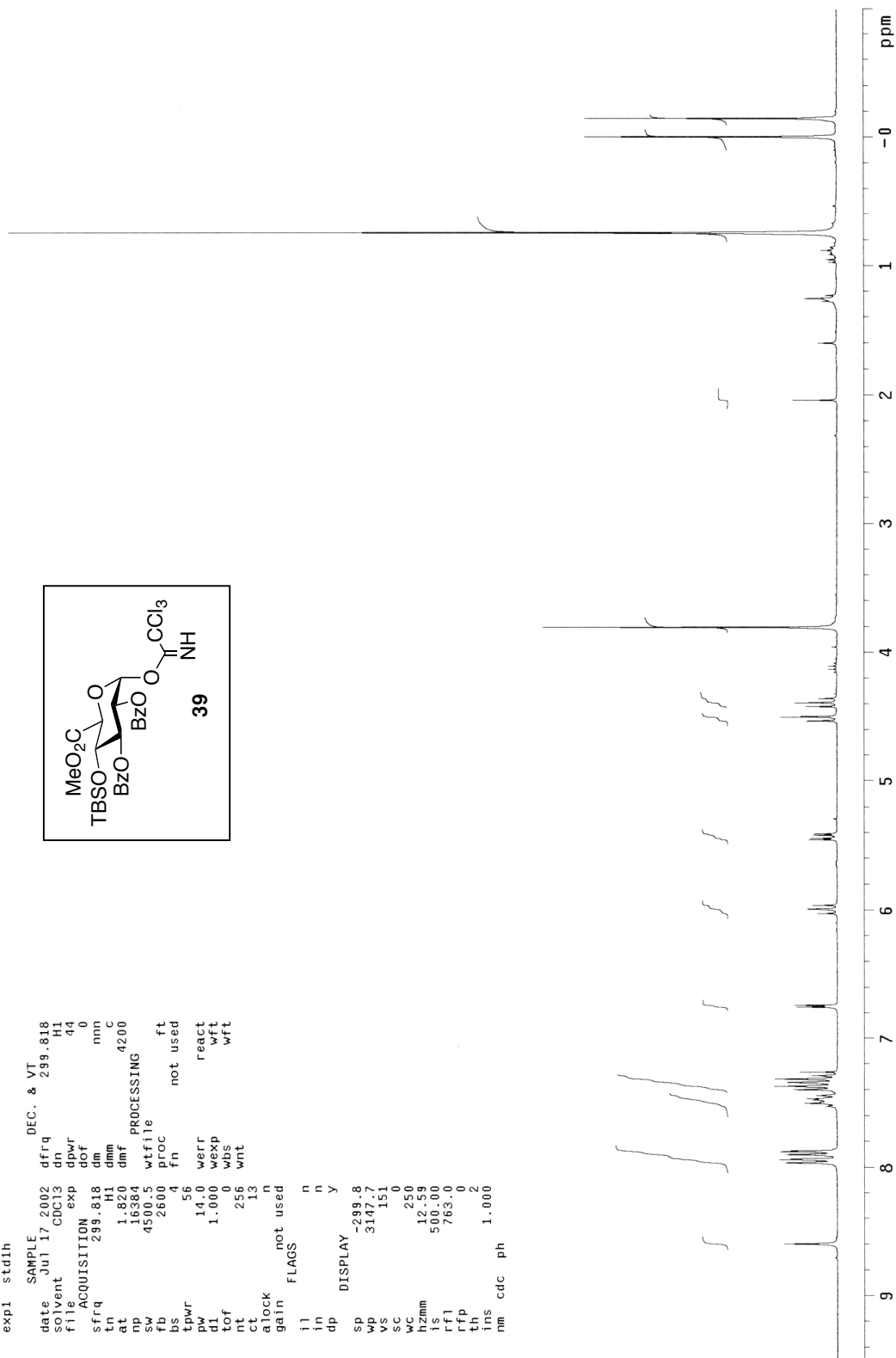
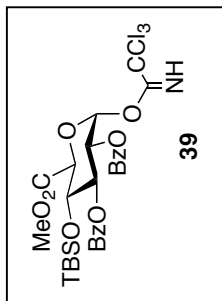
Figure A3.2: ^1H NMR (300 MHz, CDCl_3) of compound **38**.

STANDARD 1H OBSERVE

```

exp1 std1h
SAMPLE
date Jul 17 2002 dfrq DEC. & VT 299.818
solvent CDC13 dn H1
file ACQUISITION exp dpwr 44
sfrq 299.818 nmrc
at 1.820 H1 4200
np 16384 dmf
sw 4500.5 wtfile
fb 2600 proc
bs 4 fn
tpwr 56 not used
pw 14.0 werr
d1 1.000 wexp
tof 0 wbs
nt 256 wnt
ct 13
alock not used
gain
flags
il n
in n
dp y
SP DISPLAY -289.8
Wt 3147.7
VS 151
SC 0
WC 250
h2mm 12.59
IS 500.00
rfl 763.0
rfp 0
th 2
ins 1.000
nm cdc ph

```

Figure A3.3: ¹H NMR (300 MHz, CDCl₃) of compound 39.

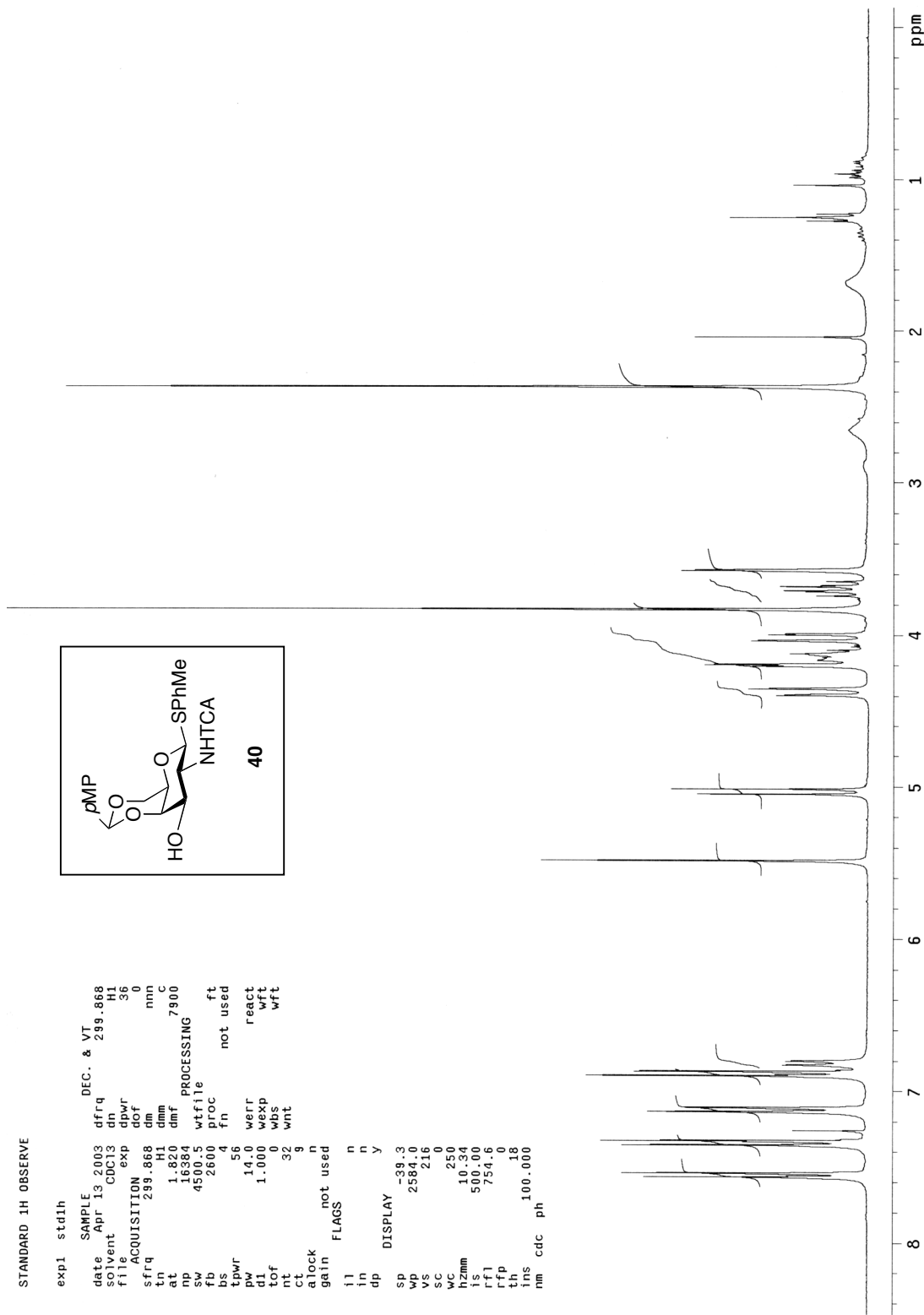
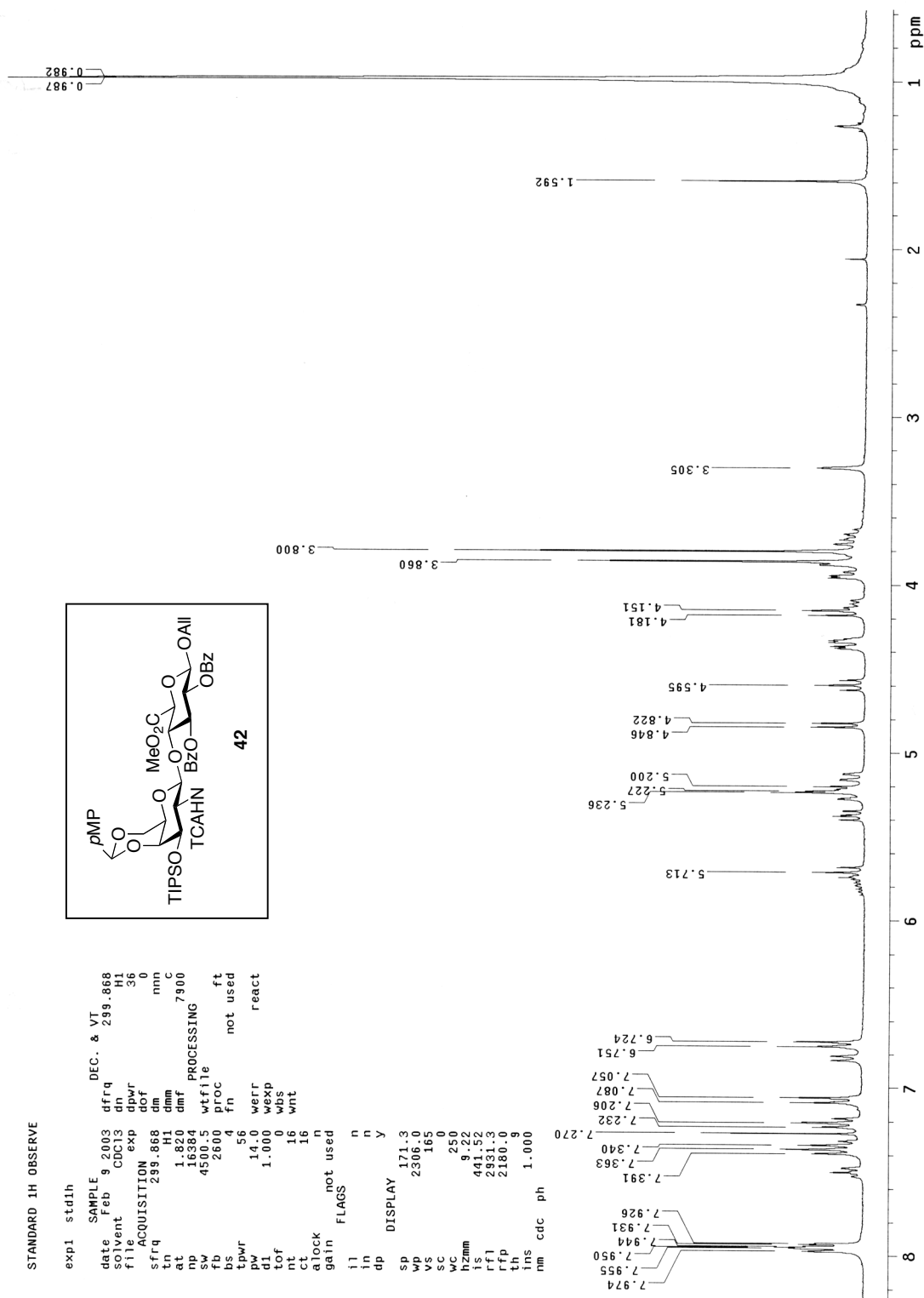


Figure A3.4: ^1H NMR (300 MHz, CDCl_3) of compound **40**.



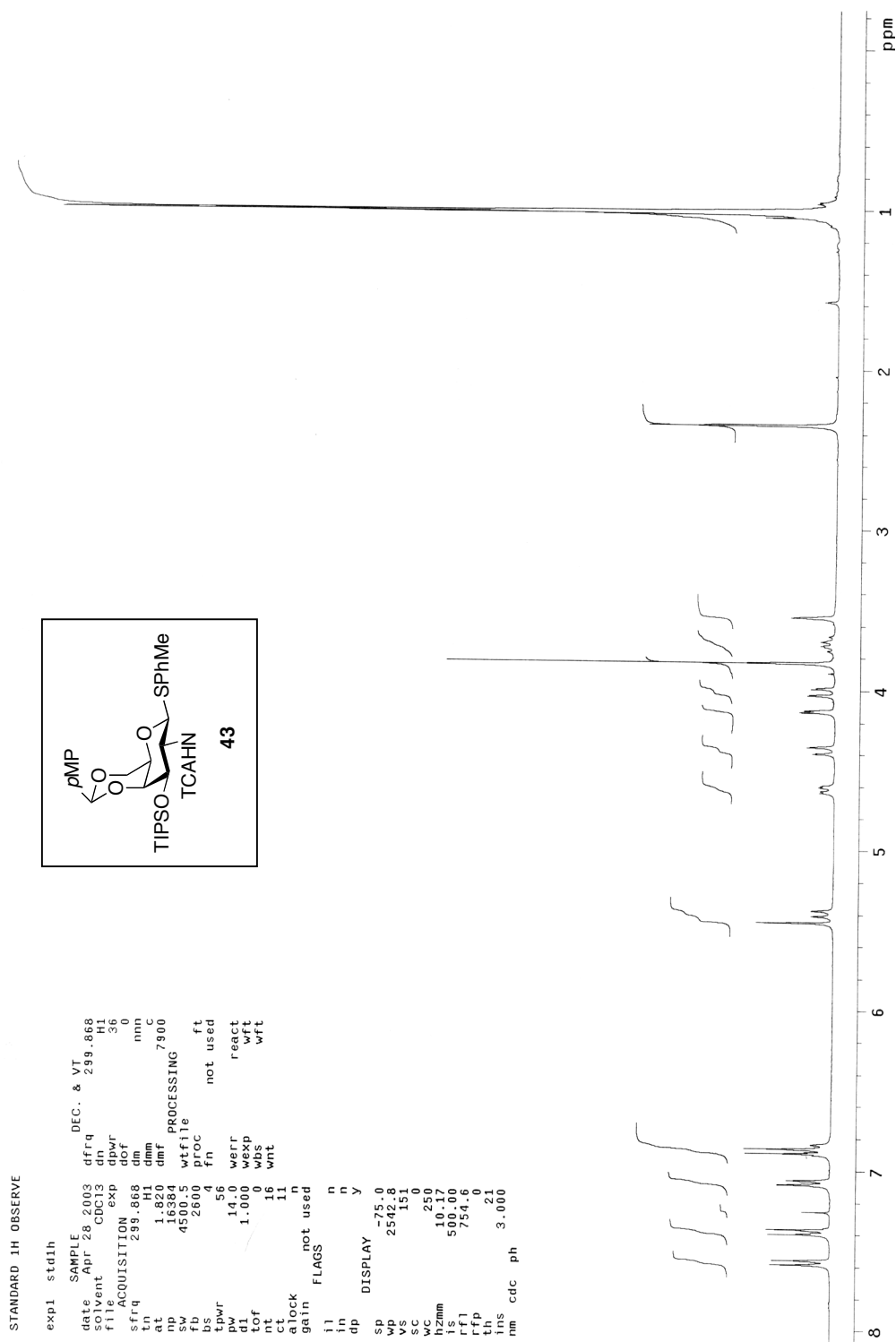


Figure A3.6: ^1H NMR (300 MHz, CDCl_3) of compound **43**.

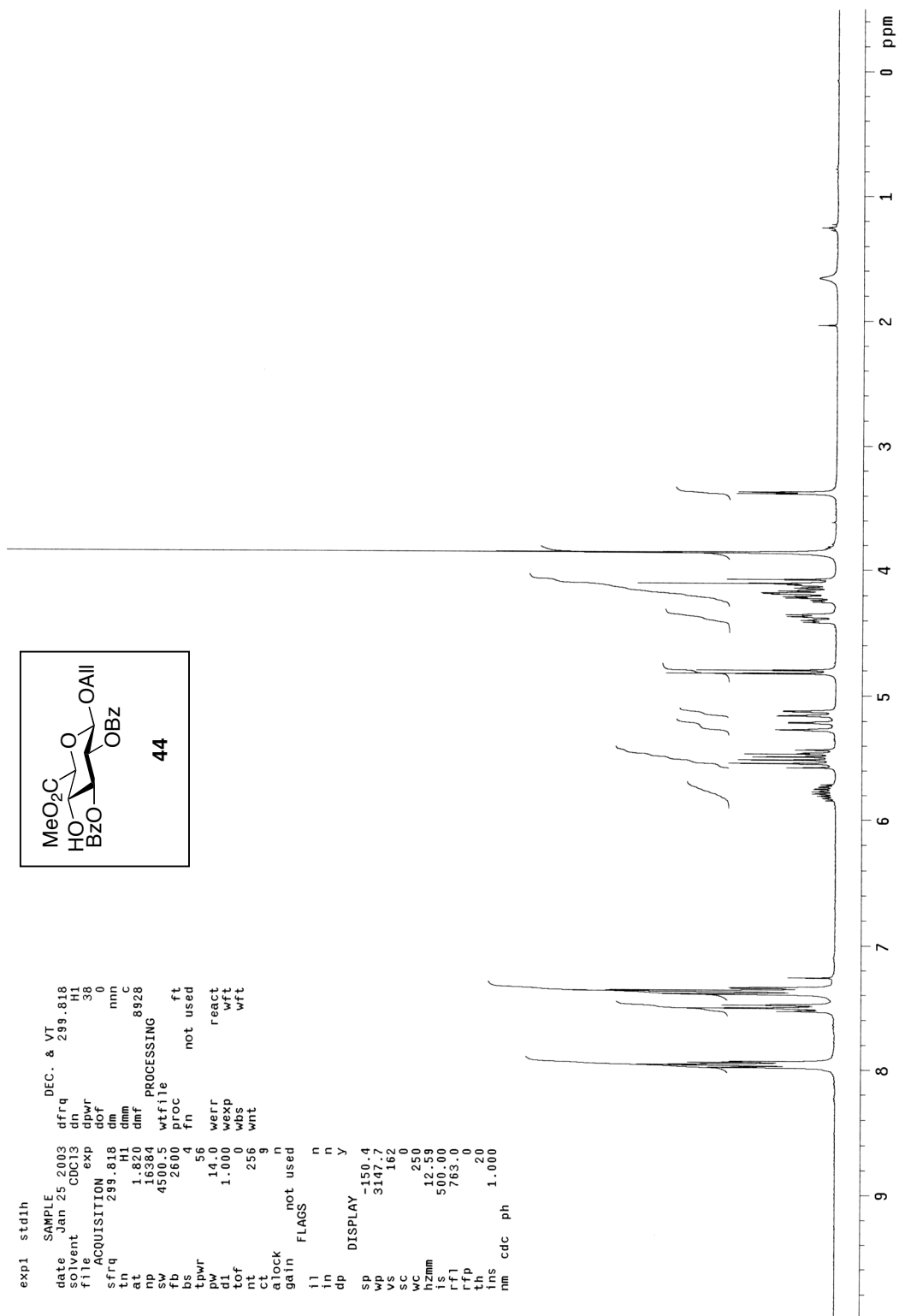


Figure A3.7: ^1H NMR (300 MHz, CDCl_3) of compound **44**.

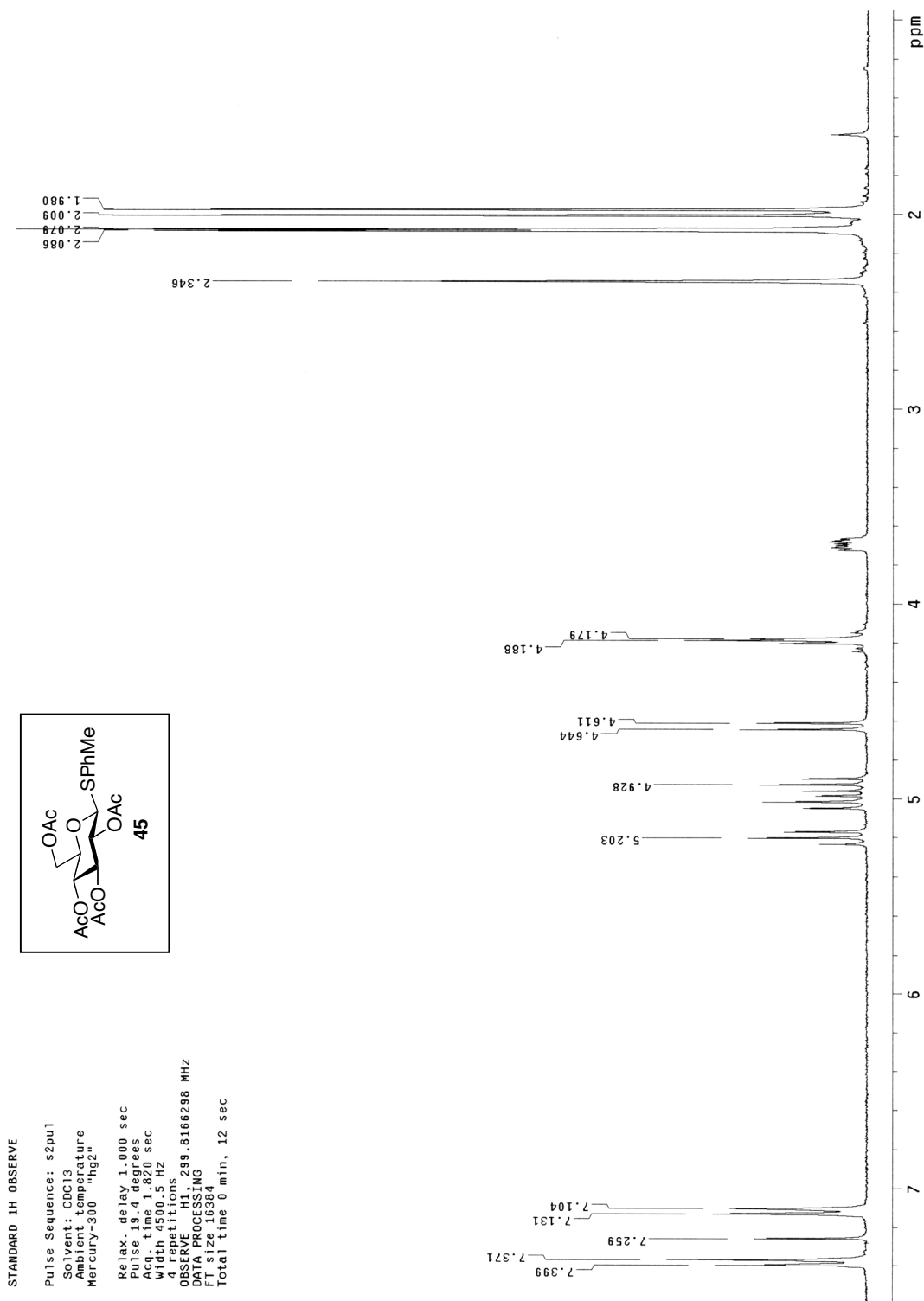
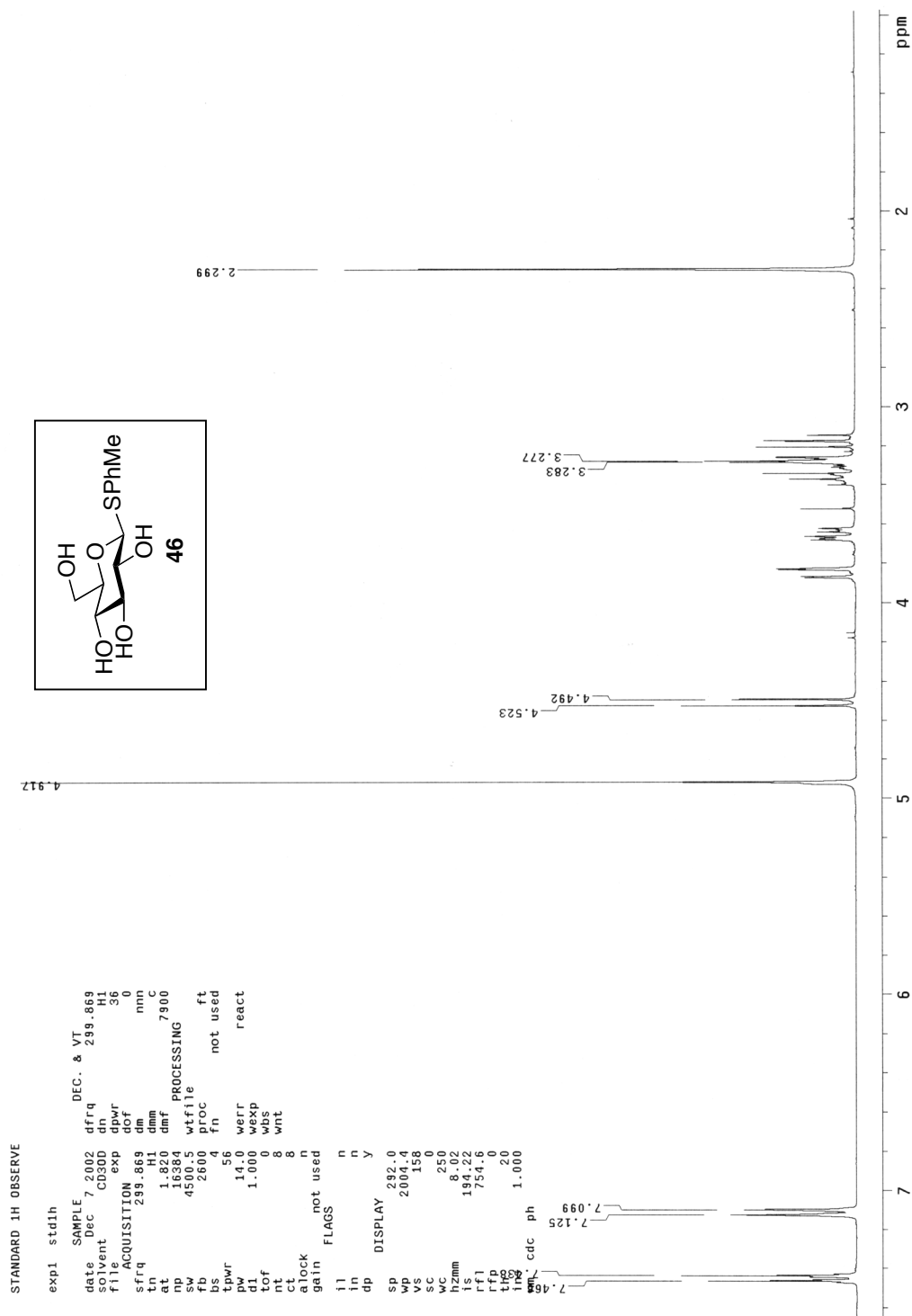


Figure A3.8: ^1H NMR (300 MHz, CDCl_3) of compound 45.



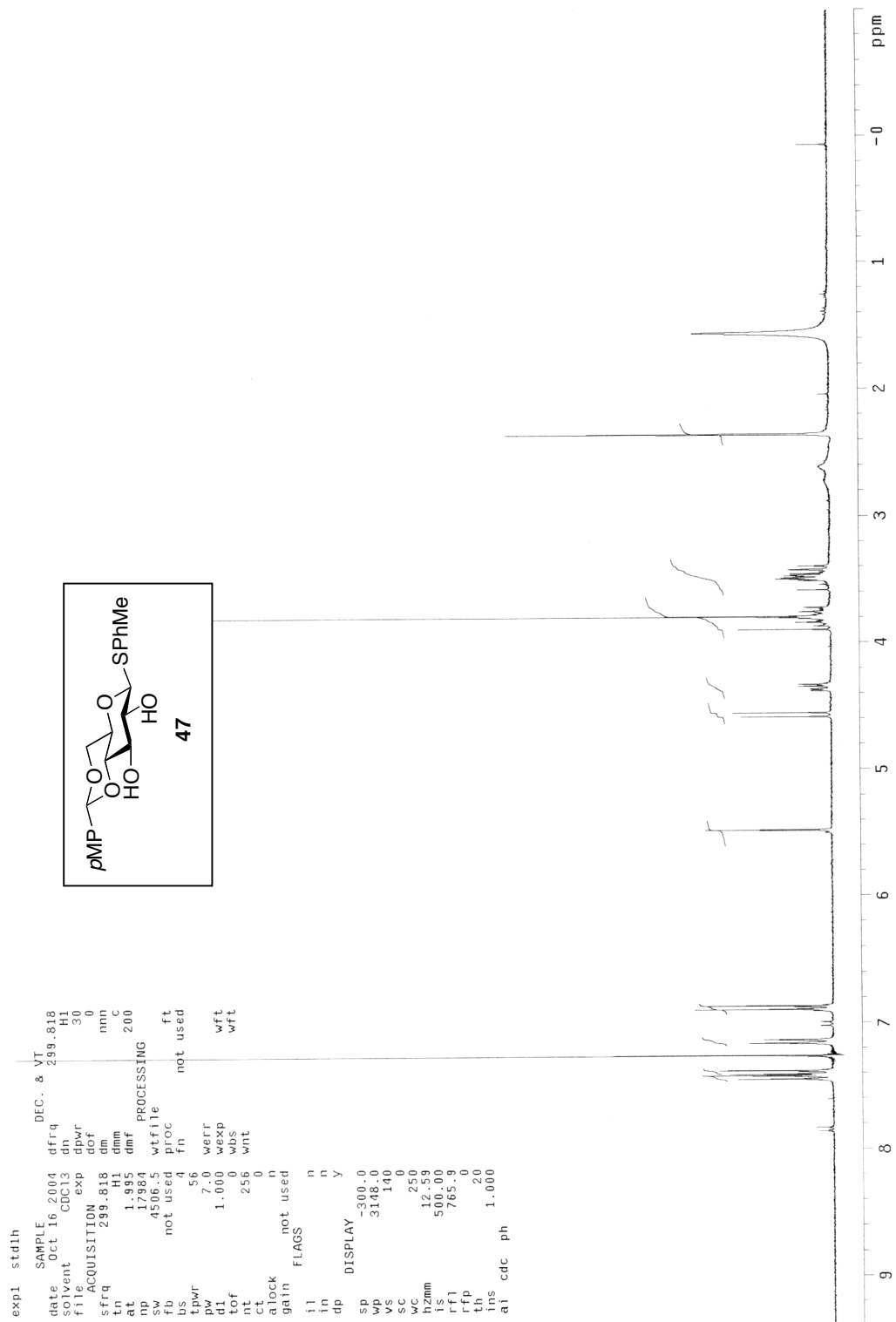


Figure A3.10: ^1H NMR (300 MHz, CDCl_3) of compound **47**.

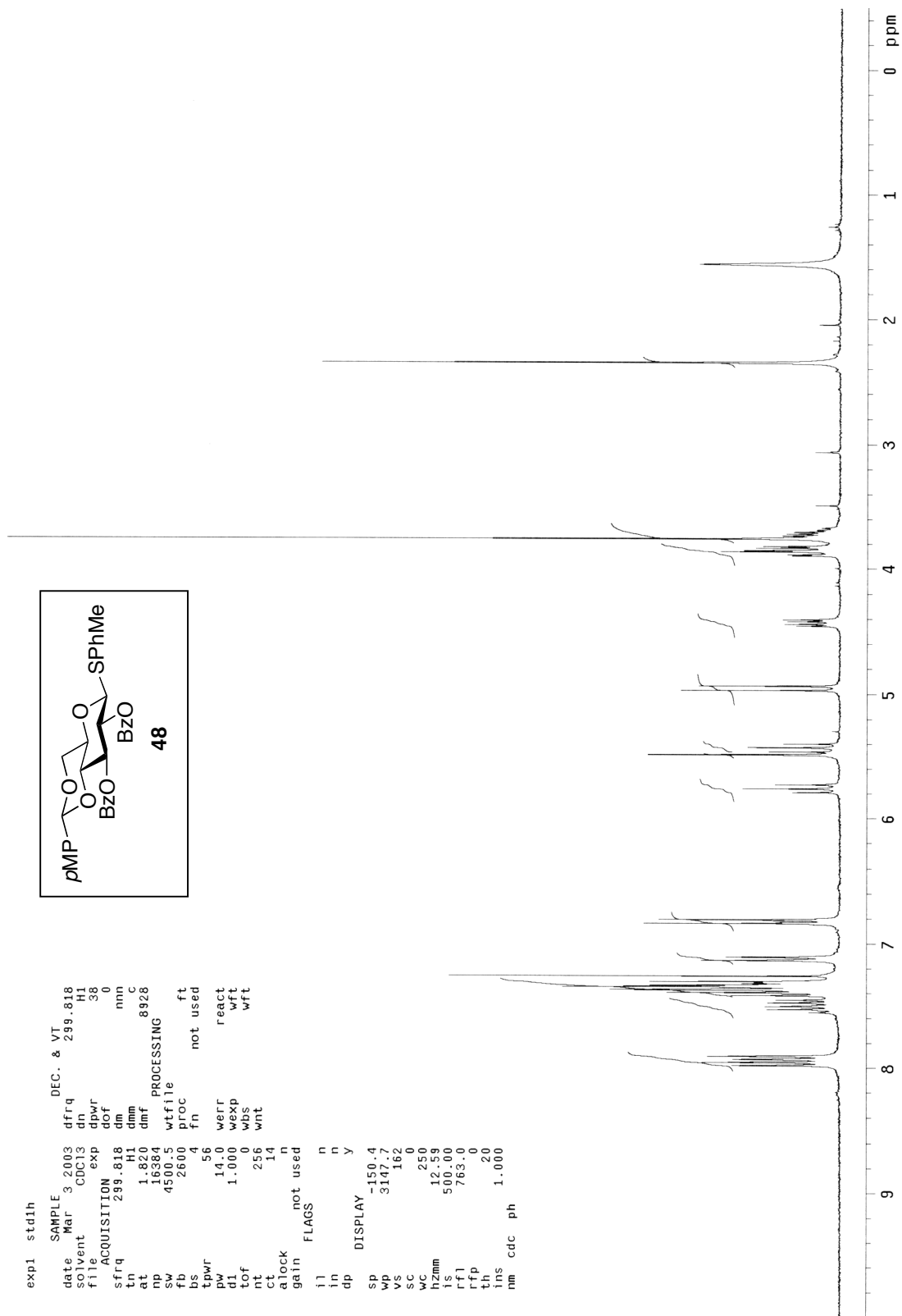
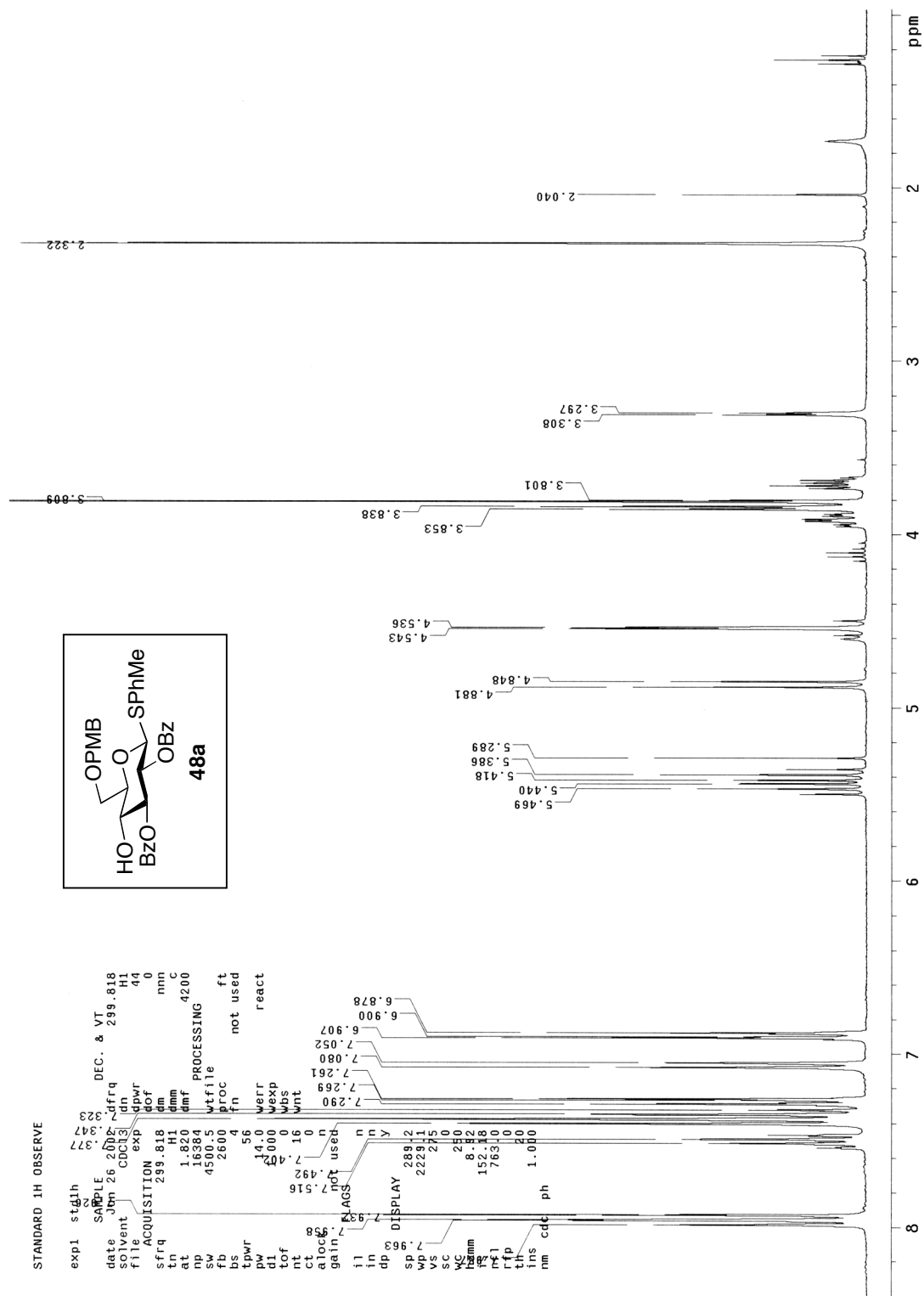


Figure A3.11: ^1H NMR (300 MHz, CDCl_3) of compound **48**.



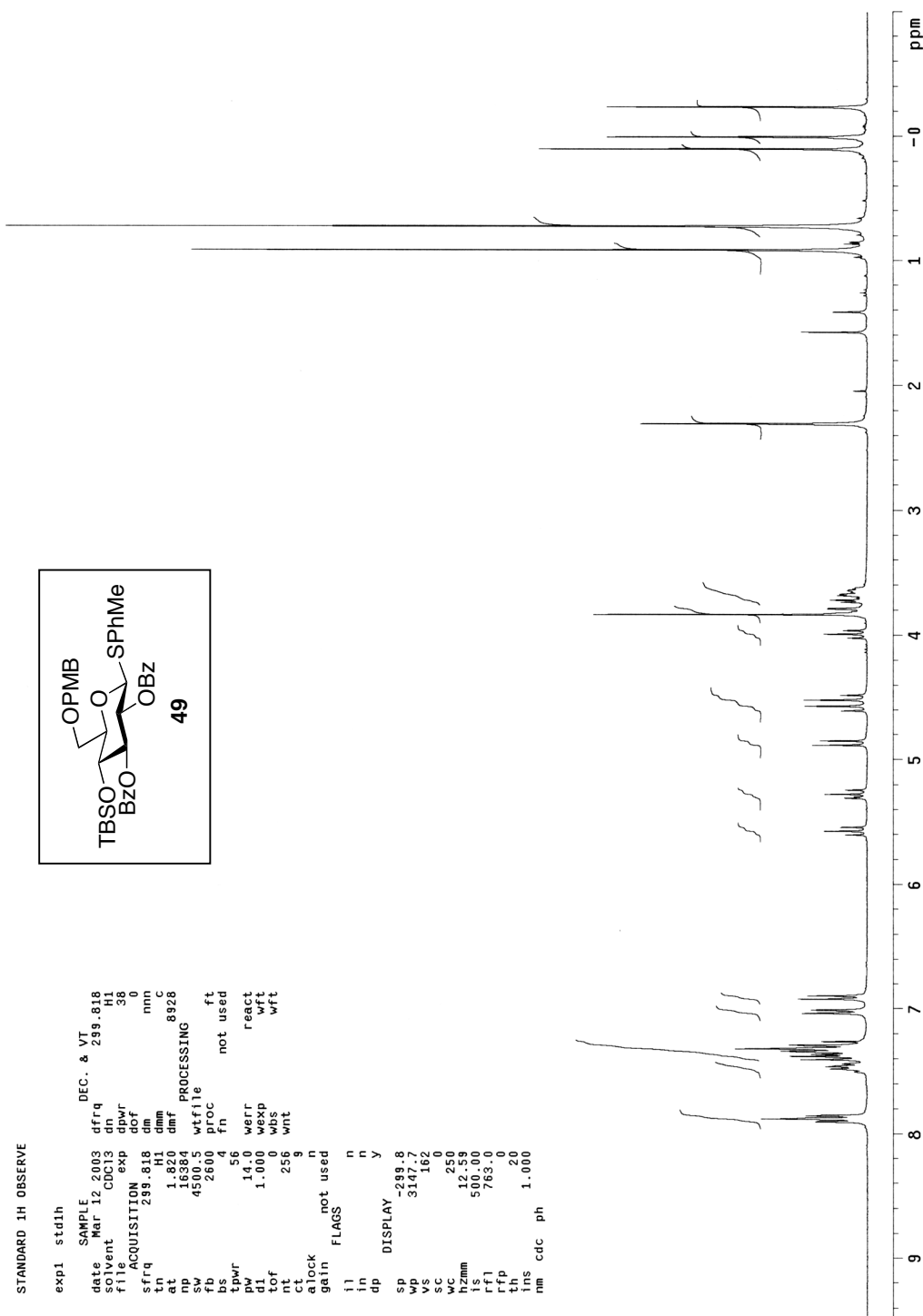


Figure A3.13: ^1H NMR (300 MHz, CDCl_3) of compound 49.

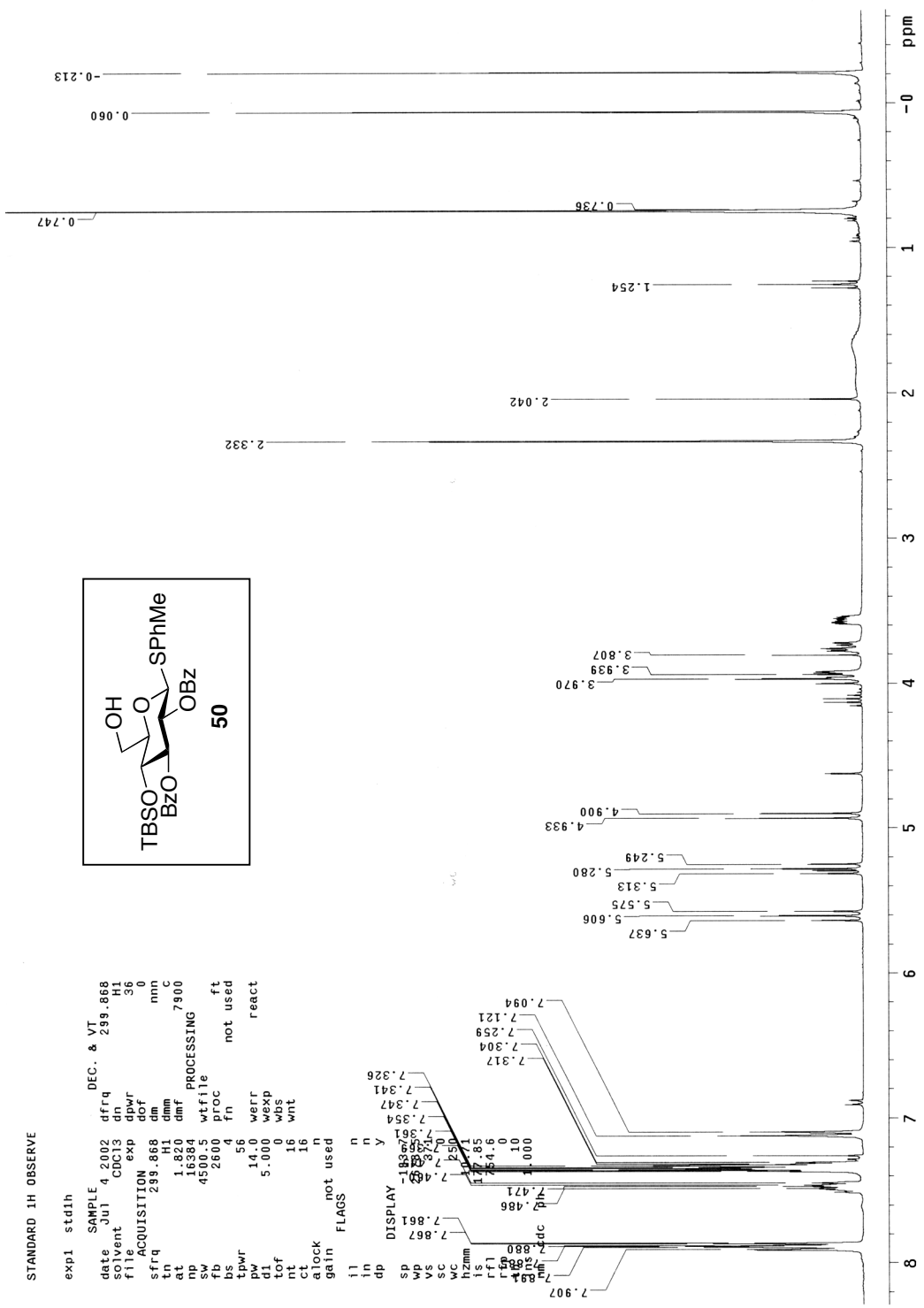


Figure A3.14: ¹H NMR (300 MHz, CDCl₃) of compound 50.

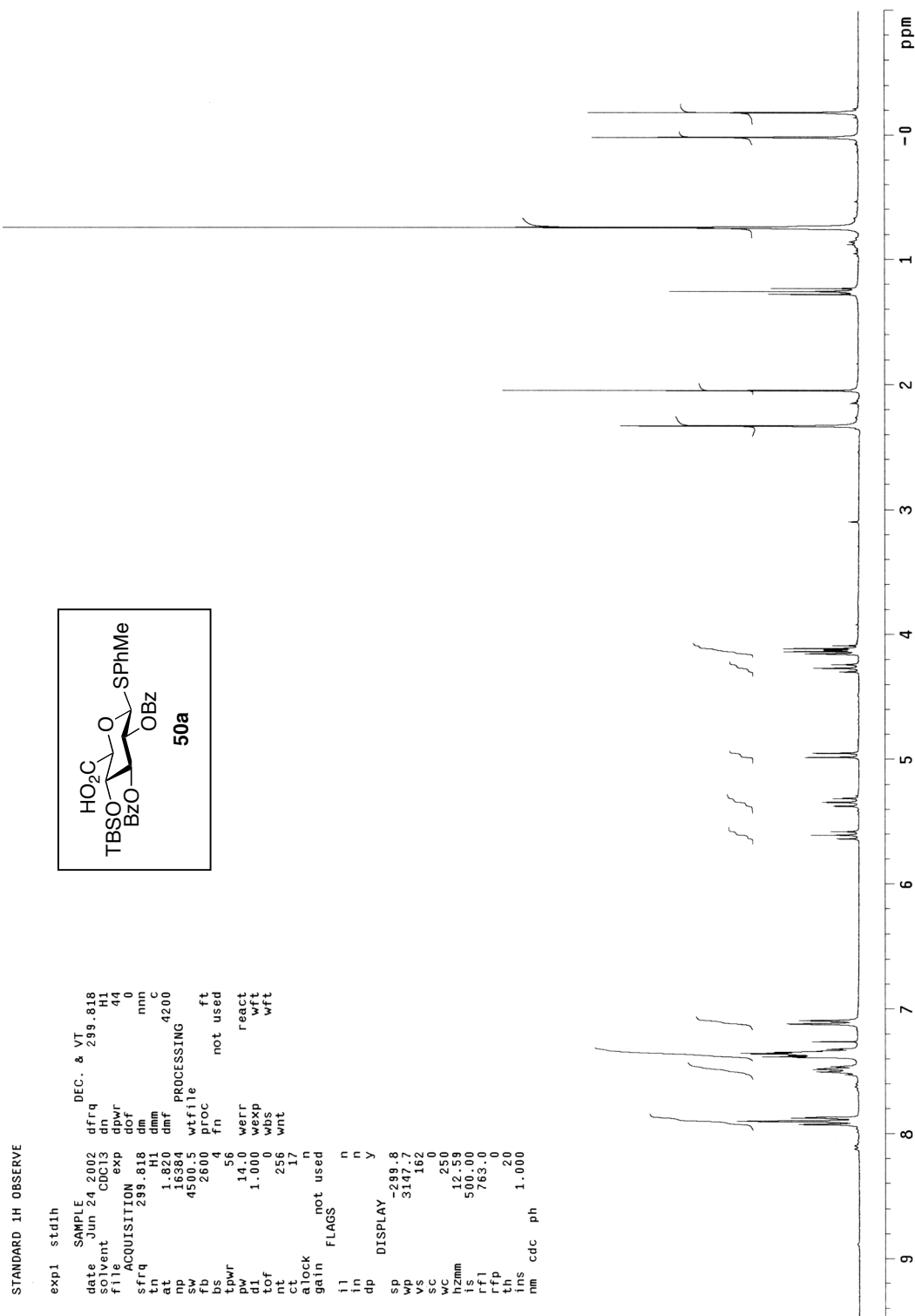


Figure A3.15: ^1H NMR (300 MHz, CDCl_3) of compound **50a**.

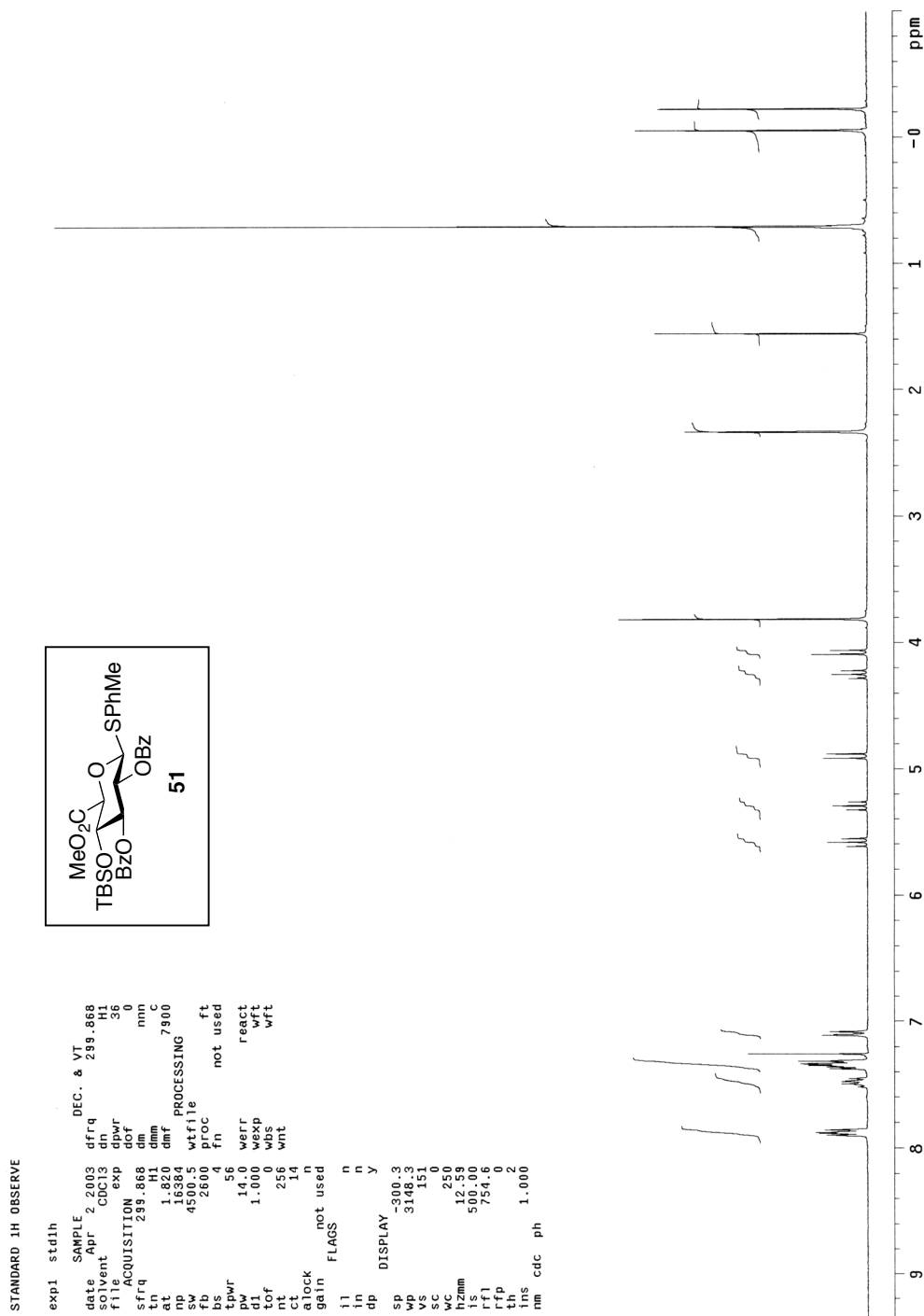


Figure A3.16: ^1H NMR (300 MHz, CDCl_3) of compound **51**.

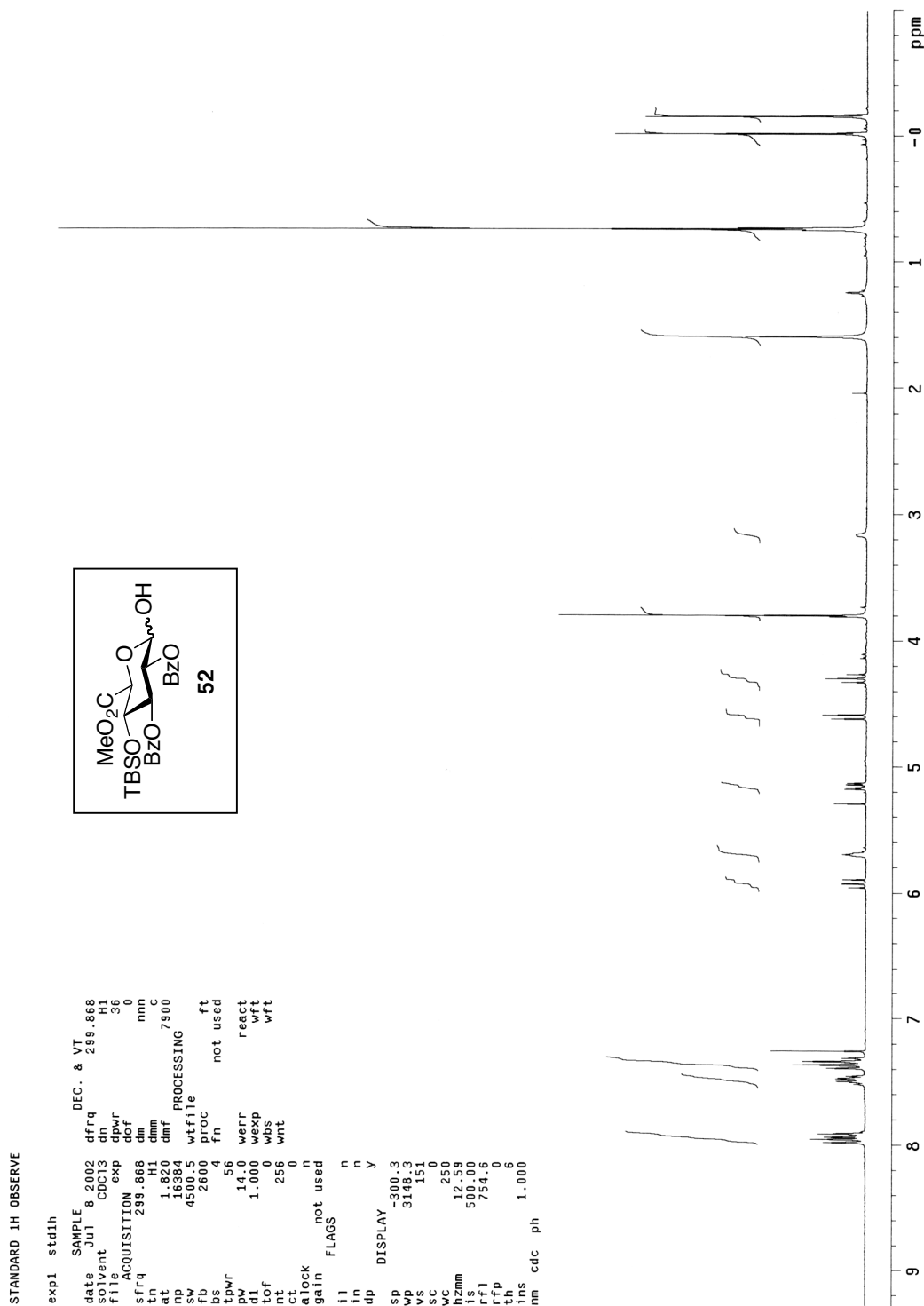


Figure A3.17: ^1H NMR (300 MHz, CDCl_3) of compound **52**.

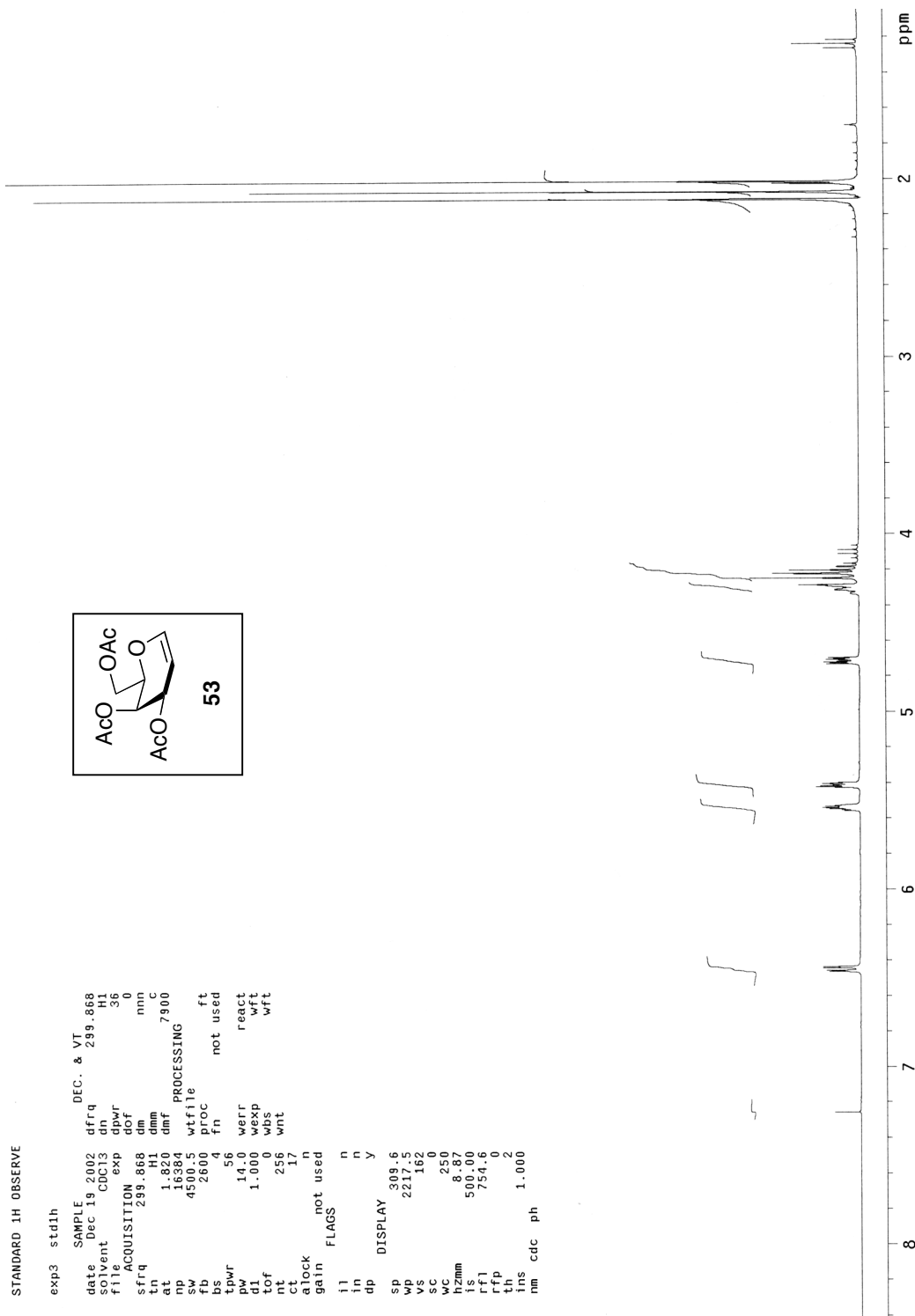


Figure A3.18: ^1H NMR (300 MHz, CDCl_3) of compound **53**.

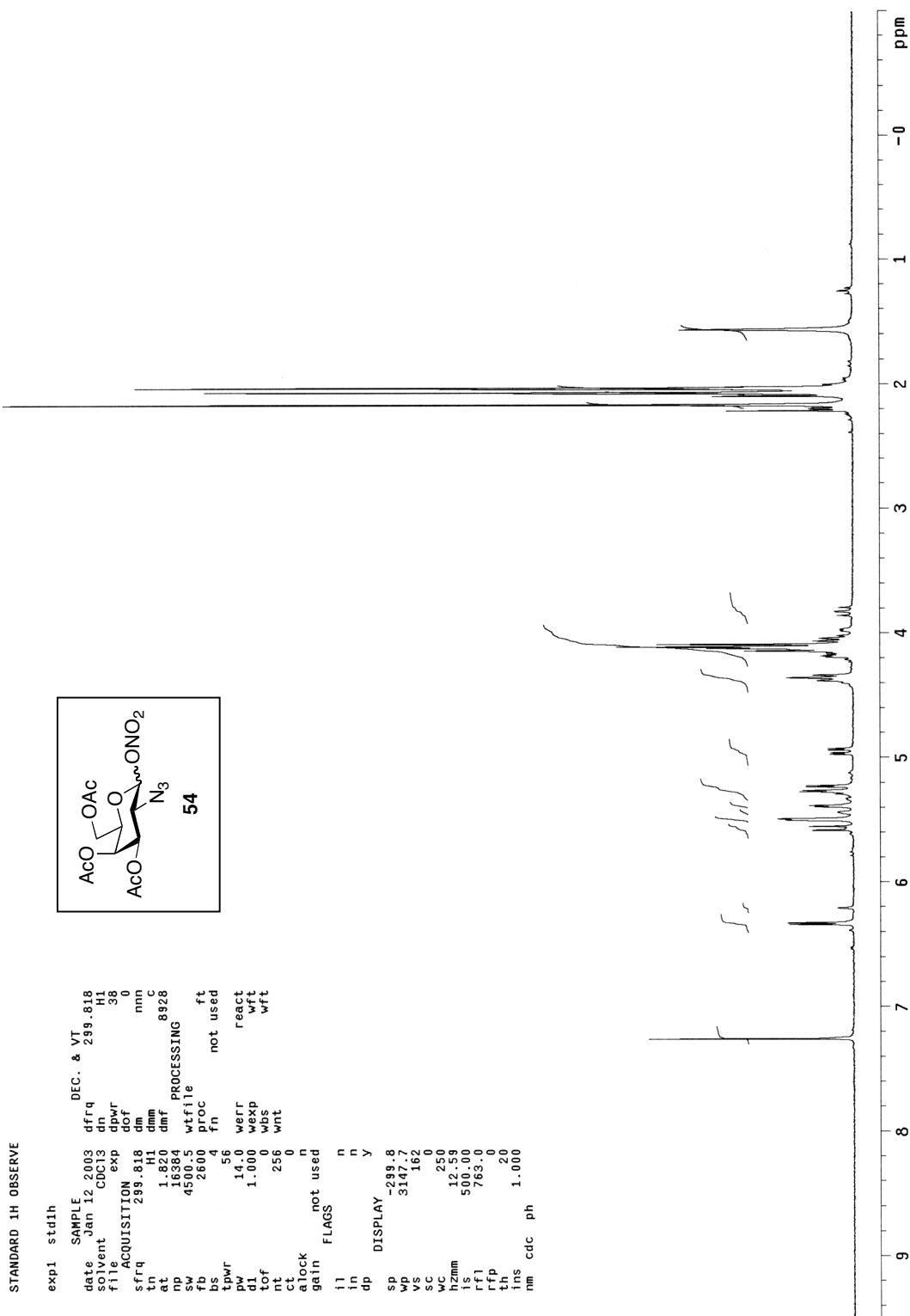


Figure A3.19: ^1H NMR (300 MHz, CDCl_3) of compound 54.

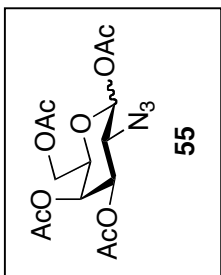
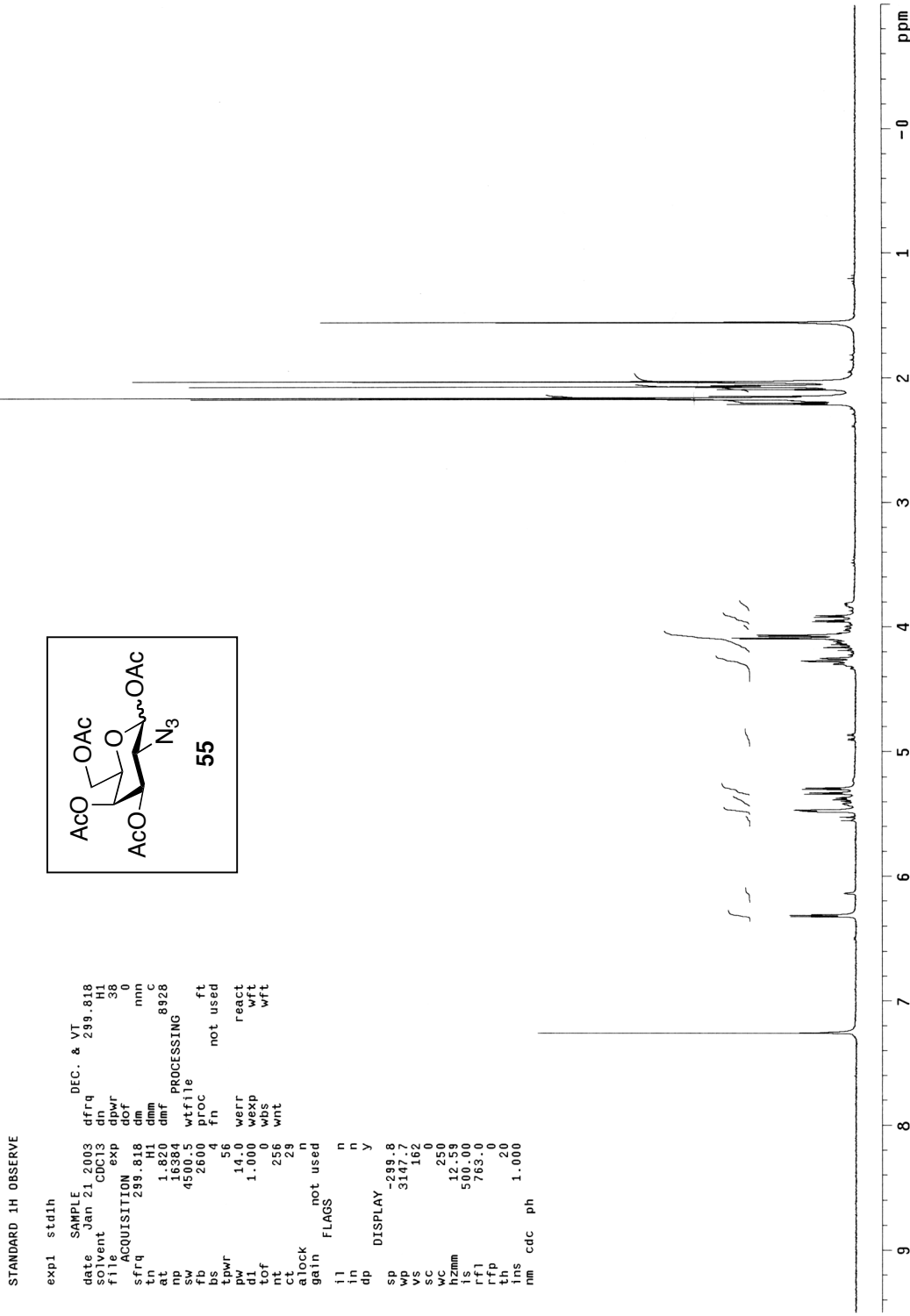


Figure A3.20: ¹H NMR (300 MHz, CDCl₃) of compound 55.

STANDARD 1H OBSERVE

```

exp1 std1h
SAMPLE
date Feb 13 2003          DEC. & VT 299.818
solvent CDC13            dn          H1
f1file ACQUISITION.exp  dpr          30
sfrq    299.818          dm          nmn
tn      1.820            dmf          8928
ap      16384            wtfile
sw      4500.5           proc
fb      2600             fn          not used
bs
cpwr    56              werr
dr      14              wexp
dt      1.000           wps
tof     0                wnt
nt      32              wnt
ct      10
alock   not used
gain    not used
il      n
in      n
dp      y
DISPLAY
SP      23.2
WP      2436.2
VS      151
SC      0
WC      250
Hzmm    500.04
fl      763.0
rfp     0
th      20
ins     100.000
nm      cdc ph

```

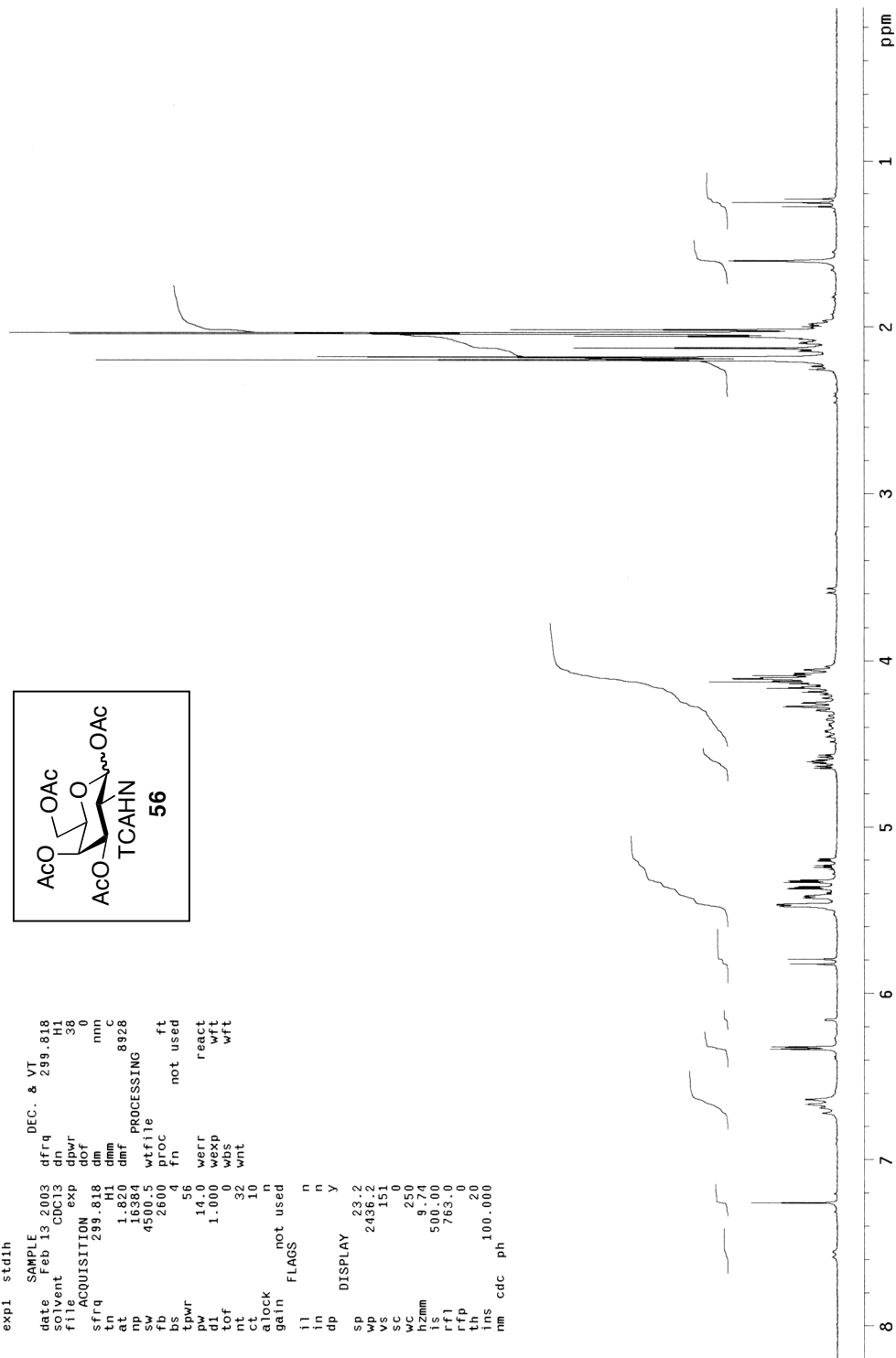
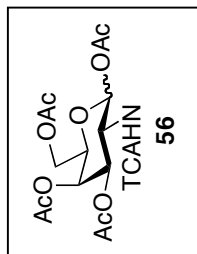


Figure A3.21: ¹H NMR (300 MHz, CDCl₃) of compound 56.

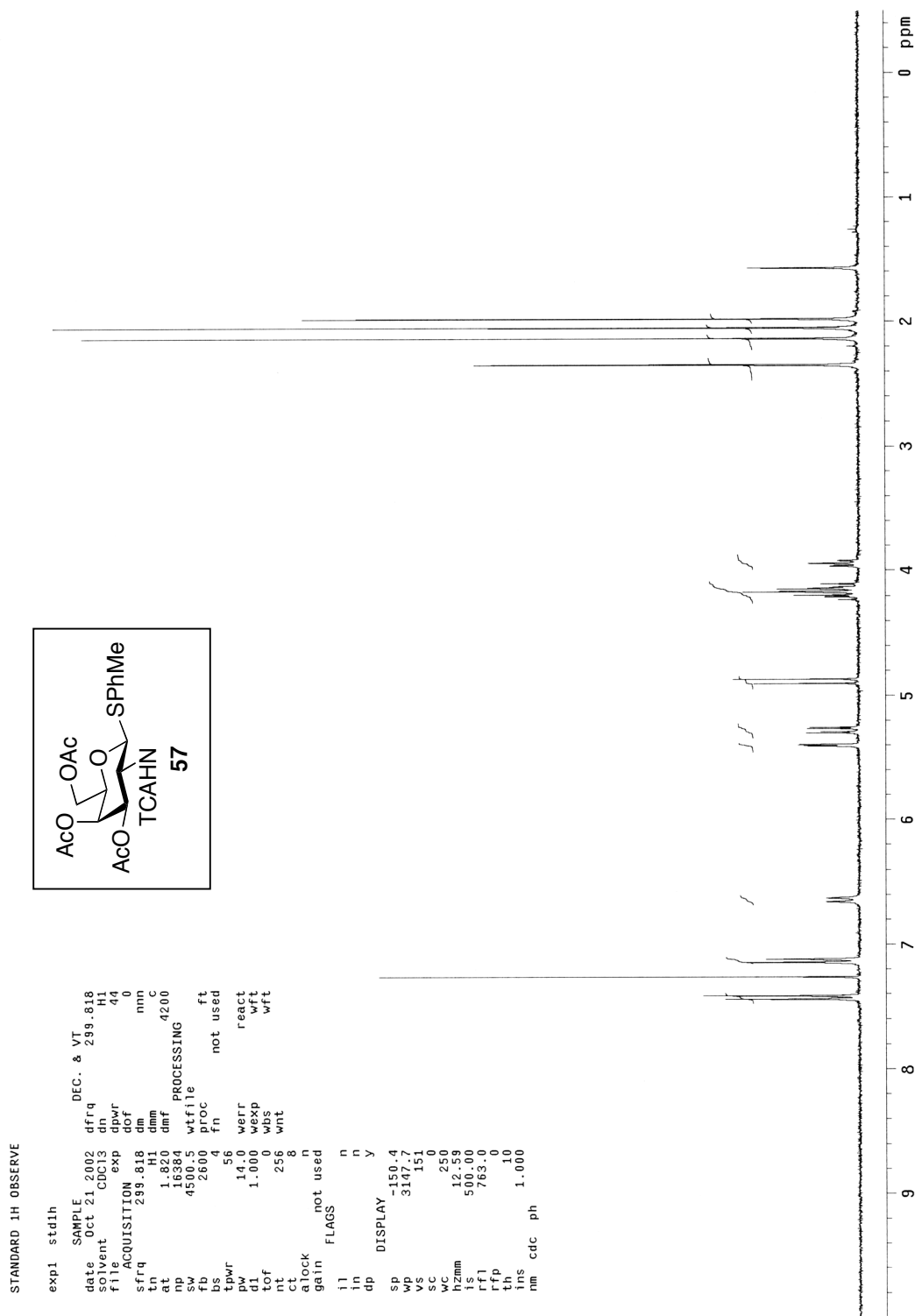
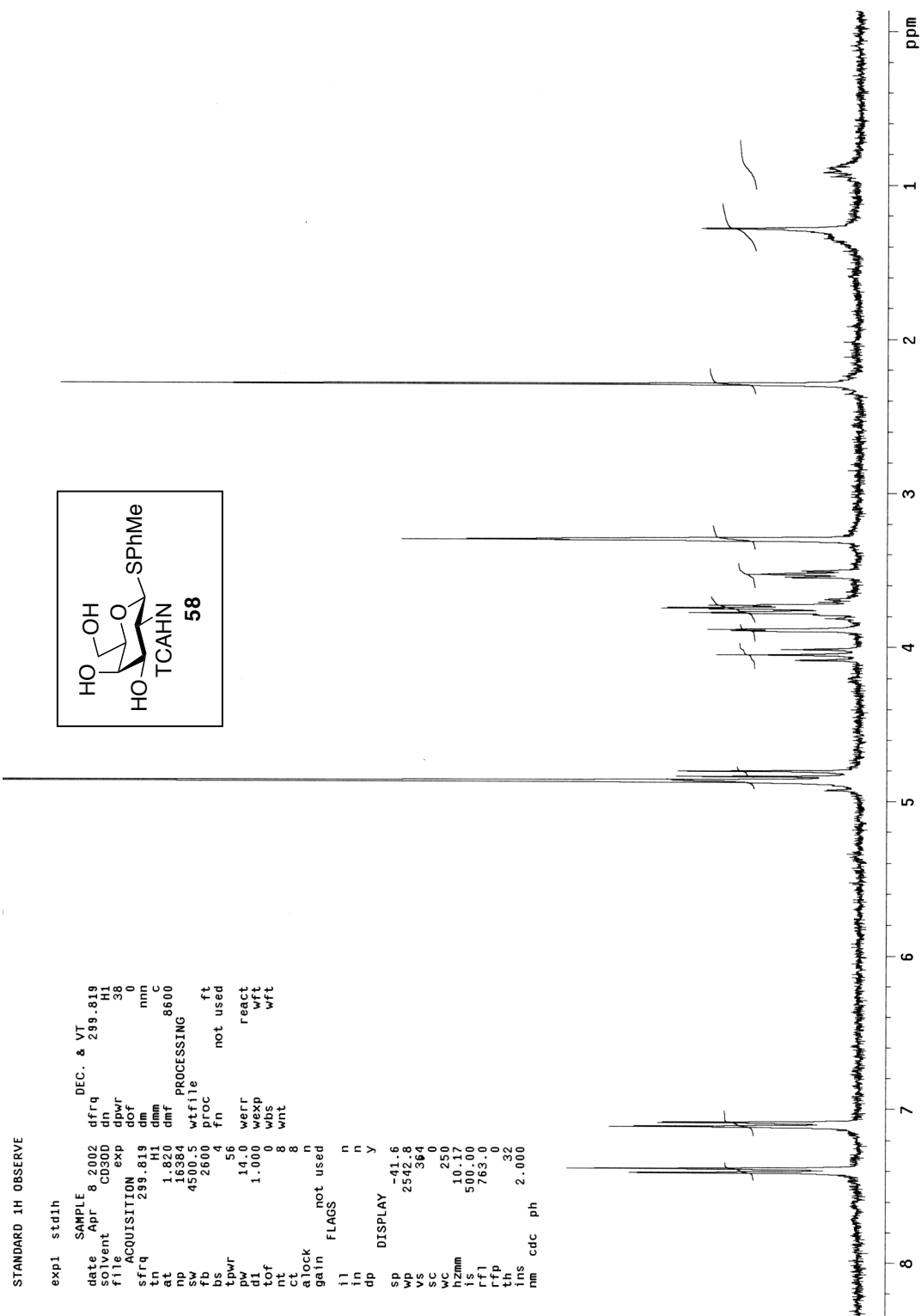


Figure A3.22: ^1H NMR (300 MHz, CDCl_3) of compound **57**.

Figure A3.23: ^1H NMR (300 MHz, CD_3OD) of compound 58.

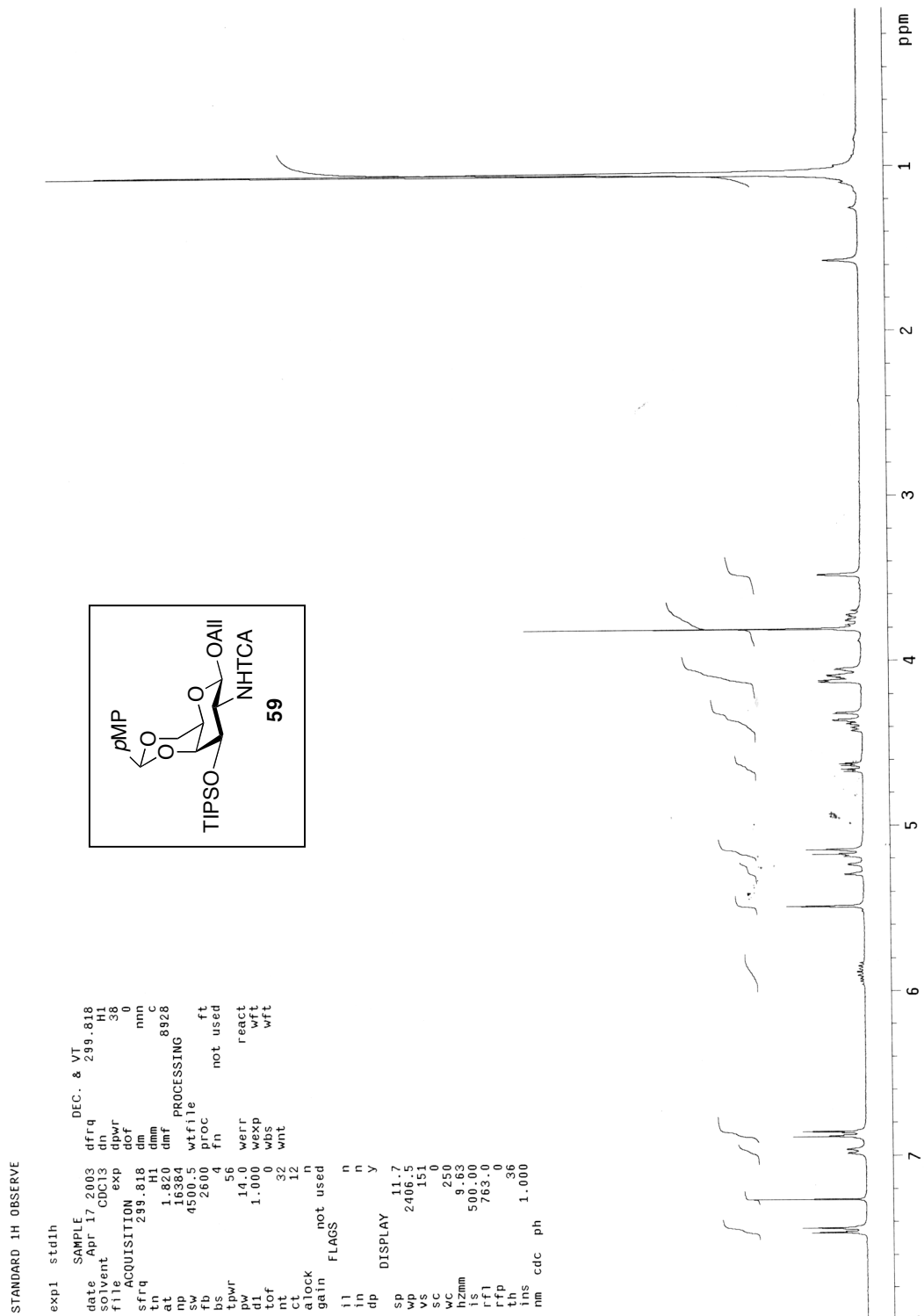


Figure A3.24: ^1H NMR (300 MHz, CDCl_3) of compound **59**.

STANDARD 1H OBSERVE

```

exp1 std1h
SAMPLE
date Apr 16 2003
solvent CDCl3
file ACQUISITION exp
sfrq 299.868
tn H1
at 1.820
np 16384
sw 4500.5
fb 2600
bs 4
tpwr 56
pw 14.0
d1 1.000
tof 0
nt 32
ct 13
atock gain not used
in n
in n
dp DISPLAY y
sp -51.4
wp 2631.3
vs 151
sc 0
wc 250
hzmm 10.53
is 500.00
rfl 754.6
rfp 0
th 17
ins nm cdc ph
nm 1.000
DEC. & VT
dn 299.868
dpwr 36
dof 0
dm nnn
dmm C
dmf 7900
wtfile PROFILE
proc ft
fn not used
werr react
wexp wft
wbs wft
wnt wft

```

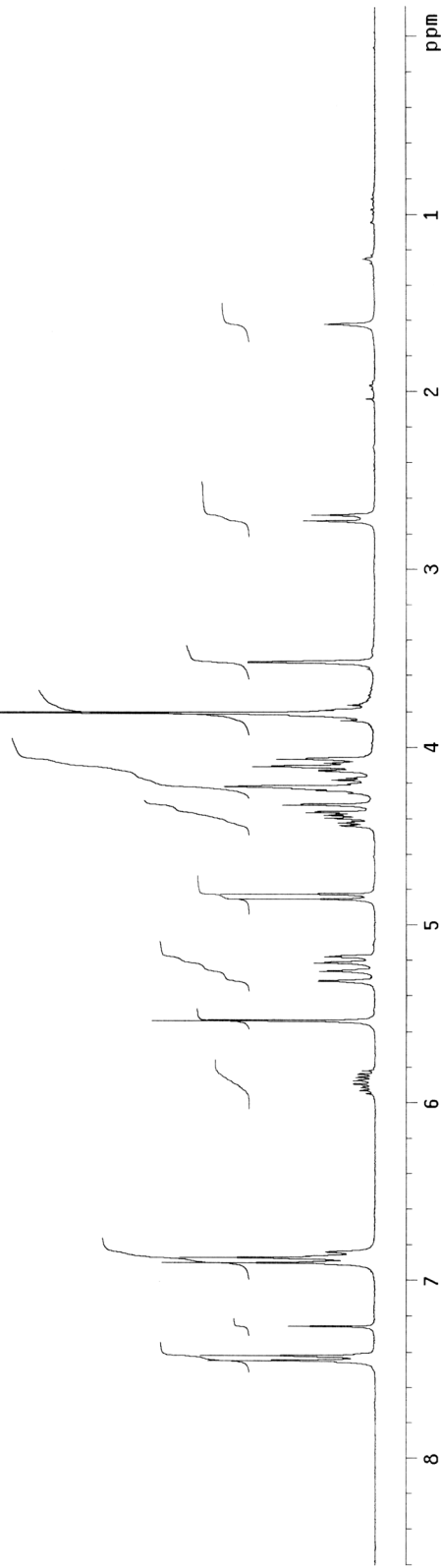
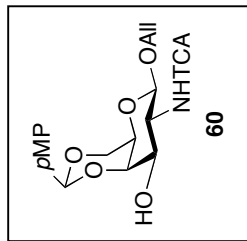
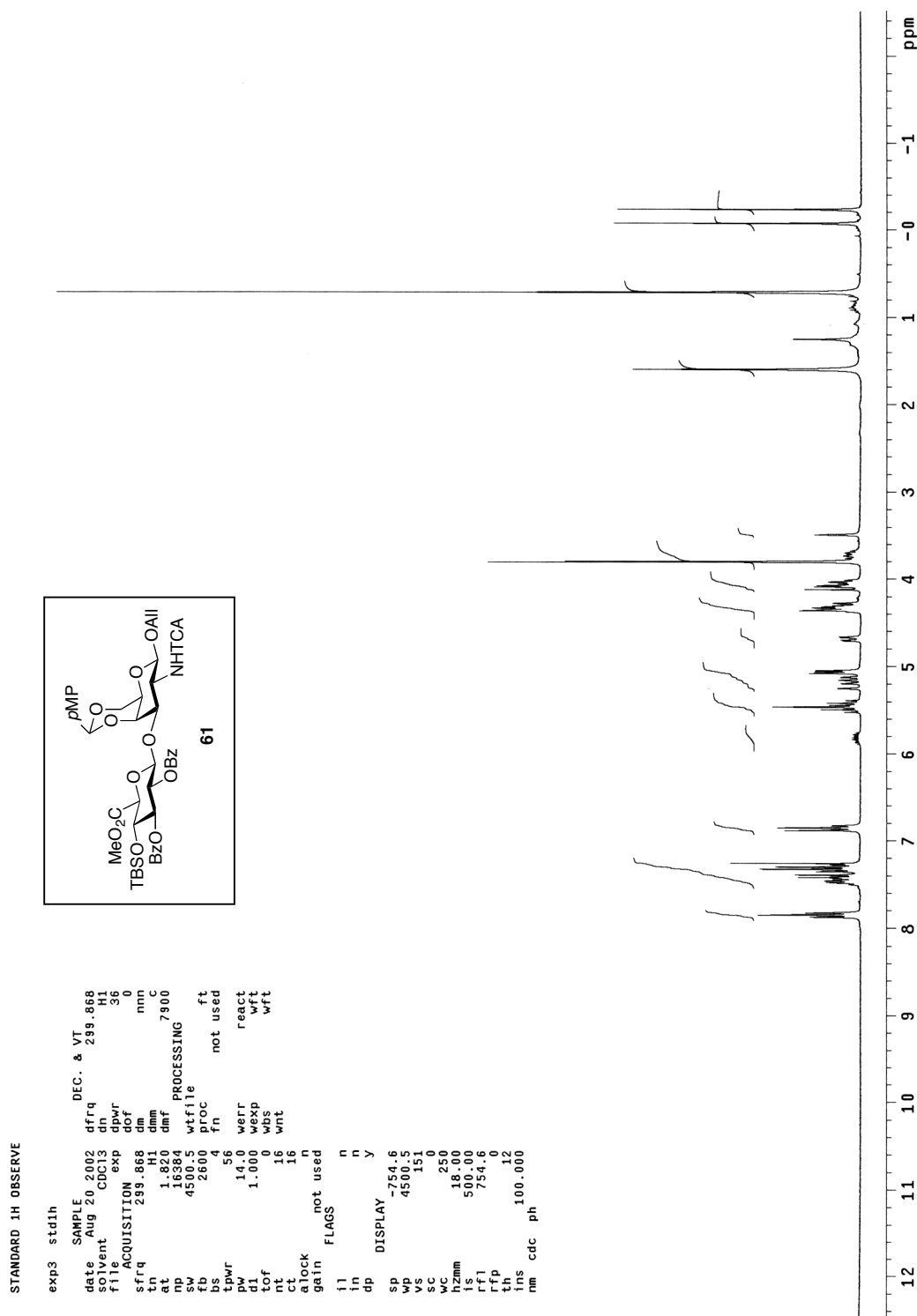


Figure A3.25: ¹H NMR (300 MHz, CDCl₃) of compound 60.

Figure A3.26: ¹H NMR (300 MHz, CDCl₃) of compound **61**.

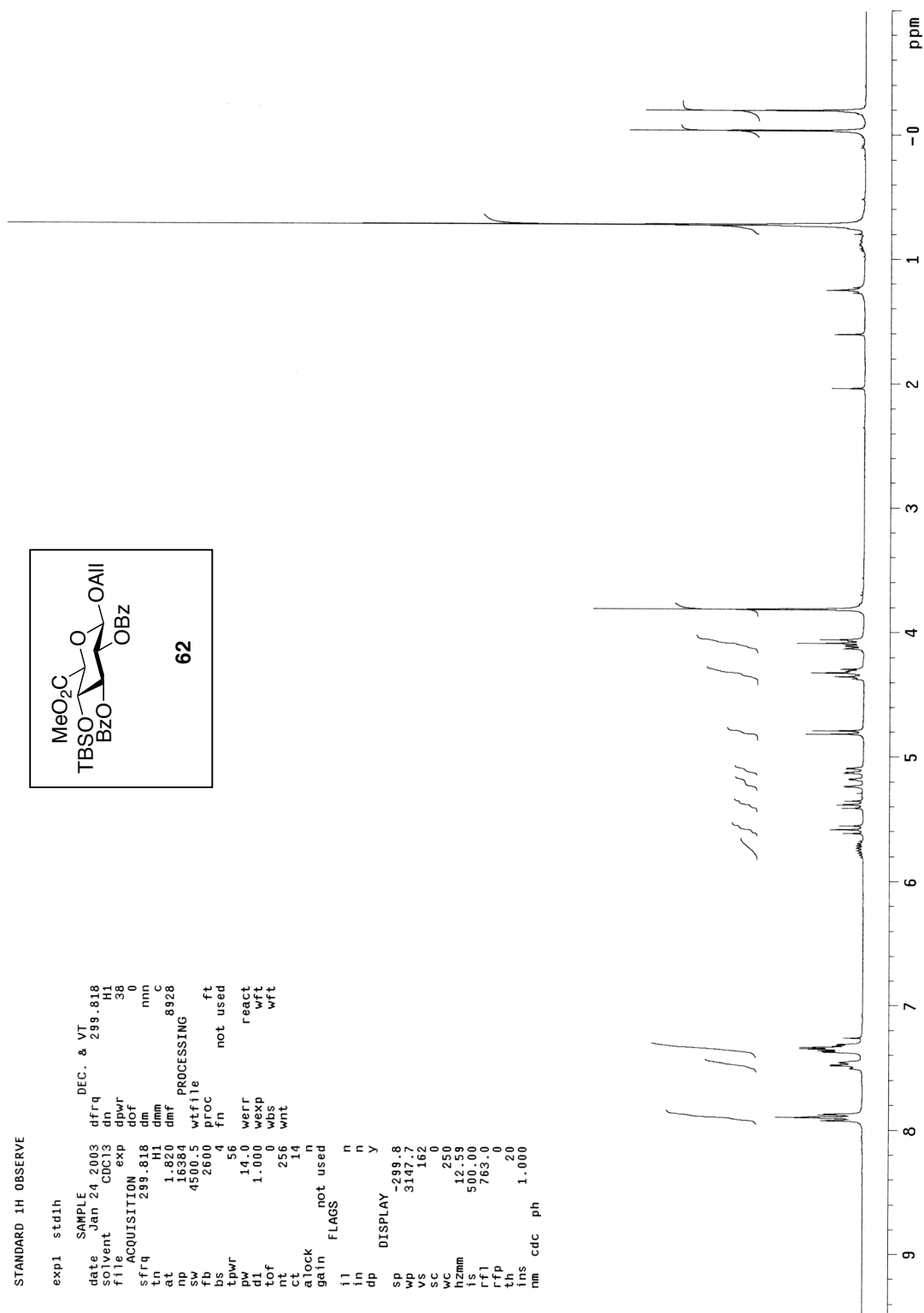
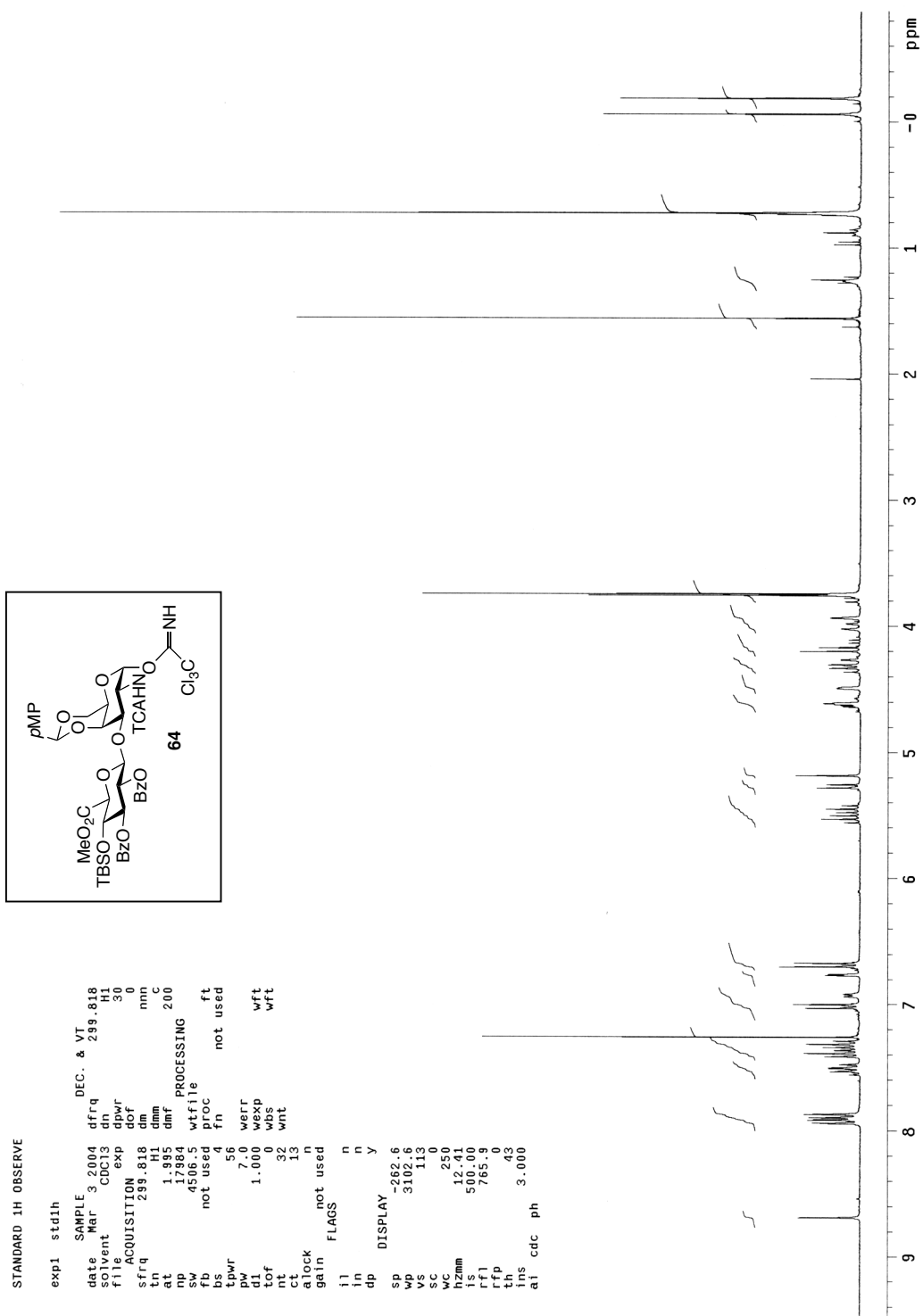
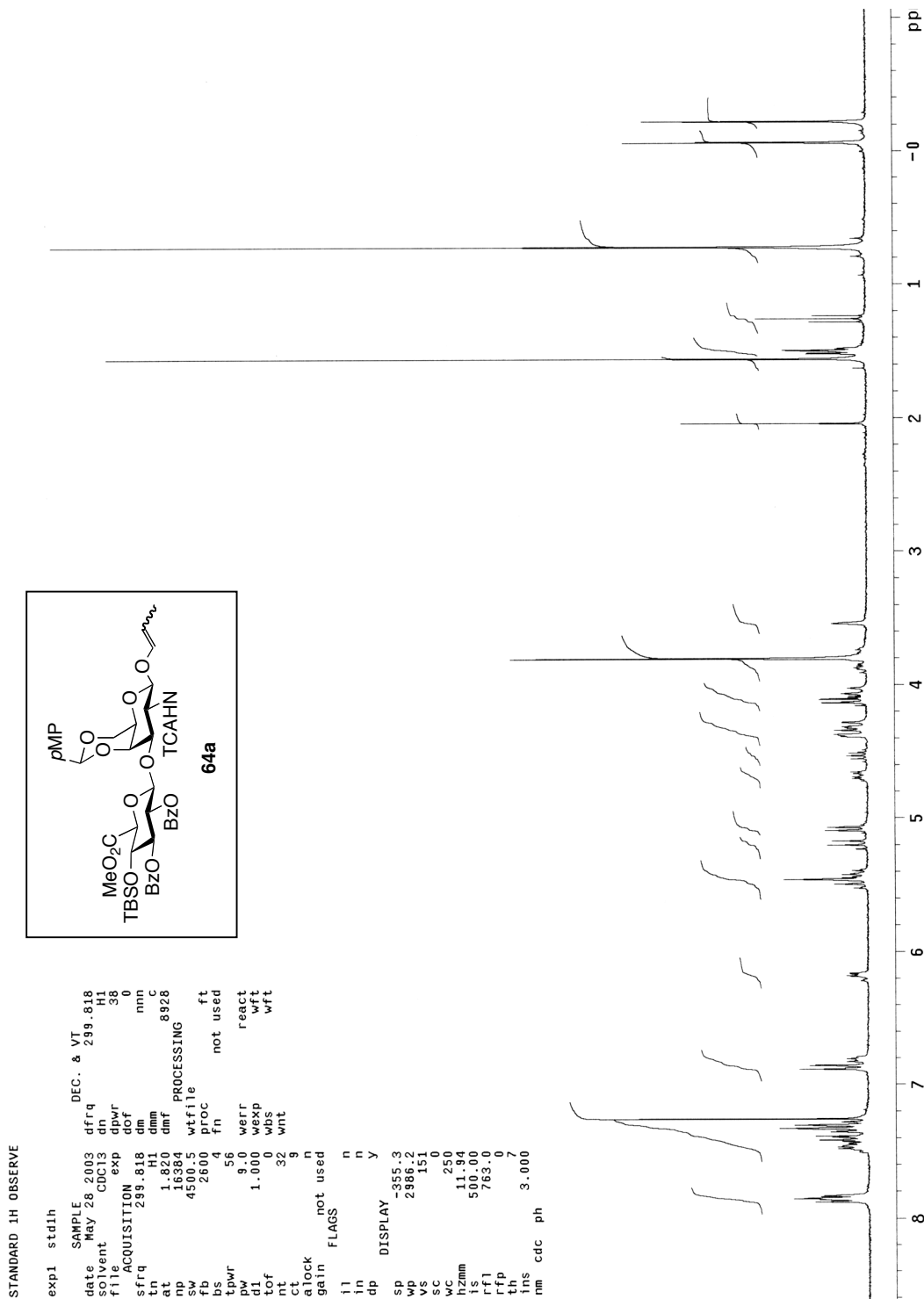


Figure A3.27: ^1H NMR (300 MHz, CDCl_3) of compound **62**.

Figure A3.28: ¹H NMR (300 MHz, CDCl₃) of compound **64**.



STANDARD 1H OBSERVE

```

exp1 std1h
SAMPLE
date May 30 2003
file ent CDC15
file ACQUISITION exp 0
sfrq 289.818
tn H1
np 16384
sw 4500.5
b 2000
b1 56
b2 9.0
pw 1.000
d1 32
nt 13
ct 13
alock n
gain not used
flags n
il n
in n
dp DISPLAY
sp -331.7
wp 3045.5
vs 151
vc 0
wc 250
h2mm 12.18
is 500.00
rfl 763.0
rfp 0
th 12
ins cdc
nm ph 3.000
DEC. & VT
dfrq 289.818
dpr 38
dpr 0
dof nnn
dm dmm
dmf 828
wtfile PROCESSING
proc not used
fn react
werr wft
wexp wbs
wnt wft
  
```

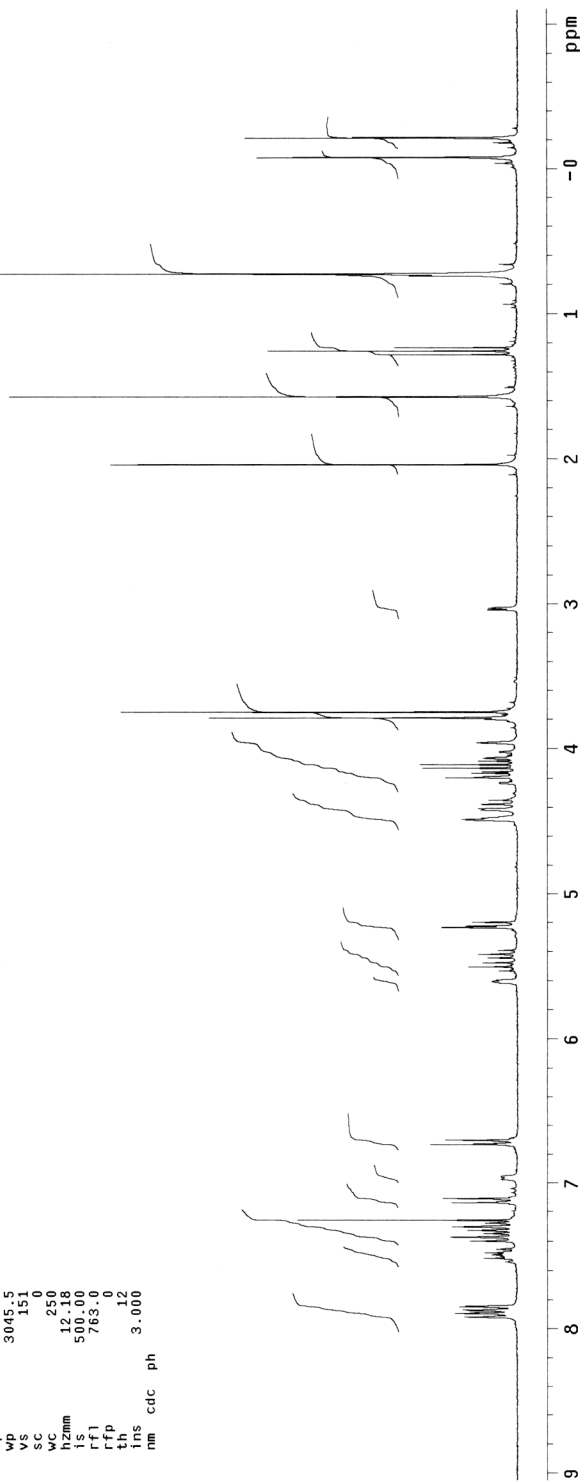
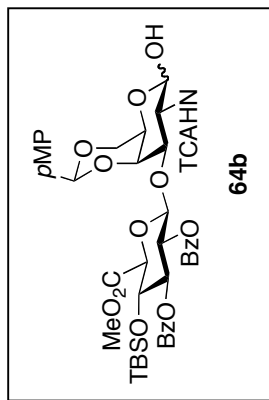


Figure A3.30: ¹H NMR (300 MHz, CDCl₃) of compound **64b**.

STANDARD 1H OBSERVE

```

exp1 std1h
SAMPLE
date Apr 24 2003
solvent CDCl3
file ACQUISITION
sfrq 299.868
at 1.820
np 16384
sw 4500.5
f2 2000
b2 56
t2wrr 14.0
d1 1.000
tof 0
nt 256
ct 14
alock n
galn not used
i1 n
in n
dp n
Sp -150.3
wp 3148.3
vs 151
sc 0
wc 250
hizmm 12.59
ls 500.00
rfl 754.6
rfp 0
th 7
tms cdc ph 1.000
DEC. & VT
dn 299.868
dpwr 36
dof 0
dm nnn
dmf 7900
wf file
proc not used
werr react
wexp wft
wbs wft
wnt wft

```

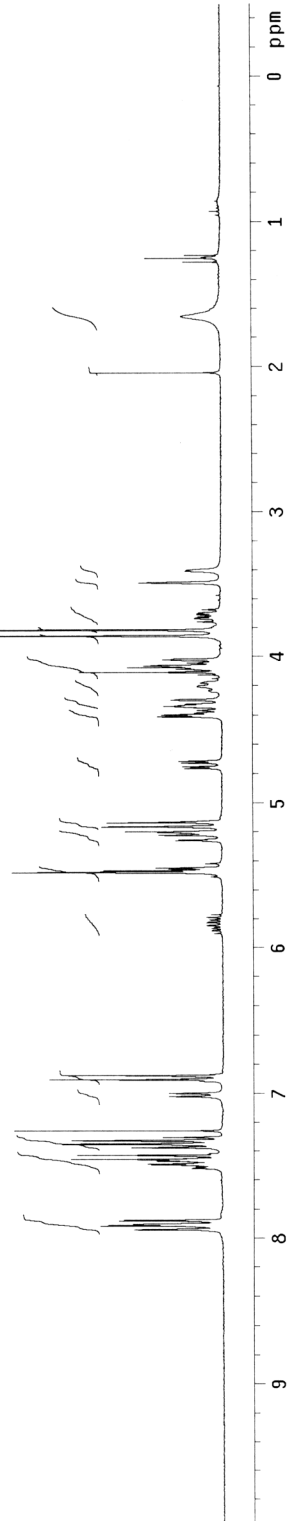
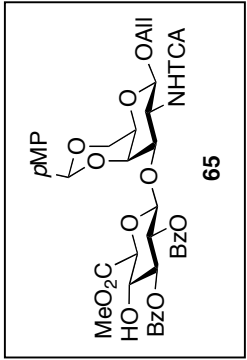


Figure A3.31: ¹H NMR (300 MHz, CDCl₃) of compound 65.

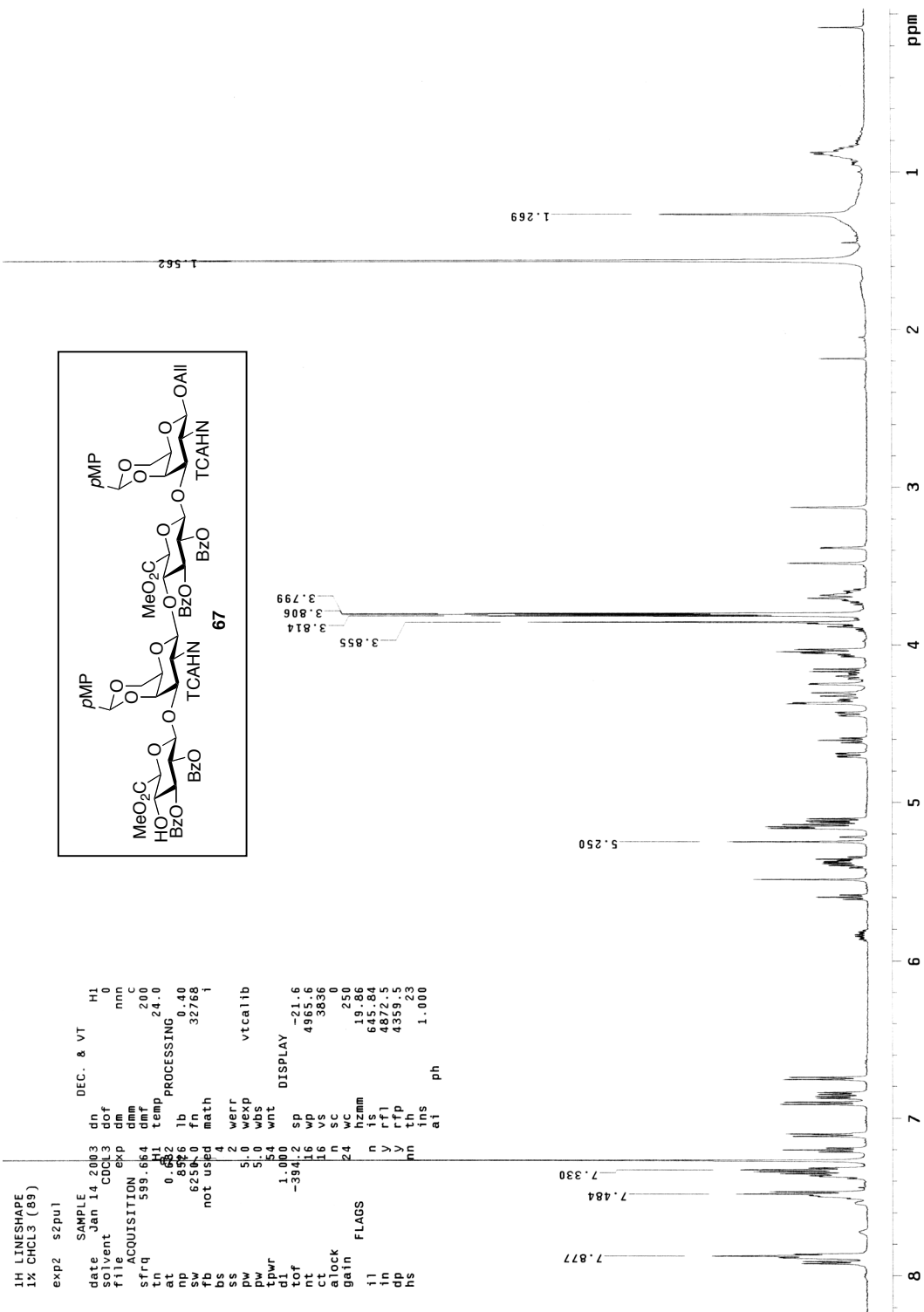


Figure A3.32: ¹H NMR (600 MHz, CDCl₃) of compound **67**.

```

1H LINESHAPE
1X CHCL3 (89)
exp2 s2pu1
DEC. & VT
SAMPLE dn H1
date Jan 14 2003 dn 0
solvent CDCL3 dof 0
file dm nnn
exp dm c
ACQUISITION dmm 200
sfrq 599.864 dmf 24.0
tn 0.852 lb temp PROCESSING 0.40
at 8.920 fn 32768
cp 6256.0
sp not used math i
bs 2
ss 4
werr 2
wexp vtcal lb
pw 5.0
wbs 5.0
wnt 54
tpwr 1.000
DISSOLV -21.6
tof -394.2 sp 499.956
nt 16 wp 389.0
sl 16 vc 250
slock 24
gain 24
h1zmm 19.86
f1 1s 645.84
in y rfl 4872.5
dp y rfp 4359.5
hs nn th 23
al 1ns 1.000
ph
  
```

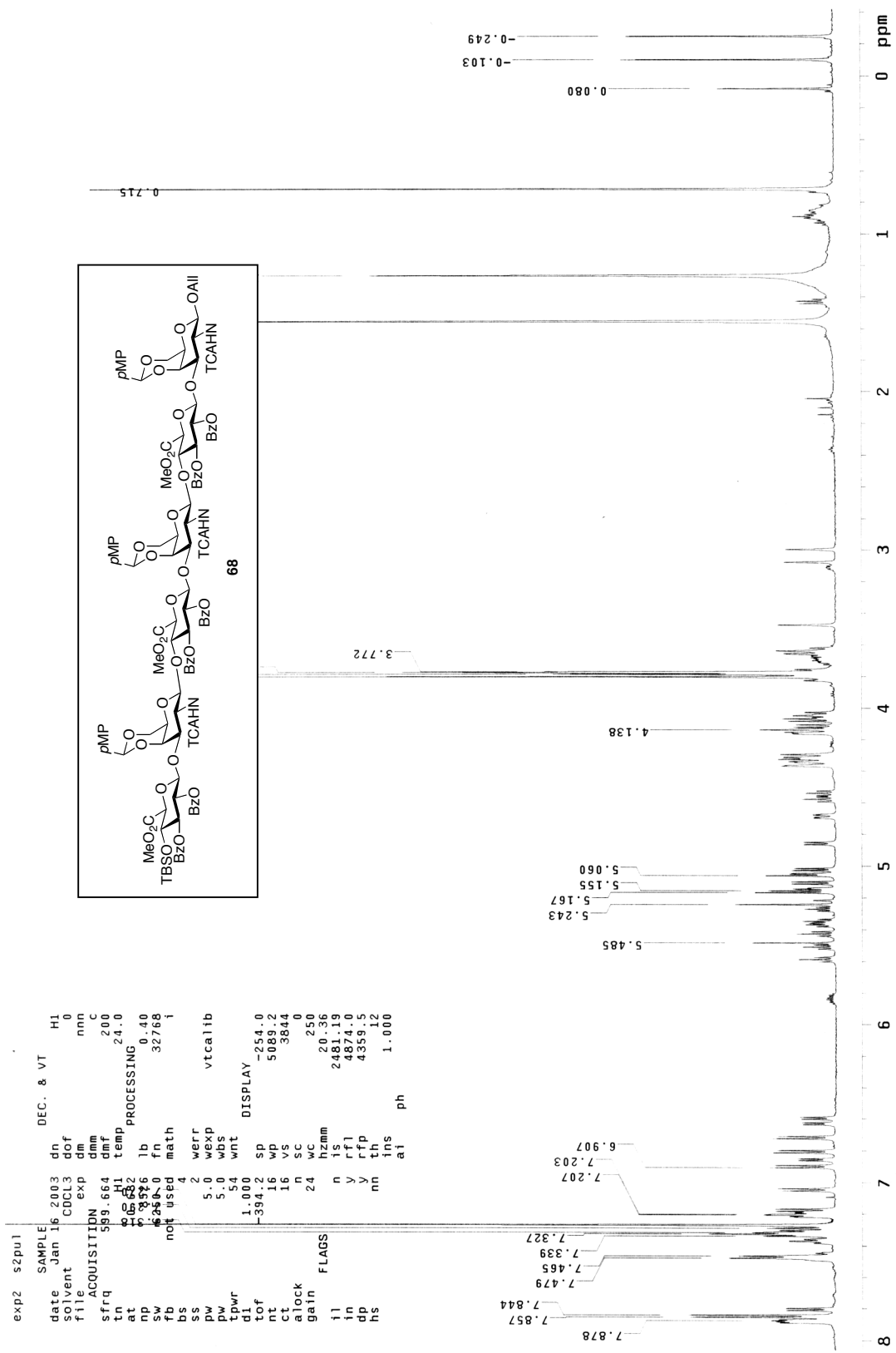



Figure A3.33: ¹H NMR (600 MHz, CDCl₃) of compound 68.

STANDARD 1H OBSERVE

```

exp1 stdih
SAMPLE      DEC. & VT
date      NOV 11 2002   dfrq      299.868
solvent    CDCl3        dr         H1
file      MOV11_0001    dpwr       36
ACQUISITION exp        dcf         0
sfrq      299.868      dm         nnn
tn        1.820        dnm         C
ap        16384        dmf         7800
sw        4500.5      wtfille
fb        2600        proc
ts        54          fn         not used
tpwr      14.5        werr
d1        1.000       wexp
tof       0           wbs
nt        256        wnt
ct        10
alock    not used
gain
FLAGS
i1        n
in        n
dp        y
SP        300.3
Ww        3148.3
VS        162
SC        0
WC        250
hzmm      12.59
is        500.00
rfl       754.6
rfp       0
th        0
ins       1.000
nm        cdc
ph

```

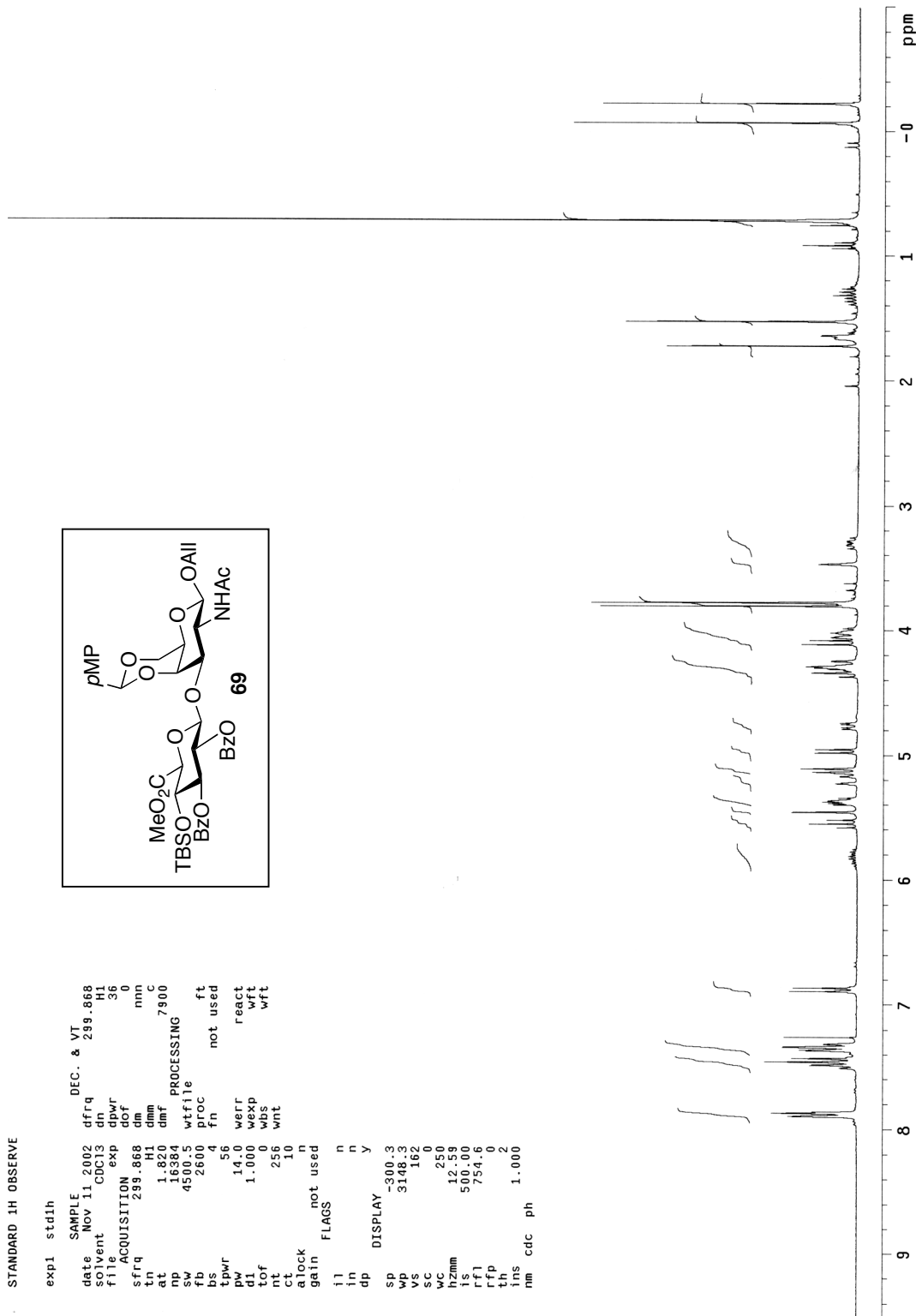
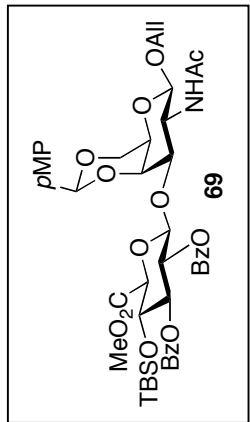


Figure A3.34: ¹H NMR (300 MHz, CDCl₃) of compound **69**.

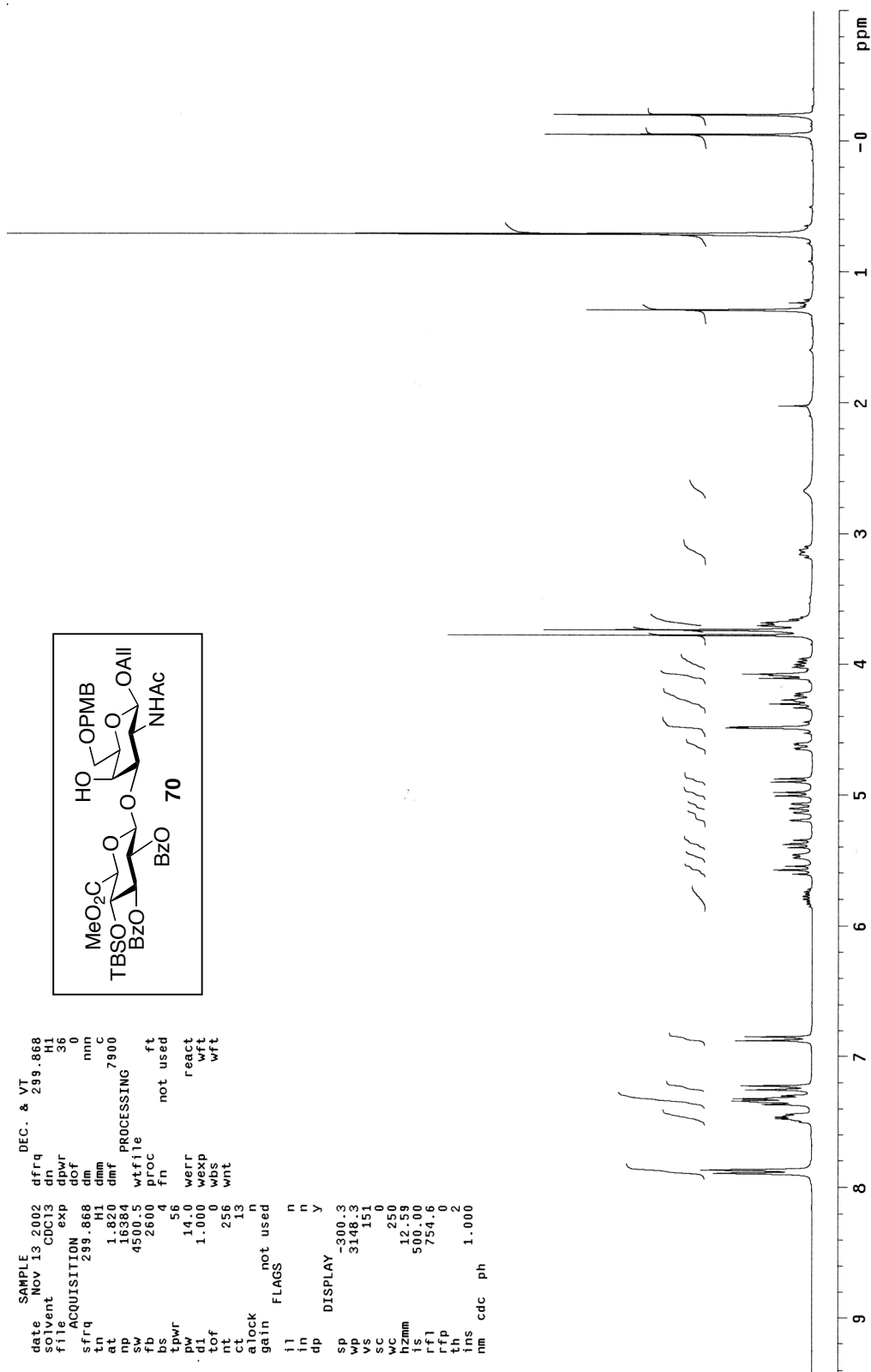


Figure A3.35: ^1H NMR (300 MHz, CDCl_3) of compound **70**.

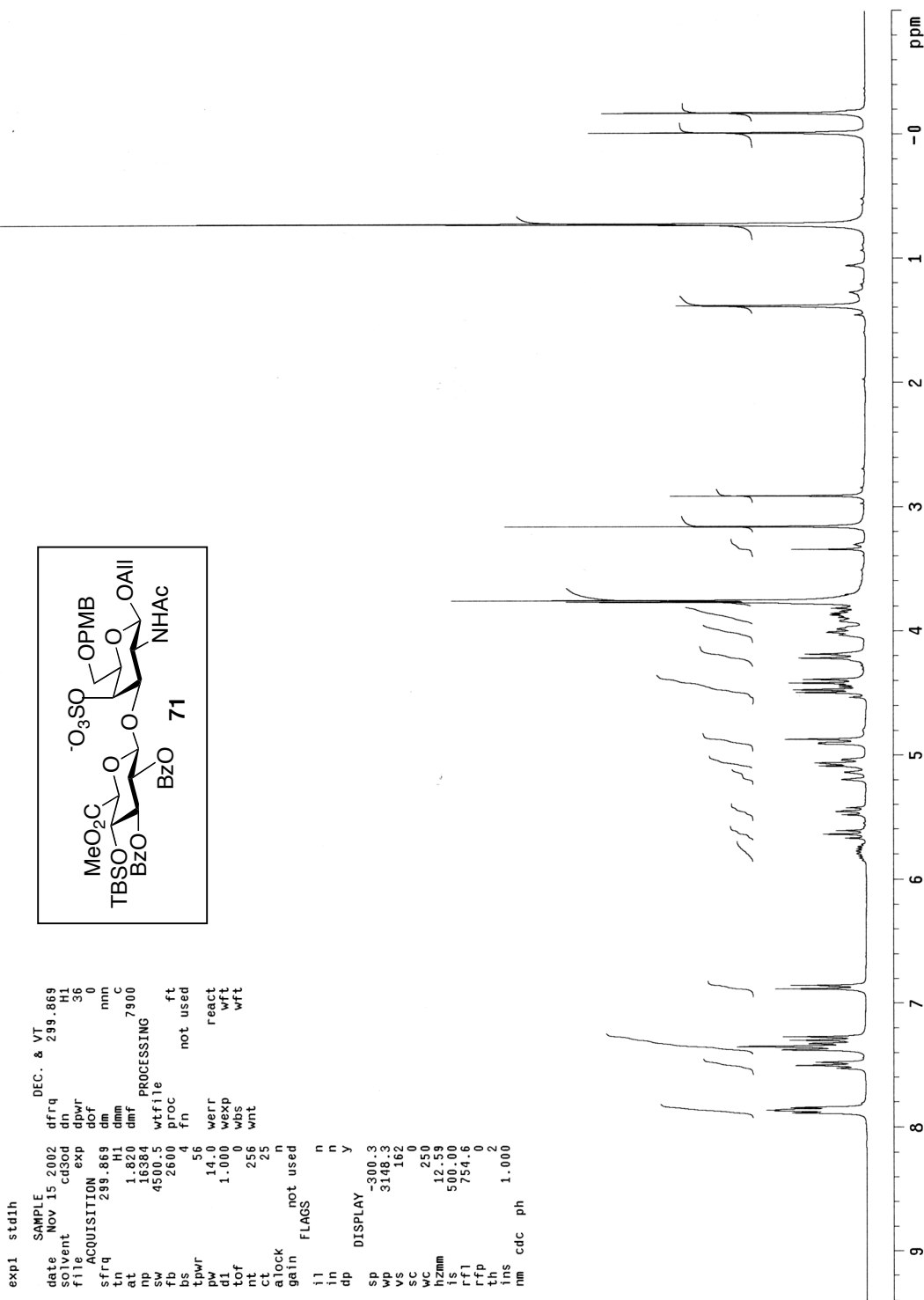
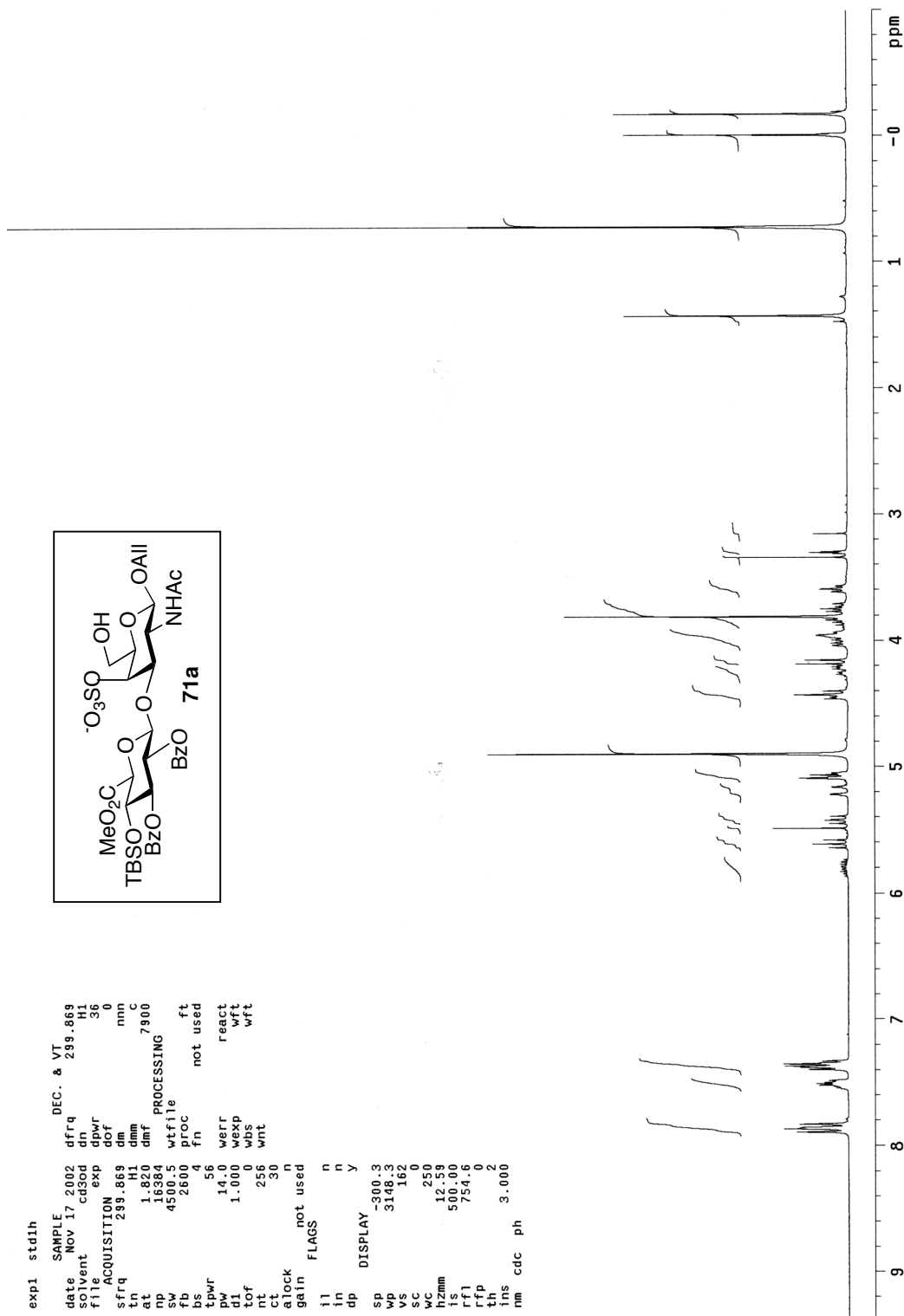


Figure A3.36: ^1H NMR (300 MHz, CD_3OD) of compound **71**.

Figure A3.37: ¹H NMR (300 MHz, CD₃OD) of compound 71a.

STANDARD 1H OBSERVE

```

exp1 std1h
SAMPLE
date Nov 21 2002 dfrq DEC. & VT 299.869
solvent cd3od dn H1
file exp dpwr 36
ACQUISITION exp dof 0
sfrq 299.869 dm nnn
tn H1 dnm 7900 C
at 1.820 dmf wtfile
pw 4500.00 proc
ds 2800.4 fn not used
tpwr 56
pw 14.0 werr react
d1 1.000 wexp wft
tof 0 wbs wft
nt 256 wnt
ct 0
alock n
gain not used
FLAGS
il n
in n
dp y
DISPLAY
sp -300.3
wp 3148.3
vs 151
sc 250
h2mm 12.59
ls 500.00
rfl 754.6
rfp
th 2
ins 1.000
nm cdc ph

```

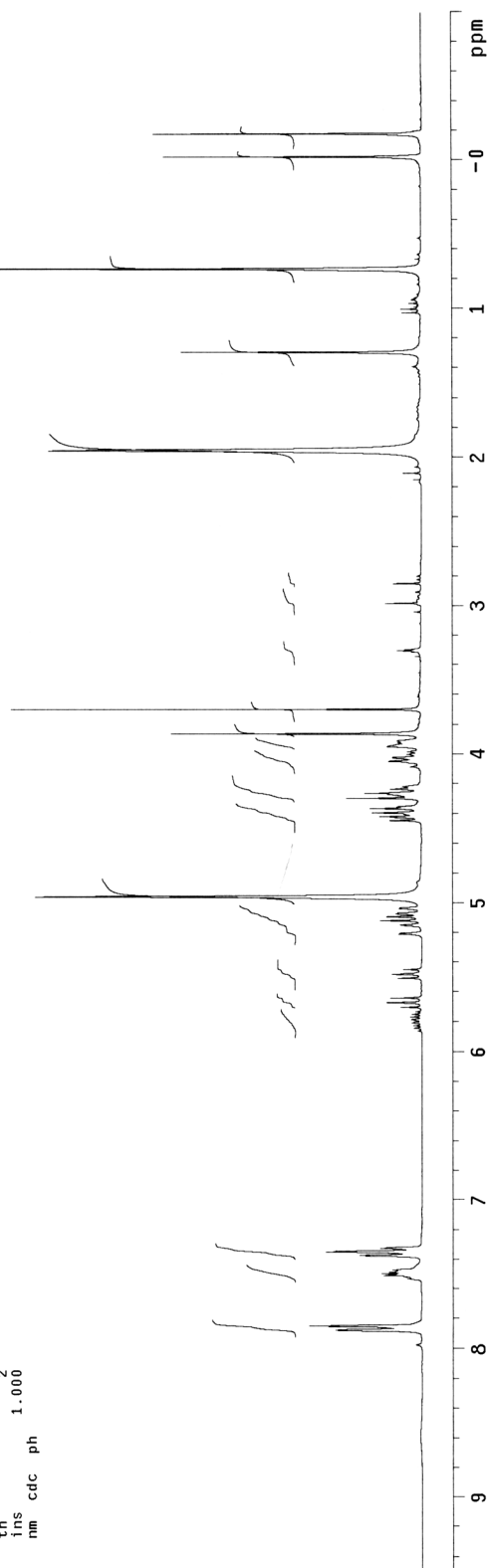
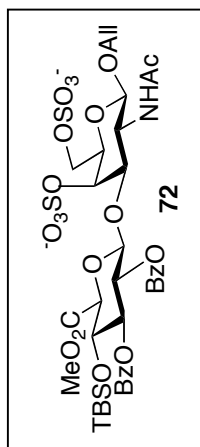


Figure A3.38: ^1H NMR (300 MHz, CD_3OD) of compound **72**.

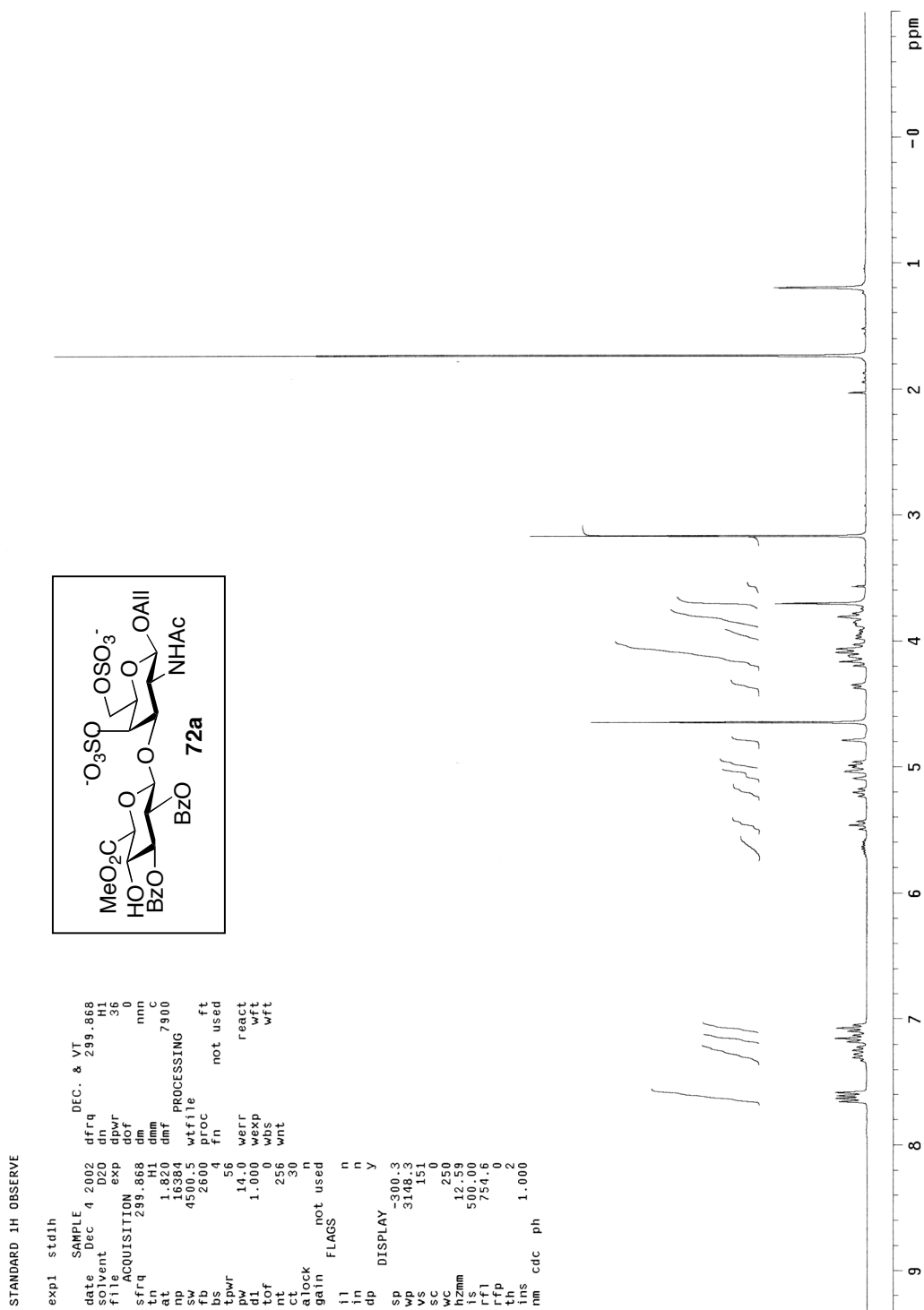


Figure A3.39: ^1H NMR (300 MHz, CD_3OD) of compound **72a**.

STANDARD 1H OBSERVE

```

exp1 std1h
SAMPLE
date Dec 10 2002 DEC. & VT
solvent D2O dfrq 299.868
file exp dn 36
ACQUISITION exp dpwr 0
sfrq 299.868 dm nnn
tn H1 dmm 7900
at 1.820 dmf
sw 18384 wtfile
fb 4500.5 proc not used
ts 4 fn
tpwr 50 werr
d1 14.0 wexp react
nt 1.000 wps wft
ct 256 wnt
alock 22 n
gain not used
FLAGS
il n
in n
dp y
DISPLAY
sp -300.3
wp 3148.3
vs 151
sc 0
hzmm 255
is 500.00
rfl 754.6
th 2
ins 2.000
nm cdc ph
  
```

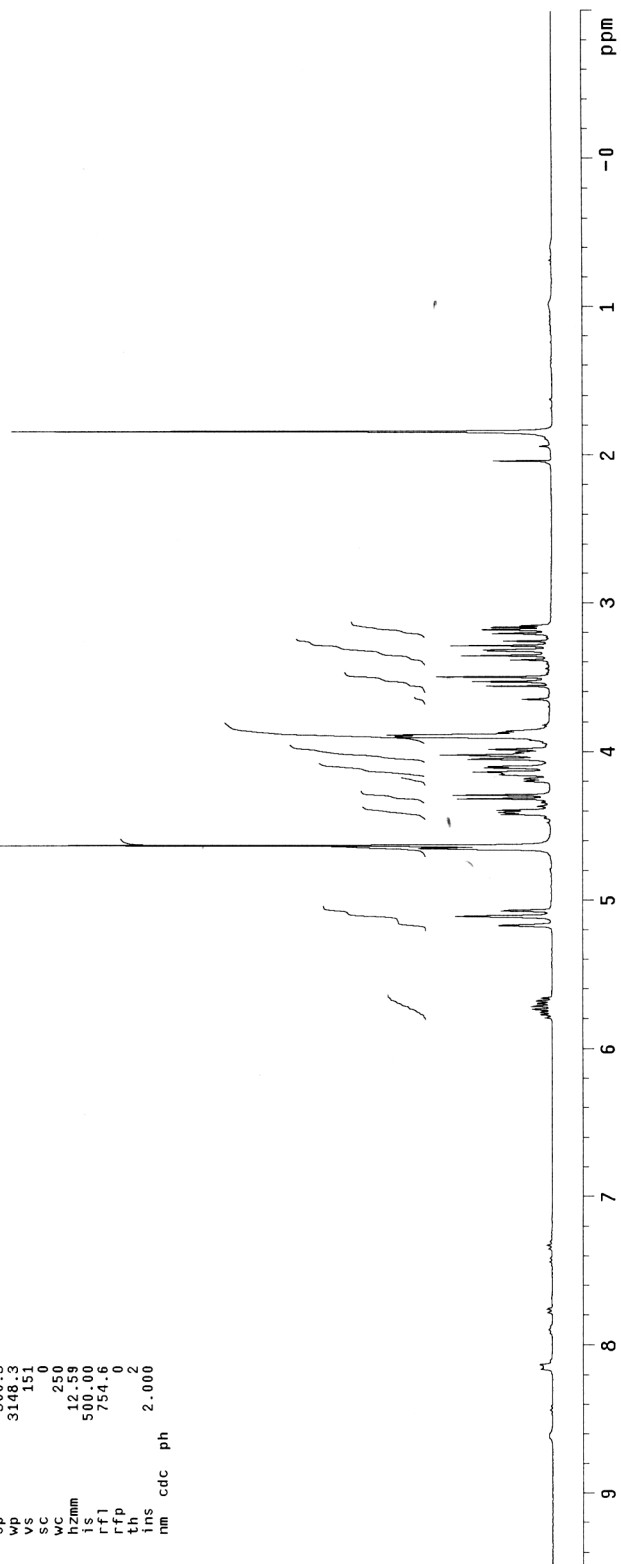
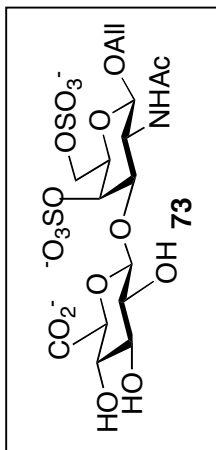


Figure A3.40: ¹H NMR (300 MHz, D₂O) of compound 73.

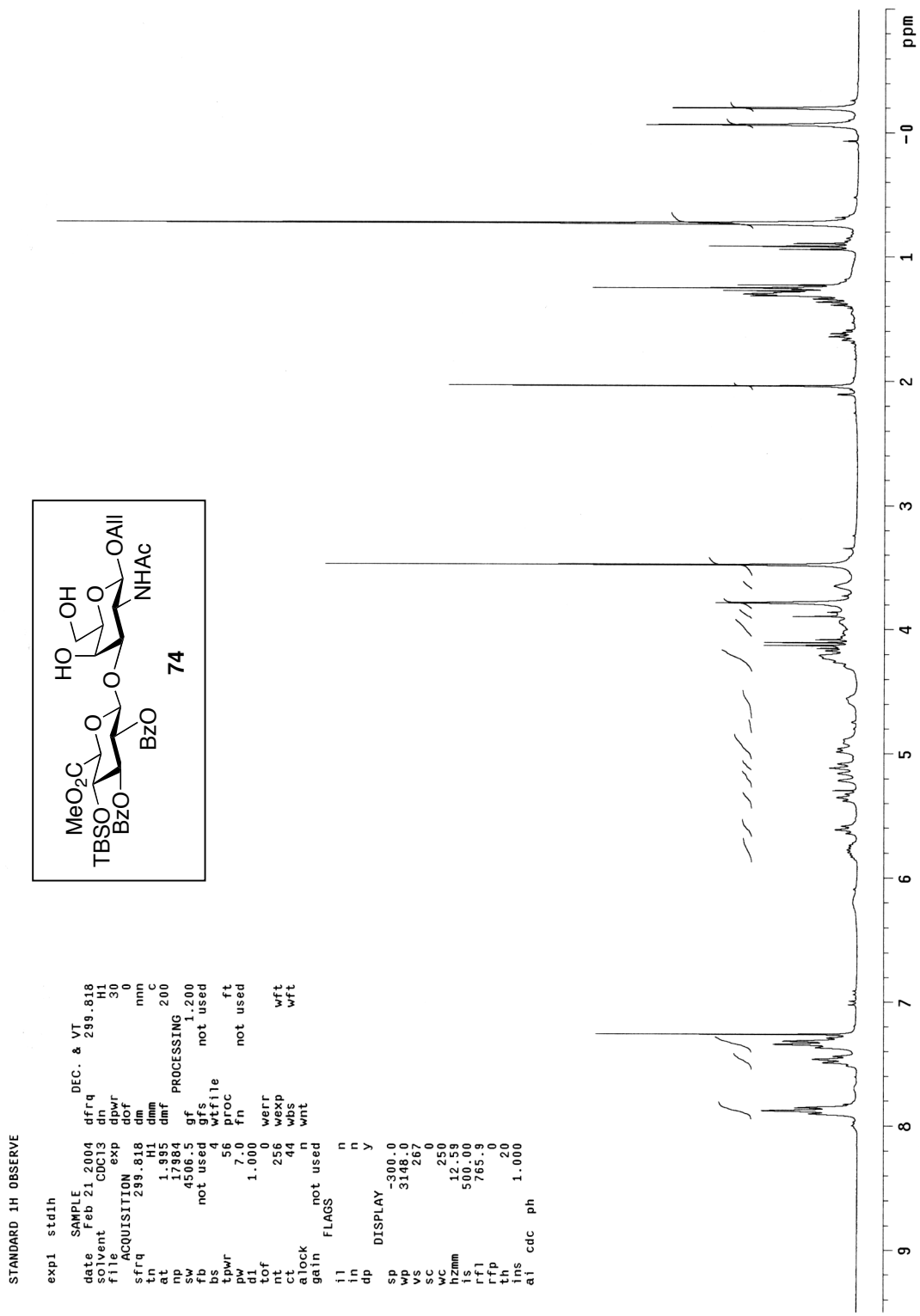
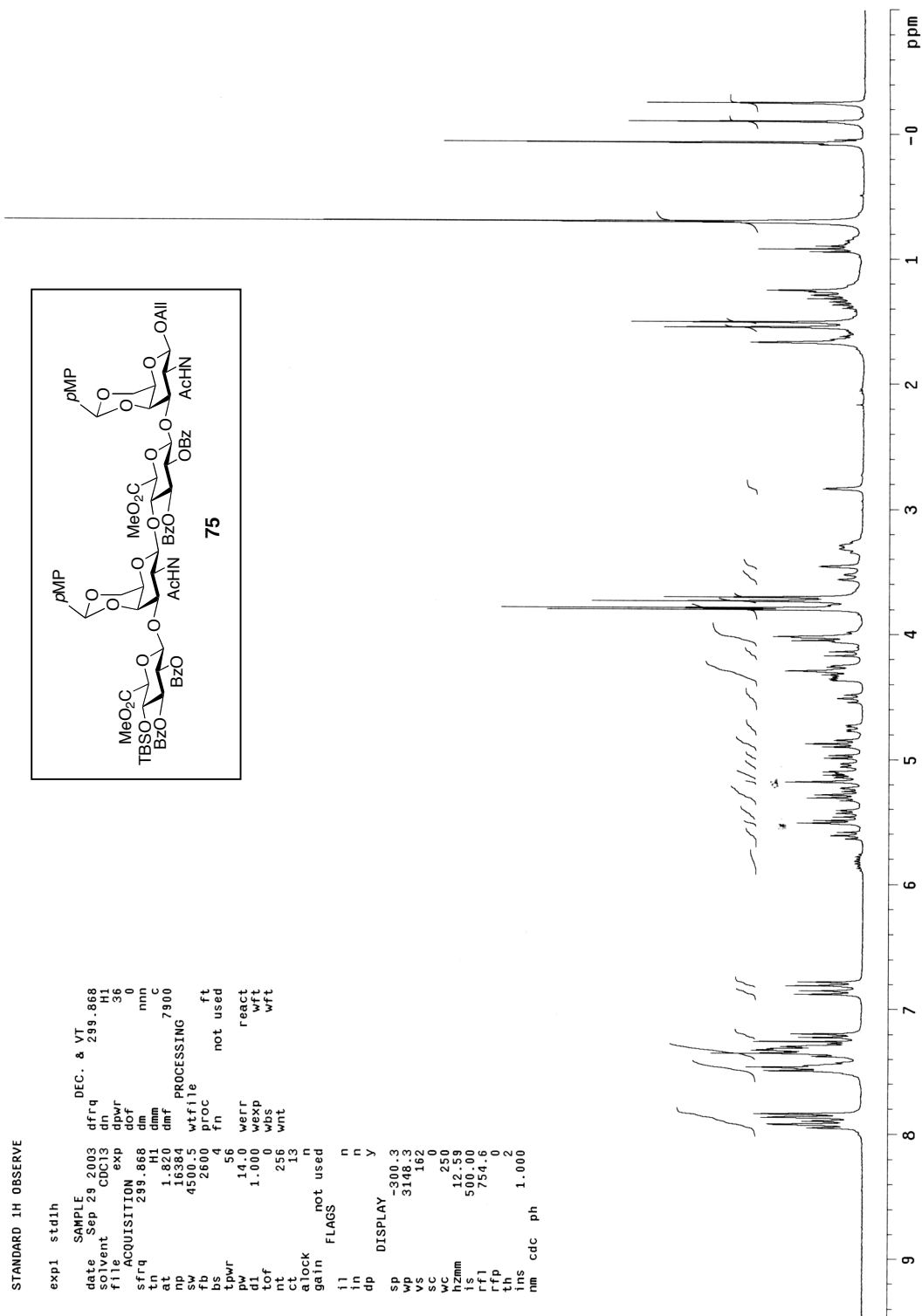
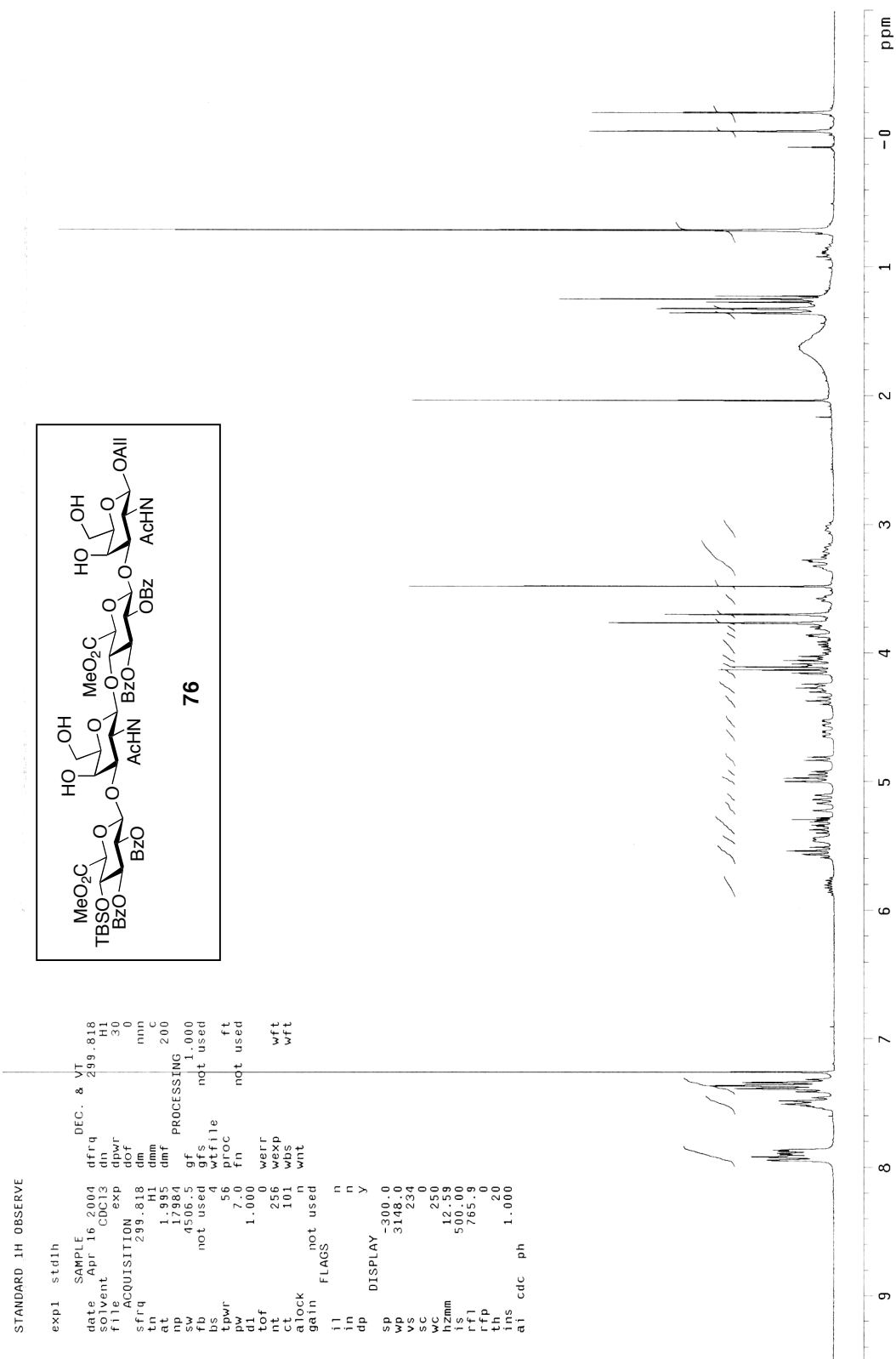
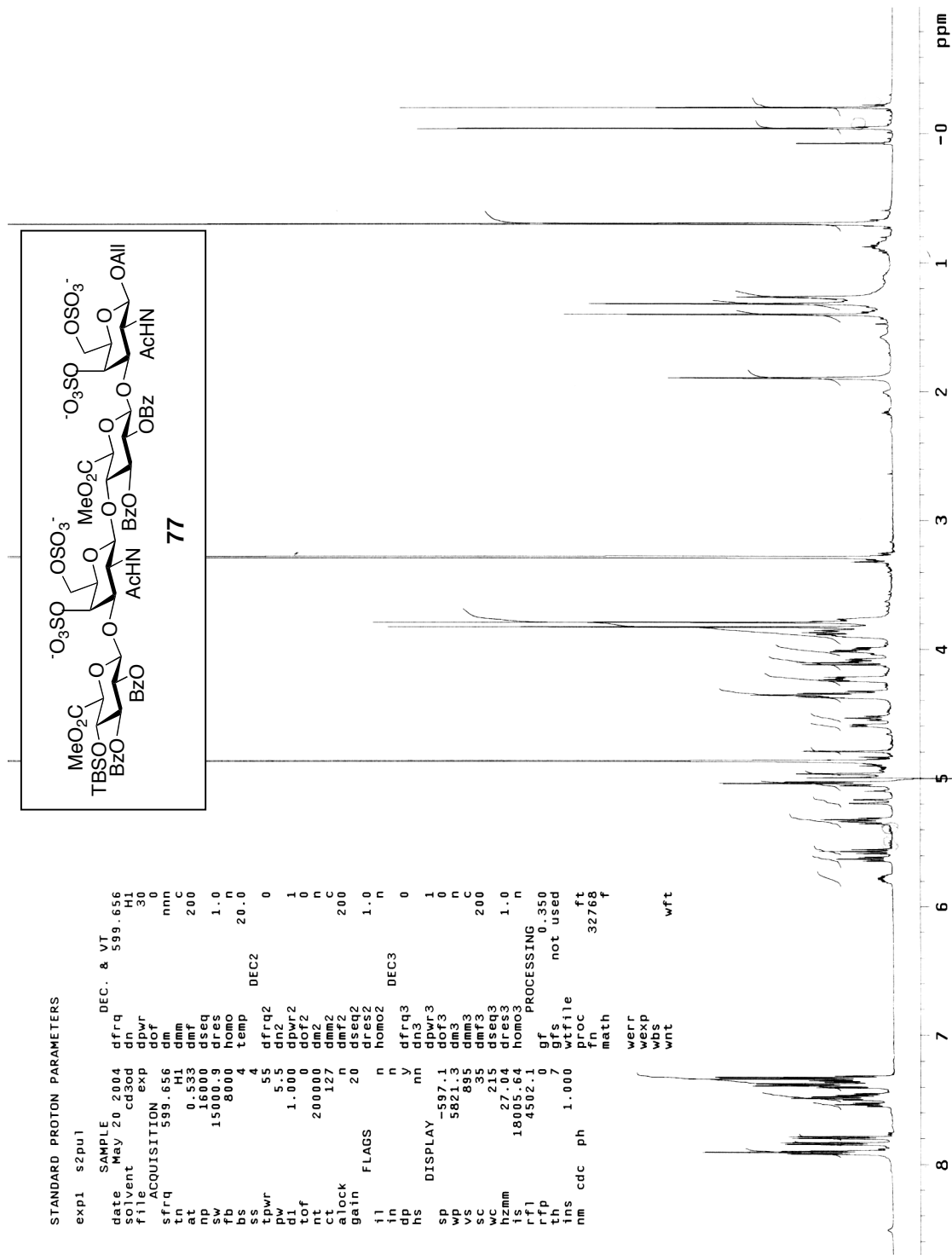


Figure A3.41: ¹H NMR (300 MHz, CDCl₃) of compound 74.

Figure A3.42: ^1H NMR (300 MHz, CDCl_3) of compound 75.

Figure A3.43: ^1H NMR (300 MHz, CDCl_3) of compound **76**.

Figure A3.44: ¹H NMR (600 MHz, CD₃OD) of compound 77.

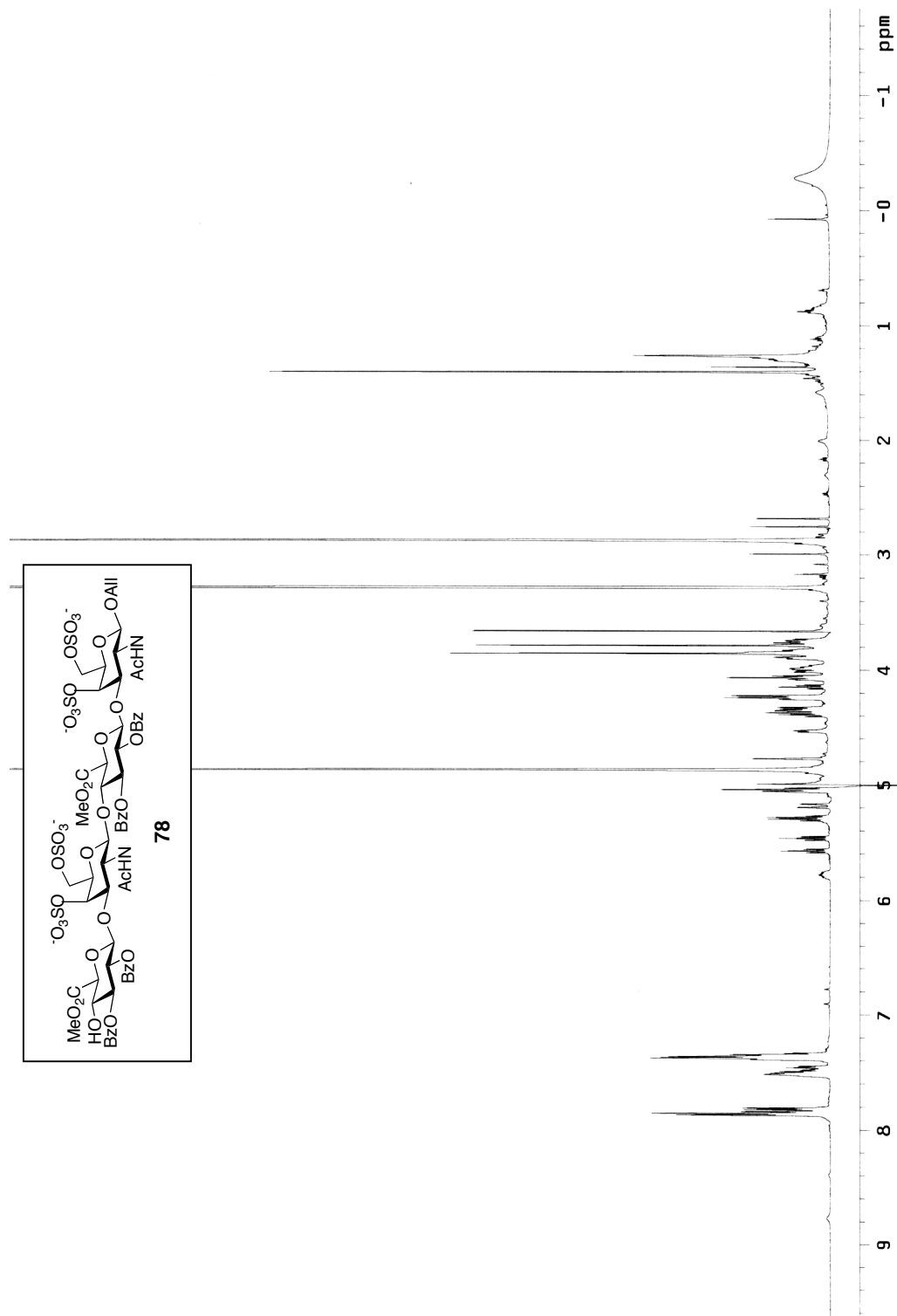


Figure A3.45: ^1H NMR (600 MHz, CD_3OD) of compound **78**.

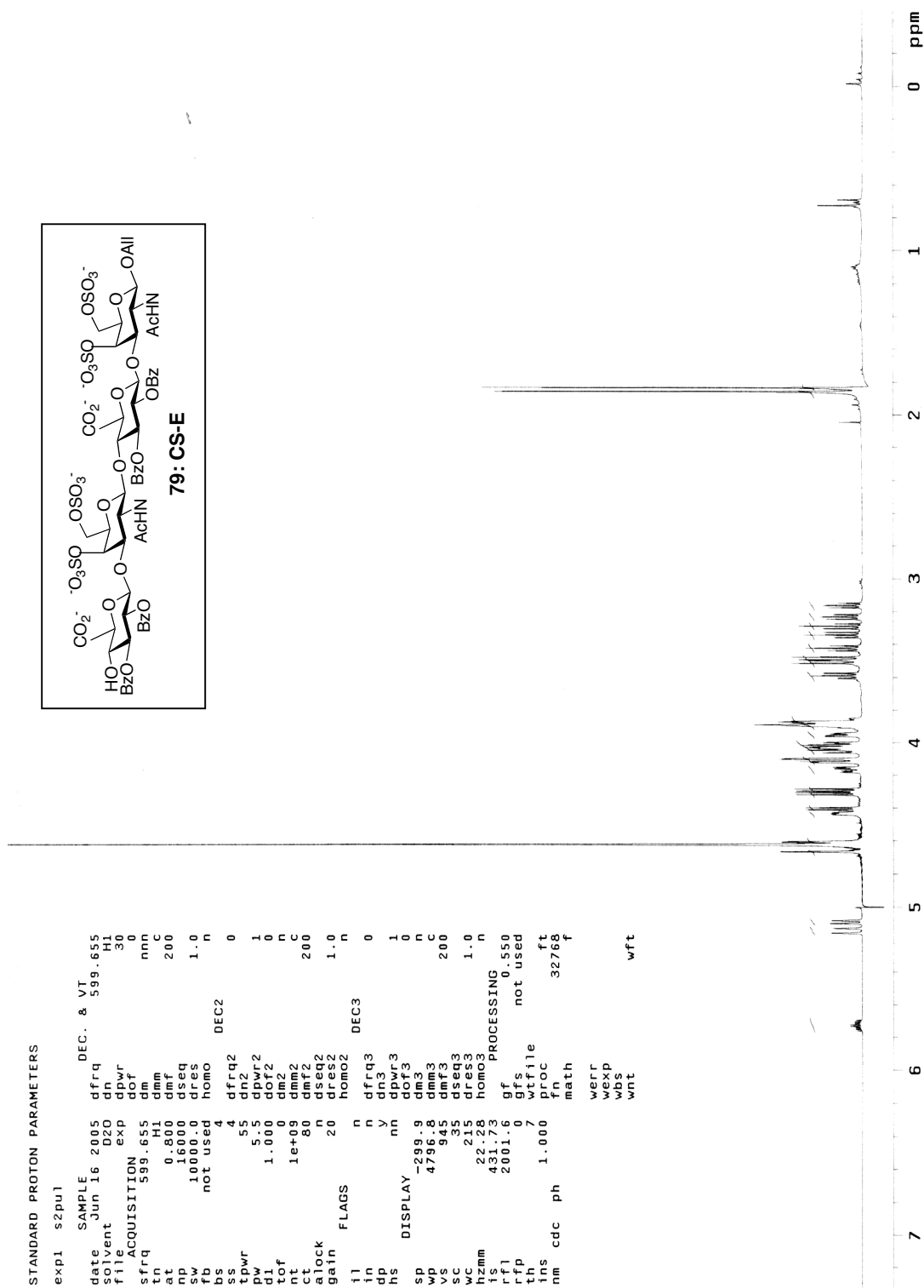


Figure A3.46: ^1H NMR (600 MHz, D_2O) of compound 79: CS-E.

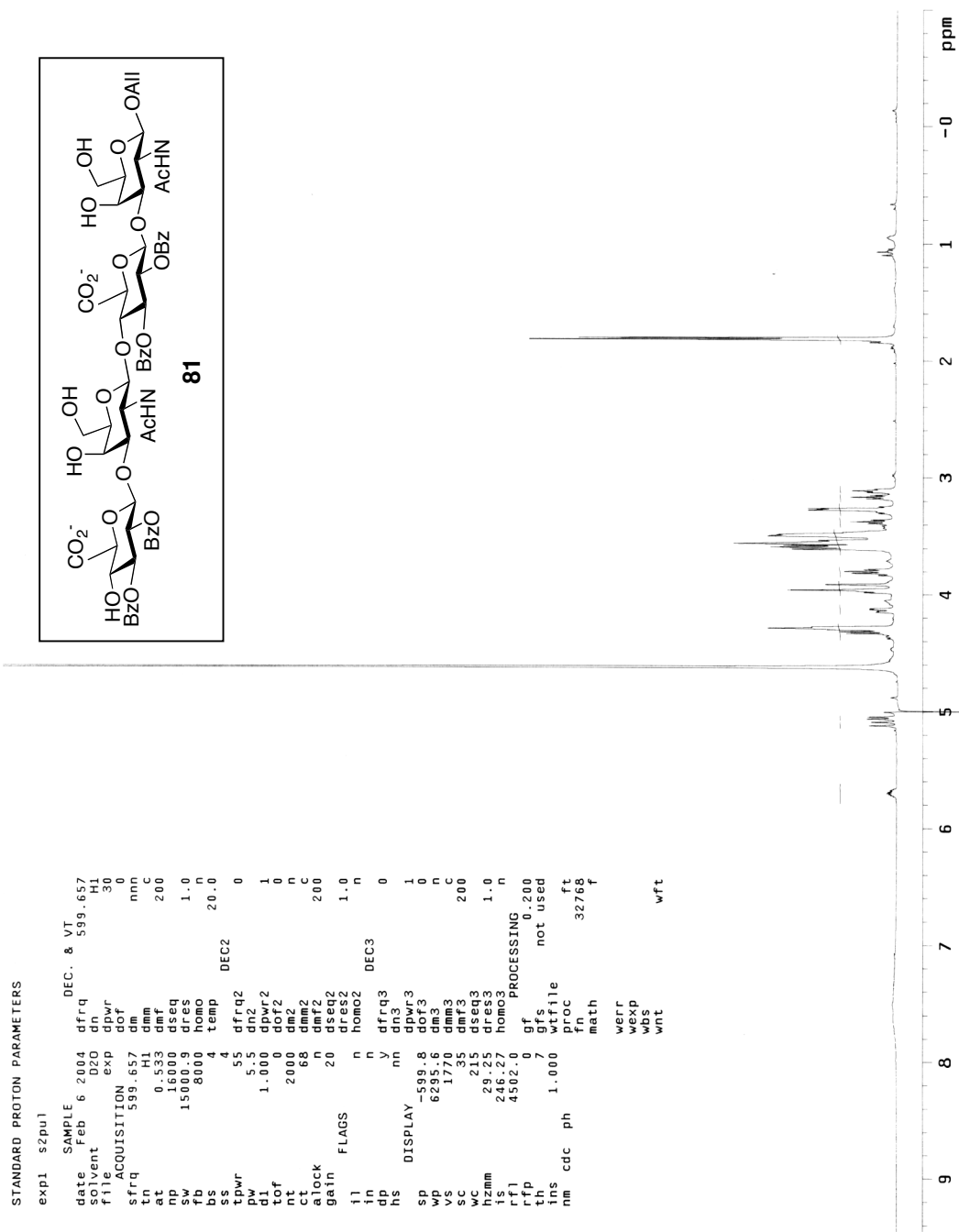


Figure A3.47: ^1H NMR (600 MHz, D_2O) of compound **81**.